SSCL-SR-1152Rev. 1

SSCL-SR-1152Rev. 1

Superconducting Super Collider Laboratory

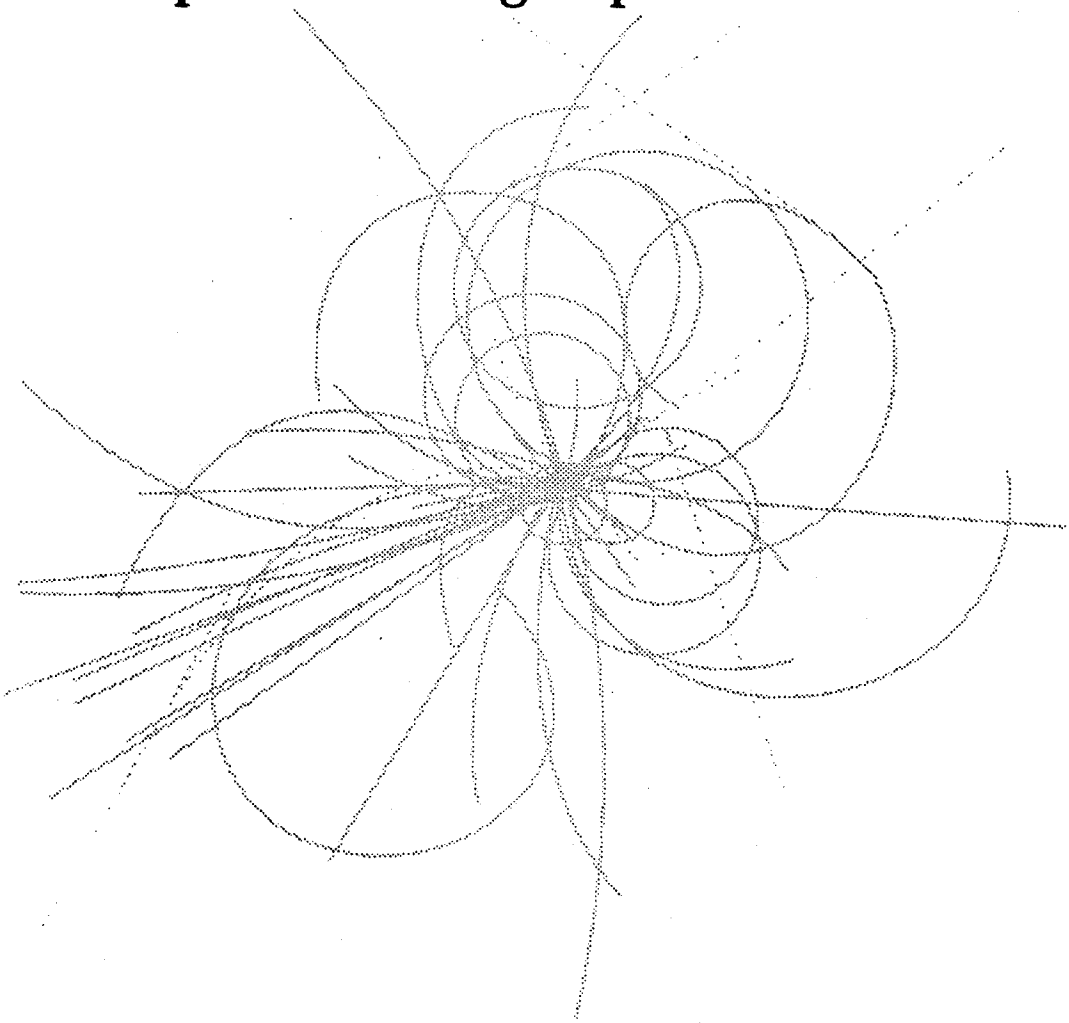

A Design Study of Interaction Halls and Assembly Procedures for a Solenoidal Detector at the SSC

M. Riddle, J. Brown, L. Dittert, A. Nunez,
W. McGinley R. Kadel, W. Edwards, J. Rasson
J. Bensinger, and D. Bintinger

April 1991

SSCL-SR-1152Rev. 1

A Design Study of Interaction Halls and Assembly Procedures for a Solenoidal Detector at the SSC

M. Riddle, J. Brown, L. Dittert, A. Nunez, and W. McGinley

RTK
Oakland, California

R.W. Kadel, W. Edwards, and J. Rasson

Lawrence Berkeley Laboratory
Berkeley, California

J. Bensinger and D. Bintinger

Physics Research Division
Superconducting Super Collider Laboratory*
2550 Beckleymeade Avenue
Dallas, Texas 75237

April 1991

* Operated by the Universities Research Association, Inc., for the U.S. Department of Energy under Contract No. DE–AC02–89ER40486.

CONTENTS

1.0 INTRODUCTION 1
2.0 INTRODUCTION TO DETECTORS AND HALLS 3
2.1 Introduction to Detectors 3
2.2 Introduction to Collision Halls 7
3.0 BASELINE DETECTOR 11
3.1 Baseline Detector Description 11
3.2 Baseline Hall Design 16
3.2.1 Overview and General Hall Plan 16
3.2.2 Detector Basement and Support 18
3.2.3 Operating Floor Construction 21
3.2.4 Access and Utility Shafts 21
3.3 Detector Assembly 24
3.3.1 Muon Steel Barrel Assembly 24
3.3.2 Muon Steel End Toroids Assembly 34
3.3.3 Calorimeter Assembly 38
3.3.4 Muon Chambers 48
3.3.5 Solenoidal Coil 48
3.3.6 Central Tracking Device 52
3.3.7 Beam Pipe 52
3.3.8 Forward Calorimeters 52
3.3.9 Electronics/Triggering 52
3.3.10 Accelerator Components 52
3.4 Schedule and Sequential Construction Drawing 53
3.4.1 Schedule 53
3.4.2 Sequential Construction Drawings 55
3.5 Disassembly and Repair Sequences 72
3.5.1 Minor Repairs 72
3.5.2 Endcap Calorimeter Module Replacement 72
3.5.3 Silicon Tracking Repair 81
4.0 AIR CORE TOROID DETECTOR 86
4.1 Air Core Toroid Detector Description 86
4.2 Air Core Toroid Detector Hall Design 92
4.2.1 Overview and General Hall Plan 92
4.2.2 Detector Basement and Support 95
4.2.3 Operating Floor Construction 99
4.2.4 Access and Utility Shafts 99

4.3 Air Core Toroid Detector Assembly 103
4.3.1 Muon Steel Barrel Assembly 103
4.3.2 Muon Air Core Toroid Assembly 112
4.3.3 Calorimeter Assembly 124
4.3.4 Muon Chambers 136
4.3.5 Solenoidal Coil 136
4.3.6 Central Tracking Device 138
4.3.7 Beam Pipe 138
4.3.8 Forward Calorimeters 138
4.3.9 Electronics/Triggering 140
4.3.10 Accelerator Components 140
4.3.11 Calorimeter Assembly Above Ground 140
4.4 Schedule and Sequential Construction Drawings 150
4.4.1 ACT Detector Schedule 150
4.4.2 Detector Assembly Sequence 152
4.5 Disassembly and Repair Sequences 169
4.5.1 Minor Repairs 169
4.5.2 Endcap Calorimeter Module Repair 169
4.5.3 Silicon Tracking Repair 169
5.0 LIQUID ARGON CALORIMETER DETECTOR 176
5.1 Liquid Argon Calorimeter Detector Description 176
5.2 Liquid Argon Calorimeter Detector Hall Design 182
5.2.1 Overview and General Hall Plan 182
5.2.2 Safety Considerations 189
5.2.3 Detector Basement and Support 190
5.2.4 Operating Floor Construction 193
5.2.5 Access and Utility Shafts 193
5.3 Liquid Argon Calorimeter Detector Assembly 196
5.3.1 Muon Steel Barrel Assembly 196
5.3.2 Muon Endcap Toroid Construction 209
5.3.3 Calorimeter Assembly 215
5.3.4 Muon Chambers 219
5.3.5 Solenoidal Coil 219
5.3.6 Central Tracking Device 220
5.3.7 Beam Pipe 220
5.3.8 Forward Calorimeters 223
5.3.9 Electronics/Triggering 223
5.3.10 Accelerator Components 223
5.4 Schedule and Sequential Construction Drawings 223
5.4.1 Construction Schedule 223
5.4.2 LAC Sequential Construction Drawings 227

5.5 Disassembly and Repair 246
5.5.1 Minor Repairs 246
5.5.2 Major Repairs 250
REFFERENCE 253
APPENDIX A: DETECTOR UTILITIES 255
APPENDIX B: HVAC CONSIDERATIONS 263
1.0 System Requirements 263
2.0 System Options 264
2.1 System A 265
2.2 System B 267
2.3 System Recommendations 269

FIGURES

2.1 Side View of a Generic SSC Detector 4
2.2 Cut and Cover Construction—Elastic Rock Movements 10
3.1 Overall Baseline Detector Layout (3-D View) 12
3.2 Cross-Section of Baseline Detector 13
3.3 Elevation View of Baseline Detector 14
3.4 Baseline Detector—Hall General Arrangement 17
3.5 Baseline Detector—Support Base Plate 20
3.6 Baseline Detector—Personnel and Equipment Shaft Plans 23
3.7 Baseline Detector—Cable and Utility Shaft Plans 25
3.8 Baseline Detector—Muon Steel Barrel 28
3.9 Baseline Detector—Hall Section 29
3.10 Baseline Detector—Muon Steel Barrel Construction (Steps 1-4) 30
3.11 Baseline Detector—Muon Steel Barrel Construction (Steps 5-6) 32
3.12 Baseline Detector—Moveable Barrel Steel Toroid 33
3.13 Baseline Detector—End Toroid General Arrangement 35
3.14 Baseline Detector—End Toroid Construction (Steps 1-4) 36
3.15 Baseline Detector—End Toroid Construction (Steps 5-6) 37
3.16 Baseline Detector—Hall Plan: Detector Assembly Layout 39
3.17 Baseline Detector—Central Calorimeter 40
3.18 Baseline Detector—Endcap Calorimeter 41
3.19 Baseline Detector—Central Calorimeter Bay Assembly 43
3.20 Baseline Detector—Central Calorimeter Washer Analysis (All Modules Inserted) 44
3.21 Baseline Detector—Central Calorimeter Washer Analysis (8 Modules Inserted) 45
3.22 Baseline Detector—Calorimeter Assembly Frame 47
3.23 (a) Baseline Detector—Solenoid Coil Installation (Step 1) 49
3.23 (b) Baseline Detector—Solenoid Coil Installation (Step 2) 50
3.24 Solenoid Cryogenic System Schematic 51
3.25 Baseline Detector Construction Schedule 54
3.26 Baseline Detector Construction Sequence (Month 0) 56
3.27 Baseline Detector Construction Sequence (Month 3) 57
3.28 Baseline Detector Construction Sequence (Month 6) 59

3.29 Baseline Detector Construction Sequence (Month 9) 60
3.30 Baseline Detector Construction Sequence (Month 10) 61
3.31 Baseline Detector Construction Sequence (Month 12) 62
3.32 Baseline Detector Construction Sequence (Month 15) 64
3.33 Baseline Detector Construction Sequence (Month 18) 65
3.34 Baseline Detector Construction Sequence (Month 21) 66
3.35 Baseline Detector Construction Sequence (Month 23) 67
3.36 Baseline Detector Construction Sequence (Month 30). 68
3.37 Baseline Detector Construction Sequence (Month 30.5) 69
3.38 Baseline Detector Construction Sequence (Month 33) 70
3.39 Baseline Detector Construction Sequence (Month 36) 71
3.40 Baseline Detector Construction Sequence (Month 36.5) 73
3.41 Baseline Detector Construction Sequence (Month 38) 74
3.42 Baseline Detector Construction Sequence (Month 40) 75
3.43 Baseline Detector Construction Sequence (Month 42) 76
3.44 Baseline Detector—Minor Repairs 77
3.45 Baseline Detector—Endcap Calorimeter Module Replacement (Step 1) 78
3.46 Baseline Detector—Endcap Calorimeter Module Replacement (Step 2) 79
3.47 Baseline Detector—Endcap Calorimeter Module Replacement (Step 3) 80
3.48 Baseline Detector—Silicon Tracking Repair (Step 1) 82
3.49 Baseline Detector—Silicon Tracking Repair (Step 2) 83
3.50 Baseline Detector—Silicon Tracking Repair (Step 3) 84
3.51 Baseline Detector—Silicon Tracking Repair (Step 4) 85
4.1 Overall ACT Detector Layout (3-D View) 87
4.2 Cross-Section of Air Core Toroid Detector 88
4.3 Elevation View of Air Core Toroid Detector 89
4.4 ACT Detector—Hall Floor Plan 93
4.5 ACT Detector—Section at Beam Line 94
4.6 ACT Detector—Section through Interaction Point 96
4.7 ACT Detector—Inclined Plate Barrel Support 98
4.8 ACT Detector—Personnel and Equipment Shaft Profiles 101
4.9 ACT Detector—Cable and Utility Shaft Plans 102
4.10 ACT Detector—Muon Steel Barrel Dimensions 104
4.11 ACT Detector—Muon Steel Barrel Construction 106
4.12 ACT Detector—Muon Steel Barrel Supports 108
4.13 ACT Detector—Muon Steel Assembly Frame 109

4.14 ACT Detector—Muon Toroid Construction 110
4.15 ACT Detector—Muon Steel Barrel Assembly (Step 1) 111
4.16 ACT Detector—Muon Steel Barrel Assembly (Step 2) 113
4.17 ACT Detector—Muon Steel Barrel Assembly (Step 3) 114
4.18 ACT Detector—Air Core Toroid Assembly 115
4.19 ACT Detector—Muon Steel End Toroid (Elevation) 116
4.20 ACT Detector—Muon Steel End Toroid (Under Construction) 118
4.21 ACT Detector—Muon Steel End Toroid 119
4.22 ACT Detector—Absorber Under Construction 120
4.23 ACT Detector—Jacking Frame 121
4.24 ACT Detector—Jacking Frame Lowering an Air Core Toroid 123
4.25 ACT/Absorber/Muon Steel Assembly (Steps 1-4) 125
4.26 ACT/Absorber/Muon Steel Assembly (Steps 5-8) 126
4.27 ACT Detector—Detector Assembly Layout 127
4.28 ACT Detector—Central Calorimeter 128
4.29 ACT Detector—Endcap Calorimeter 129
4.30 ACT Detector—Central Calorimeter Bay Assembly 131
4.31 ACT Detector—Central Calorimeter Washer Analysis (All Modules Inserted) 133
4.32 ACT Detector—Central Calorimeter Washer Analysis (8 Modules Inserted) 134
4.33 ACT Detector—Endcap Calorimeter Assembly Frame 135
4.34 ACT Detector—Solenoid Coil Installation 137
4.35 Solenoid Cryogenic System Schematic 139
4.36 ACT Detector—Surface Facilities—Calorimeter Assembly Above Ground (Plan View) 141
4.37 ACT Detector—Surface Facilities—Calorimeter Assembly Above Ground (3-D View) 142
4.38 ACT Detector—Surface Construction Facilities (Front Section) 143
4.39 ACT Detector—Surface Construction Facilities (End Section) 144
4.40 ACT Detector—Surface Construction Facilities (Phase 1) 146
4.41 ACT Detector—Surface Construction Facilities (Phase 2) 147
4.42 ACT Detector—Surface Construction Facilities (Phase 3) 148
4.43 ACT Detector—Surface Construction Facilities (Phase 4) 149
4.44 Air Core Toroid Detector Construction Schedule 151
4.45 ACT Detector Construction Sequence (Month 0) 153
4.46 ACT Detector Construction Sequence (Month 3) 154

4.47 ACT Detector Construction Sequence (Month 6) 155
4.48 ACT Detector Construction Sequence (Month 9) 156
4.49 ACT Detector Construction Sequence (Month 12) 157
4.50 ACT Detector Construction Sequence (Month 15) 158
4.51 ACT Detector Construction Sequence (Month 18) 160
4.52 ACT Detector Construction Sequence (Month 21) 161
4.53 ACT Detector Construction Sequence (Month 24) 162
4.54 ACT Detector Construction Sequence (Month 27) 163
4.55 ACT Detector Construction Sequence (Month 30) 164
4.56 ACT Detector Construction Sequence (Month 33) 165
4.57 ACT Detector Construction Sequence (Month 36) 166
4.58 ACT Detector Construction Sequence (Month 39) 167
4.59 ACT Detector Construction Sequence (Month 42) 168
4.60 ACT Detector Open for Minor Repairs 170
4.61 ACT Detector—Endcap Calorimeter Module Replacement (Step 1) 171
4.62 ACT Detector—Endcap Calorimeter Module Replacement (Step 2) 172
4.63 ACT Detector—Silicon Tracking Replacement (Step 1) 173
4.64 ACT Detector—Silicon Tracking Replacement (Step 2) 174
4.65 ACT Detector—Silicon Tracking Replacement (Step 3) 175
5.1 Overall LAC Detector Layout (3-D View) 177
5.2 Cross-Section and Plan View of LAC Detector 178
5.3 LAC Detector—Plan View of Cryogenic Equipment on Gallery (Schematic) 183
5.4 LAC Detector Shown Without Muon Barrel 184
5.5 LAC Detector—Plan Section of Detector Hall 185
5.6 LAC Detector—Section through Interaction Point 187
5.7 LAC Detector—Section through Beam Line 188
5.8 LAC Detector—Inclined Plate Barrel Support 192
5.9 LAC Detector—Personnel and Equipment Shaft Profiles 195
5.10 LAC Detector—Cable and Utility Shaft Plans 197
5.11 LAC Detector—Muon Steel Barrel Dimensions 198
5.12 LAC Detector—Muon Steel Barrel Construction 199
5.13 LAC Detector—Muon Steel Barrel Supports 203
5.14 LAC Detector—Muon Steel Assembly Frame 204
5.15 LAC Detector—Muon Toroid Construction. 205
5.16 LAC Detector—Muon Steel Barrel Assembly (Step 1) 206

5.17 LAC Detector—Muon Steel Barrel Assembly (Step 2) 207
5.18 LAC Detector—Muon Steel Barrel Assembly (Step 3) 208
5.19 LAC Detector—Muon Toroid Assembly 210
5.20 LAC Detector—Muon Toroid Assembly (Open for Minor Repair) 211
5.21 LAC Detector—Muon Steel End Toroid Plates 212
5.22 LAC Detector—Muon Steel Toroid Erection 213
5.23 LAC Detector—Muon Toroid Half (Fitted with Disassembly Frame and Rollers) 214
5.24 LAC Detector—Barrel Calorimeter (Exploded View) 216
5.25 LAC Detector—Tool for Hadronic Module Placement 217
5.26 LAC Detector—Barrel Calorimeter Being Inserted into Vacuum Vessel 218
5.27 LAC Detector—Solenoid Coil Installation 221
5.28 Solenoid Cryogenic System Schematic 222
5.29 LAC Detector—Forward Calorimeter Support System 224
5.30 LAC Detector Construction Schedule 225
5.31 LAC Detector Construction Sequence (Month 0) 228
5.32 LAC Detector Construction Sequence (Month 3) 229
5.33 LAC Detector Construction Sequence (Month 6) 230
5.34 LAC Detector Construction Sequence (Month 9) 232
5.35 LAC Detector Construction Sequence (Month 12) 233
5.36 LAC Detector Construction Sequence (Month 15) 234
5.37 LAC Detector Construction Sequence (Month 18) 235
5.38 LAC Detector Construction Sequence (Month 21) 237
5.39 LAC Detector Construction Sequence (Month 24) 238
5.40 LAC Detector Construction Sequence (Month 27) 239
5.41 LAC Detector Construction Sequence (Month 30) 241
5.42 LAC Detector Construction Sequence (Month 33) 242
5.43 LAC Detector Construction Sequence (Month 36) 243
5.44 LAC Detector Construction Sequence (Month 39) 244
5.45 LAC Detector Construction Sequence (Month 42) 245
5.46 LAC Detector Construction Sequence (Month 45) 247
5.47 LAC Detector Construction Sequence (Month 48) 248
5.48 LAC Detector Open for Minor Repairs 249
5.49 LAC Detector Open for Endcap Calorimeter Repair 251
5.50 LAC Detector Open for Barrel Calorimeter Repair 252

B.1 HVAC System A Schematic—A/C Units in Hall 266
B.2 HVAC System B Schematic—A/C Units Above Ground 268

TABLES

2.1 Common Materials in Calorimeters or Tracking Detectors 5
3.1 Baseline Detector Mechanical Parameters 15
3.2 Hall Shafts 22
3.3 Mechanical Specifications for Baseline Detector Muon Toroids 24
3.4 Muon Barrel Toroid Plate Specifications 26
4.1 ACT Detector Mechanical Parameters 91
4.2 Hall Shafts 99
4.3 Mechanical Specification for ACT Detector Muon Toroids 103
4.4 Plate Count for Muon Barrel Steel Toroid 107
4.5 Unit Labor and Rental Costs for Hydraulic Jacking System 122
4.6 ACT Jacking Frame Cost Summary 122
5.1 LAC Detector Mechanical Parameters 181
5.2 Liquid Argon Cryogenic Equipment 186
5.3 Hall Shafts 194
5.4 Mechanical Specification for LAC Detector Muon Toroids 196
5.5 Plate Count for Muon Barrel Steel Toroid 201
A.1 Power Consumption 256
A.2 Primary Cooling Requirements 259
A.3 Secondary Cooling Requirements 262
B.1 Design Criteria for Temperature, Humidity, and Ventilatin 264
B.2 HVAC Power Requirements (System A) 265
B.3 HVAC Power Requirements (System B) 267

1.0 INTRODUCTION

This report presents conceptual designs for interaction halls and assembly procedures for solenoidal-type detectors at the Superconducting Super Collider (SSC). Previous design studies for detector halls and related facilities can be found in the SSC Conceptual Design Report (1986), the Proceedings of the Summer Study on the Physics of the Super Collider (Snowmass, 1986), the Proceedings of the Workshop on Experiments, Detectors, and Experimental Areas for the Super Collider (1987), the Site-Specific Study of SSC Support Facilities for Four Generic Detector Designs (1989), and the SSC Site-Specific Conceptual Design Report (1990). These previous reports of necessity focussed on a variety of detectors and provided only roughly sized facilities and outlines of detector assembly and schedules. This report focuses on a solenoidal-type detector and presents in further detail the assembly procedures for several options for such a detector. Based on these assembly studies, interaction halls and surface facilities are conceptually designed and detector assembly schedules are formulated.

The specific goals of this study are:

1. To assemble detector designs for major design options of the solenoidal-type detector. The options include a baseline detector with square muon steel and a modularized scintillator or warm liquid calorimeter, a detector with octagonal muon barrel steel and endcap air core toroids, and a detector with liquid argon calorimetry.
2. To model the assembly sequence for each option in detail, including required assembly tooling and environment.
3. To develop the required hall design for each option, including space requirements, floor loading and movement requirements, crane requirements, shaft specifications, and safety requirements.
4. To obtain from the above a detector assembly schedule. Some manpower estimates are also given.

Each detector option study began with physicists and engineers working through plausible assembly procedures based on information gathered about the detector's subsystems, such as muon steel, calorimetry, and solenoid. This assembly procedure was then modeled in three dimensions on a CAD system. The CAD model includes the detector with its subsystems, assembly procedures and tooling, and interaction hall and shafts. Careful examination of space requirements is possible because of CAD modeling.

This report is organized as follows: Chapter 2 introduces the general reader to detectors at the SSC and underground halls for detectors. Chapters 3, 4, and 5 present hall and assembly studies of the baseline, air core toroid (ACT), and liquid argon calorimeter (LAC) detectors, respectively. Each detector study chapter includes a detector description, a hall description, assembly description, assembly schedule, assembly sequence drawings, and disassembly drawings. Each of

Chapters 3, 4, and 5 may be read independently. Appendixes A and B present general utilities and HVAC considerations, respectively.

2.0 INTRODUCTION TO DETECTORS AND HALLS

2.1 Introduction to Detectors

Large-scale detectors at the SSC will consist of several different subsystems, each of which contributes some piece of information about an individual event produced at the SSCL. Individual events produce an average rate of 100,000,000 per second at the design luminosity, and each event consists of hundreds of particles emerging from the event vertex.

Two particles, electrons and muons, are of particular interest when designing a detector. Both are among the class of particles called leptons. Leptons are very rare in high energy collisions: about one in every 10,000 particles emerging from the interactions is a lepton. The presence of leptons usually points to the occurrence of some interesting physics phenomenon. Hence, a great deal of care is used in the design of the experiments to optimize the identification of leptons, particularly electrons and muons. As we indicate below, both of these particles have systems dedicated to their detection. We use both these particles to illustrate the overall logic of detectors at colliders. The reader should keep in mind, however, that there are many interesting issues in physics that do not rely on identification of electrons or muons. These two particles are used only as an example.

Figure 2.1 shows a cross-section of a generic solenoidal detector for the SSC. All of the detector subsystems work by sensing energy left behind by individual tracks as particles emerge from the interaction region. In some cases it is only a tiny fraction of a particle's total energy that is detected. A tracking chamber, which is used to measure the direction of charge tracks, is an example of such a detector. Putting tracking detectors inside a solenoidal magnetic field allows the momentum and direction of charged tracks to be measured. These particle trajectories and momenta can be compared with measurements in other parts of the detector to help clarify the underlying physics process that produced the event. Note that neutral particles will not leave a track in a tracking chamber. Tracking detectors are typically manufactured using lightweight materials to minimize their effect on the particle they are trying to measure.

Other detectors—a calorimeter, for example—sense particles by measuring all of their energy. A calorimeter is made of interleaving layers of a sensitive detector material and an "absorber." Particles entering the calorimeter interact, mostly in the absorber, creating a cascade of lower energy particles, each of which in turn interacts further along the absorber. As this cascade develops in the absorber, its energy is sampled at regular intervals in the "detector layers." Examples of material used in these detector layers are plastic scintillator, liquid argon (a cryogenic fluid at about

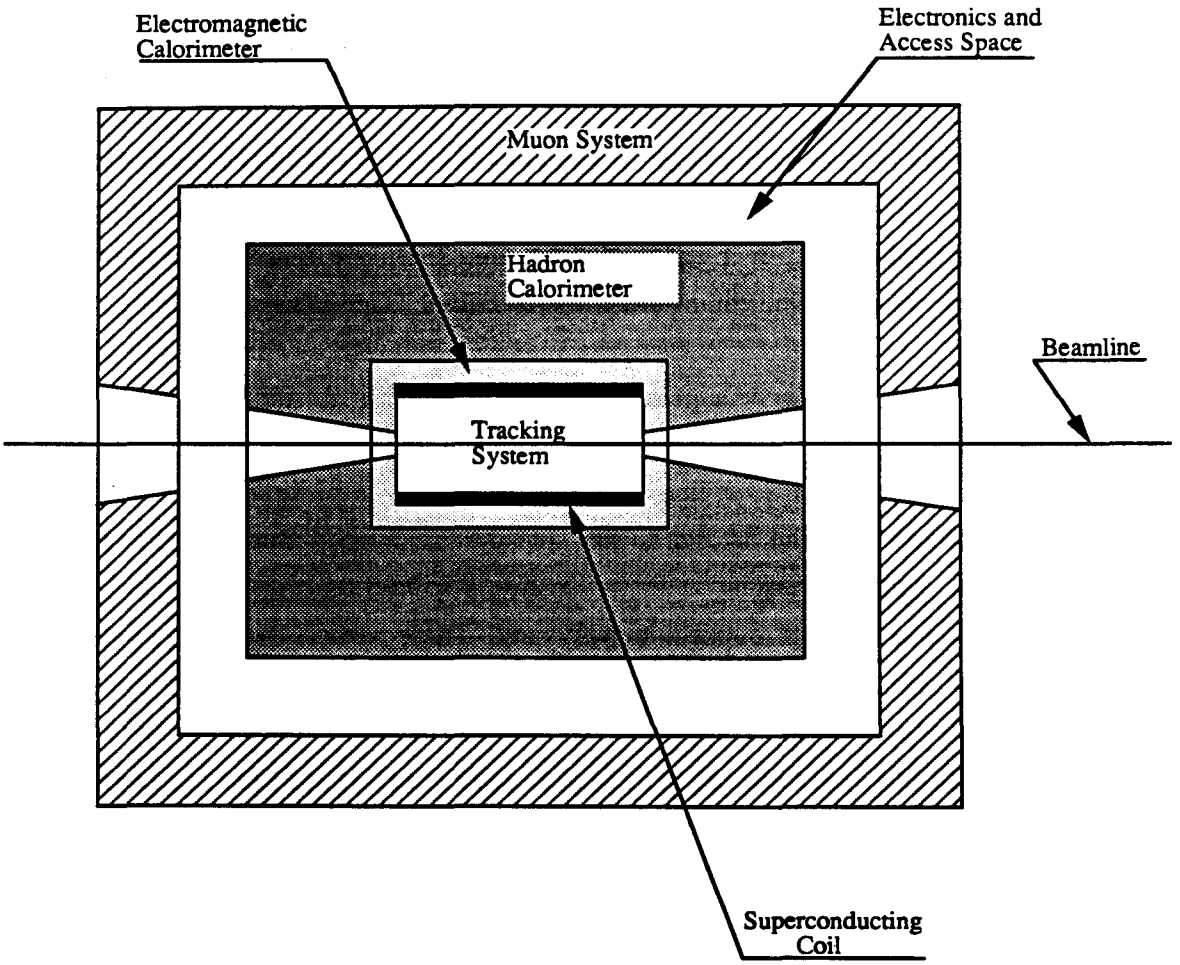

Figure 2.1 Side View of a Generic SSC Detector

80 K) and so-called "warm liquids" (special, very pure, hydrocarbons at room temperature). The absorber typically can be lead, iron, tungsten, or depleted uranium. The absorber contributes 80% to 90% of the volume of a calorimeter and 95% of the weight. Typically, the calorimeter is divided into at least two longitudinal sections: the electromagnetic compartment and the hadronic compartment.

The electromagnetic compartment obtains its name because it is optimized to measure the energy and position of electrons (and photons) which interact via the electromagnetic force. These particles interact very quickly at the front of the calorimeter, and their energy can be measured very accurately.

The depth or thickness of the electromagnetic calorimeter is measured in "radiation lengths," which indicate the probability that an electron will interact in the absorber. About 60% of electrons will interact in one radiation length. The longer the radiation length, the less likely a particle will interact given a fixed thickness of material. The first column of Table 2.1 lists typical values for the radiation length of some common materials used in calorimeters or tracking devices. In order to contain a high-energy electron shower at the SSC, the electromagnetic (or EM) calorimeter is usually designed to be about 25 radiation lengths thick. The maximum radiation dose in the detector occurs at electromagnetic shower maximum, between 6 and 9 radiation lengths from the front face of the calorimeter.

Table 2.1. Common Materials in Calorimeters or Tracking Detectors

Material	Typical Use	Radiation Length (mm)	Nuclear Interaction Length (mm)
Beryllium	Supports	353	408
Carbon Fiber	Supports	~400	392
Aluminum	Supports	89	394
Uranium	Absorber	3.2	105
Lead	Absorber	5.6	171
Tungsten	Absorber	3.5	96
Iron	Absorber/Supports	17	167
Liquid Argon	Detector	140	835
Scintillator	Detector	424	565
TMP (Warm Liquid) Detector	~565	~753	

Consider an electromagnetic calorimeter constructed from equal, alternating layers of lead and scintillator. The radiation lengths of lead and scintillator are about 5.6 mm and 424 mm, respectively. Table 2.1 implies that the scintillator contributes about 5.6 mm/428 mm, or 1.3%, of the total thickness of a scintillator/lead calorimeter when measured in radiation lengths. Hence, most

interactions take place in the absorber, not the detector layer. The most popular choice for an absorber in an electromagnetic calorimeter is lead because it is cheap, it has a small value for the ratio of radiation length to nuclear interaction length (see below), and it is relatively safe. Uranium also works well, but it is expensive and it has some serious safety problems. Tungsten is prohibitively expensive, and iron does not work as well as lead because the ratio of radiation length to nuclear interaction length is larger.

Unlike electrons, most of the particles interact in the calorimeter via the "strong" or nuclear force. Particles which interact via this strong force are called hadrons, and a calorimeter which measures their energy is called a hadron calorimeter. The distance between interactions (nuclear interaction length) of this type is much greater than in the case of the electromagnetic force, as can be seen by comparing the last two columns in Table 2.1. Materials with a small ratio of radiation length to nuclear interaction length are used in electromagnetic calorimeters. This is because the shape of the electron cascade differs greatly from a hadronic cascade in such a material. Electrons are easy to identify because they interact near the beginning of the calorimeter. To contain 95% of the energy in 95% of the events (a typical depth specification for a hadron calorimeter), the total depth of a hadron calorimeter at the SSC needs to be from 10 to 12 nuclear-interaction-lengths deep, including the electromagnetic calorimeter, which is typically one interaction-length thick.

Clearly, if one wants to accurately measure the total energy of a particle, the amount of dead material for support and cable pathways through the detector needs to be minimized. Use of light materials (beryllium, carbon-fiber-reinforced plastics, or aluminum) for supports will affect operation of the calorimeter the least, because the probability of an interaction is much smaller in these materials. Both beryllium and carbon-fiber-reinforced plastics are expensive, however, and the latter can undergo radiation damage at high luminosities. These materials are used successfully in tracking chambers where the volume of material needed is small and the radiation doses are smaller. Mechanical supports inside the active volume of a calorimeter are more commonly made of aluminum. Supports outside the active volume of the calorimeter are typically structural steel.

Given these three components of a detector (a tracking chamber in a magnetic field, an electromagnetic calorimeter, and a hadron calorimeter), we can outline the strategy for identifying an electron among the hundreds of particles in an event:

1) The electron is charged, so it should leave a path in the tracking chamber. Usually we are looking for high-energy electrons, so the path in the magnetic field will be an almost-straight line.

2) An electron should leave most of its energy in the electromagnetic calorimeter, and there should be little energy in the hadron calorimeter directly behind.

3) Since the electron mass is very small, the energy measured in the EM calorimeter should agree with the momentum measured in the tracking chambers.

4) The track in the chamber should point in the same direction as the energy deposit in the EM calorimeter.

The second particle we wish to identify is the muon, a heavy cousin of the electron. The muon is unusual in its ability to penetrate very dense materials, even calorimeters. A muon will leave little of its energy in a calorimeter. Typically, the presence of a muon is observed by a detector (usually tracking chambers) outside the calorimeter. Because muons are charged, they also leave a track in the central tracking chambers, where their initial momentum is measured. In order to reduce backgrounds, magnetized iron toroids are used to remeasure the muon momentum, and comparison is made with the initial measurement made in the central tracking system inside the solenoid coil. Muons, for the most part, will remeasure at about the same momentum, while decay fragments or particles which leak out the back of the calorimeter will have significantly lower momentum.

Hence the strategy for detecting a muon: a straight track in the tracking chamber, no significant energy deposit in the calorimeter along the path of the track, and a track outside the calorimeter, consistent in direction, location, and momentum with extrapolated track from the central tracking chamber.

Before proceeding to the description of specific detectors and halls, it is useful to introduce a detector coordinate system. The x axis points radially outward in the plane of the collider, y is upward, and z points along the beam bisector to complete a right-handed coordinate system. Spherical polar (r,θ,ϕ) and cylindrical (r,ϕ,z) coordinate systems are obtained from the Cartesian coordinates in the usual way. To relate this detector Cartesian coordinate system to the hall, we identify the positive z axis with project North and the positive x axis with project West.

It is also useful to introduce the concept of pseudo-rapidity (η), an angular coordinate defined by

$$\eta = - \ln (\tan (\theta/2)).$$

Note that $\eta = 0$ corresponds to $\theta = 90^o$, and larger (smaller) values of η lie closer to the positive (negative) z axis. This coordinate is frequently used in high-energy physics because the number of particles seen in the detector is roughly constant in a fixed interval in η. For example, we expect as many particles in the interval $0 < \eta < 1$ ($90^o > \theta > 40.4^o$) as we would in the interval $3 < \eta < 4$ ($5.7^o > \theta > 2.1^o$).

With this information in hand, we now turn to the general design of detector halls for the SSC.

2.2 Introduction to Collision Halls

The solenoidal detector is installed in an air-conditioned underground hall connected to the surface by several access and utility shafts. The single long hall is constructed with its major axis parallel to the collider beam line. The hall is designed to house all components of the detector and

its electronics rack and to allow servicing of the assembly and disassembly of the detector. Adequate space must be provided around the completed detector for moving fixtures, for retracting the detector components for maintenance, and for upgrading of the detector.

Assembly of the muon steel toroids and other components of the detector is performed by two top-running bridge cranes. The larger of the cranes is used to assemble muon steel toroids and absorbers, and to move heavy steel saddles and support frames of the movable end toroids and other components. This crane is equipped with a 100-tonne and a 50-tonne hook, each on a separate trolley. The second crane is used for moving the calorimeter modules, installing muon chambers and other lighter components in the hall during assembly, and performing maintenance. This crane is equipped with a 50-tonne and a 25-tonne hook, both on the same trolley. Both bridge cranes run on the same set of rails. To provide maximum hook coverage over the hall floor below, the rails rest directly on top of the side walls of the halls.

One of the most important considerations in the selection and design of the hall floor is maintaining the vertical floor movements within acceptable limits. Excessive floor movement would require the realignment of the entire detector, weighing over 20,000 tonnes, and may require the adjustment of hundreds of other components of the detector, which must be installed to very close tolerances. For example, the muon system requires chamber placement accuracy on the order of 0.1 mm. Time spent to perform alignment checks and adjustments may reduce the time the detector is available for experiments. Excessive floor movement could also result in redistribution of the gravity loads on the detector supports, resulting in local overstress and distortion.

For these reasons the concrete slab under the detector must be made very rigid. The most effective means of reducing floor movement is to reduce the effective spans (width and length) of the floor to the minimum, and to provide a rigid support at the four sides of the floor. To this end, we have raised the hall floor at each end of the detector to approximately the top of the bottom segment of the muon steel barrel, and introduced a transverse wall approximately 5 m (16.4 ft.) deep between the two floors at the ends of the detector. These walls, and the side walls of the hall, will restrain the edges of the slab supporting the detector, and therefore, reduce floor movement.

Reducing the floor movement by structural considerations is even more important when heaving of the rock underlying the detector hall is considered. Assuming that the SDC detector is located at the west cluster, the hall floor will rest directly on the soft Eagle Ford Shale, and, therefore, will be subjected to short-term mass movement and long-term creep. The clay shales of this formation have a moderate to very high self pressure of up to 122 kg/m^2 (25 ksf). The gravity loading on the detector support floor (basement) is about 135 kg/m^2 (27.7 ksf), while loading on the raised floor supporting only accelerator components is practically nil. If the floor arrangement described above is used, the movement of the detector support floor should be minimal because detector loading and self pressure almost match; the raised floor, on the other hand, should experi-

ence long-term heave. This requires that the support frames of the accelerator components be furnished with adjustable base plates. If the detector support floor is not isolated structurally from the rest of the hall floor (as in a single floor level construction), the average gravity loading on the hall floor will be reduced by about 60%. As a result, the swell pressure of the underlying shale can cause long-term heaving of the entire hall floor.

The magnitude and duration of this movement is difficult to estimate without knowing the actual swell pressures and other physical data of the rock. We have performed a preliminary finite element analysis to assess the anticipated rock movements. Assuming a benched open excavation as shown in Figure 2.2, the elastic (immediate) vertical rock movement at the center of the excavation is 154 mm to 350 mm (6.1 in. to 13.8 in.), and the net heave is 83 mm to 199 mm (3.3 in. to 7.8 in.) depending on the elasticity of the rock. Long-term heave could be as much as 50% to 75% of the elastic heave. However, this must be substantiated by *in situ* testing at the selected site.

There are other operational and safety features of the raised operating floor arrangement. Because the floor is at or near the level of the top of the muon steel barrel floor, there is no need for special movable make-up cradles to support the 4000-tonne end toroids and the calorimeters when disassembling the detector to gain access to the calorimeter bays. The cost of the hall is somewhat reduced as the need to excavate and the amount of concrete in the walls are reduced. A detector basement or pit, however, might restrict future expansion of the detector. Also, the edges of a pit might be subject to crumbling. A full study of the tradeoffs of two level floor versus one level floor has not been made in this report. For either floor configuration it is important that the planned geotechnical investigations, particularly the *in situ* swelling pressure measurements, are carried out as soon as possible. Also, the design of the detector hall floor and of the detector supports must be closely coordinated.

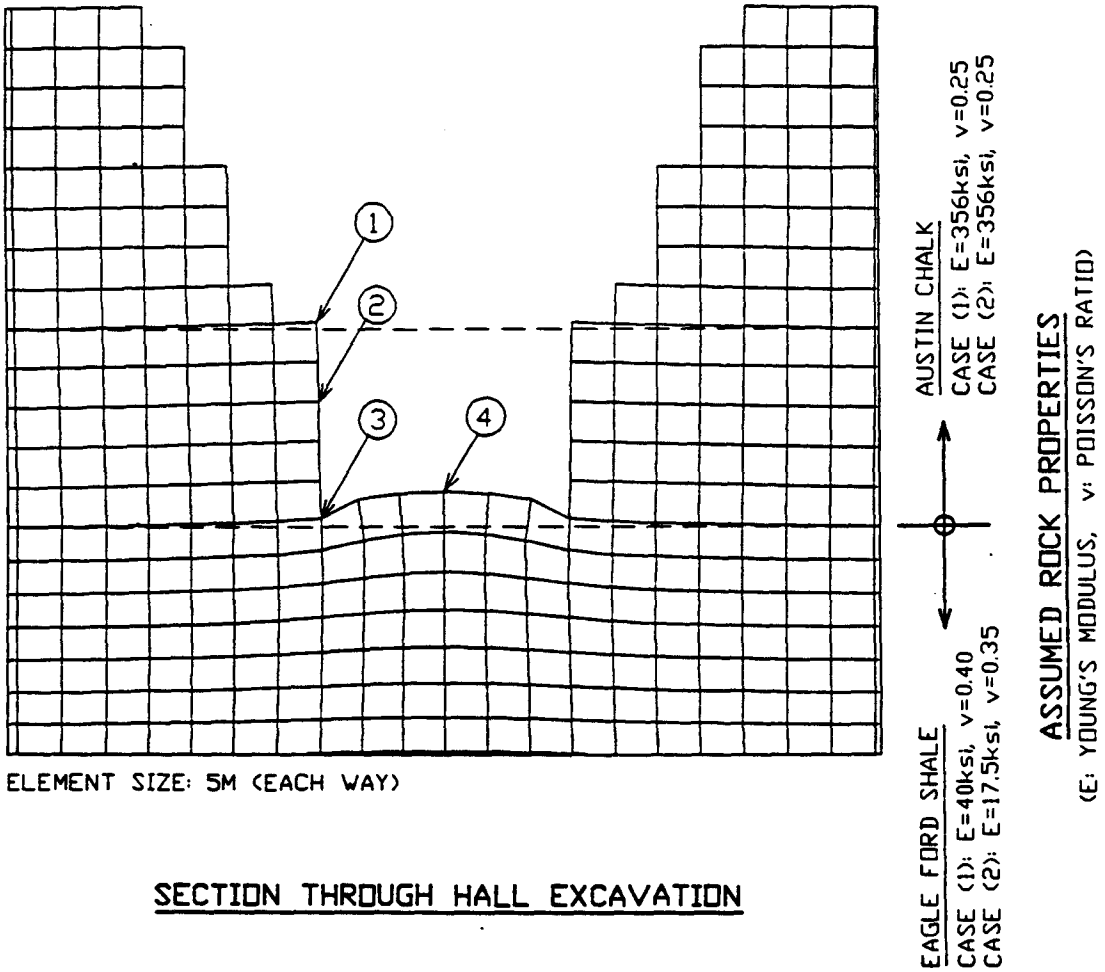

SECTION THROUGH HALL EXCAVATION

ESTIMATED ELASTIC ROCK MOVEMENTS (millimeters)

ROCK PROPERTY CASE	MOVEMENT	LOCATION				NET HEAVE (4-3)
		1	2	3	4	
1	VERTICAL	67	64	71	154	83
	HORIZONTAL	2	6	13	0	N/A
2	VERTICAL	143	141	151	350	199
	HORIZONTAL	2	8	18	0	N/A

Figure 2.2 Cut and Cover Construction—Elastic Rock Movements

3.0 BASELINE DETECTOR

3.1 Baseline Detector Description

For the baseline detector we chose a simple design, but with sufficient complexity so that realistic studies can be made. The intent is not only to study a particular detector, but to begin to develop tools and collect information that can be applied to a broad range of detectors based on solenoidal magnets. In order to concentrate our efforts on hall design, rather than detector design, we chose a baseline detector configuration which minimizes the mechanical interaction between sub-systems.

Figure 3.1 is a three-dimensional view of the detector, which is also shown in cross-section in Figure 3.2. The elevation view of the detector is shown in Figure 3.3. The solenoidal coil design is based on an "air-core" or short solenoid design.[1] This magnet does not use iron near the ends of the coil; hence, the external forces on the coil cryostat and the calorimeter are dominated by gravity. Any electromagnetic forces between the calorimeter and coil have been ignored. The tracking system selected is divided into a silicon inner tracker and an outer tracker. The outer tracker is further divided into central and intermediate tracking chambers.

The calorimeter is loosely based on the Warm Liquid design by EG&G;[2] however, the studies described here would apply equally to any self-supporting calorimeter built from "modules" of 20 to 50 tonnes. The calorimeter modules are assembled into five cylindrical bays: three central bays and two endcap bays. Each bay extends about 3 m along the beam line and weighs about 1200 tonnes. One essential ingredient of the calorimeter bays is the inclusion of return iron in the individual calorimeter modules to create a field-free region for electronics or photomultiplier tubes (PMT) on the outside of the calorimeter. About 65% of the flux is returned through the volume of the non-magnetic calorimeter, and the remaining 35% is returned through the steel at the outside of the calorimeter. There are small forward ($5 > |\eta| > 3$) calorimeters for missing energy measurements. These are located just in front of the interaction region quadrupoles.

The calorimeter is surrounded by magnetized iron muon toroids, 1.2 m thick in the barrel region ($|\eta| < 1.5$) and about 3.5 m thick in the endplug region between $2.5 > |\eta| > 1.5$. In the barrel region the steel is divided into two independent, 60-cm-thick iron toroids. Each of these toroids has 8 coils located near the corners, for a total of 16 coils. There are four planes of muon chambers in the barrel region, with one measuring station in the gap between the two barrel toroids. The momentum resolution of the exterior system is limited by the resolution of the chambers, and the 1-m gap between the two exterior chambers enables charge determination up to momenta of 1 TeV/c.

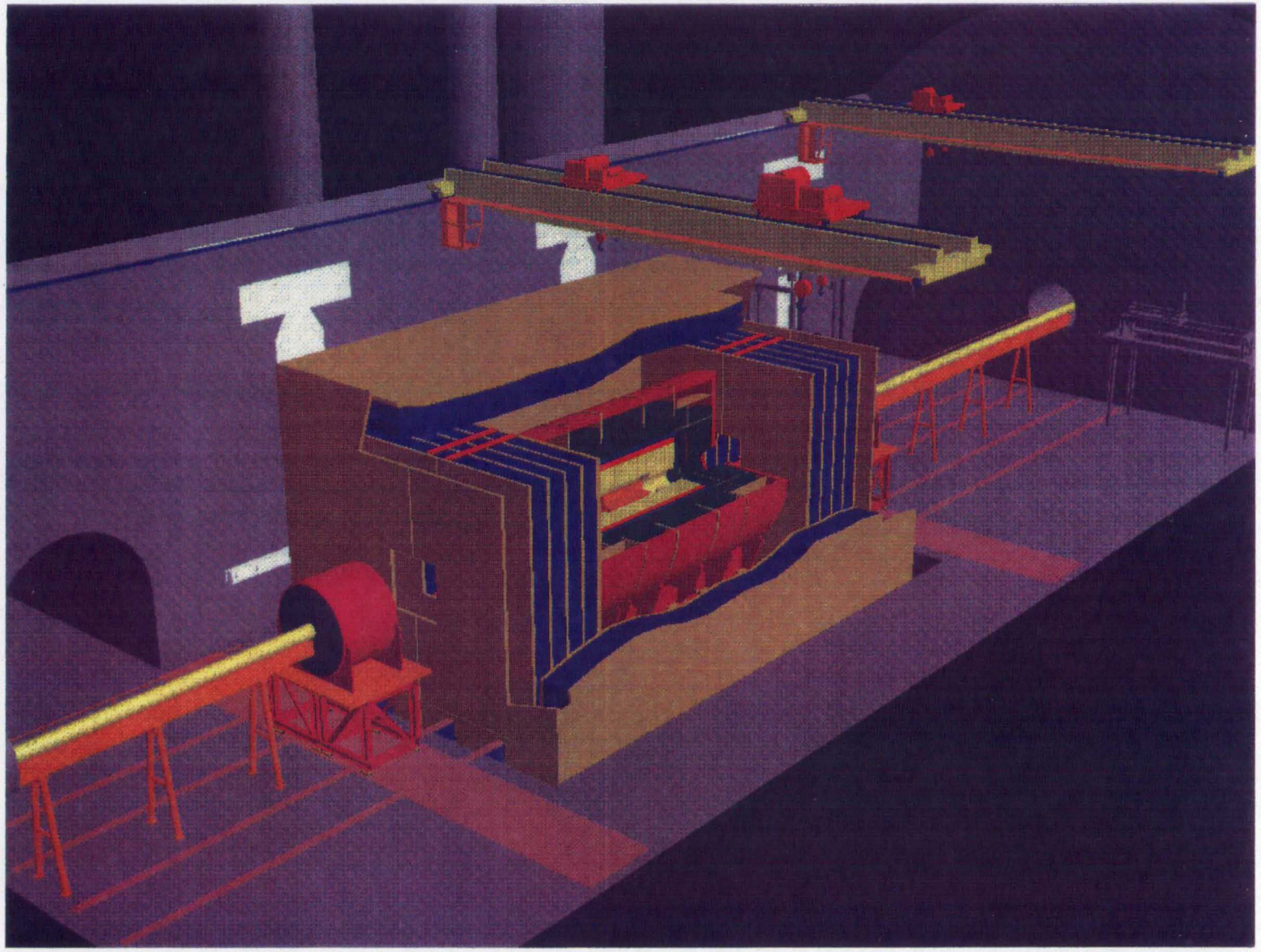

Figure 3.1.Overall Baseline Detector Layout (3D View)

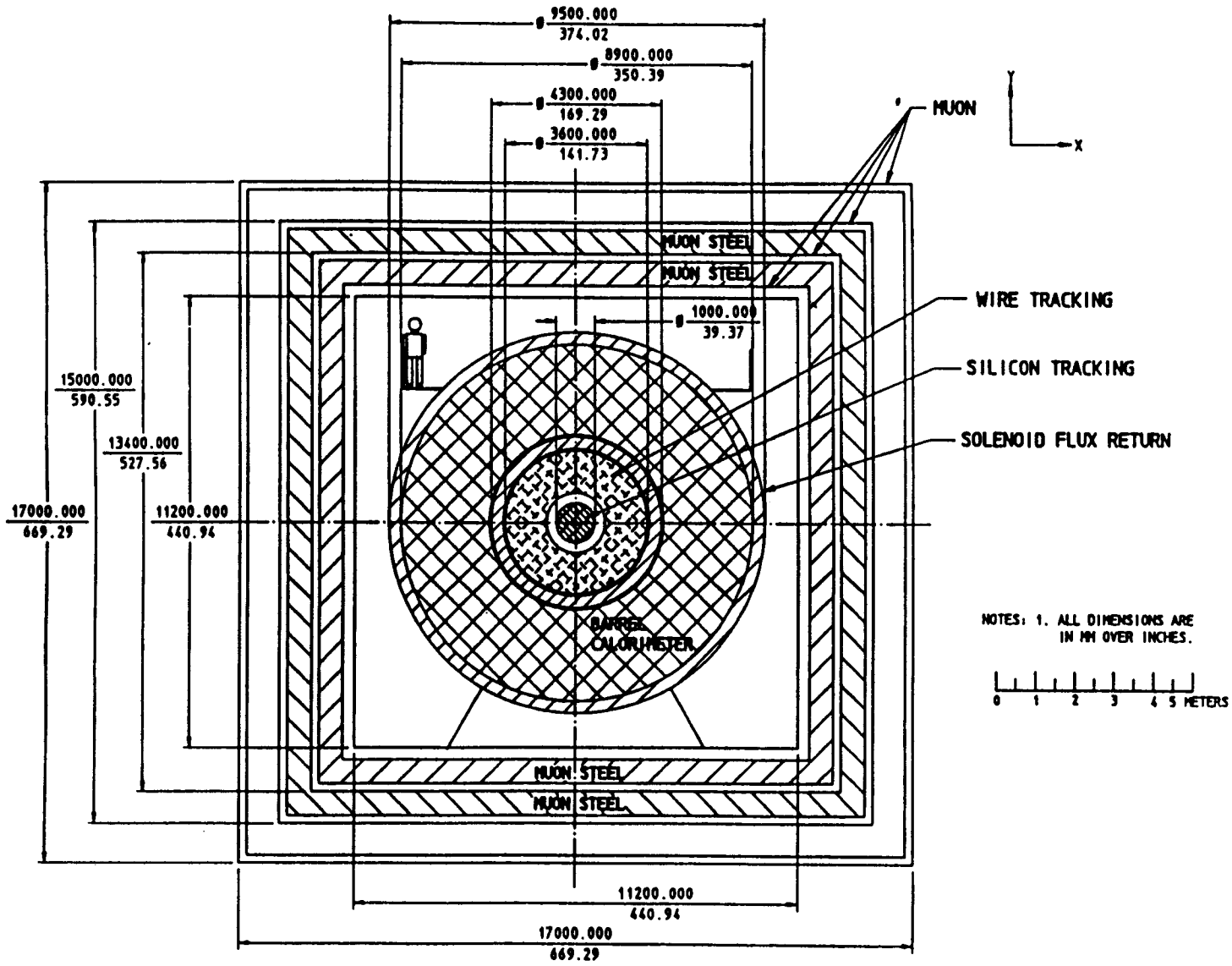

Figure 3.2. Cross-Section of Baseline Detector

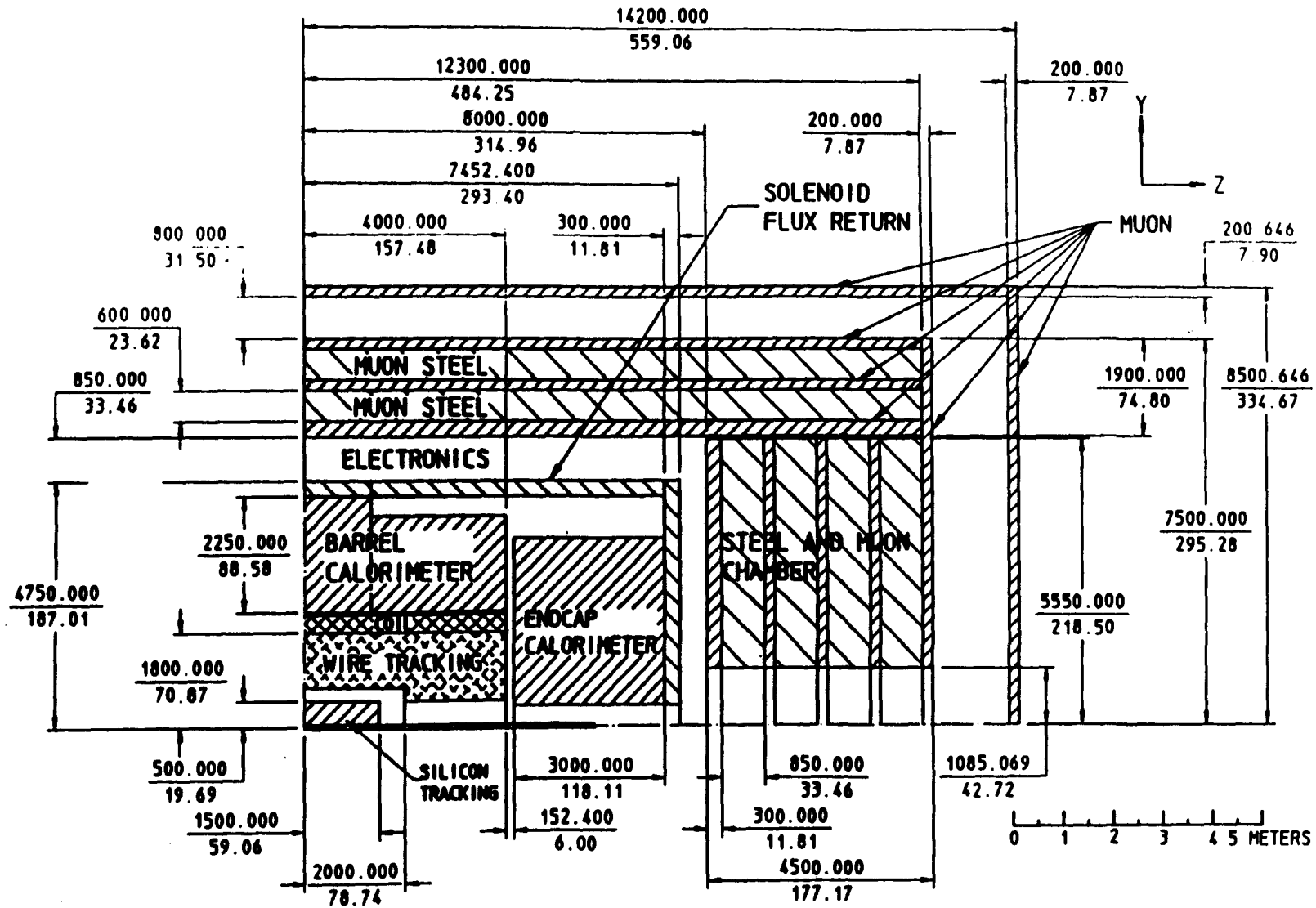

NOTES: 1. ALL DIMENSIONS ARE IN MM OVER INCHES.

Figure 3.3. Elevation View of Baseline Detector

Each end plug has four 0.85-m-thick iron toroids. These toroids have a square cross-section and are designed to split vertically along the beam line. There are four coils per toroid set installed near the location where the toroids split. In order to equalize the flux distribution we have added tapered stainless steel shims between the diagonal corners of the toroids; these equalize the reluctance paths for different radii. An end plug toroid muon detector consists of six planes of chambers, four planes inside the steel and two outside.

A major concern for the configuration of the muon steel is access to the calorimeter. We consider two alternatives for the base line detector: 1) The barrel muon steel fixed in the hall with sufficient space inside to allow personnel access between the muon steel and calorimeter for electronics repairs, and 2) Movable barrel muon toroids to allow crane access to the barrel calorimeter.

Table 3.1 summarizes some of the mechanical aspects of the baseline detector:

Table 3.1. Baseline Detector Mechanical Parameters.

Detector	Size	Units	Comments
Tracking Volume	3.7 × 8.0	m	od × length
Total Channels	200	K	incl. inter & central
Silicon Tracking	1.0 × 3.0	m	diameter × length
Coil	3.7 × 4.3 × 8.0	m	id × od × length
Barrel Calorimeter	4.4 × 9.5* × 8.0	m	id × od × length
Weight	3910	tonne	includes return steel
Total Channels	120	K	includes endcaps
Endcap Calorimeter	0.8 × 9.5* × 3.5	m	id × od × length
Weight	3000	tonne	both ends
Muon Barrel Toroids	14.6 × 14.6 × 24.6	m	w × h × length
Weight	12,920	tonne	
Muon EC Toroids	11.1× 11.1 ×4.1	m	w × h × length
Weight	7848	tonne	both ends
Muon Chambers	17.0 × 17.0 × 28.4	m	w × h × length
Total Channels	118	K	includes endcaps

*includes return steel

Each subsystem in the detector will require a variety of connections for proper operation and to meet safety requirements. The connections to each subsystems consist of:

- Mechanical supports
- Trigger and data acquisition cables
- Power, including low and high voltage connections
- Cooling fluids or gases

- Sub-system speciality fluids or gases
- Alignment monitoring and adjustment
- Environmental monitoring (temperature, oxygen concentration, explosive gas concentrations, smoke detectors, etc.).

The details of these connections will depend greatly on technology chosen for each subsystem, and planning will have to consider the interactions between subsystems as well as the needs of an individual detector element. However, the general strategy for the "hookup" of the detector to external systems is as follows.

For all detector subsystems, the front-end electronics, level 1 trigger electronics, and temporary data storage for about 100 crossings (including data buffering between the level 1 and level 2 trigger decisions) are mounted directly on the mechanical structure of the subsystem. These electronics are connected via flexible cable trays to global trigger and data acquisition electronics located in a multi-story gallery next to the detector inside the collision hall. The flexible cable trays allows access to the internal portions of the detector without disconnecting cables or utilities.

The layout of the hall currently allocates the second and third floors for trigger and data acquisition areas. Each floor of the gallery is approximately 4 m wide by 30 m long. These two floors are fully air-conditioned enclosures and are provided with computer (false) floors for routing of cables between electronics racks. Data acquisition and trigger signals are communicated to the surface via the 3-m-diameter cable shaft, located 8 m inside the wall next to the gallery. The upper floors of the gallery are reserved for mechanical systems, gas and fluid handling, and cryogenics systems for the detector; they do not have separate air-conditioning or computer floors. Utilities for these areas, as well as any heavy-duty power lines, are connected to the surface via a separate utility shaft to avoid pickup of switching noise from the heavy-duty power cables on the data acquisition cables .

3.2 Baseline Hall Design

3.2.1 Overview and General Hall Plan

The baseline collision hall is 28.0 m wide and 81.0 m long, constructed with its long axis parallel to the collider beam line, as shown in Figure 3.4. To best utilize the floor areas reserved for muon steel and calorimeter assembly, the center of the detector is offset by 2.0 m and 6.5 m from the long and short axes of the hall, respectively. Dimensions of the hall are based on access around the completed detector, space requirements for assembly and checkout of the calorimeters and end muon toroids, and clearance requirements for retracting the detector components for maintenance access. In-place upgrading of the detector has also been considered. A temporary air-

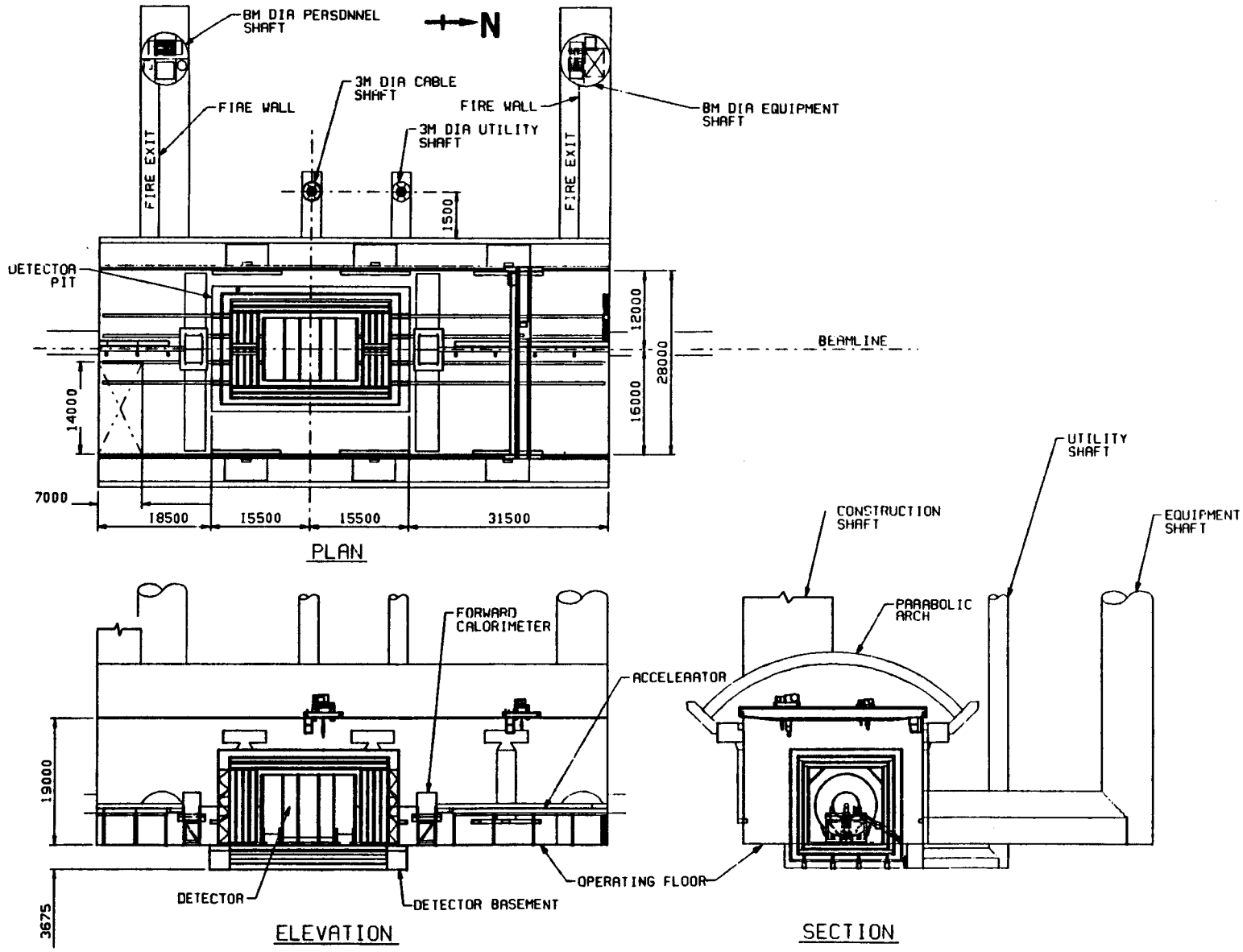

Figure 3.4. Baseline Detector—Hall General Arrangement

tight partition between the muon steel assembly and the calorimeter assembly areas of the hall is erected to provide a clean area for calorimeter assembly.

The top of the main operating floor is set level with the top of the roller tracks in the barrel muon steel, and the basement under the detector is about 3.57 m below that. Also provided are a 3-m-wide passage for moving small equipment on the operating floor and a 7-m-wide passage for transporting large items by the hall crane from one end of the hall to the other.

The basement is extended to the side wall of the hall under the 3-m-wide passage to provide room for pumps, compressors, utility distribution, and other equipment, and for structural requirements.

The walls of the hall are tied to the rock behind by rock anchors. The walls extend about 19.0 m above the operating floor. The crane runways rest directly on the top of the side walls, which are provided with vertical recesses for the flush-mounted air-conditioning ductwork.

The roof of the collision hall is a parabolic concrete arch supported on independent foundations just behind the top of the side walls. This low-rise arch imposes an outward force on the rock mass behind the side walls of the hall, thereby reducing the heave forces on the side walls. The arch foundations are not tied to the walls, so that any change in the overburden or surface loading above the arch will not affect the walls or the floors of the hall. Placing the roof of the hall on top of the walls would impose a high vertical load on the walls, and in turn on the edge of the hall floor slabs, which may be just above the weak Eagle Ford Shale if the hall is located at the west cluster. The resulting immediate and long-term floor movements would be significant and could be influenced by changes in the overburden pressure on the roof.

The space between the top of the wall and the base of the arch can be used for distribution of some of the hall utilities, and for servicing of the cranes, the fans of the air-conditioning system, and the roof drainage sumps.

The proposed hall configuration may be constructed by conventional open excavation, or by excavating to the top of the walls and constructing the roof arch while the excavation proceeds to the hall floor. The latter arrangement will permit an earlier start of the backfill operation, thereby reducing construction time of the hall.

3.2.2 Detector Basement and Support

The adopted maximum floor movement is 2.5 mm for short duration (one week) loading and 25 mm for long duration (one year or more) loading after all components of the detector are in place. These floor movement specifications require a very rigid concrete basemat under the detector. The floor movement during erection of the muon steel and after the central calorimeters are installed is also restricted to 25 mm; however, this could be compensated for by pre-setting the main steel barrel supports before erection of the muon steel begins. Weight calculations indicate

that the detector loading on the basement floor is about 110% of the present vertical rock pressure at this elevation. This means that movement of the floor due to the weight of the detector will be very small; therefore, floor movement will be largely controlled by the heaving pressure of the underlying rock. In the operating floor areas, the floor loading is very low—less than 10% of the present rock pressure—and, therefore, the upward floor movement due to the unopposed heave could be significant.

To reduce floor movements, the detector basement is made very rigid. The stiffness of the basemat depends on the thickness and uncracked moment of inertia and modules of elasticity of the concrete, as well as on the length and aspect ratio of the floor spans. The vertical restraint of the perimeter walls also effects the deflection of the slab.

To construct a basement slab to be as rigid as possible, the edge of the detector floor is restrained by the stiff walls of the hall on two sides and by the heavily reinforced retaining walls at the ends of the detector. Using a higher strength (and Young's modulus) concrete also reduces deflections. Our preliminary finite element calculations indicate that floor deflections caused by the stationary and moving components of the detector will not exceed the adopted maximum floor movements. Floor movement caused by heaving of the underlying rock mass may be large, however, and could require special design considerations as outlined below.

Detailed design of the floor will be based on the actual detector loadings and deflection limitations, and on the results of a geotechnical investigation of the physical properties of the underlying rock at the selected hall location. However, if the hall is located at the west cluster, the detector support floor will rest on or directly above the Eagle Ford Shale, and will, therefore, be subjected to the long term heave forces of the shale. Assuming that the excavation is stable, the immediate (elastic) heave of the rock is not a problem until the concrete floor has hardened. After that, swelling due to the migration of the moisture in the rock and to creep and redistribution of stresses caused by the uneven overburden pressure may cause a slow upward floor movement. The magnitude and duration of this movement would be difficult to estimate. However, there are several ways to overcome the heave problem. A simple solution is to provide the means to adjust the height of the base plates of the four barrel support beams. This may be accomplished by supporting the base plate on a sole plate and shims, as shown on Figure 3.5. To adjust the elevation of the detector, low-height hydraulic jacks placed under the base plate are used to unload the shim plates; after the shim thickness is adjusted, the jacks lower the detector to the required elevation. After the nuts are locked to the base plates, the jacks are removed.

A more direct solution to the heave problem is to post-tension the floor slab to the underlying rock. This is done by drilling into the rock through several rows of blockouts near the midspan of the floor and installing rock bolts to a depth of approximately 1.5 times the width of the hall. The lower 1/3 of the bolt length is grouted into the rock, while the upper 2/3 is sleeved to permit

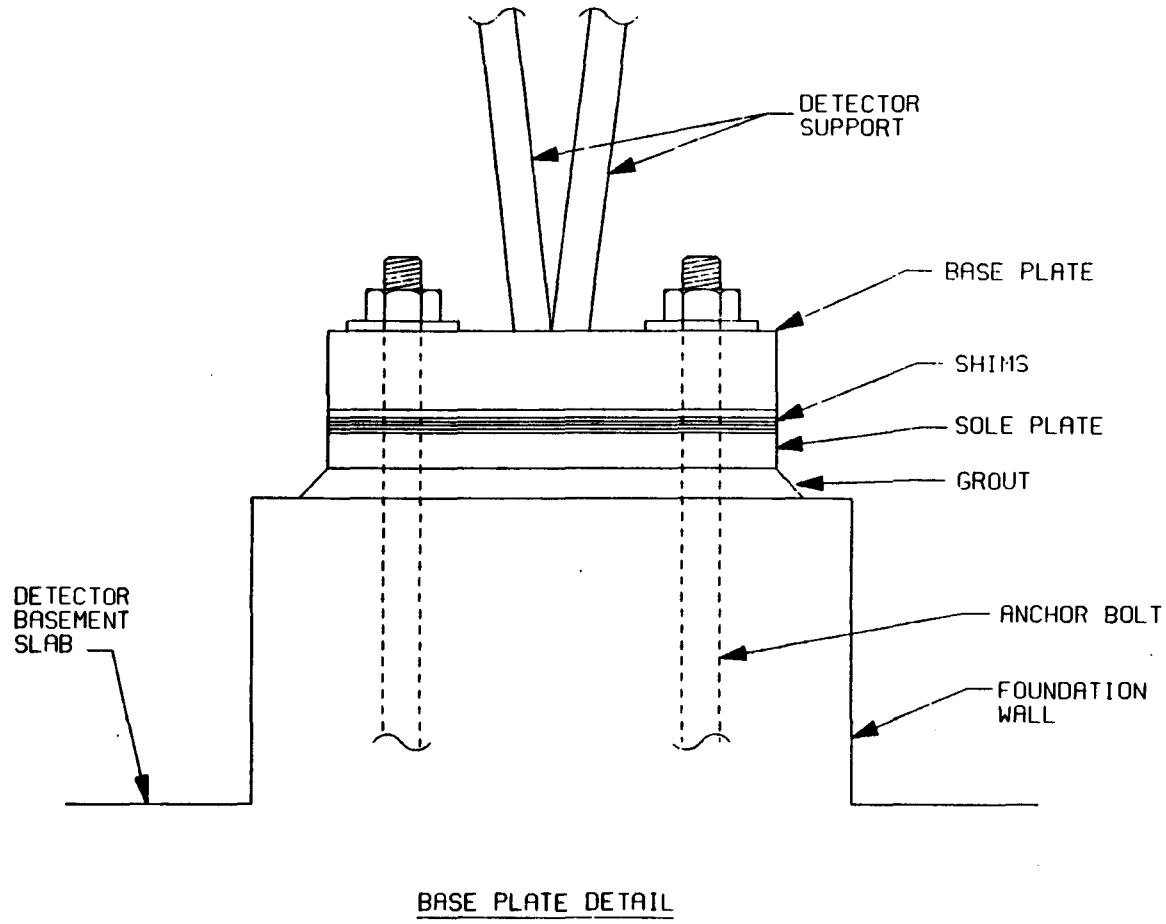

Figure 3.5. Baseline Detector—Support Base Plate

slippage. The bolts are initially tensioned for the weight of the detector and, if required, are further tensioned to reduce heave. The floor movements are continuously monitored by lasers, and if required, the bolts may be retensioned or slackened to adjust the floor elevation.

3.2.3 Operating Floor Construction

To facilitate disassembly of the detector components and access to the detector, the top of the operating floor is set level with the top of the roller tracks in the barrel. Unlike the detector basement floor, the operating floor will be loaded to less than 10% of the present vertical rock pressure at this elevation. This means that to reduce floor movement to acceptable levels, the heave pressure from the underlying rock will have to be restrained by the floor slab. Excessive floor heaving could slow down disassembly operations of the detector because rolling the heavy components on a sloping floor will require special procedures to insure safety. The supports of the forward calorimeter and of the acceleration magnets will have to be made adjustable to maintain proper alignment.

Floor heave could be reduced by post-tensioning the floor slab to the underlying rock, as described in Section 3.2.2, or by separating the floor slab from the rock by a layer of compressible materials. This problem should be studied further as soon as the results of the geotechnical investigation become available.

To facilitate movement of the detector components during construction and major disassembly, the entire floor area north and south of the detector basement is covered by a 12-mm-thick steel plate. The plate is leveled before it is anchored to the floor slab by high-strength grout. This arrangement provides the proper rolling surface and distributes the high rolling pressures of the rollers under the end toroids and calorimeters. Some components of the detector are moved to predetermined areas via guided paths to provide access to the central tracking device and calorimeters for testing and maintenance. To facilitate this work, the floor plate in these areas is thickened to about 36 mm and is machined flat to reduce rolling resistance. Tapped holes for anchoring the push/pull jacks are provided in these areas.

3.2.4 Access and Utility Shafts

Access to the hall is provided by a rectangular construction shaft penetrating the hall roof in the southeast corner of the hall and by two circular shafts, both with stairs and one equipped with an elevator. Separate shafts for utilities, cabling, and for the air-conditioning ducts are also provided. The location of these shafts is shown on Figure 3.4, and some of their features are described in Table 3.2.

Table 3.2. Hall Shafts.

Name or Use	Size	Cross-section	Access
Construction Shaft	7 m × 14 m	rectangular	crane only
Equipment Shaft	8 m	round	stairwell / crane
Personnel Shaft	8 m	round	stairwell elevator
Cable Shaft	3 m	round	stairwell
Utility Shaft	3 m	round	stairwell / dumbwaiter

The construction shaft provides a 14-m by 7-m access into the hall for lowering all steel used in constructing the muon barrel and the end toroids, the support beams and erection rigs of the barrel, and the saddles, washers and return flux steel of the calorimeters. The solenoidal coil, central tracking device, and the muon chamber panels are also brought down through the construction shaft. To maximize the usable floor area for detector assembly and for possible major repair or modification work on the detector in the future, the construction shaft is located in the corner of the detector hall. Placing the shaft on the center line of the hall would require a longer hall for detector assembly and would locate the shaft over the beam line. Location of the construction shaft over the beam line would inhibit the use of the shaft after beam line components are in place. Once the detector assembly has been completed, this shaft is closed at the top by overlapping precast concrete slabs to block radiation. These slabs may be removed later to regain access to the hall for lowering large objects.

The equipment shaft is 8 m in diameter and is located a sufficient distance from the northwest corner of the detector hall so that the shaft surfaces outside of the area excavated during hall construction. This allows the shaft to be built earlier to provide access to the hall before the hall roof is constructed and backfilled. The bottom of the shaft is connected to the operating floor by an 8-m-wide concrete-lined tunnel. The equipment shaft and tunnel are partitioned by a fire wall to enclose the fire escape stairs and egress route from the hall (Figure 3.6). The stairwell and egress route in the tunnel are slightly pressurized to prevent smoke from entering this region in the event of a fire. The equipment shaft also incorporates a 3-m by 4-m hoisting well for lowering calorimeter modules, electronics, and other equipment. Space for a 900 kg capacity construction elevator and for the ductwork of the hall ventilation system is also provided.

The personnel shaft is located a distance from the southwest wall of the detector hall. For the reasons given above, this shaft is also situated outside of the region excavated during hall construction. As shown in Figure 3.6, this 8-m-diameter shaft and the connecting tunnel house the second fire escape stairwell and egress route. The personnel shaft contains the passenger/light freight elevator connecting the operations center on the surface to the main hall floor, the ductwork

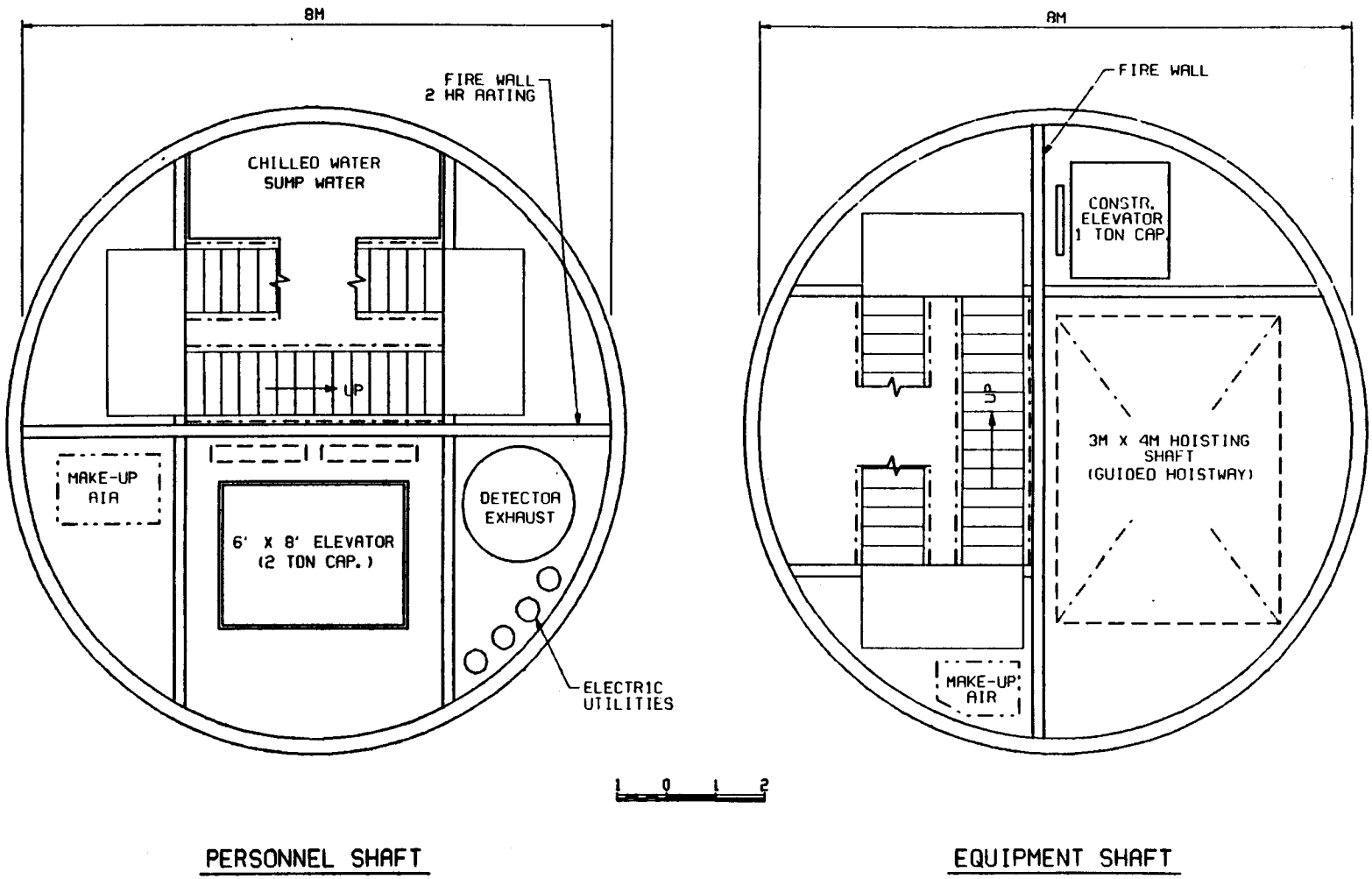

Figure 3.6. Baseline Detector—Personnel and Equipment Shaft Plans

for the hall ventilation system, and the piping and power supply for the conventional hall services (e.g., lighting, power outlets, cranes, and sumps).

The cable shaft is 3 m in diameter and is located approximately 15 m from the west wall of the hall in line with the center of the detector. This shaft will carry all signal cables from the hall to the data acquisition and control rooms of the operations center on the surface. As shown in Figure 3.7, the shaft is equipped with vertical cable trays—60 cm by 15 cm (24 in. by 6 in.) and 90 cm by 15 cm (36 in. by 6 in.)—and a 1.5-m-diameter spiral staircase to provide access to the cables. The cable trays are arranged to be within arm's reach of the staircase. The bottom of the cable shaft is at the operating floor level of the hall; however, additional cable passages from the shaft to the floors supporting the electronics cabinets are also provided.

The utility shaft, also 3 m in diameter, is located at least 9 m away from the west wall of the hall in order to bypass the hall roof foundation. The location of this shaft is coordinated with the layout of the surface facilities. The bottom of the shaft is at the floor level of the detector support. As shown in Figure 3.7, the utility shaft will have several compartments for the 400 Hz, 60 Hz, and DC power lines, the tracking chamber gases and helium and nitrogen gases, and the cryogenics and safety systems. Also provided are a 1.5-m-diameter spiral staircase with frequent landings and a 250-kg-capacity dumbwaiter to carry maintenance tools and equipment for servicing these utilities.

3.3 Detector Assembly

3.3.1 Muon Steel Barrel Assembly

The configuration of the muon steel barrel is shown in Figure 3.8, and some properties of the muon toroids are listed in Table 3.3.

Table 3.3. Mechanical Specifications for Baseline Detector Muon Toroids

Thickness of steel at $\theta = 90^{\circ}$	1.2 m
Thickness of steel parallel to beam in endcaps	3.4 m
Magnetic field	1.8 T
Maximum allowed gap in steel	3 mm
Minimum fraction of steel along any radial path	98 %

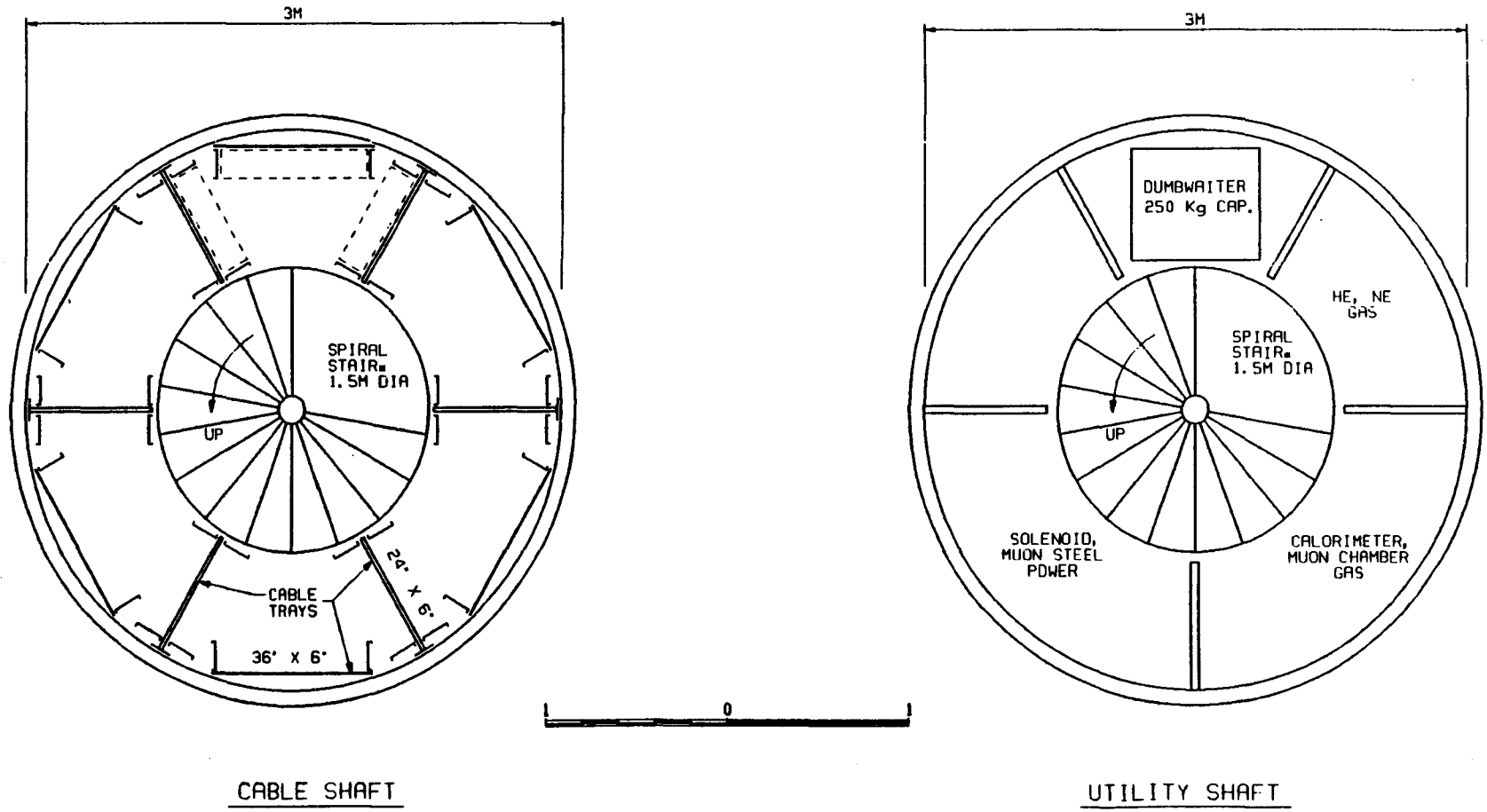

Figure 3.7. Baseline Detector—Cable and Utility Shaft Plans

The barrel consists of two concentric, open-end boxes separated by a 200 mm gap. Each barrel is constructed from 600-mm-wide steel plates, 200-mm (8 in.)-thick (along Z) except in a limited area around the interaction point. Here the thickness is increased to about 350 mm (14 in.) to meet the required minimum of 98% solid material along a ray. The plates are arranged to lie in planes perpendicular to the beamline and parallel to the toroidal flux lines. The steel plates are pulled together by 38-mm (1.5 in)-diameter high-strength bolts to reduce the gaps between the plates to 3 mm maximum, to provide structural stiffness for stability, and to resist magnetic and other forces. The plates are drilled with oversized holes to facilitate installation of the longitudinal bolts. The spacing of the bolts is 1250 mm maximum. This combination of plate thickness and bolt size and spacing permits the use of plates furnished by the rolling mills to standard (ASTM A6) industry tolerances. Using thicker plates would require larger diameter and/or more bolts in order to pull the plates together to the above criteria. Thicker plates cost more per tonne, and the machining and general handling costs are also higher. Thicker plates would reduce the number of plates to be installed, but this is not considered a real advantage since the plates can be handled in groups of four or more during shipping and installation.

To reduce bolt length and facilitate installation, the plates are pulled together in groups of eight. The outside plates (in a group of eight) have recessed holes on both sides to receive the bolts from the adjacent group of plates. The length of the plates depends on their position. For the inner barrel, the floor and roof plates are 13,000 mm long and the sidewalls are 11,800 mm long. For the outer barrel, the floor and roof plates are 14,600 mm long and the sidewalls are 13,400 mm long. The number of each plate type required for the barrel is shown in Table 3.4.

Table 3.4. Muon Barrel Toroid Plate Specifications.

Plate Location	Length ¥ Thickness (mm)	Number Required	Weight of Each Plate (tonnes)
Inner Roof and Floor	13000 × 200	236	12.25
Inner Roof and Floor	13000 × 350	6	21.43
Inner Walls	11800 × 200	236	11.11
Inner Walls	11800 × 350	6	19.45
Outer Roof and Floor	14600 × 200	236	13.75
Outer Roof and Floor	14600 × 350	6	24.07
Outer Walls	13400 × 200	236	12.62
Outer Walls	13400 × 350	6	22.08

Note: All plates are 600 mm wide.

Each end of the wall plates and one edge of the roof and floor plates are machined for bearing surfaces. The machined areas of the roof and floor plates are recessed and intended to provide clearance for the coil packs. Guide pins at the bottom and top of the walls are provided to position the sidewalls between the roof and floor plates.

To provide maximum muon chamber coverage the barrel steel is supported on four "knife-edge" plates resting on individual concrete supports (Figure 3.8). The four concrete supports run the entire length of the detector basement, but the knife-edges run only the length of the barrel. The knife-edges are braced together at about 3 m longitudinal (z) spacing to resist lateral forces. The bracings are between the two outer layers of muon chambers to avoid interference. The base of these supports, as shown in Figure 3.5, are designed to facilitate vertical adjustment of the barrel elevation to compensate for the floor movements described in Section 3.2.2.

Prior to the muon steel barrel assembly, the two inner knife-edge supports of the barrel are installed. The two outer supports are not placed until after the barrel floor coil packs have been installed and tested.

The steel barrel assembly proceeds as follows. The pre-drilled and painted steel plates are assembled into jigs on the surface and are lowered into the hall through the construction shaft by the yard crane in groups of four (Figure 3.9). From the construction shaft laydown area in the hall the plates are moved to the muon steel staging area by winched carts. After final checkout the plates are lifted into place in groups of four by the hall crane. Two erection crews proceed with the construction, each beginning in the middle of the detector and working out toward opposite ends. After eight plates are in place, the longitudinal high-strength bolts are installed and tightened to pull the plates together. The last plate in any group of eight is tied to the next group by overlapping the bolts. Using this procedure, the lower floor of the barrel is assembled first (Figure 3.10). Once the lower floor is complete, the 200-mm-wide vertical spacer plates are installed, and work proceeds with the installation of the upper floor in an identical fashion.

After the construction of the upper and lower floors is complete, the four preassembled coil packs are lowered into the hall. The coil packs are aligned with the end of the barrel floor, and the shipping spool of the coils are bolted temporarily to the floor. After final checkout the coil packs are moved onto the end of the floor steel and are secured. Following the installation of the four floor coil packs, the two remaining knife-edge floor supports are installed.

The erection of the barrel walls proceeds in a similar fashion, as shown in Figure 3.10. Using temporary bracings to stabilize the plates from a wall of the hall, the outer walls are constructed first. The inner walls, supported during construction by temporary struts and spacers from the barrel floor, are erected next.

Installation of the lower coil packs of the walls is a two-step process. First the coils are lowered to the top of the temporary wall bracings, then new bracings are installed above the coils and the lower bracings are removed to permit lowering of the coils to the bottom of the walls. Installation of the upper wall coils is similar to the installation of the floor coils described previously.

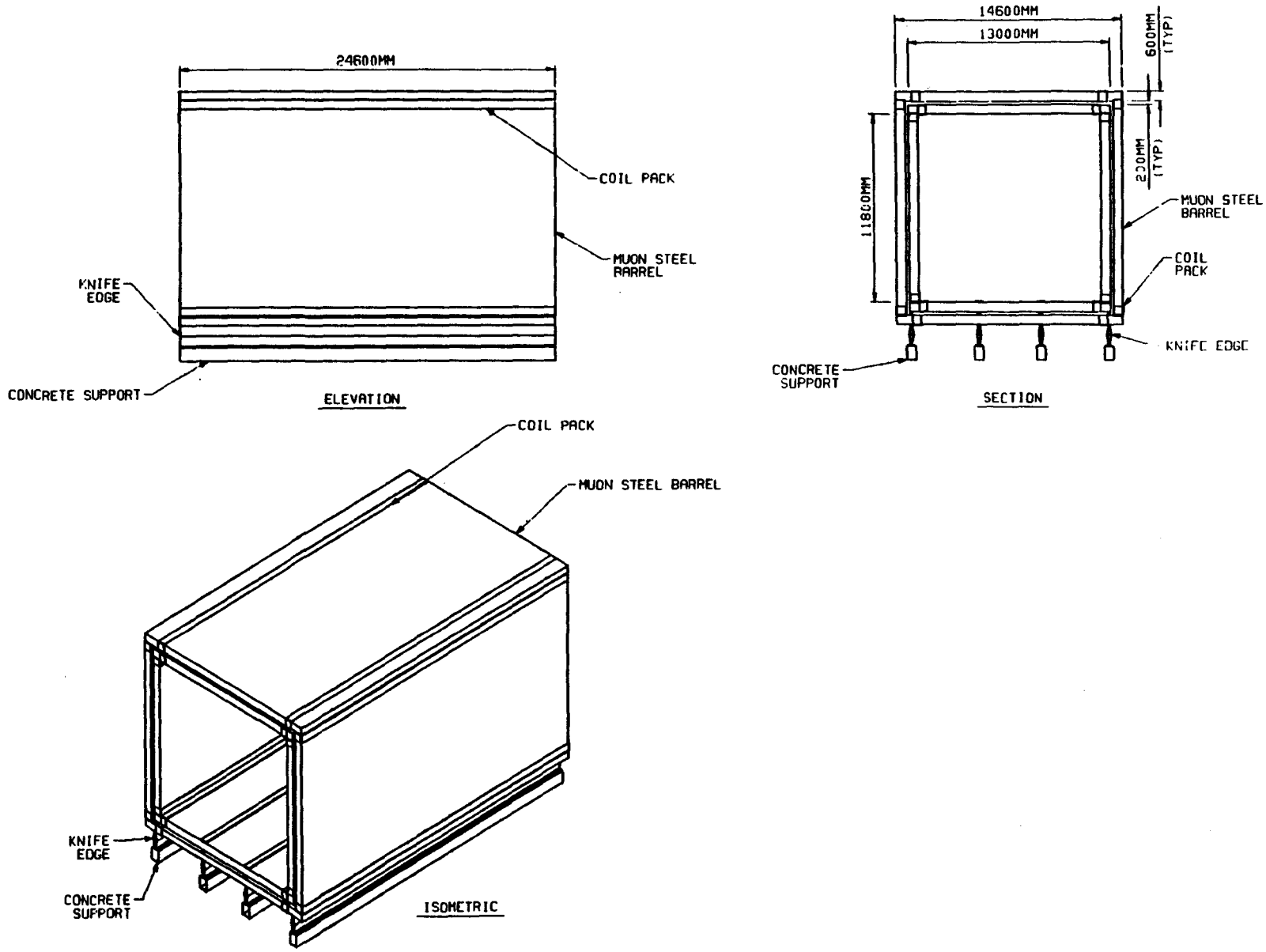

Figure 3.8. Baseline Detector—Muon Steel Barrel

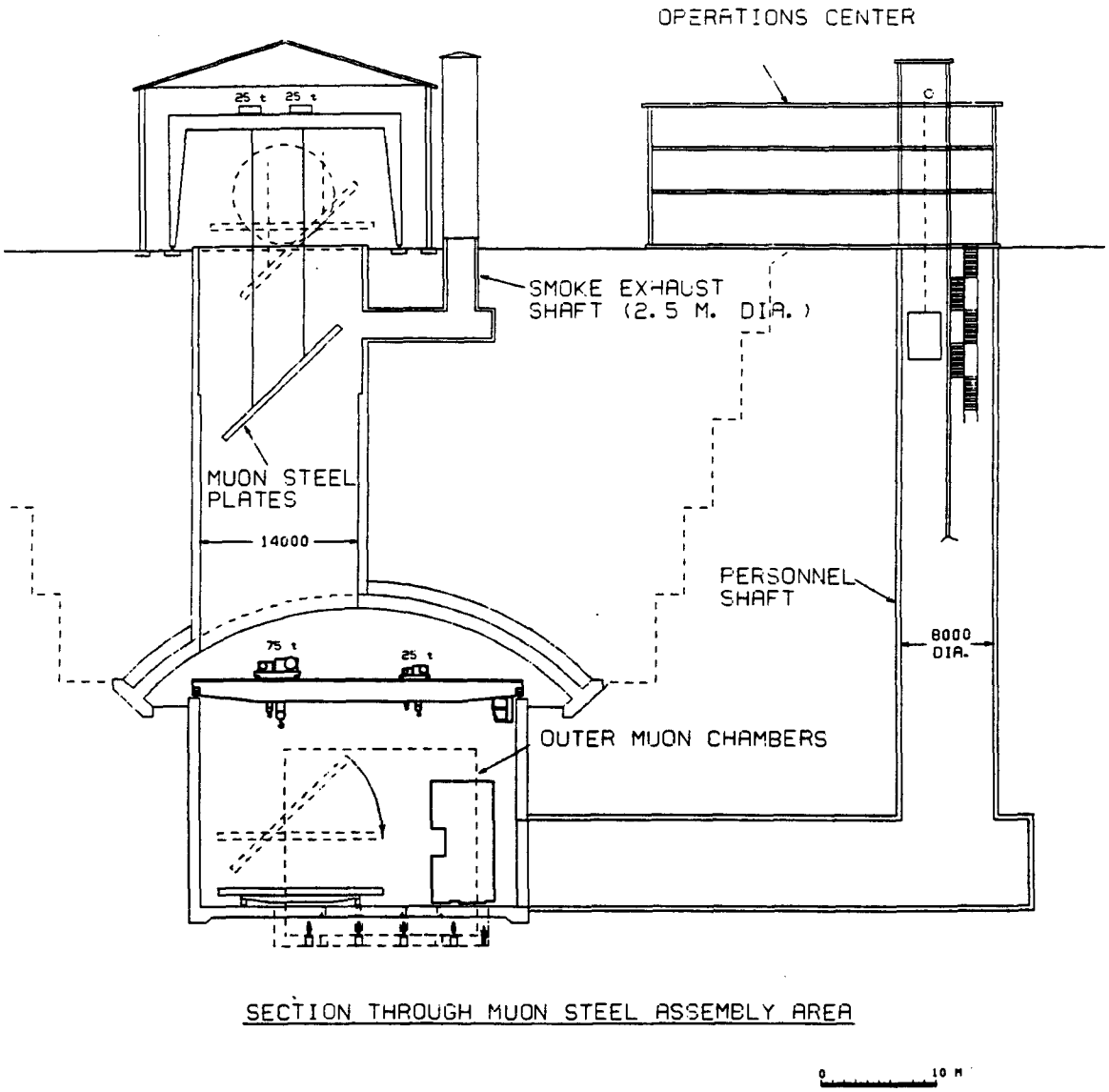

Figure 3.9 Baseline Detector—Hall Section

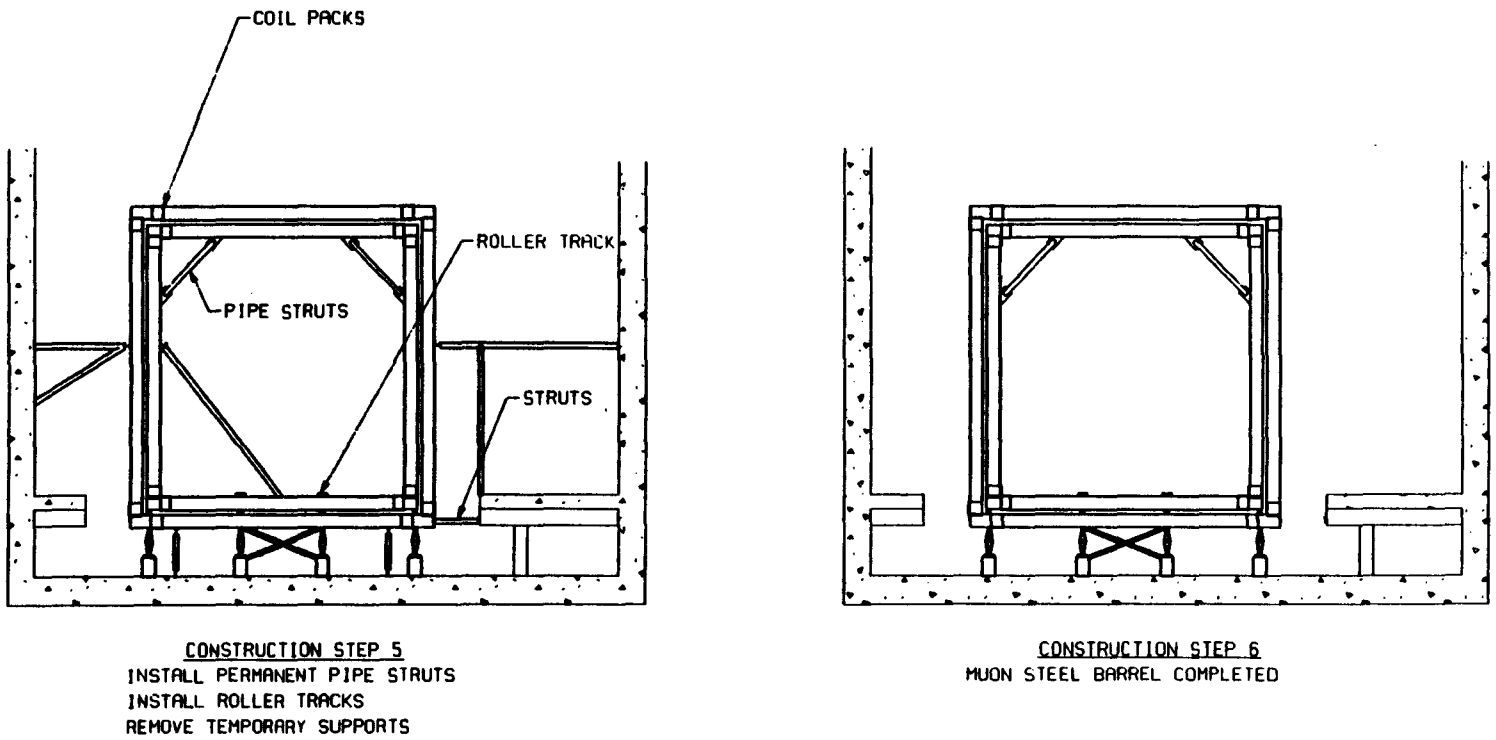

Figure 3.10. Baseline Detector—Muon Steel Barrel Construction (Steps 1-4)

To permit the installation of the four prefabricated coil packs on the roof of the barrel, the inner and outer roof steel is installed on a temporary structure as shown in Figure 3.10, construction step 4. The assembly of the two roof layers and the installation of their coil packs is the same as for the floors. After checkout of the coils and installation of the locating pins on top of the walls, the roof is lowered by jacks onto the temporary structure to complete the barrel. The lateral alignment of the roof is checked and adjusted by the temporary wall struts as required. The lateral stability of the barrel is provided by welding eight stainless steel pipe bracings between the wall and the roof (Figure 3.11). The removal of the temporary wall bracing completes the barrel assembly.

The estimated manpower requirement for muon steel barrel assembly for this detector using a single crew is as follows:

- Unloading, topside subassembly, and lowering plates to hall floor—6 men.
- Receiving plates in hall—4 men.
- Plate assembly and bolting—6 men.

Using two crews to assemble the plates would require eight more men in the hall.

In addition to the fixed-barrel muon steel described above, we have investigated the feasibility of movable-barrel muon toroids. The walls and the roof of the barrel are split at the center of the detector, and each half-section is mounted on rollers, as shown in Figure 3.12. To gain access to the central calorimeters for normal servicing, the end steel toroids and endcap calorimeters as well as the barrel muon steel sections move approximately 2 m. To provide room for major repair work or modification of the detector, the moveable barrel sections move further out onto the operating floor. This requires a deep trench in the concrete floor, which severely limits the movement of the heavy components of the detector. Also the rigidity of the floor, so important to limit floor movement due to heave, is impaired.

Structural analysis of the movable section of the barrel steel indicates that extensive field welding between the walls and roof of the barrel steel is required to resist the lateral stability forces and to maintain rigidity and alignment during the moving operation. Heavy steel framing and rollers for guiding the bottom of the walls must be installed. These framings and other provisions for moving the barrel steel reduce muon chamber coverage and require an extra operation during disassembly since the end toroids and calorimeters have to moved in any case.

For the above reasons, and due to the added cost and maintenance of the rolling equipment, the movable-barrel muon toroid alternate has not been pursued further.

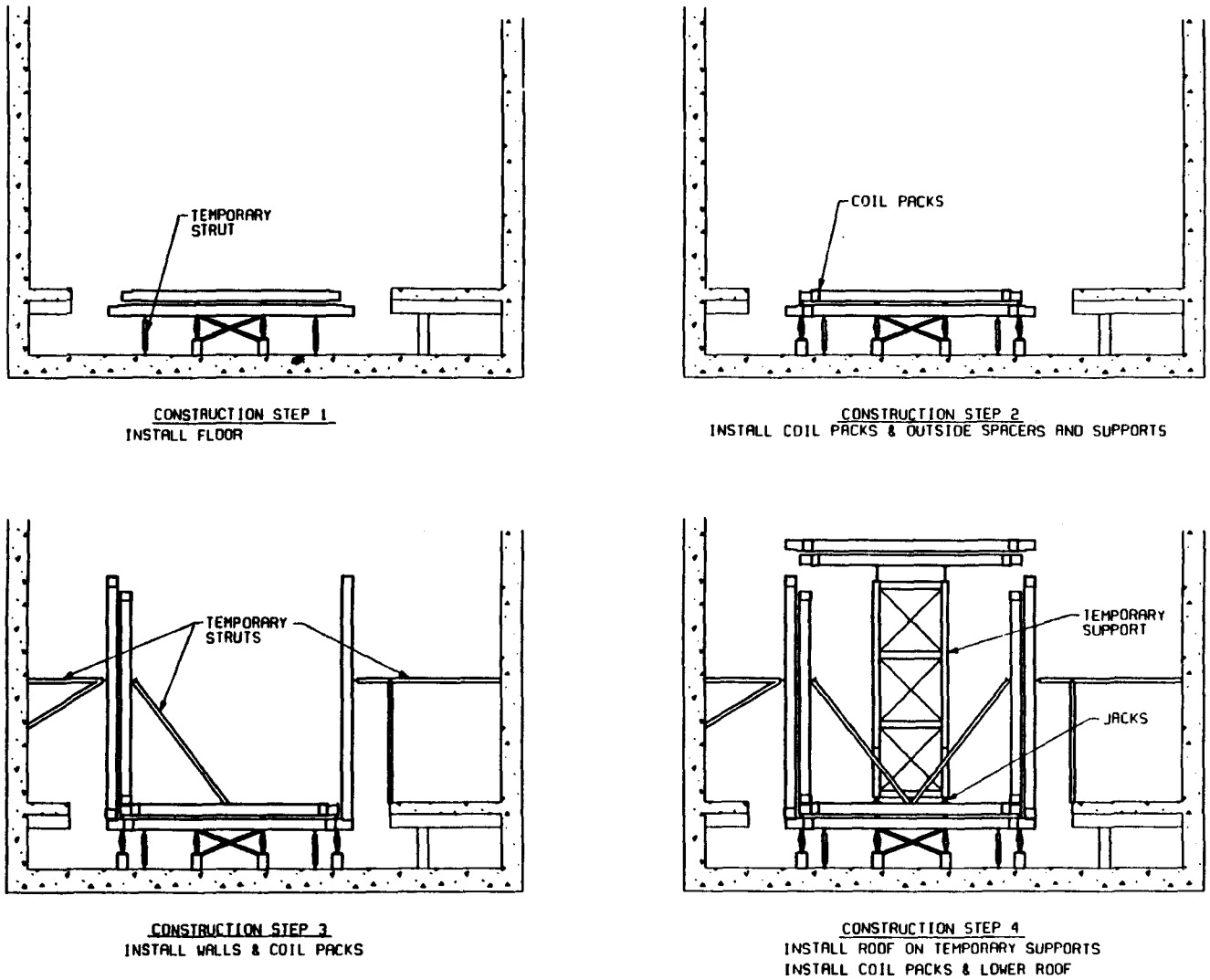

Figure 3.11. Baseline Detector—Muon Steel Barrel Construction (Steps 5-6)

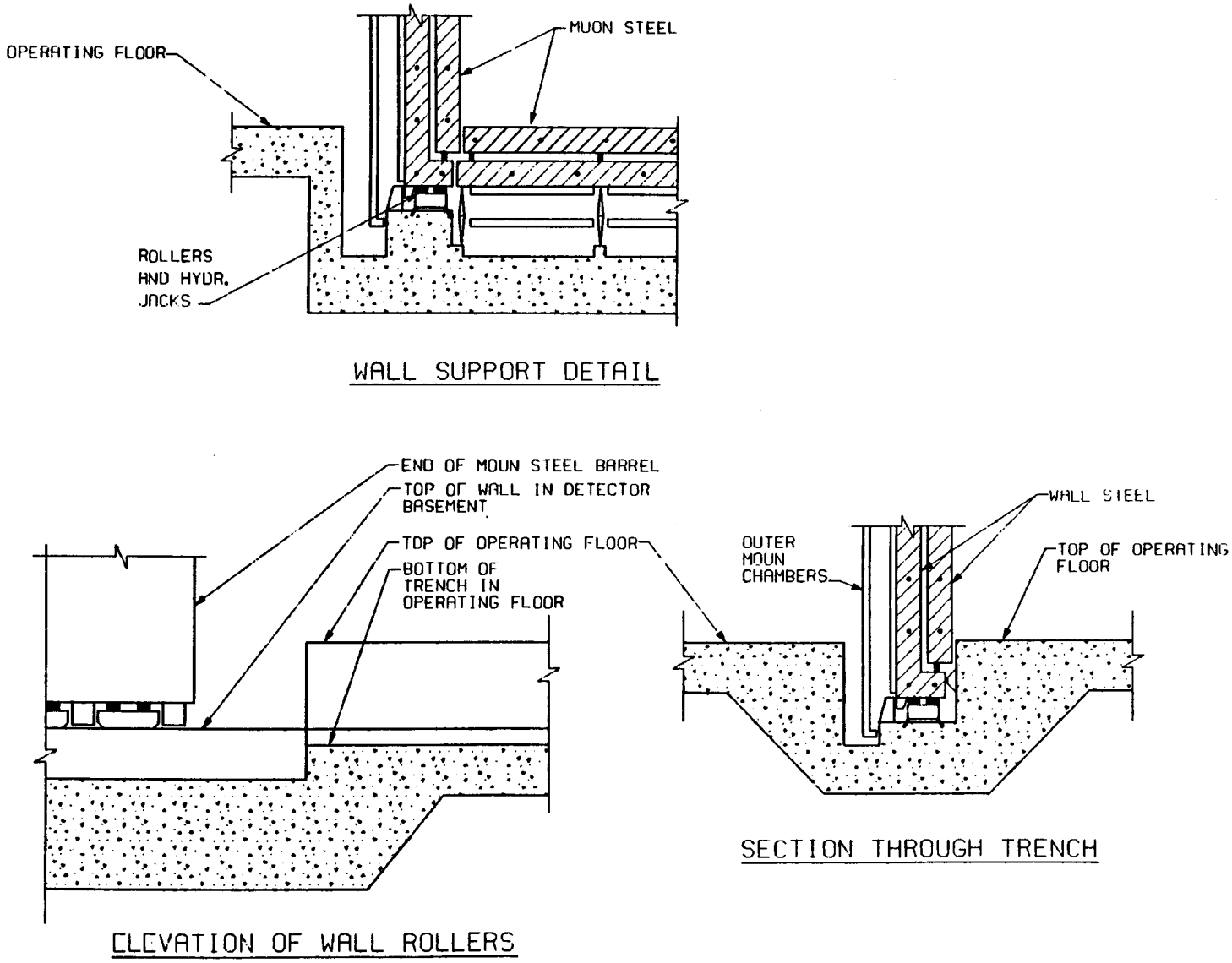

Figure 3.12. Baseline Detector—Moveable Barrel Steel Toroid

3.3.2 Muon Steel End Toroids Assembly

The end toroids of the baseline detector consist of four 850-mm-thick "wafers" separated by 200 mm gaps, as shown in Figure 3.13. Each half of these wafers is assembled from two 200-mm-thick and two 225-mm-thick plates shop fabricated from four segments (A, B, C and D). The three plates of segment B are butt-welded to each other using a tapered stainless steel spacer plate. This tapered non-magnetic gap and a similar shimmed gap between segments C and D give a uniform flux distribution around the corners of the toroids.

The four plates of each wafer are pulled together with 38-mm (1.5 in.)-diameter high-strength bolts which reduce the gaps between the plates to less than 3 mm (1/8 in.). The plates may be furnished to standard (ASTM-A6) mill tolerances. The mating surfaces of the half toroids and the edges of all plates at the tapered gap are machined.

The end toroids are assembled in the south end of the detector hall following the muon steel barrel construction. The plates are lowered through the construction shaft and installed in the erection frame, as shown in Figure 3.14. The four wafers of each end toroid are constructed separately. All plates of segment A are installed first, followed by the plates of segments B, C and D. The overlapping plates between the segments may be bolted with fitted bolts or field-welded. Final tightening of the high-strength bolts is carried out after the alignment of all plates in the wafer has been checked.

After the four wafers of a toroid have been assembled, two of the wafers are aligned and pulled together, as shown on Figure 3.15. The tie plates between the two wafers are installed next. This procedure is repeated until all four wafers of the toroid are assembled into a single unit. Each half-toroid is fitted with eight permanent rollers, moved away from the assembly area for installation of the coil packs and muon chambers, then temporarily stored. The above assembly procedure is repeated until all four half-toroids are completed.

Horizontal locating pins and clamping bolts are provided at the top and bottom of each wafer to maintain alignment of a half-toroid pair and structural integrity while moving in and out of the barrel.

Manpower requirement for the end toroid assembly is approximately the same as for the muon steel barrel assembly; however, because of the limited space in the hall, only one wafer with one crew can be constructed at a time.

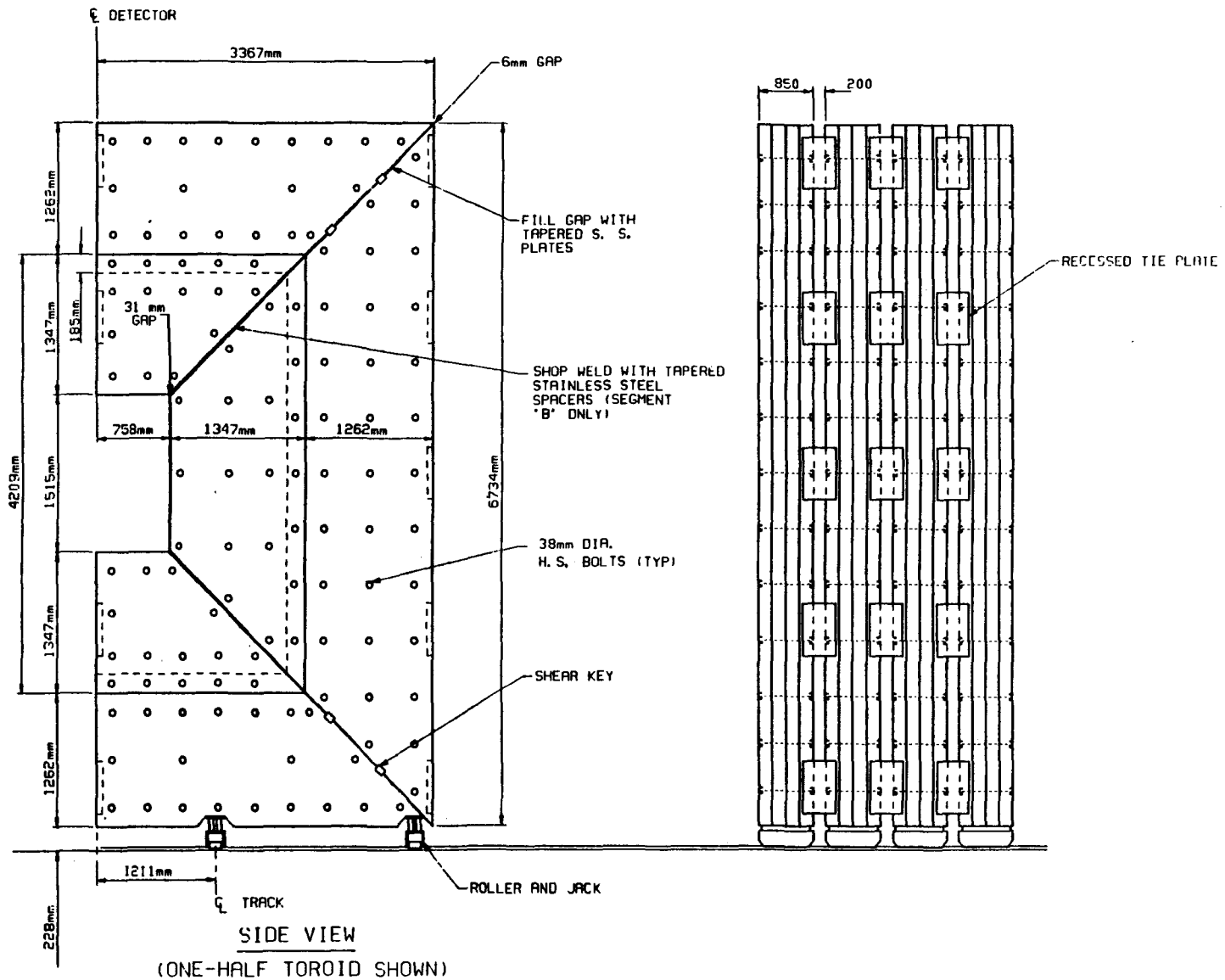

Figure 3.13. Baseline Detector—End Toroid General Arrangement

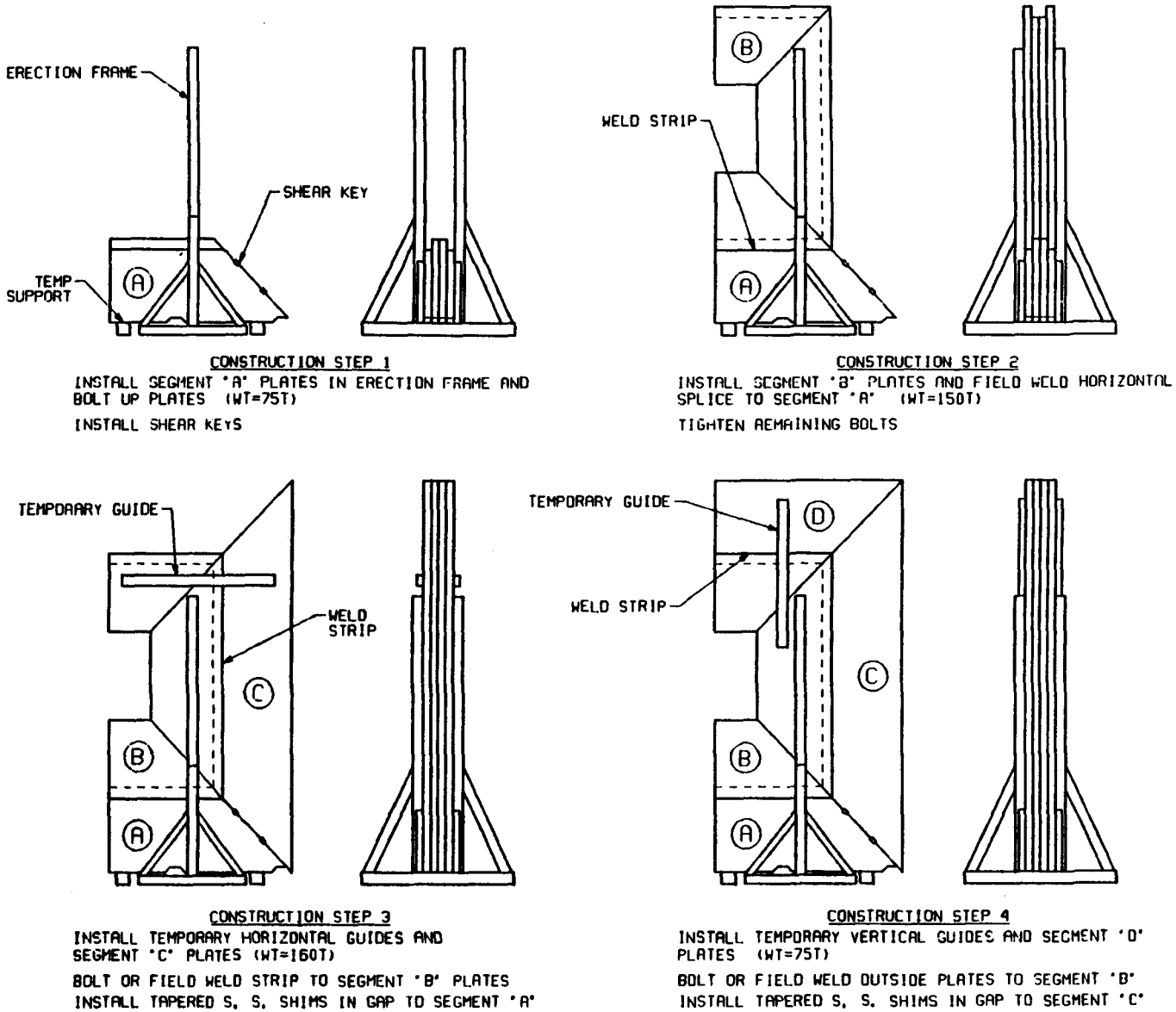

Figure 3.14. Baseline Detector—End Toroid Construction (Steps 1-4)

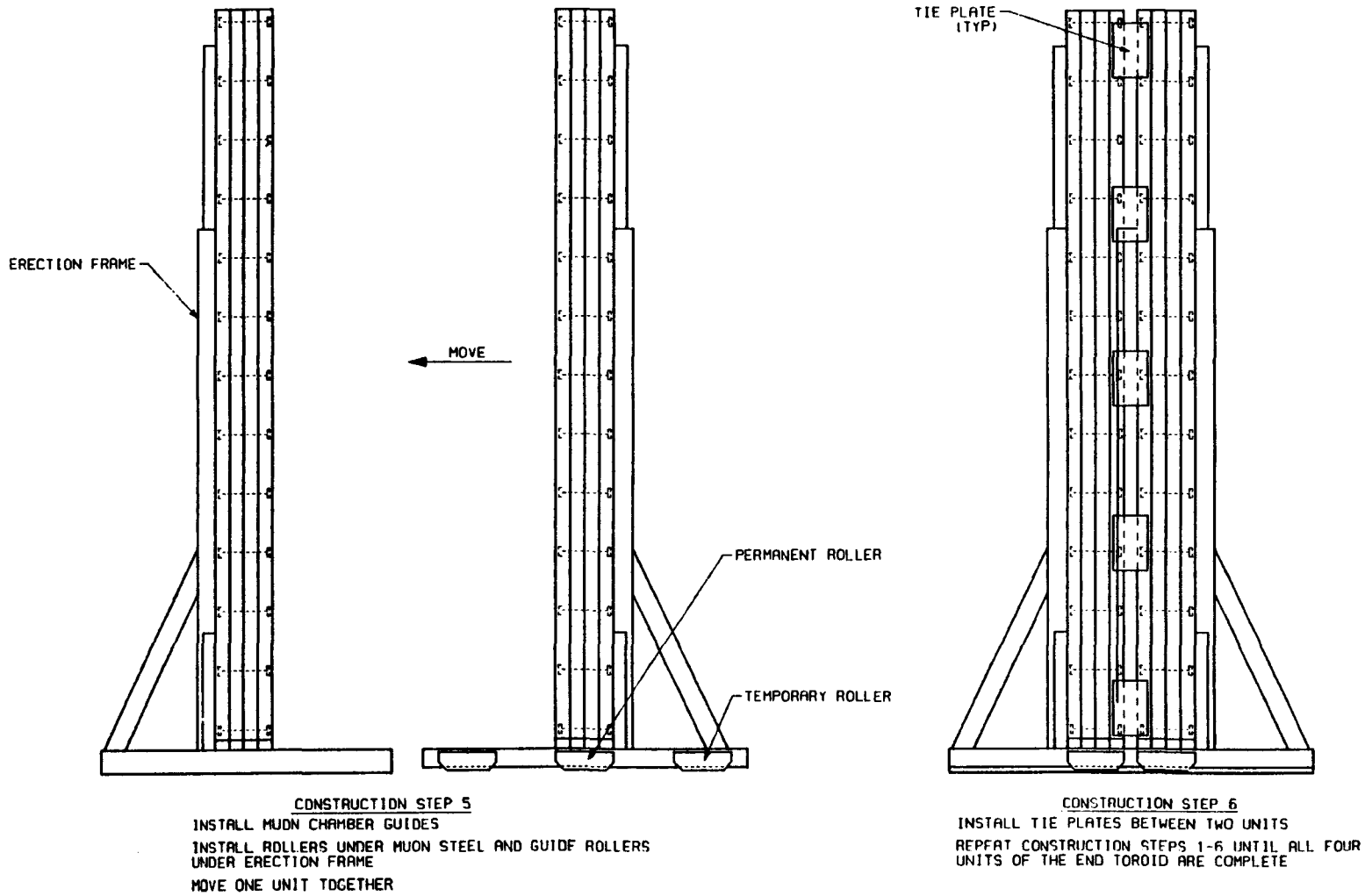

Figure 3.15. Baseline Detector—End Toroid Construction (Steps 5-6)

3.3.3 Calorimeter Assembly

The central and endcap calorimeters of the baseline detector are assembled in the north end of the hall. As shown in Figure 3.16, this area is sealed off from the rest of the hall by a temporary air-tight partition. The HVAC system of the hall is temporarily adjusted to maintain a slight overpressure in the calorimeter assembly area to prevent entry of dust and fumes generated by the muon steel assembly and other work. A total area of about 25.5 m by 15 m is provided for calorimeter assembly. (Note that this area does not include the space set aside for the clean room.) This area allows the construction of one calorimeter bay at a time while still providing room for mobility of all construction equipment and access to the equipment shaft. The calorimetry of the baseline detector consists of three central and two endcap calorimeter bays, shown in Figures 3.17 and 3.18.

Testing of the assembled calorimeter bays is performed in a clean room constructed to the east of the calorimeter assembly area, as shown in Figure 3.16. The clean room is separated from the assembly area by strip doors (overlapping flexible strips of heavy plastic) to allow unrestricted movement of the bays. The room has a steel deck roof to provide support and a working area for a self-contained pumping/filtration unit used to fill the modules of a bay with an ionization liquid such as TMP. The clean room, pressurized by filtered air, is sized to hold up to four calorimeter bays with an allowance of 3 m of clearance between them. This clearance permits mobility of the telescoping work platforms used to reach any area of the calorimeter assemblies during checkouts and filling of the modules.

Each calorimeter bay is constructed from preassembled modules weighing on the order of 20 tonnes. These modules are delivered to the calorimeter storage and staging building at the surface. From the staging area the modules are lowered to the hall through the equipment shaft, then moved to the assembly area on carts. The steel saddles and aluminum washers and frames of the calorimeter bays are lowered to the hall through the construction shaft, then moved to the calorimeter assembly area by the hall crane.

The support saddles are interconnected by box members equipped with four sets of Hillman rollers and hydraulic jacks. Normally, the weight of the calorimeter bay is carried by the box beam resting on steel blockage on the roller tracks. When the calorimeter bay must be moved, the rollers are lowered by the hydraulic cylinders, and the entire bay is rolled on steel tracks laid on the operating floor or installed in the muon steel barrel. The rollers can pivot through 360 degrees, allowing the movement of the calorimeter bays in any direction required.

The central calorimeter bays are constructed of 32 inner modules and 32 outer modules bolted to two aluminum washers that are supported on steel saddles (Figure 3.17).

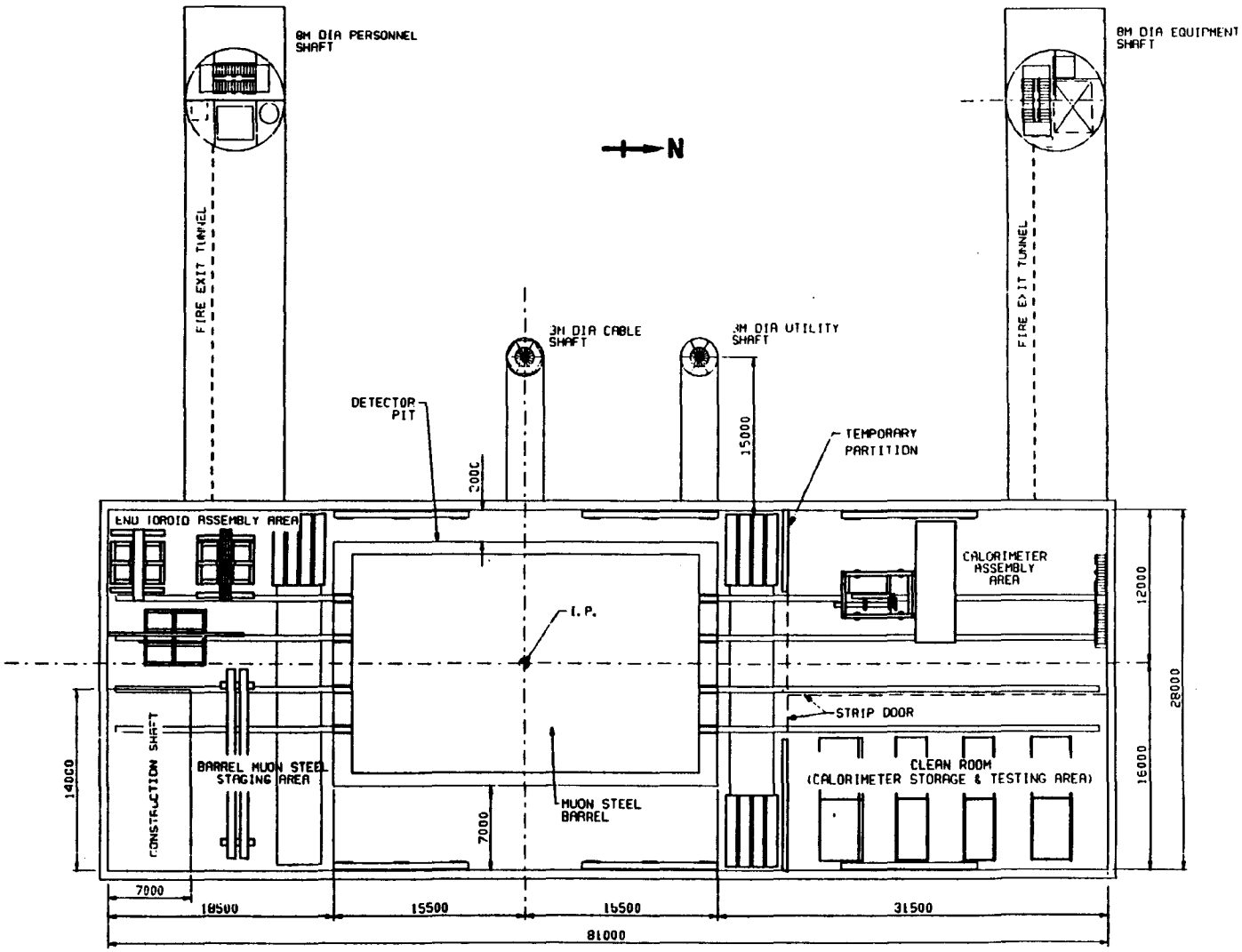

Figure 3.16. Baseline Detector—Hall Plan: Detector Assembly Layout

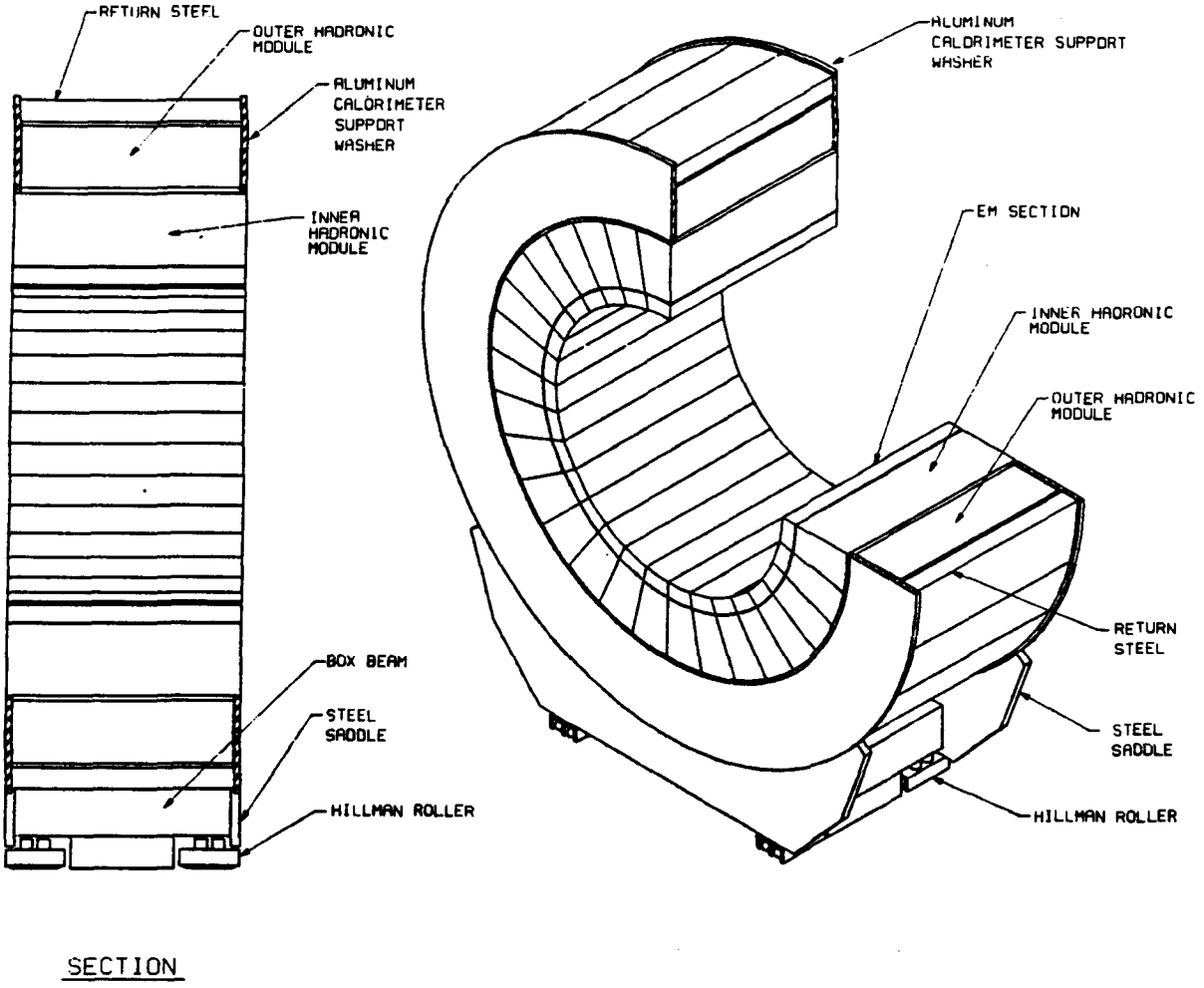

Figure 3.17 Baseline Detector—Central Calorimeter

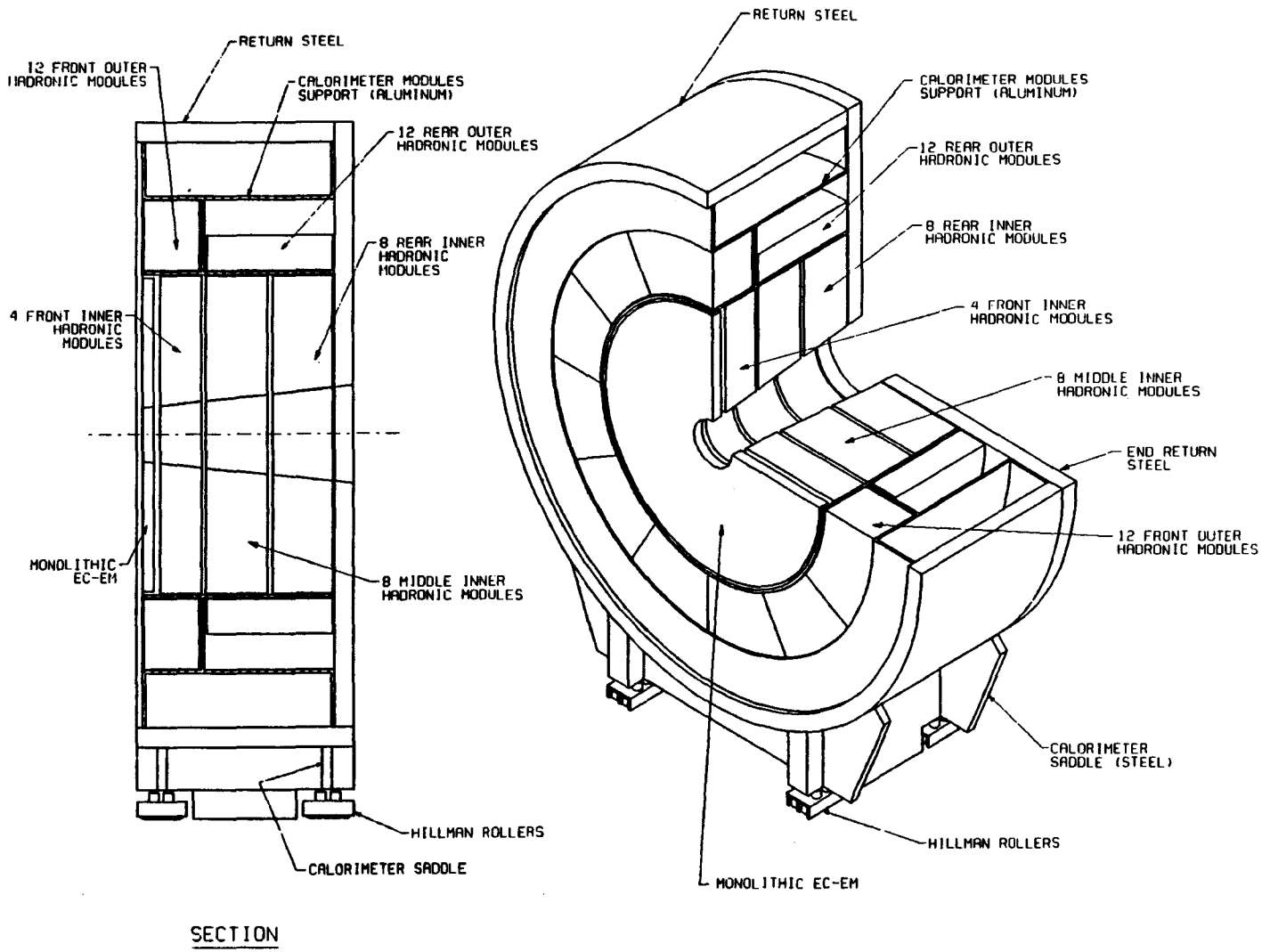

Figure 3.18. Baseline Detector—Endcap Calorimeter

Assembly of the central calorimeter bay (Figure 3.19) proceeds as follows:

1. Assemble the steel saddles and box beams onto the four rollers and anchor the assembly to the floor.
2. Install temporary spacer struts between two washers and lift this subassembly onto the saddles. The top of the saddles are fitted with lubricated bronze bearing bars to facilitate rolling of the washers during assembly of the modules.
3. Install brackets and hydraulic cylinders to washers and saddle. These cylinders provide the rotational motion needed during the assembly process.
4. Lift in four inner calorimeter modules and bolt to the inside edge of the washers in the topmost position. Since the inner calorimeter modules are longer (along the beam line) than the clearance between the two washers, they are lifted through the washers perpendicular to the position they will assume once installed.
5. Lift in four outer modules with flux return steel and install in topmost position using bolts recessed in the outside face of the washers.
6. Rotate the washer/module assembly 45° clockwise using the hydraulic cylinders, remove the temporary spacer struts at the top of the washers, and repeat these two steps until all but the last five inner modules are installed. Because of the limited space between the two washers, the last five inner modules are installed with the fixture used for the installation of the end calorimeter modules.
7. After all modules of a central calorimeter bay are installed, lock the saddle to the washer with bolts tapped into the washer, remove the hydraulic cylinders, and move the completed bay into the clean room.

We have performed several finite-element computer analyses to insure that deformation of the washer will not interfere with the installation of the modules during assembly. As shown in Figures 3.20 and 3.21, the maximum stress and deflection of the 100-mm (4 in.)-thick aluminum washers during and after assembly of the modules is acceptable.

The endcap calorimeter bays are made up of 20 inner hadronic modules and 24 outer hadronic modules, plus a monolithic EM module, as shown in Figure 3.18. The modules are bolted to a welded aluminum frame consisting of an inner and outer shell and three washers. The aluminum frame is supported by the lower portion of the flux return steel, which is welded to the support saddle to form a rigid cradle. The module support frame, the lower half of the return steel and saddle assembly, and the top half of the return steel are lowered to the floor through the construction shaft. The two halves of the return steel are field-welded, and the rollers and hydraulic jacks are installed under the saddle. The completed return steel and saddle assembly is moved to the calorimeter assembly area.

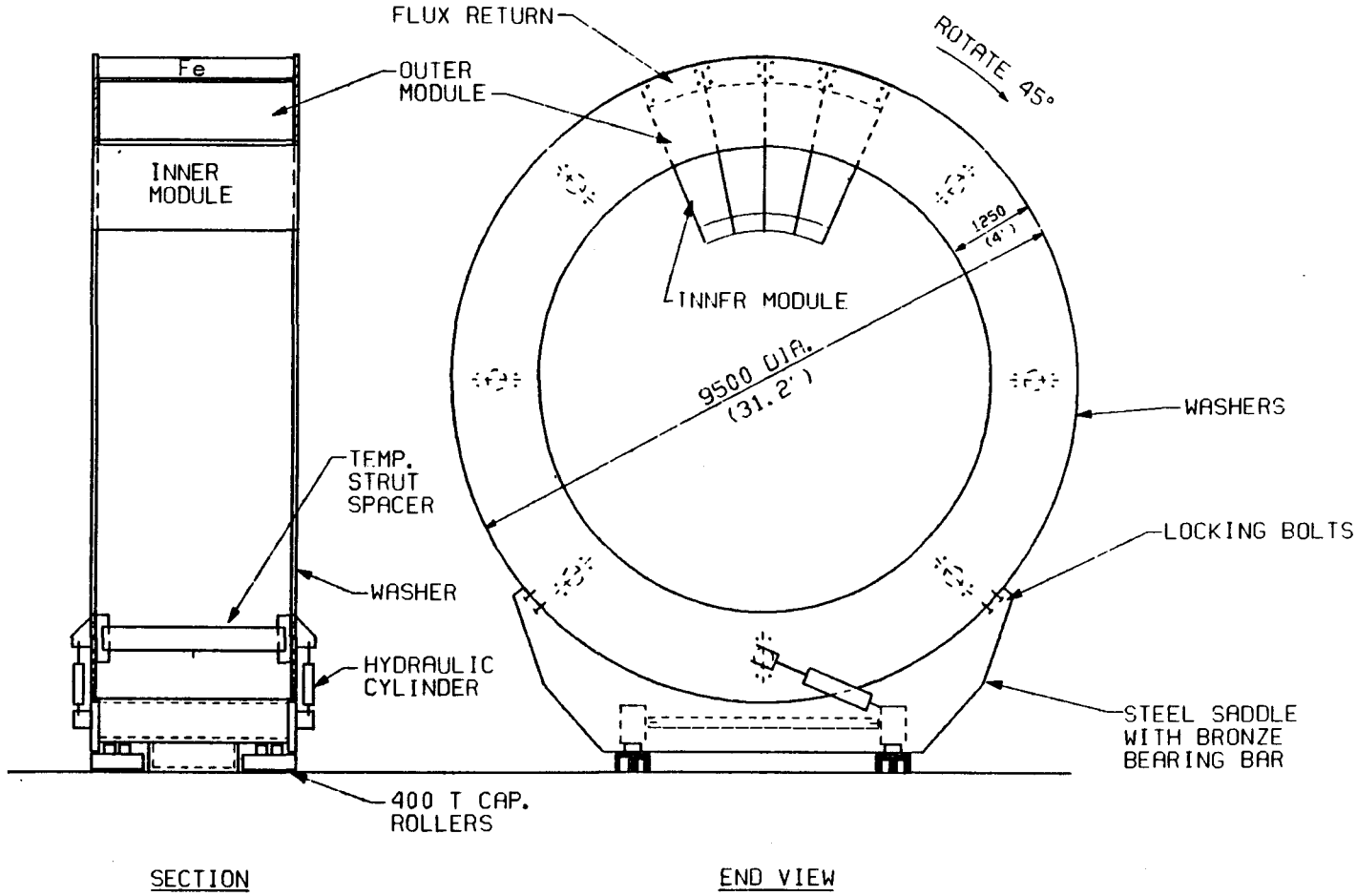

Figure 3.19. Baseline Detector—Central Calorimeter Bay Assembly

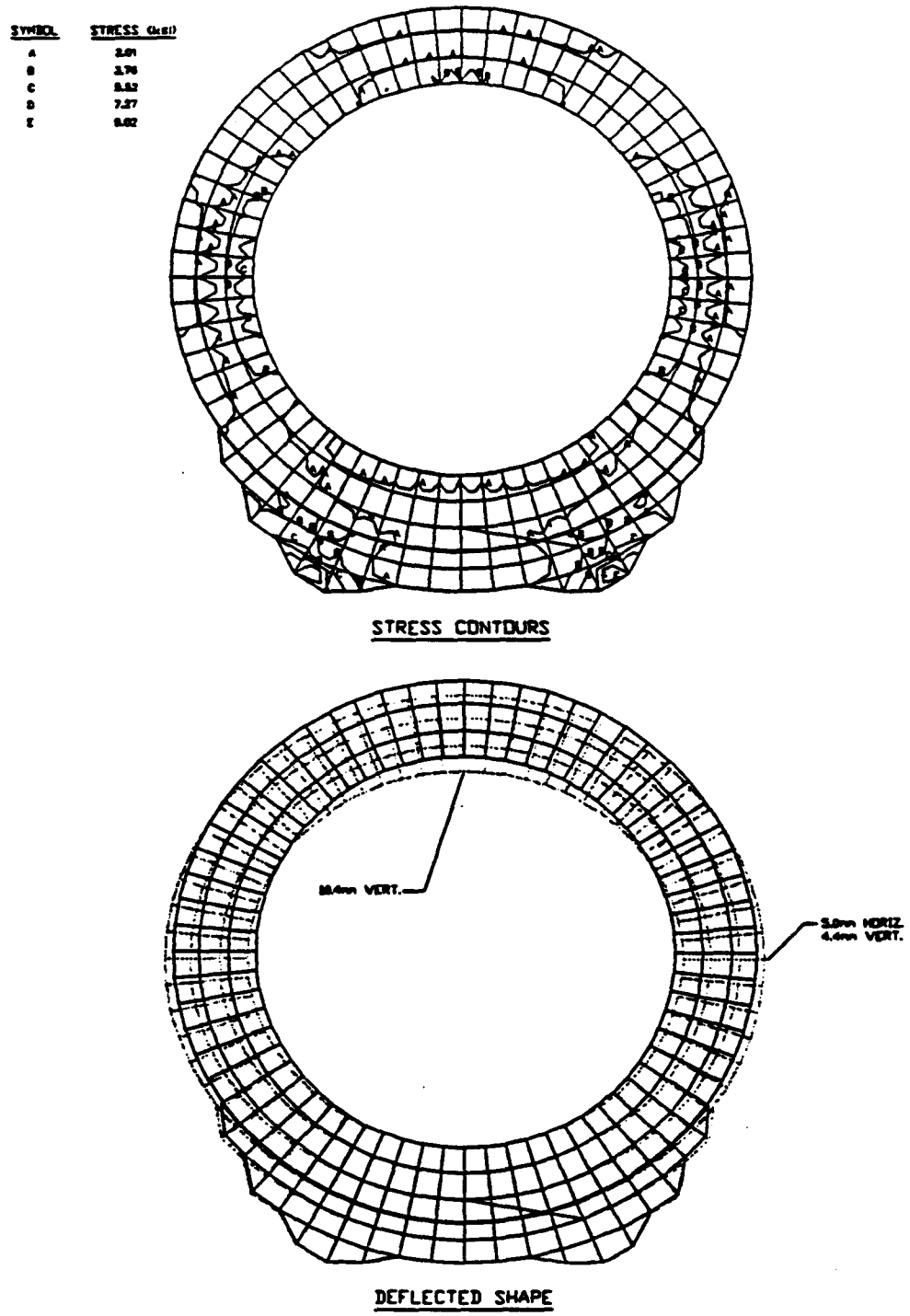

NOTE:
ALL MODULES LOADED.

Figure 3.20 Baseline Detector—Central Calorimeter Washer Analysis (All Modules Inserted)

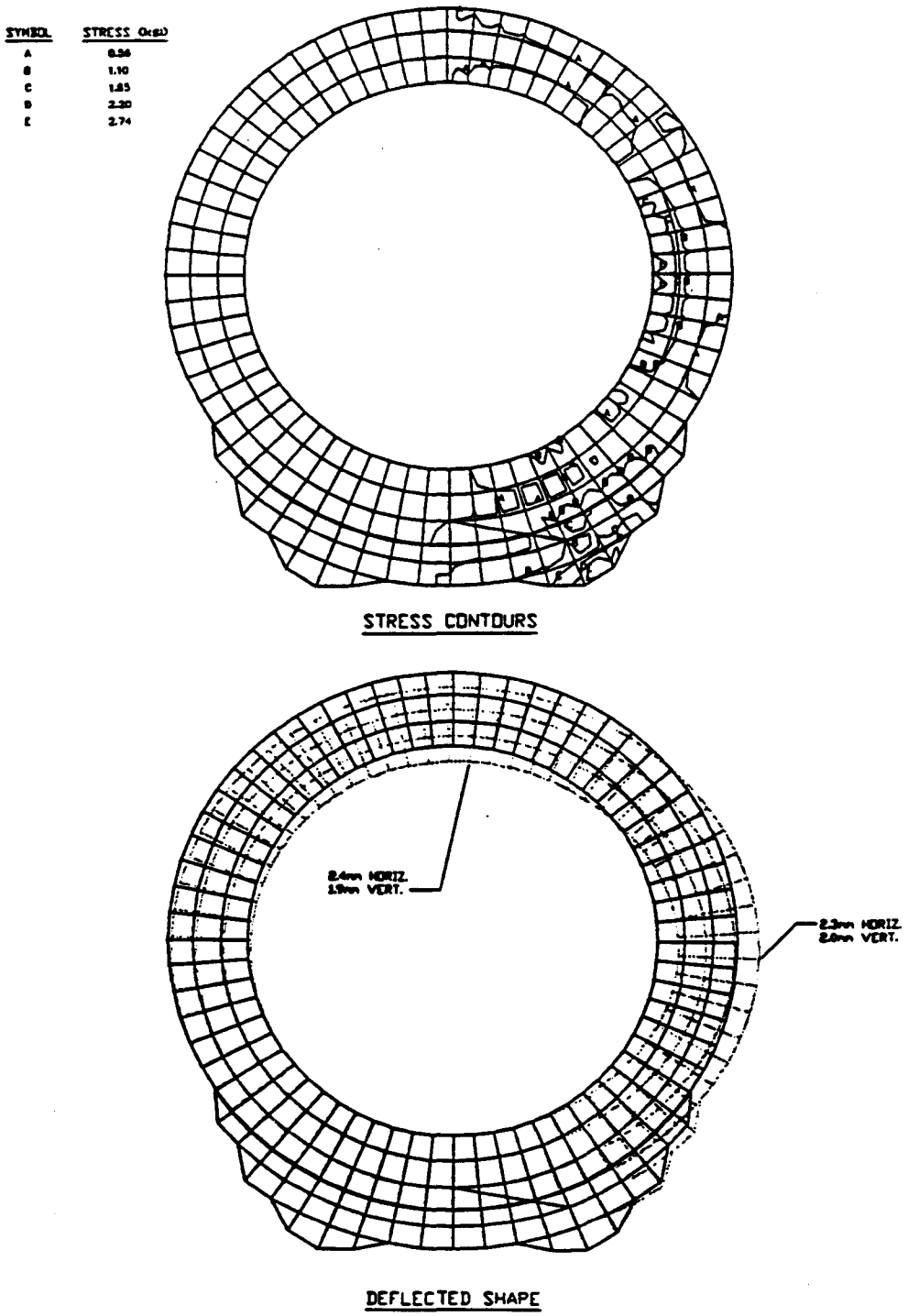

NOTE:
EIGHT MODULES LOADED AT
TWO O'CLOCK POSITION.

Figure 3.21 Baseline Detector—Central Calorimeter Washer Analysis (8 Modules Inserted)

Assembly of the endcap calorimeter bays proceeds as follows:

1. Install the module support frame inside the return steel barrel and lock in.
2. Position the special assembly fixture shown in Figure 3.22 and fasten it to the end of the return steel by temporary bolts. This prevents any movement between the fixture and the module support frame which would interfere with installation of the modules.
3. Install the 8 middle and 8 rear inner calorimeter modules, then the 12 rear outer modules. The assembly fixture is repositioned periodically to access the full face of the calorimeter assembly.
4. Move the assembly fixture to the opposite face of the endcap calorimeter bay, bolt to the return steel, and install the 4 front inner and the 12 front outer hadronic modules.
5. Install the monolithic EM module and move the assembled endcap to the clean room for the final electrical checkouts and filling of the modules.

The flat end return steel of the endcap calorimeters is installed by bolting the steel plates to the machined rear face of the curved return steel. The end return steel will be assembled from 3 to 5 segments to facilitate removal for servicing the rear face of the endcap.

As previously noted, the calorimeters are moved about the detector hall on Hillman rollers running on steel tracks. The bays are moved from the assembly area to the clean room and to their operating positions in the barrel muon steel on portable steel tracks welded to the floor plate. However, as described in Section 3.2.3, certain areas of the hall will be provided with permanent tracks. The calorimeters will be pulled along the tracks by hydraulic jacks bolted to the steel tracks.The estimated manpower requirement for assembling the calorimeters is as follows:

- Receiving, unloading, unpacking and staging the modules at topside. Lowering modules to hall—8 men.
- Receiving modules at bottom, moving to assembly area—4 men.
- Module installation—6 men.

The estimated rate of installation using the above manpower is two modules per 8-hour shift. After two modules are installed, they are tested in a second shift before installation of the next two modules. Additional physicist manpower is required to checkout modules after installation.

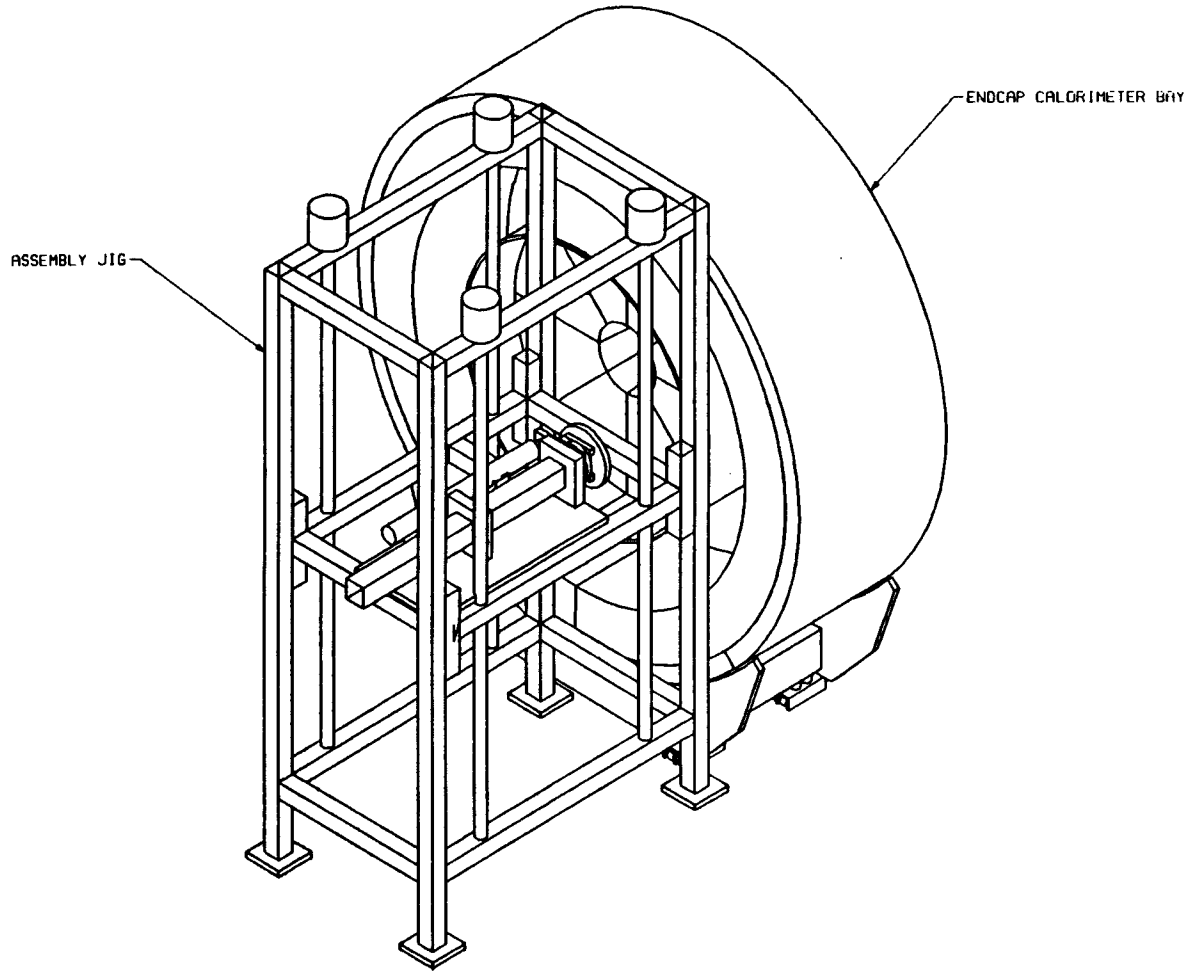

Figure 3.22. Baseline Detector—Calorimeter Assembly Frame

3.3.4 Muon Chambers

We assume that the muon chambers arrive in the hall as panels, several meters on a side, ready to be installed. Support and alignment frames are attached to the muon steel to accept the panels. Transport of the panels is by hall crane. The problems of muon chamber support and alignment have been greatly simplified in this study and need to be addressed in future studies.

3.3.5 Solenoidal Coil

The superconducting solenoidal coil arrives at the detector hall fully assembled and ready to be installed. It is assumed that the coil arrives at the hall mounted on a mandrel which is designed to support the coil during transportation to the site and during installation. The coil is lowered into the hall via the construction shaft and is carried by the overhead hall crane to the area previously used for calorimeter assembly. Mounting the coil on its temporary support trolleys, and any other pre-installation work, is done in this area. During the coil installation, all muon steel work and calorimetry assembly will have been completed, leaving sufficient space available for coil work.

After unpacking and inspection, the coil is installed in the following steps:

1. The coil is first lifted by its mandrel onto the saddles of the temporary supports located at each end of the coil, as shown in Figure 3.23 (a). These temporary supports will hold the coil on the beam line; they are designed to roll on calorimeter tracks.
2. After the shipping mandrel is extended by bolting an approximately 12-m-long beam to one end, the coil is rolled into the barrel calorimeter until the end of the cantilever mandrel extension has emerged from the calorimeter, as shown in Figure 3.23 (b). A third movable support stand is bolted to the free end of the mandrel extension, and the middle temporary support stand is removed.
3. The coil is now moved into the barrel calorimeter. After installation of the permanent support links to the calorimeter and removal of the shipping ties, the mandrel is rolled out from the coil.
4. Cryogenic and power connections are made.
5. Field mapping takes place after the coil has been cooled and the endcap calorimeters have been temporarily moved into their operating positions.

The superconducting solenoidal coil operates at a cryogenic temperature of 4.5 K by boiling liquid helium in the magnet and liquid nitrogen in shield. The cryogenic valve box is located on top of the north end of the detector. Cryo pipes and electric power are connected to the magnet via an approximately 30-cm^2-diameter chimney. Figure 3.24 shows a schematic layout of the required cryogenic cooling system in the hall and at the surface. As shown in the figure, the cryogenic and vacuum equipment, such as local dewars and pumps, is located on the gallery at the side of the

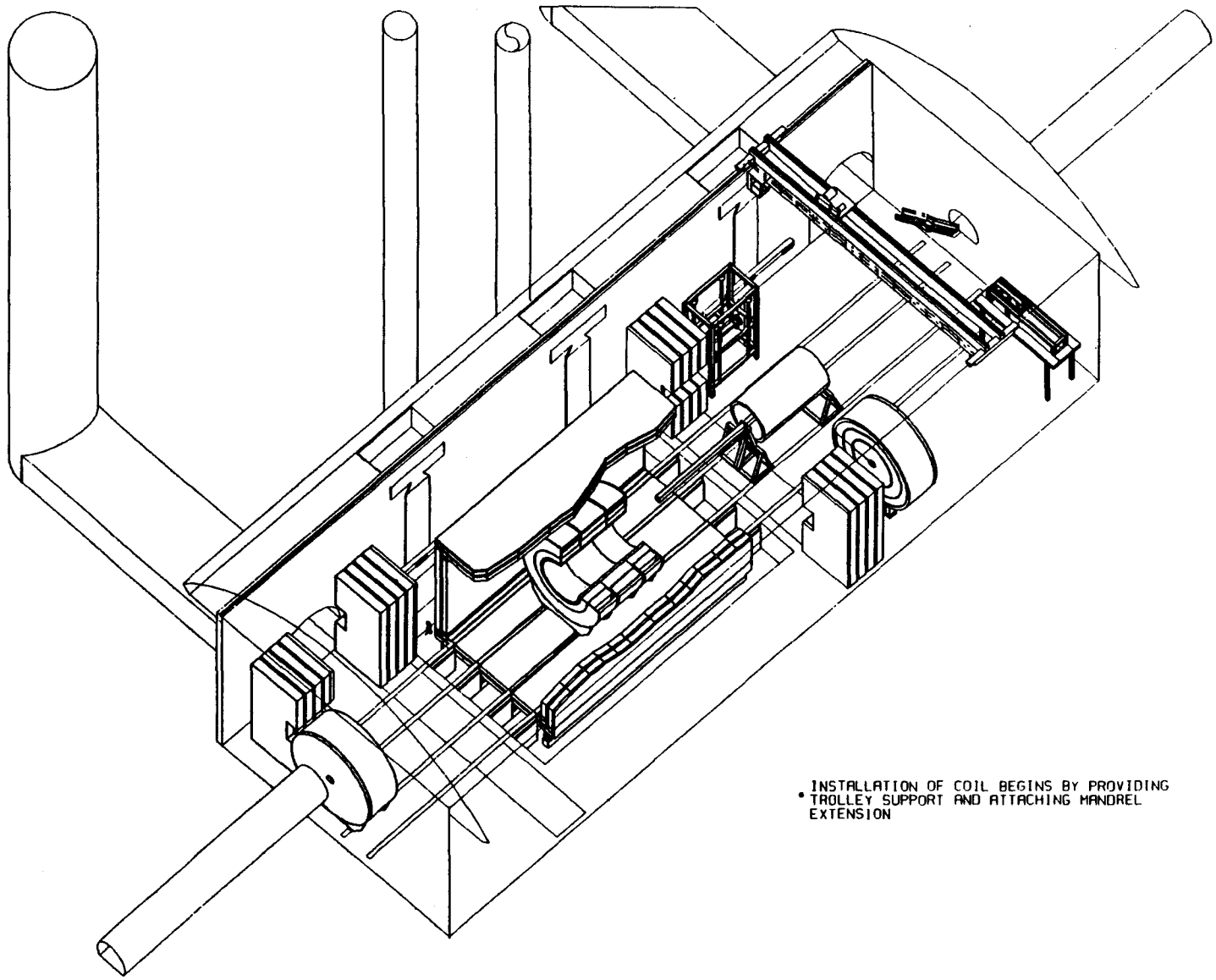

Figure 3.23 (a). Baseline Detector—Solenoid Coil Installation (Step 1)

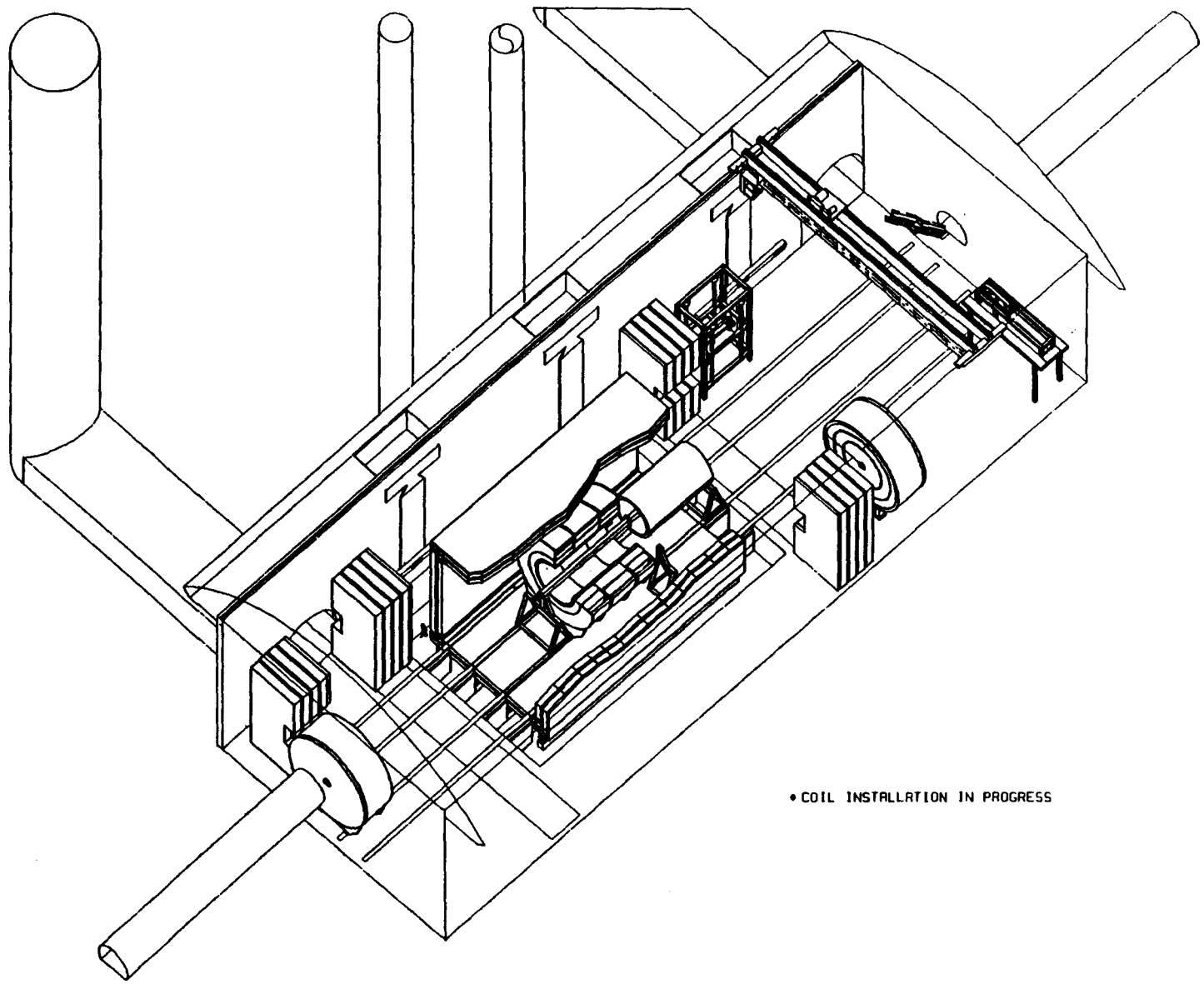

Figure 3.23 (b). Baseline Detector—Solenoid Coil Installation (Step 2)

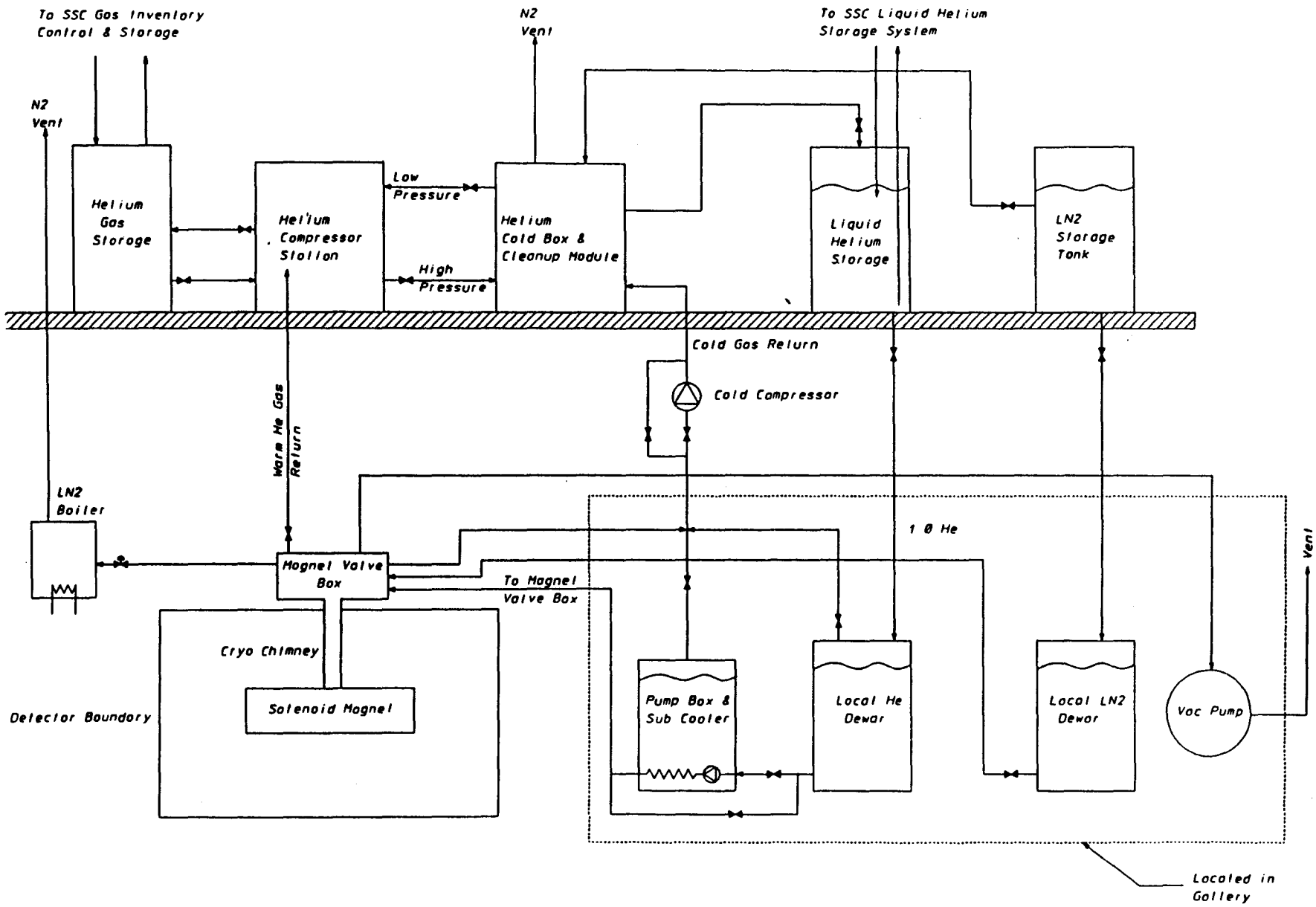

Figure 3.24. Solenoid Cryogenic System Schematic

detector. A walkway from the gallery to the top of the detector is included to facilitate access to the cryogenic valve box.

The impact of the cryogenic equipment assembly and installation on the magnet installation schedule is minimized by completing most of the cryogenic piping installation prior to inserting the magnet into the detector. Cleanup and cooldown time is accounted for in the magnet installation schedule.

3.3.6 Central Tracking Device

We assume that the central tracking unit, including the silicon tracking device, arrives at the hall fully assembled on a mandrel and ready to be installed. The central tracking device is lowered into the hall through the construction shaft and is carried to the calorimeter assembly area by a hall crane. This area is used for any necessary pre-installation work. After checkout, the tracking unit is installed using the temporary support stands of the coil, in a manner similar to the installation of the coil.

3.3.7 Beam Pipe

The beam pipe arrives at the hall in segments and is assembled on site. These segments are lowered into the hall through the construction shaft and are either rolled to their installation sites on trolleys or carried by the hall crane. Any preparatory work done on the beam pipe can be done in any area adjacent to the barrel muon steel or in the barrel itself.

3.3.8 Forward Calorimeters

We assume that the forward calorimeters arrive at the detector hall in halves, each half fully assembled. They are brought into the detector hall through the construction shaft, carried to their installation sites, and lifted onto their support cradles by the hall crane. Any work required on the forward calorimeters is accomplished *in situ* once they have been installed. Sufficient room is available for this work.

3.3.9 Electronics/Triggering

We have not studied the assembly of the readout and triggering electronics needed for this detector. We have provided space for the electronic and its cables. The cables to the surface for the electronics and triggering are carried by the cable shaft, which has been provided specifically for this purpose.

3.3.10 Accelerator Components

Assembly of accelerator components is carried out in coordination with the SSC Laboratory. We assume that the accelerator components are brought into the hall through the construction shaft

and are carried to their installation sites by either of the two cranes in the detector hall. There is space available adjacent to their installation sites for any necessary preassembly work.

3.4 Schedule and Sequential Construction Drawing

3.4.1 Schedule

The estimated schedule for construction of the baseline detector is shown in Figure 3.25. Estimates for the assembly of the muon steel have assumed that two crews are involved and that work proceeds from the middle outward in two directions. Assembly of the endcap toroid steel is done by the same crews during the periods when the coils for the barrel toroids are being connected to power and to Low Conductivity Water (LCW), and are being tested for electrical continuity and for integrity of the electrical insulation and cooling system.

Both the barrel and the endcap calorimetry assembly schedules assume that, on average, one calorimeter module can be installed and tested per day. We foresee the calorimeter installation occupying two shifts per day: the day shift to install and the evening shift to test and calibrate the installed modules. We have allowed five months contingency at the end of the calorimeter schedule; a third shift per day may also be taken as additional contingency time. The overall scheduling for the detector is easiest if at least one endcap calorimeter is completed prior to installation of the barrel system. This simplifies motion of the heavy objects inside the collision hall.

The superconducting coil cannot be installed until the barrel calorimeter is complete and has been placed in its final position on the beam line. From the argument in the previous paragraph, this would imply that at least one endcap calorimeter has also been fabricated. Prior to installation of the central tracking device, the magnetic field of the solenoid must be measured. This requires installation of the endcap calorimeters, since they provide part of the return yoke of the magnet. Initial testing of the field-mapping instrumentation can take place simultaneously with the installation and testing of the coil, but the final mapping must wait until all of the magnetic elements are installed and operational.

After the magnetic field has been mapped, the endcap calorimeters are withdrawn and installation of the central tracking device (including the silicon tracker) can proceed. The central tracking is assumed to arrive in the hall as a single, pre-tested unit that requires minimal debugging inside the collision hall prior to instillation in the detector.

Installation of the muon chambers begins with the successful testing of the barrel iron toroids and their coils. The exterior chambers are installed first, followed by the chambers on the inside of the steel (except for those on the bottom, which are installed with the barrel calorimeter). The end

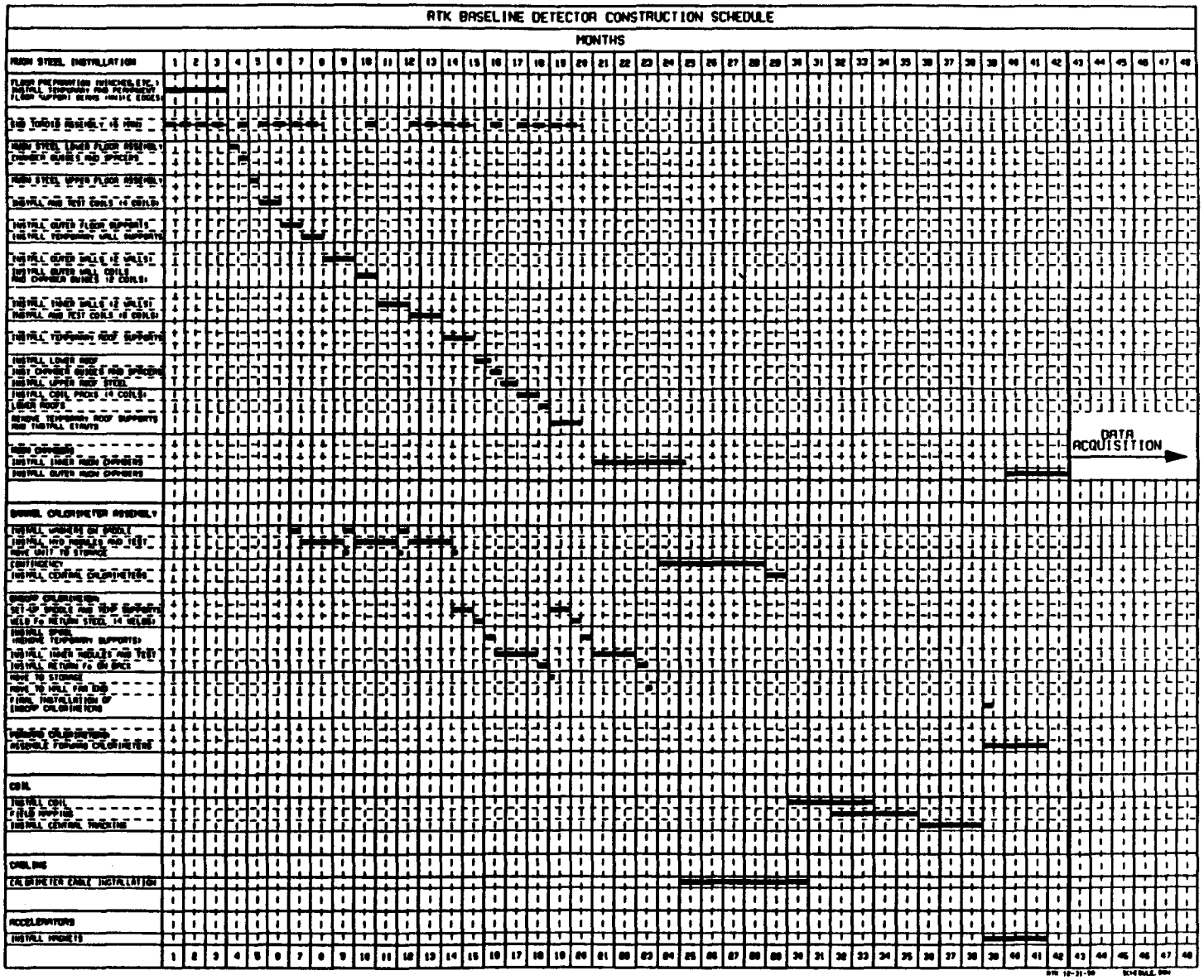

Figure 3.25. Baseline Detector Construction Schedule

cap muon chambers are installed as soon as the endcap iron toroids and their coils are assembled and have been successfully tested.

Estimating the schedule for the installation of the electronics is more problematical; we have not considered this schedule in detail. We assume that large-scale testing of the data acquisition system and pathways begins with the assembly of the first calorimeter bay. Some of this testing could provisionally be done using the electronics gallery in the hall as a temporary data acquisition location. However, prudent planning implies that beneficial occupancy of the operations center should be no later than one year after beneficial occupancy of the collision hall.

3.4.2 Sequential Construction Drawings

A full-scale, three-dimensional computer model of the baseline detector and hall has been made. An electronic model has many advantages over conventional drawing and modeling techniques; a primary example is the ability to easily manipulate the pieces that constitute the completed model. Complicated construction tasks may then be quickly simulated and potential problem areas may be pinpointed. In this manner, our model has served to help establish and verify space requirements and usage, constructibility, possible scheduling conflicts, and general construction information and needs.

The objective of the modeling exercise is to simulate the detector construction at various stages of completion. Three-month periods have been established as generally sufficient to highlight construction milestones; however, additional views have been assembled where necessary. The result of this work is a series of drawings depicting the detector construction with a high degree of detail and realism. The construction sequence is presented in Figures 3.26 through 3.43.

Figure 3.26 presents the hall at beneficial occupancy (month 0 on the construction schedule). At this time construction begins on the first muon steel end toroid in the area adjacent to the personnel shaft at the near end of the hall. Sufficient space is available for the end toroid assembly, for any necessary steel preparatory work, for temporary storage of the completed units, and for access to the personnel shaft. The end toroid steel is brought into the hall through the construction shaft.

Preparation for the barrel muon steel assembly also begins at this time with erection of the floor support beams (knife edges) and all necessary sub-floor support structures. Materials for this work are also brought into the hall through the construction shaft. A staging area adjacent to the muon steel barrel (and clear of the construction shaft access) provides room for any steel preparatory work. At the far end of the hall work begins on the hall partition and the clean room.

Figure 3.27 depicts the hall after three months of activity. The first end toroid assembly is complete, and the unit awaits movement to a temporary storage area. Construction of the barrel muon steel begins with the assembly of the lower floor. The assembly begins in the center of the

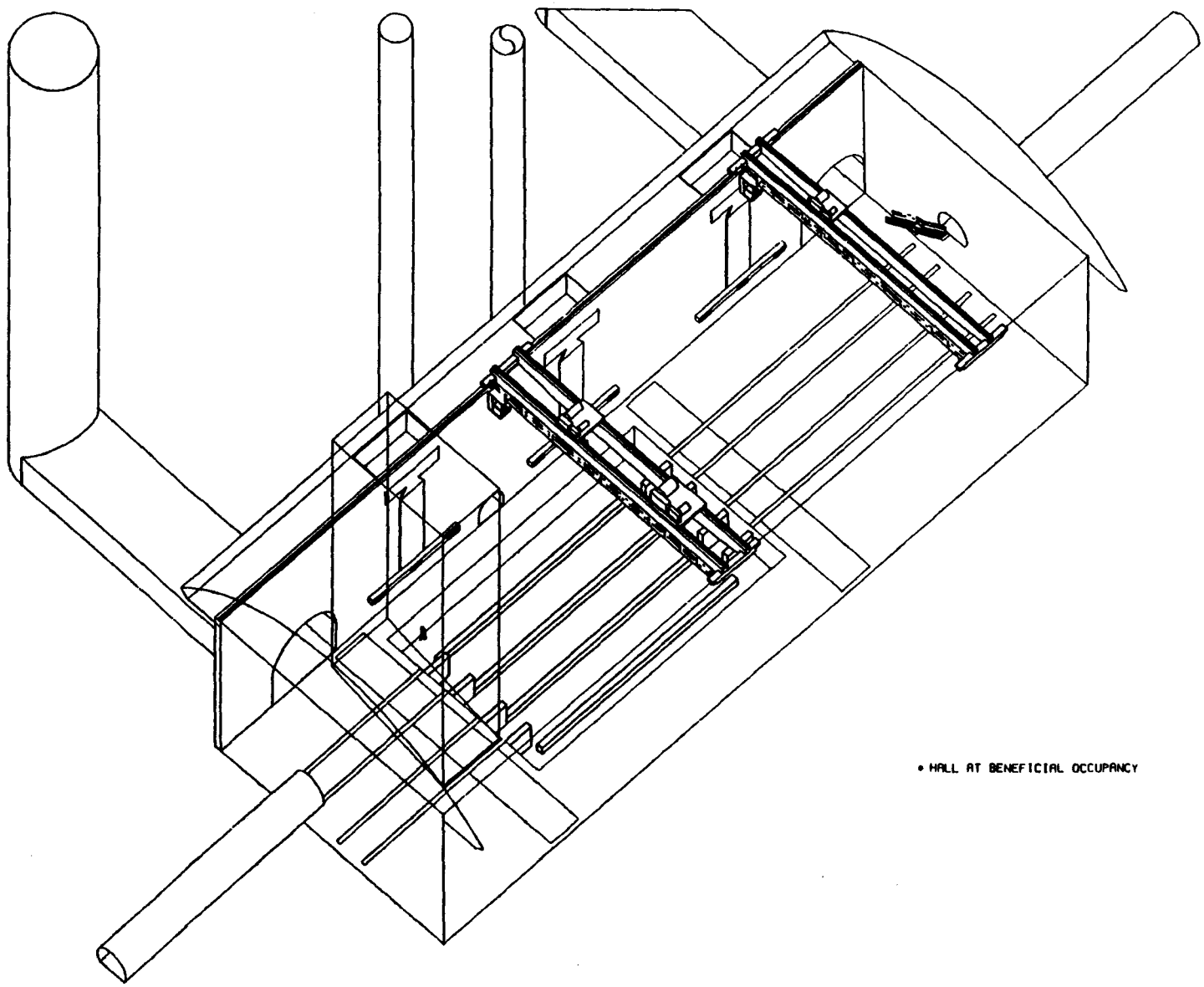

Figure 3.26. Baseline Detector Construction Sequence (Month 0)

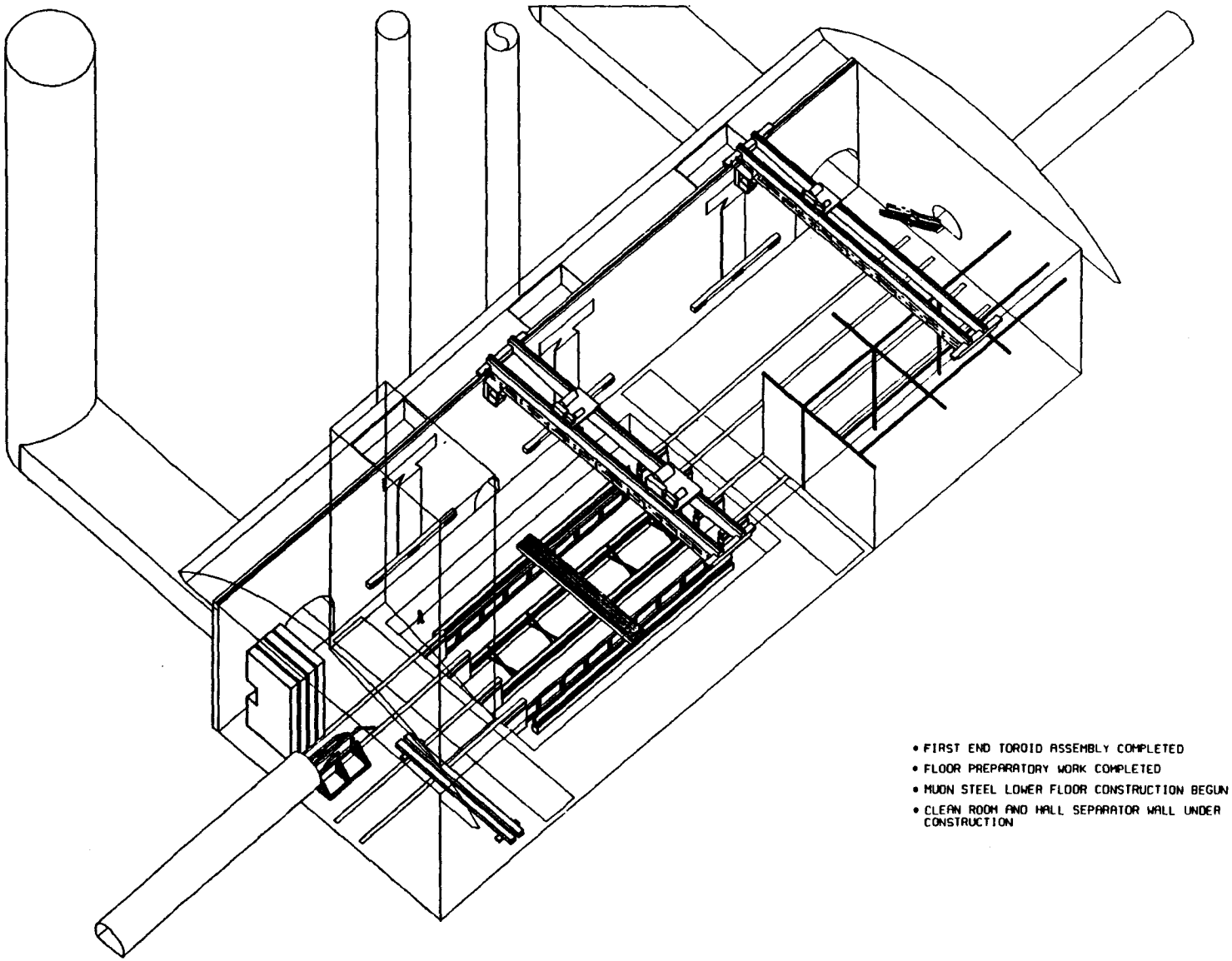

Figure 3.27. Baseline Detector Construction Sequence (Month 3)

barrel and proceeds out toward each end. Two crews are required, each working in opposite directions. Figure 3.27 also shows the staging areas available for steel preparatory work for both the end toroids and the barrel muon steel. At the far end of the hall work continues on the clean room and hall partition.

Figure 3.28 shows the hall six months into construction. The first end toroid unit has been moved to a temporary storage area and a second end toroid is approximately 50% assembled. The muon steel barrel upper and lower floors have both been completed, and their coil packs have been installed. Outer floor supports are installed at this time. At the far end of the hall the temporary partition and the clean room are complete. The first central calorimeter bay assembly is begun by erecting the support washers and saddle. The washers are lowered into the hall as fully assembled units through the construction shaft.

Hall activity at nine months is seen in Figure 3.29. The second end toroid is complete and both units await transport to the opposite end of the hall. Assembly of the barrel muon steel continues with the erection of the outer walls and their temporary supports. At the far end of the hall the first central calorimeter bay assembly is complete, and the unit has been moved into the clean room where it is undergoing electrical checkout. The saddle and support washers for the second central calorimeter bay have been assembled, and the installation of the calorimeter modules is in progress. This view also shows the tooling required for the installation of the modules. The calorimeter modules are brought down to the hall level via the equipment shaft at the far end of the hall and are rolled into the hall on trolleys. It should be noted that any material or equipment necessary for the assembly of the calorimeter bays which cannot be transported through the equipment shaft must be brought through the construction shaft. The support washers are an example. The hall partition does not permit through-access to the large crane into the calorimeter assembly area; this requires the transfer of equipment from the large crane to a trolley able to carry these pieces into this region. This transfer can be accomplished in the area adjacent to the hall partition. Three-dimensional computer simulation of this scenario shows this to be possible at this or any subsequent stage.

Figure 3.30 shows hall activity at 10 months. The two completed end toroids must be moved to the opposite end of the hall at this time. Once the toroids are moved, progress on the barrel muon steel can continue with the erection of the inner walls and their temporary supports. These temporary supports prevent passage of large objects through the barrel steel. During this period the outer wall coil packs are installed. The calorimeter modules installation is in progress on the second central bay.

The hall at 12 months is shown in Figure 3.31. The two completed end toroids can be seen in their storage positions adjacent to the hall partition. Construction has just begun on the third end toroid. The muon barrel inner walls are complete, and the installation of the coil packs is in progress. The second calorimeter bay assembly is complete and is undergoing electrical checkout

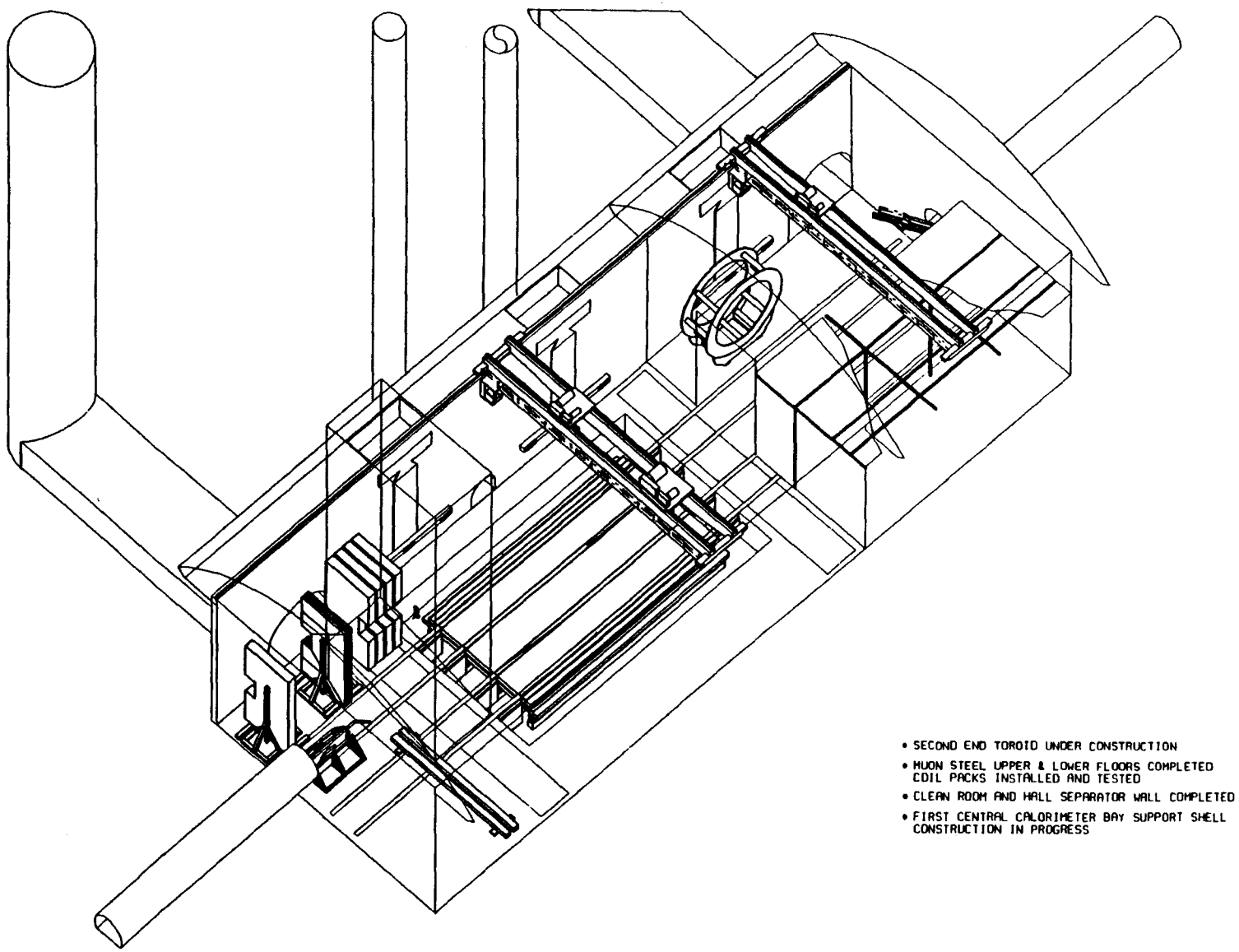

Figure 3.28. Baseline Detector Construction Sequence (Month 6)

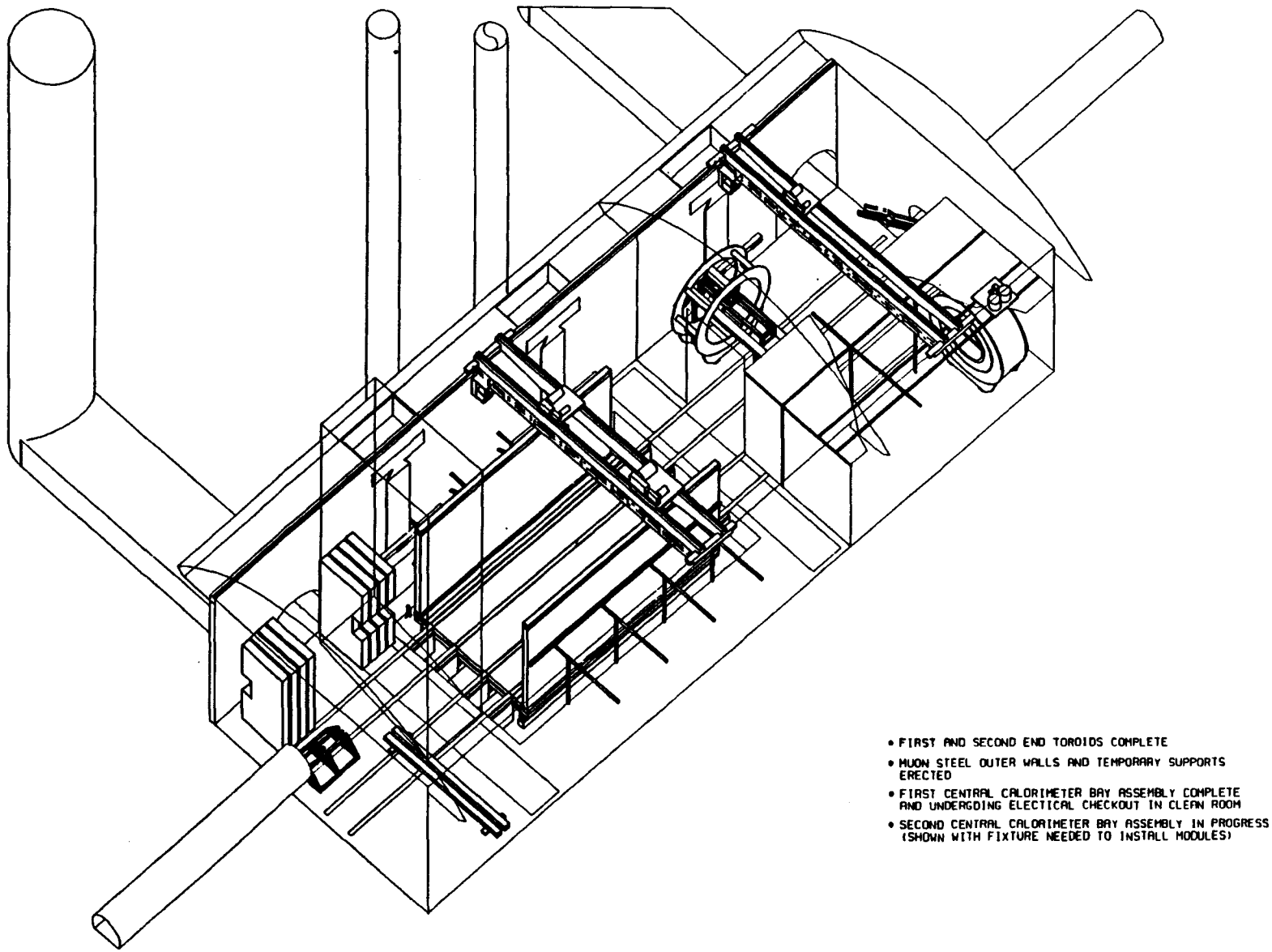

Figure 3.29. Baseline Detector Construction Sequence (Month 9)

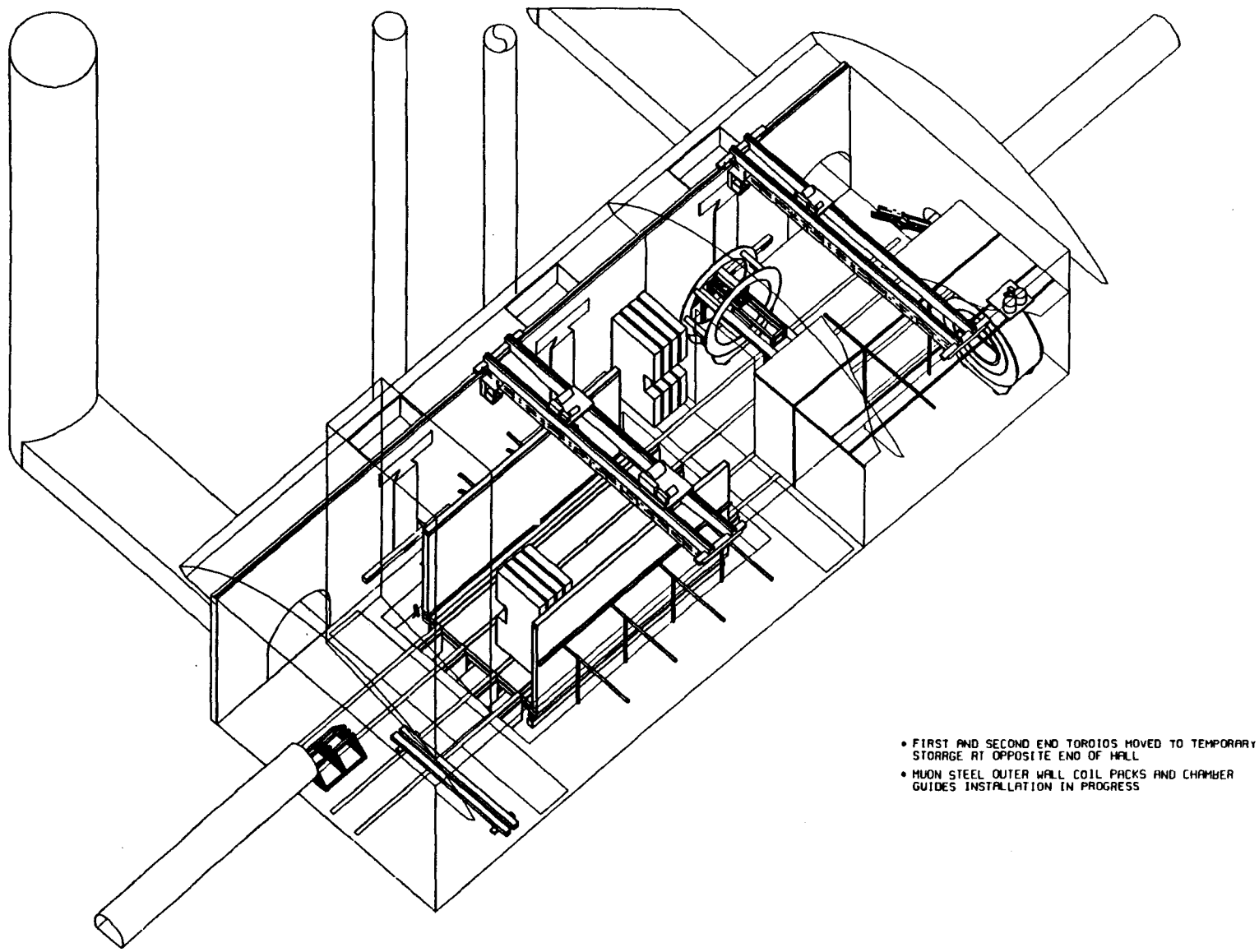

Figure 3.30. Baseline Detector Construction Sequence (Month 10)

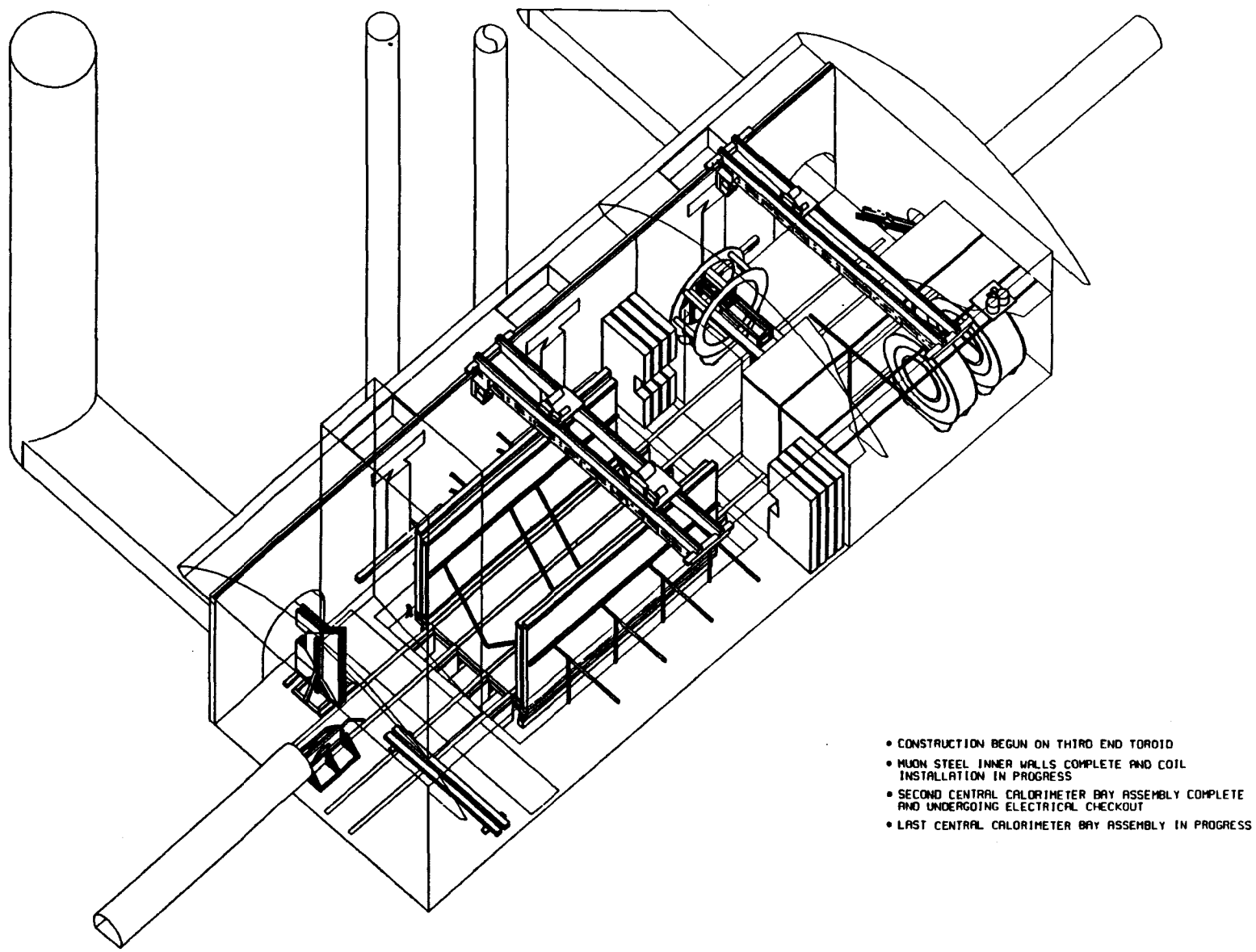

Figure 3.31. Baseline Detector Construction Sequence (Month 12)

in the clean room. The last central calorimeter bay support has been assembled, and the installation of the modules is underway.

At 15 months (Figure 3.32), the third end toroid has been completed, and the unit awaits movement to its temporary storage. The barrel muon steel roof temporary supports have been erected, and the lower roof has been assembled in a raised position. The lower roof coil packs are installed at this time. The last central calorimeter bay is complete and is undergoing electrical checkout in the clean room. The central bay's assembly fixture has been moved to storage at the far end of the hall. Assembly of the first endcap calorimeter bay begins at this time with construction of the return steel.

Figure 3.33 shows the progress made after 18 months. The third end toroid has been moved to its temporary storage, and construction is in progress on the last unit. The barrel muon steel upper roof has been completed, and both roofs are lowered into position. At the opposite end of the hall, calorimeter modules are installed into the first endcap bay. A special fixture, required to achieve this, is shown along side the calorimeter bay.

The state of the hall at 21 months is shown in Figure 3.34. At this stage the last muon end toroid assembly has been completed. All muon steel temporary supports and scaffolding have been removed, and the permanent supports have been installed. Installation has begun on the inner muon chambers. The first endcap calorimeter bay is complete and is undergoing electrical checkout in the clean room; the second endcap calorimeter is under construction.

During month 23 (Figure 3.35), the second completed endcap assembly is moved to the opposite end of the hall. Prior to moving the endcap, the hall partition and part of the clean room wall are dismantled. Installation of the inner and middle muon chambers is in progress. The endcap assembly fixture has been placed in storage.

Months 24 through 28 are a contingency period. At month 30 (Figure 3.36), the central calorimeter bays have been installed in their operating positions, and installation of the coil begins. The coil is presumed to be supplied with a mandrel support. This support is poised on a trolley system, and a mandrel extension is then attached. Dismantling of the clean room is complete.

Coil installation proceeds at 30.5 months (Figure 3.37). The coil is positioned next to the calorimeters with the mandrel extension protruding through the bays. Trolley support can then be provided on each side of the central bays. The coil is then inserted into the bay assembly, and the trolleys and mandrels are removed.

Figure 3.38 shows the hall at 33 months. The coil installation has been completed, and the endcap calorimeters are temporarily moved into operating position. The coil field mapping then proceeds.

At 36 months (Figure 3.39), the coil field mapping is complete, and the endcap calorimeter bays are pulled back to allow access in preparation for the central tracking unit installation. The

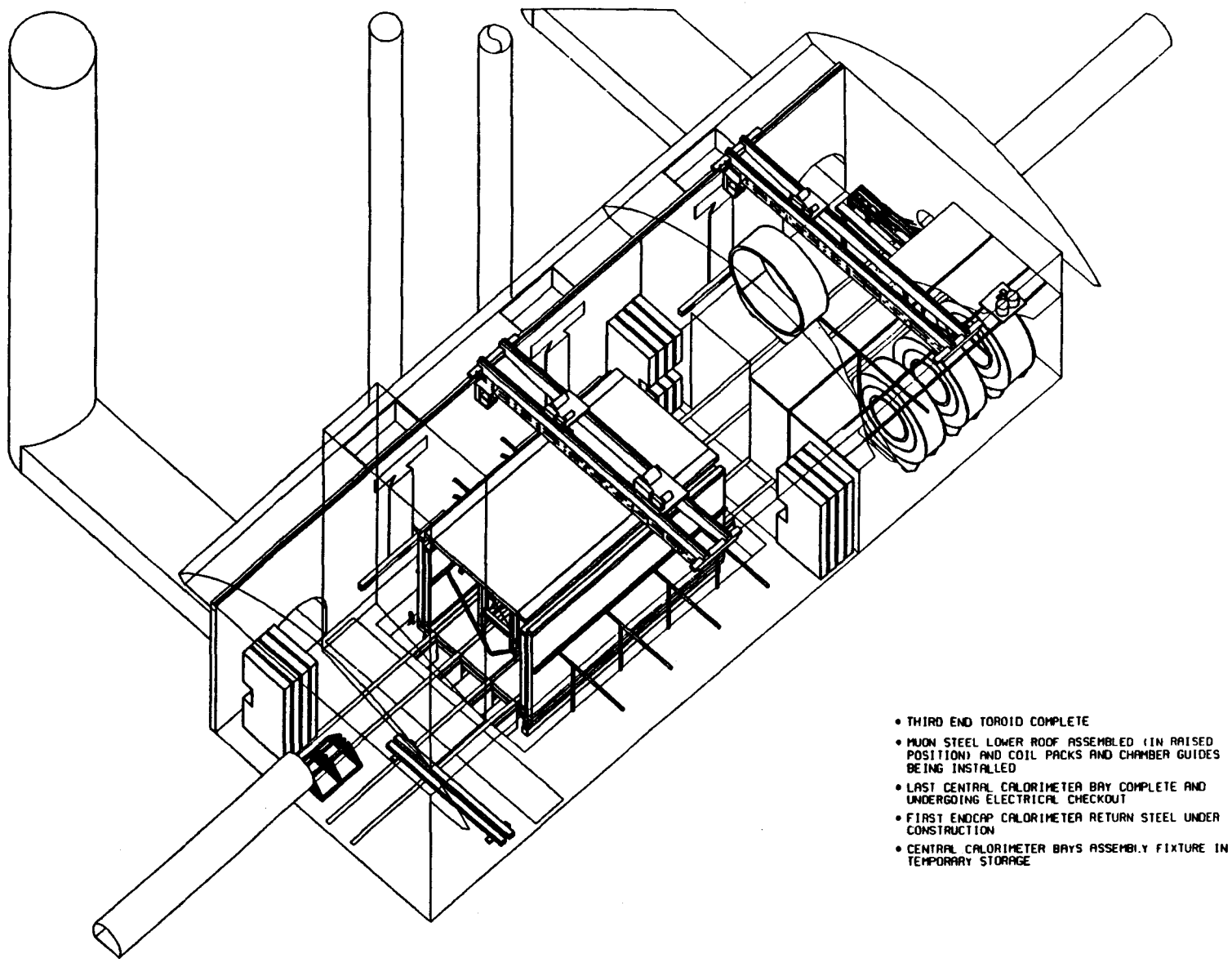

Figure 3.32. Baseline Detector Construction Sequence (Month 15)

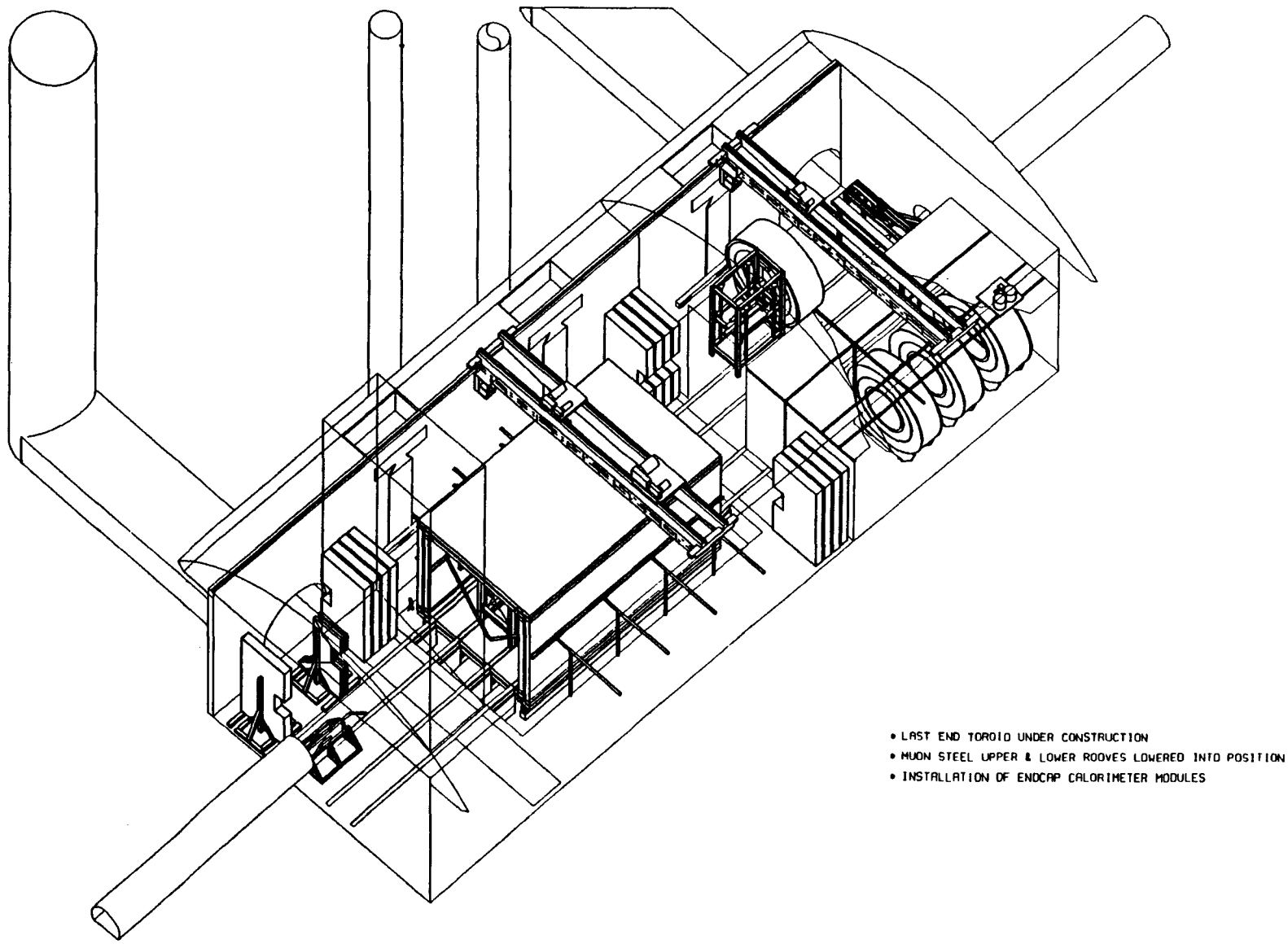

Figure 3.33. Baseline Detector Construction Sequence (Month 18)

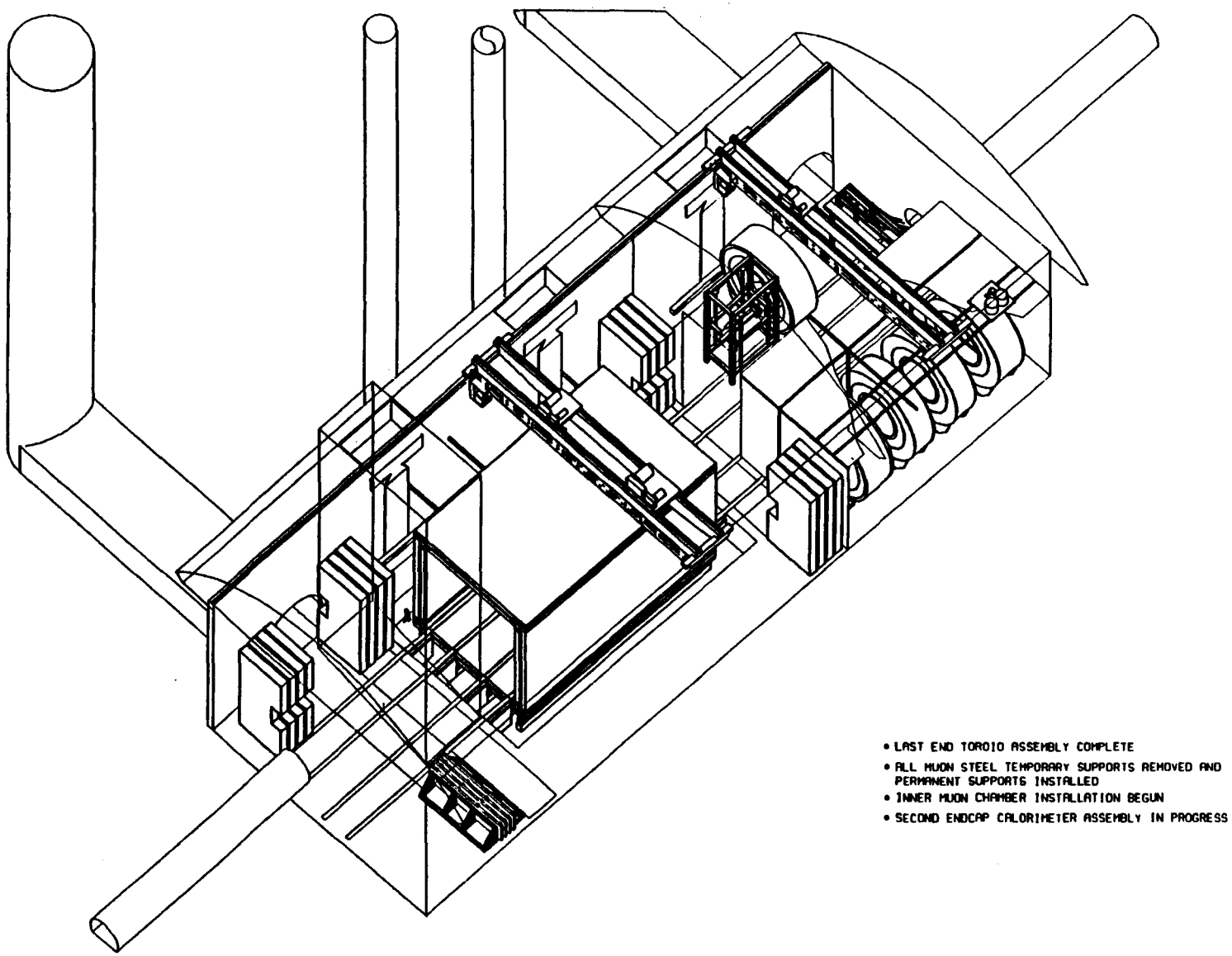

Figure 3.34 Baseline Detector Construction Sequence (Month 21)

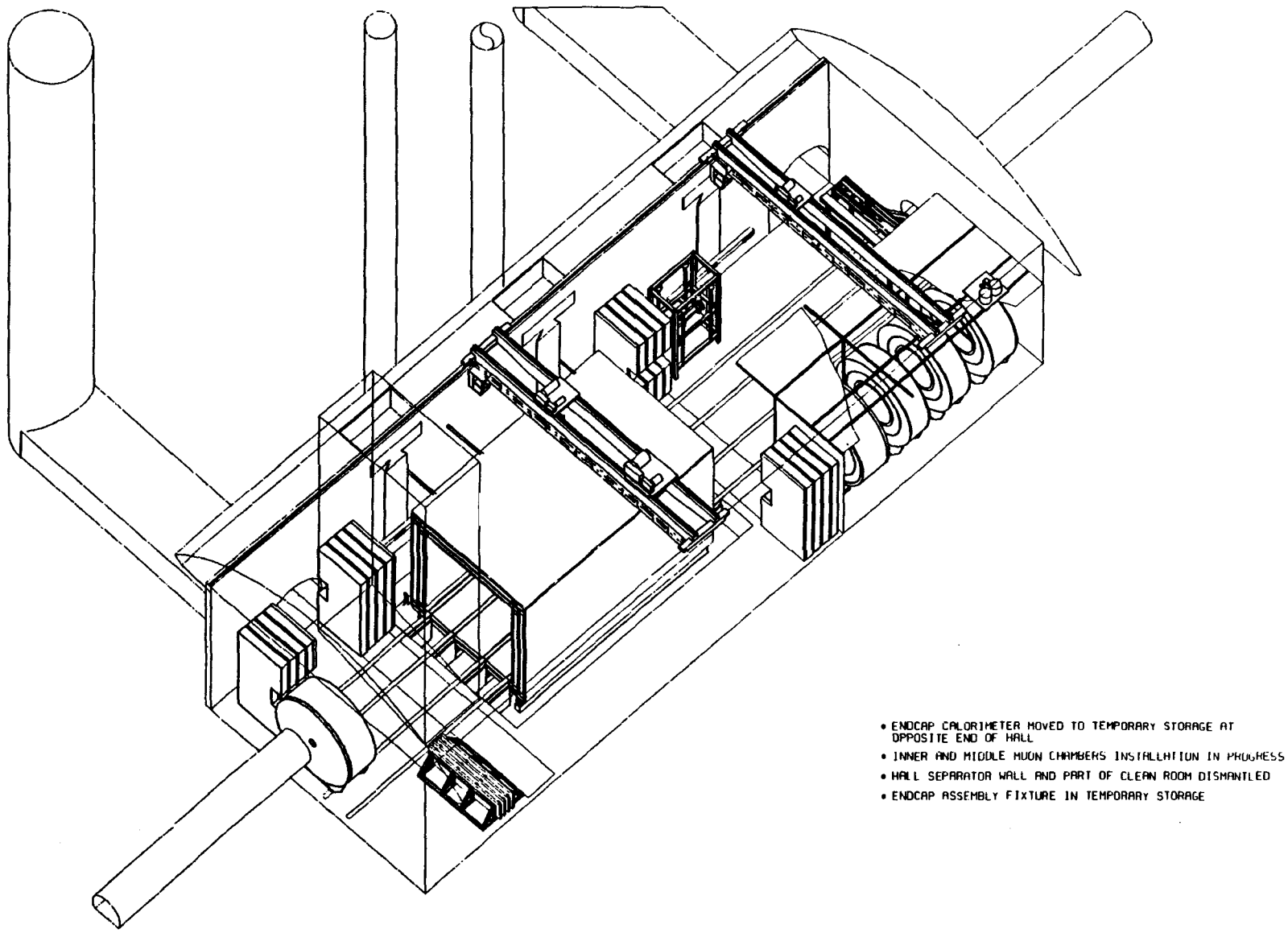

Figure 3.35. Baseline Detector Construction Sequence (Month 23)

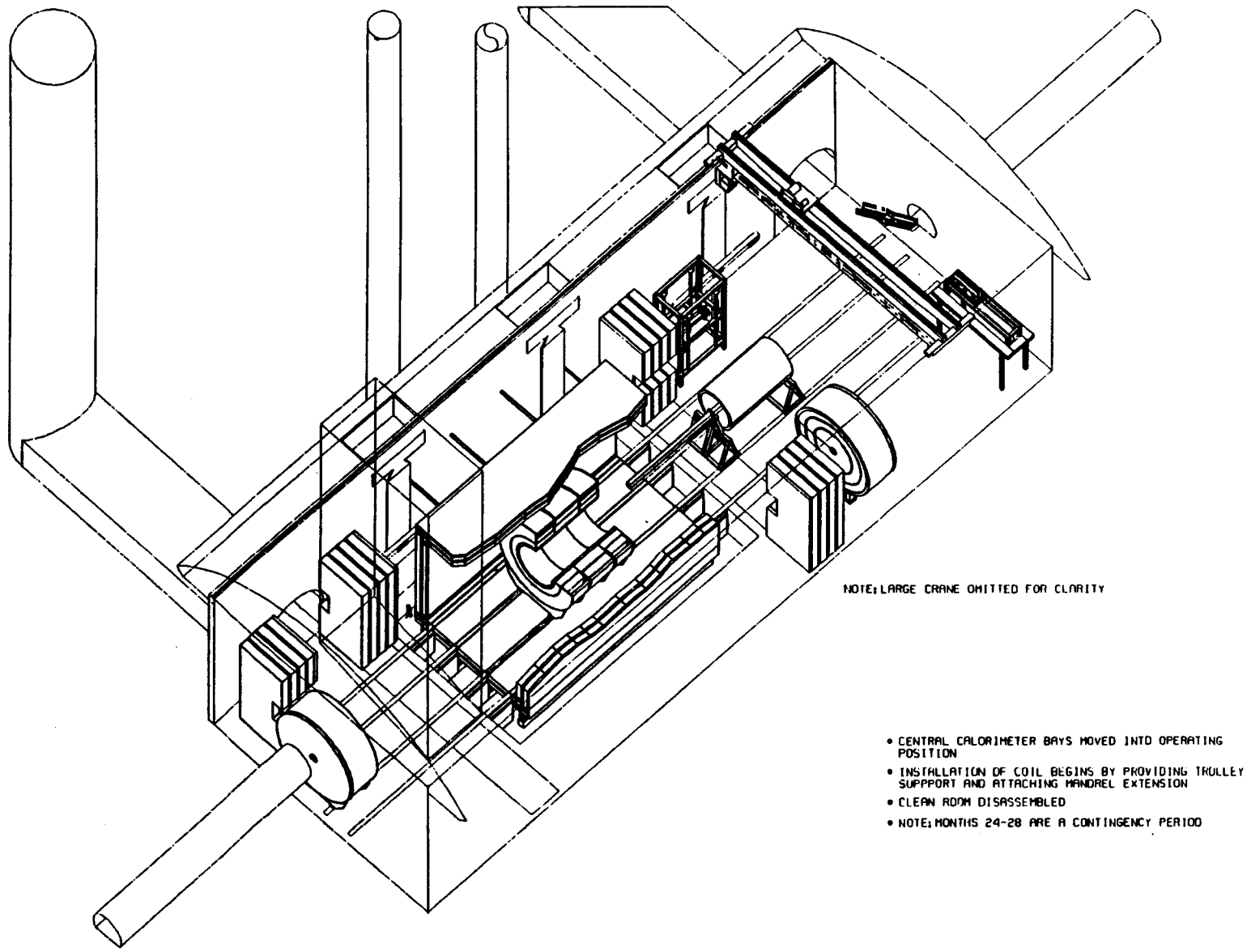

Figure 3.36. Baseline Detector Construction Sequence (Month 30)

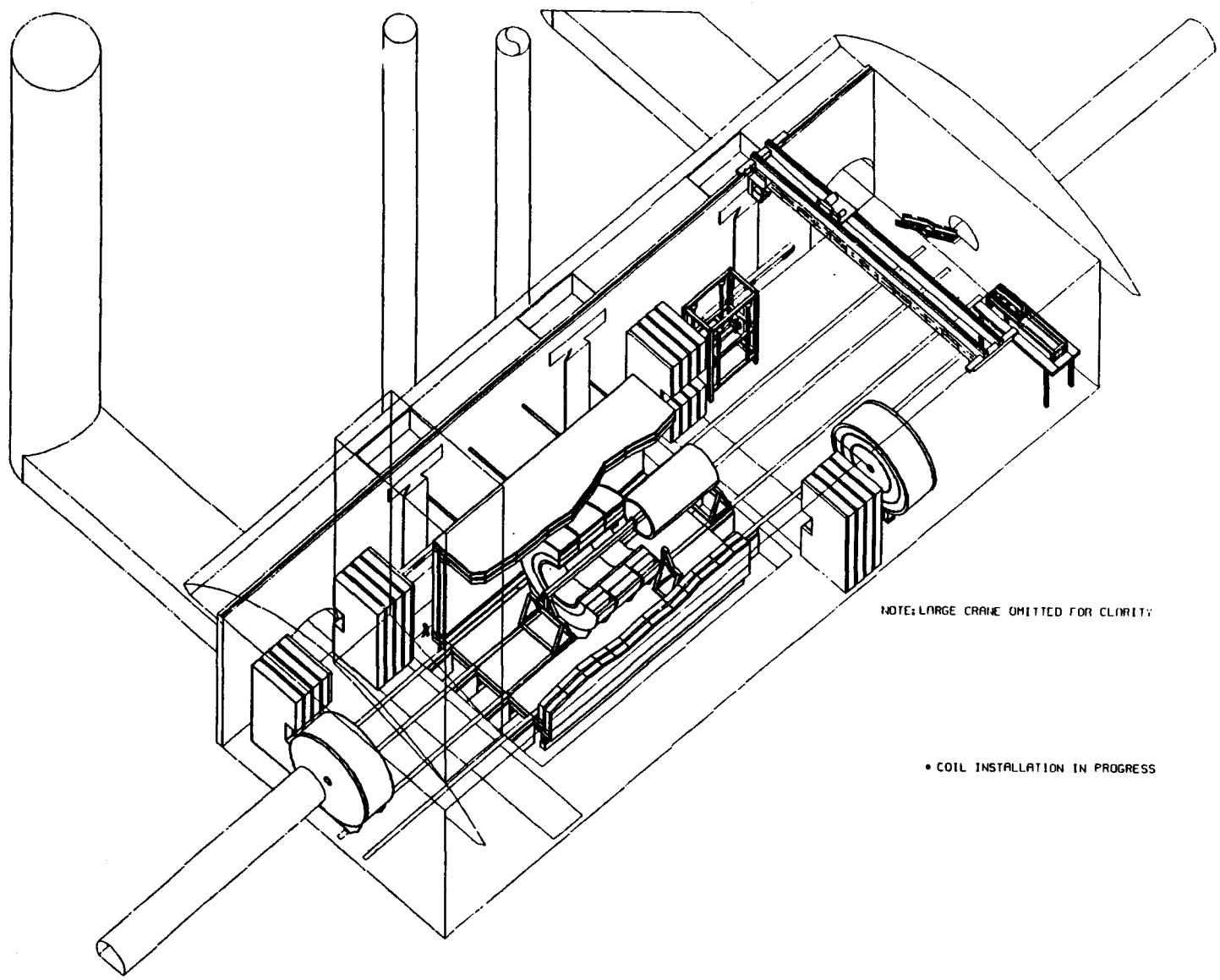

Figure 3.37. Baseline Detector Construction Sequence (Month 30.5)

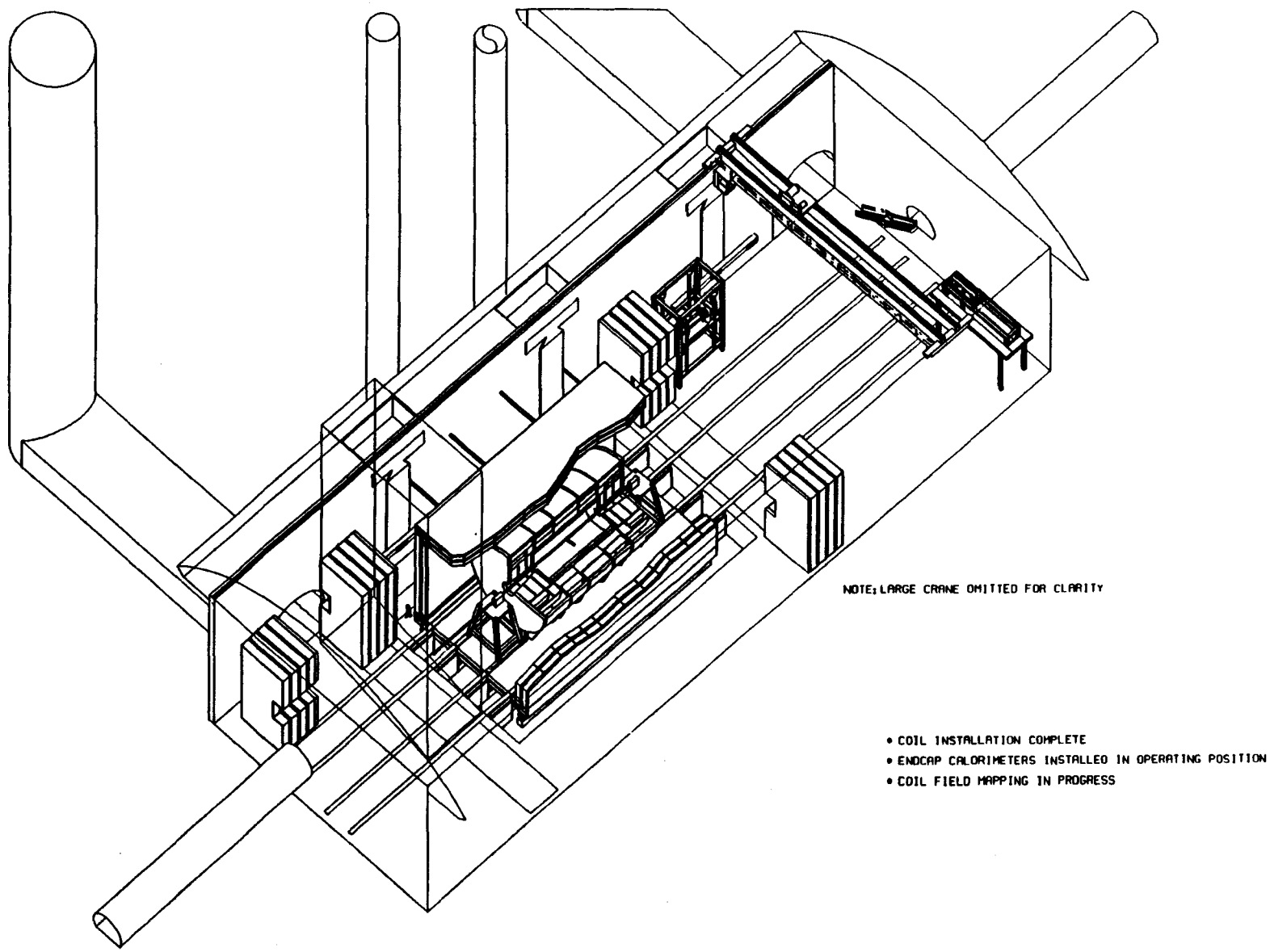

Figure 3.38. Baseline Detector Construction Sequence (Month 33)

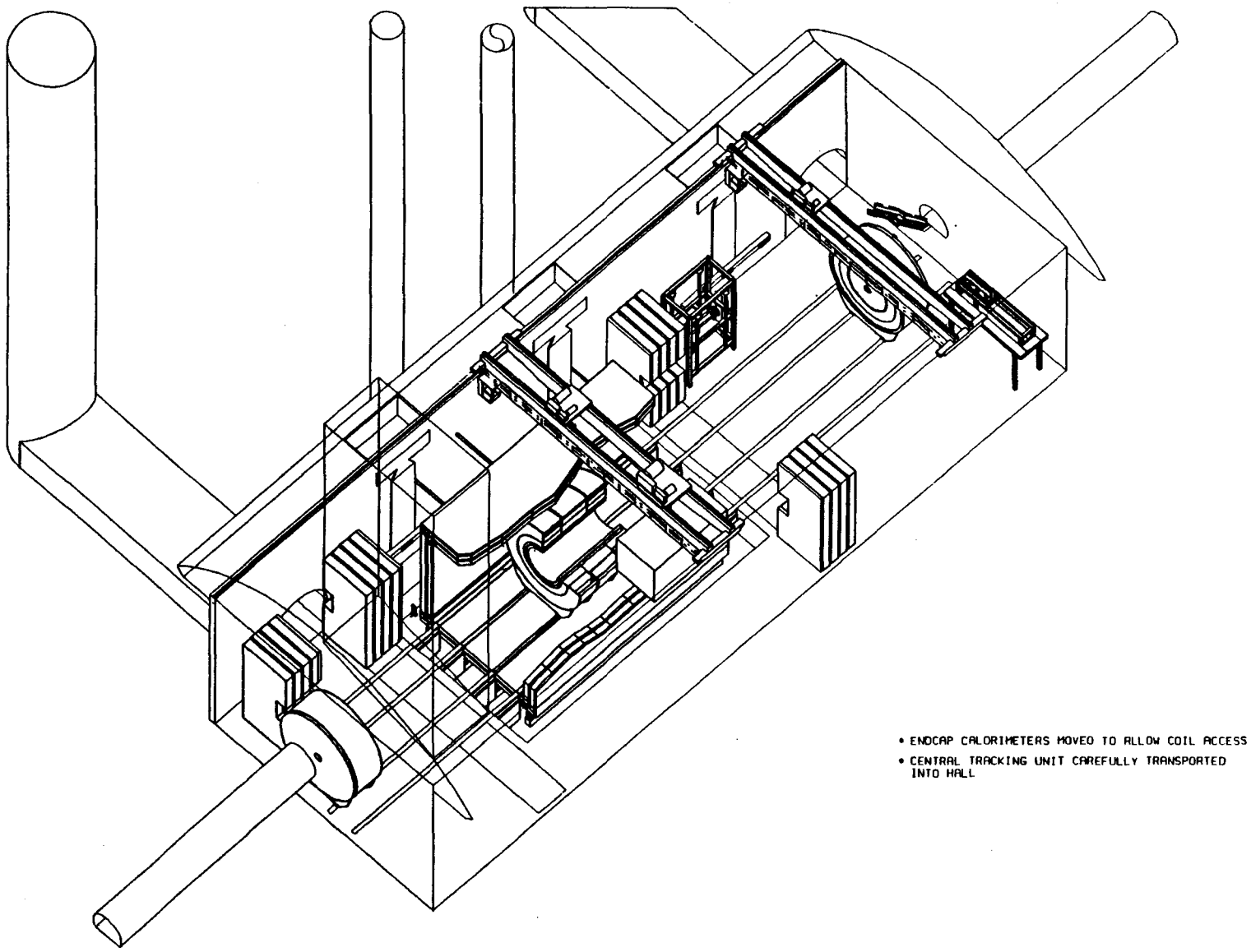

Figure 3.39. Baseline Detector Construction Sequence (Month 36)

central tracking unit is lowered into the detector hall via the construction shaft. There is sufficient clearance to transport the unit over the detector to the far end of the hall.

Figure 3.40 shows installation of the central tracking unit during month 36 using methods similar to those employed during the coil installation.

The final installation of the endcap calorimeter bays and the muon end toroids occurs at month 38 (Figure 3.41).

During month 40 (Figure 3.42), construction progresses with installation of the accelerator magnets, the outer muon chambers, and the forward calorimeters. Construction is complete at month 42 (Figure 3.43).

3.5 Disassembly and Repair Sequences

Two major repair procedures are simulated: replacement of an endcap calorimeter module, and repair of the silicon tracking unit. A primary concern is the space required to achieve these repairs. These procedures are considered to be worst-case scenarios.

3.5.1 Minor Repairs

The detector has been conceptualized so that minor repairs can be made without having to break the beam tube.

Figure 3.44 shows the detector open for minor repairs. The procedure is as follows: First, the forward calorimeter opens in two halves and moves out of the way. Second, the muon toroids move back as far as possible without interfering with the magnet support system. Third, the calorimeters move back 1 m or more, allowing access to most electronics in the detector.

3.5.2 Endcap Calorimeter Module Replacement

An endcap calorimeter module replacement is shown in Figures 3.45 through 3.47. The endcap at the near end of the hall is chosen because of the smaller working area available at that end of the hall. It is apparent that if the procedure can be accomplished here, it can also be accomplished at the opposite and larger end of the hall. We first investigated whether it is possible to perform this repair without disassembling the beam pipe. In this case, after the forward calorimeter and end toroids have been removed, the endcap calorimeter is pulled out as far as allowed by the accelerator magnets. This places the endcap in the hall, where crane coverage is possible. However, removal of a calorimeter module requires the same fixture used to assemble the unit, and positioning and maneuvering of this fixture is difficult with the beam pipe in place. Also crane coverage, which is necessary to remove the module from the disassembly fixture, becomes limited with both the endcap and its disassembly fixture in place. For these reasons we decided to perform the repairs off the beamline. The repairs are accomplished in the area adjacent to the detector and underneath

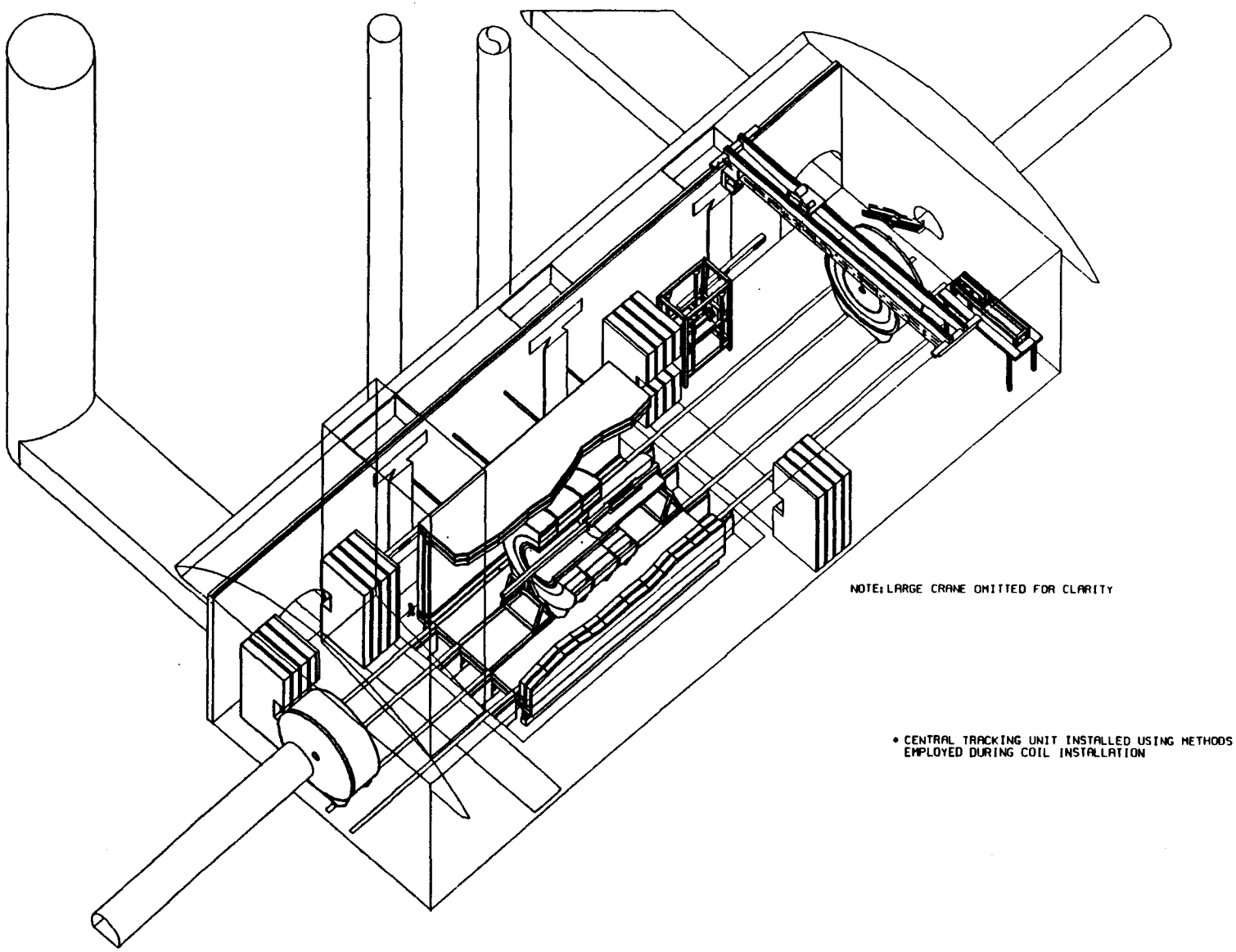

Figure 3.40. Baseline Detector Construction Sequence (Month 36.5)

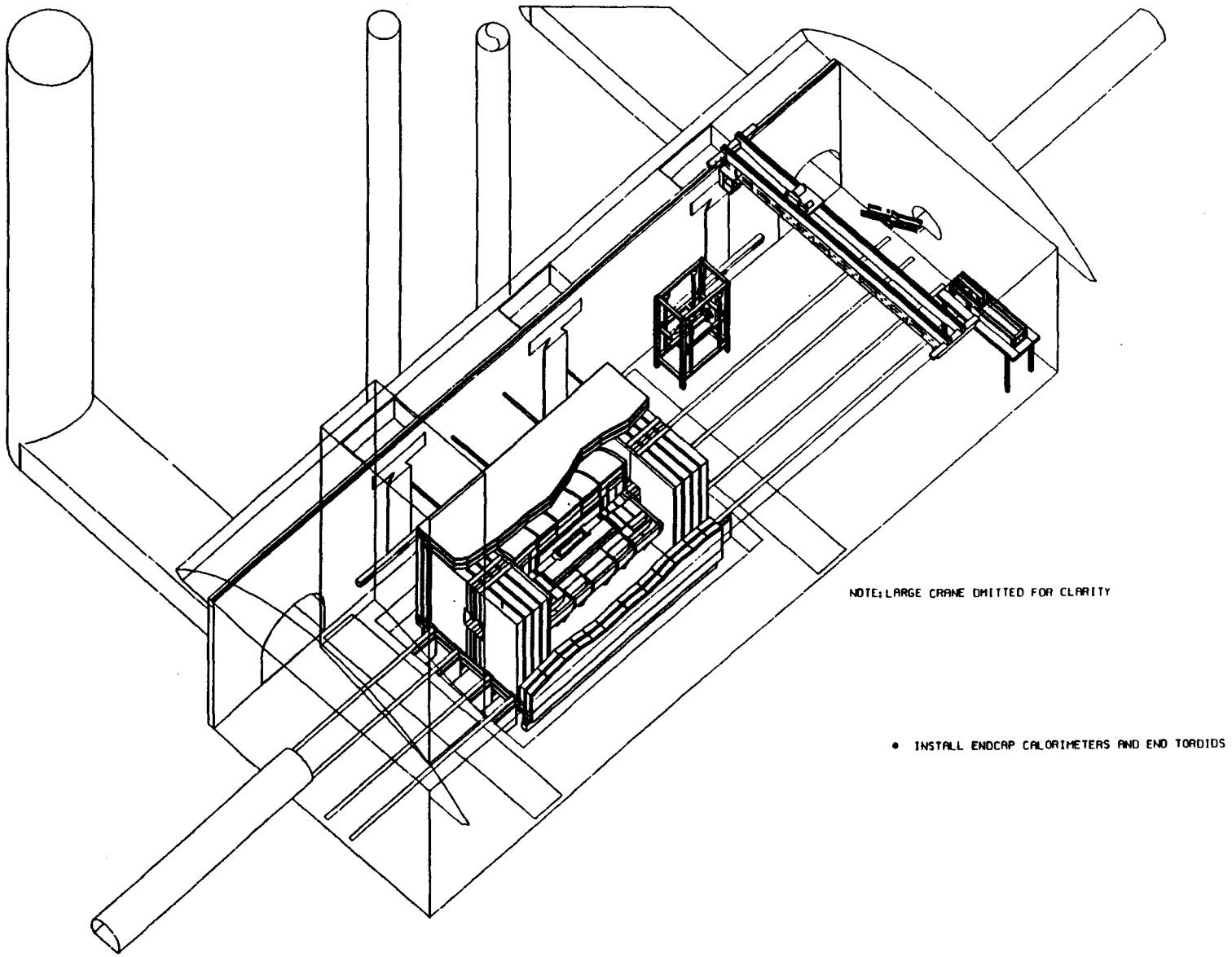

Figure 3.41. Baseline Detector Construction Sequence (Month 38)

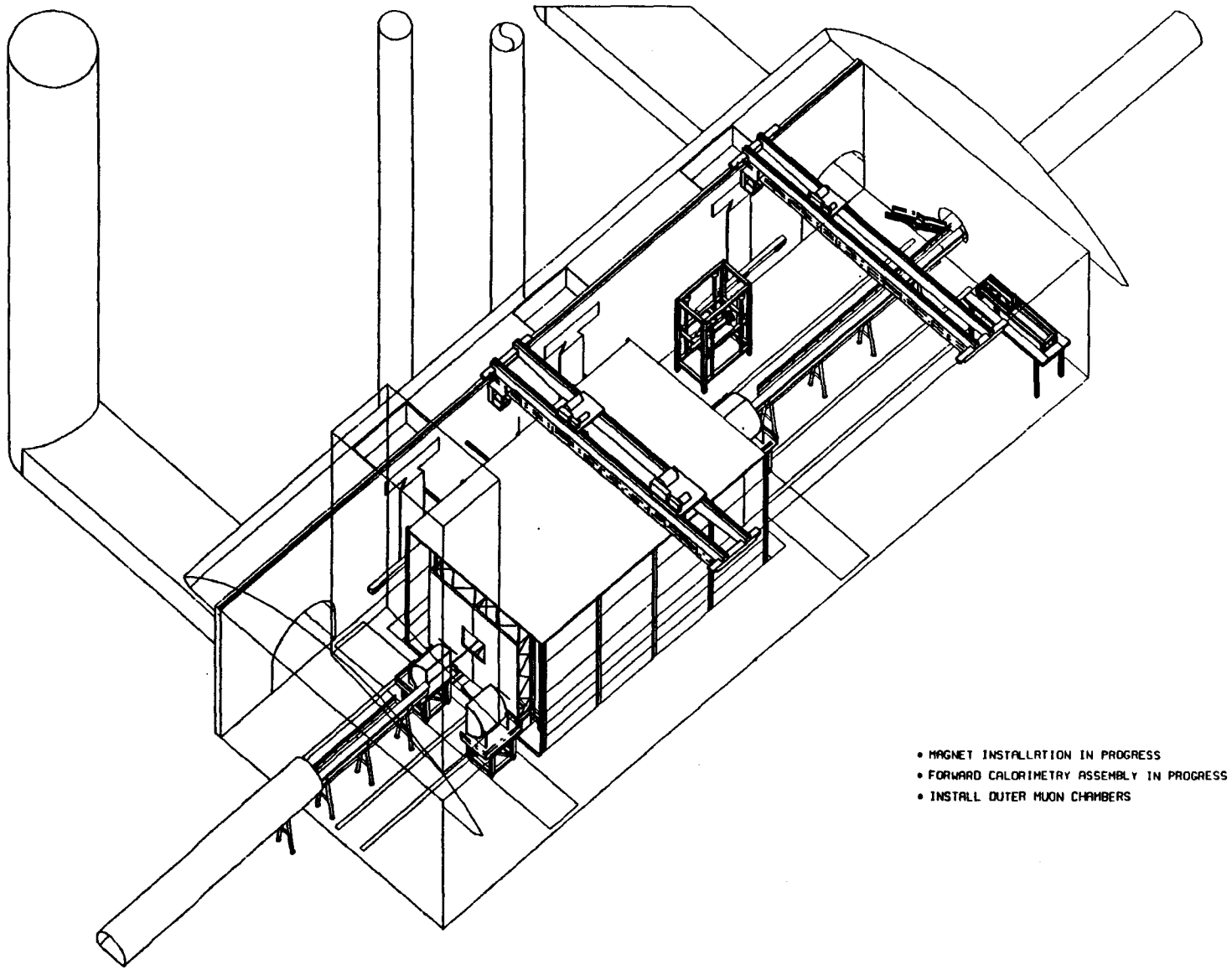

Figure 3.42. Baseline Detector Construction Sequence (Month 40)

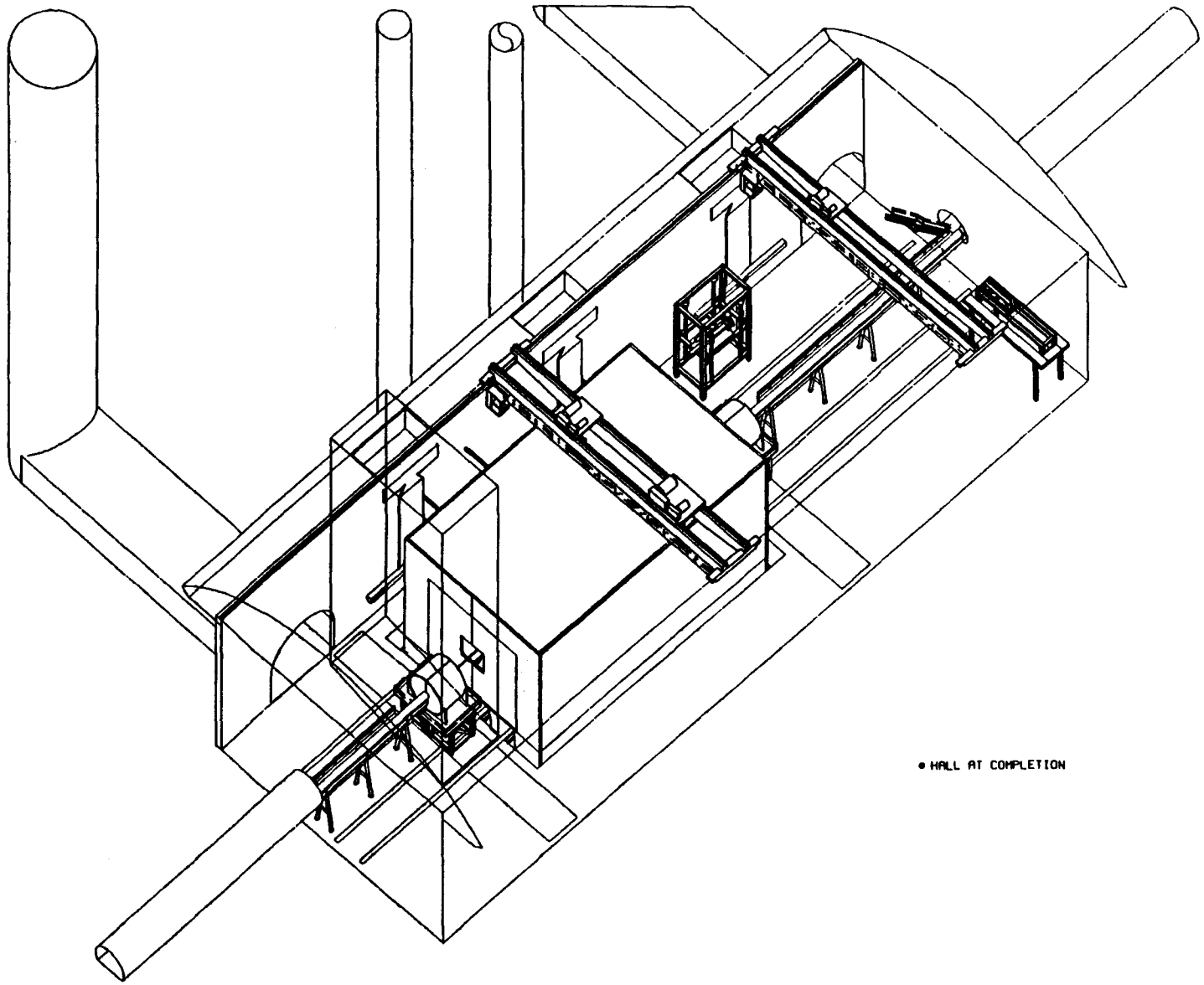

Figure 3.43. Baseline Detector Construction Sequence (Month 42)

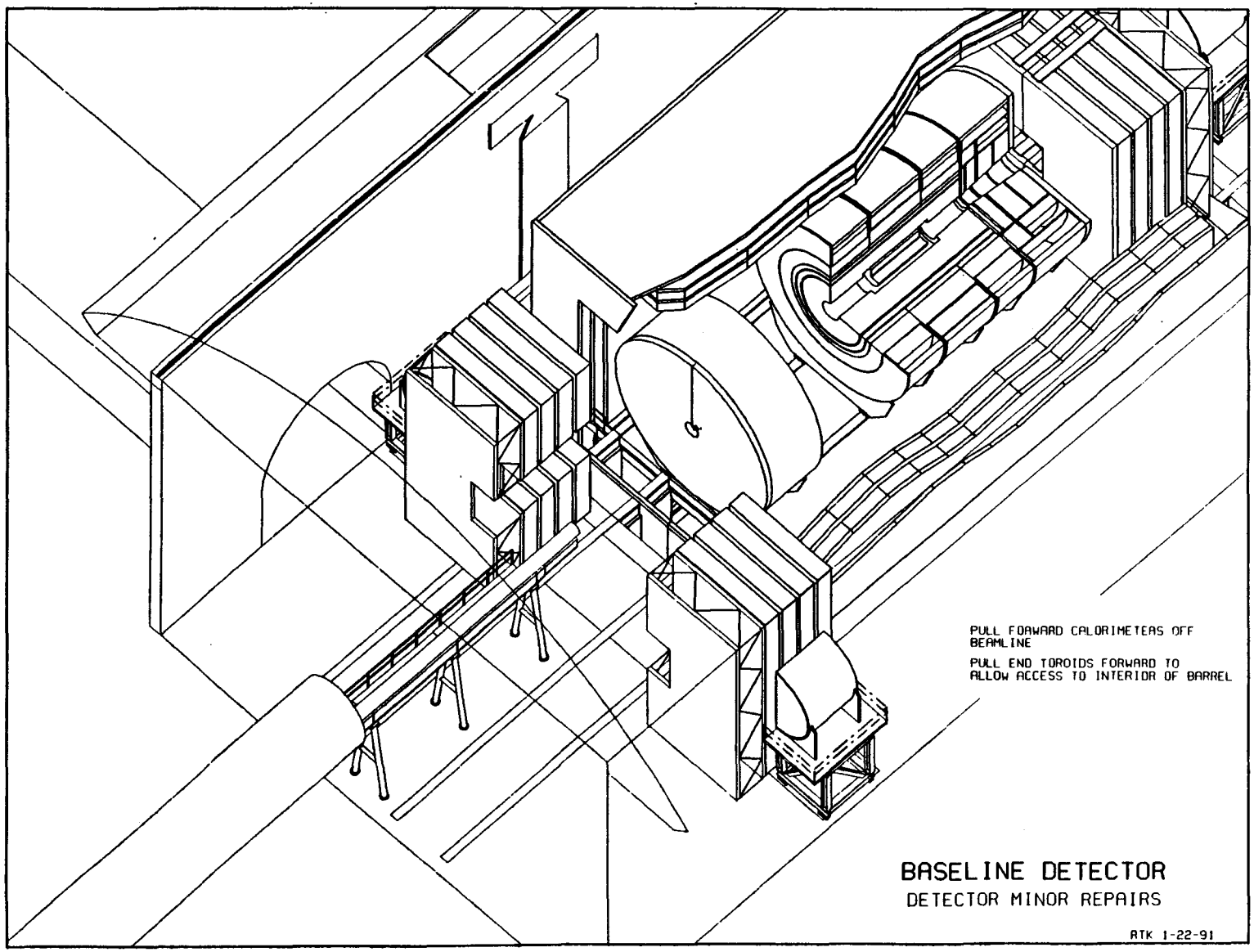

Figure 3.44. Baseline Detector—Minor Repairs

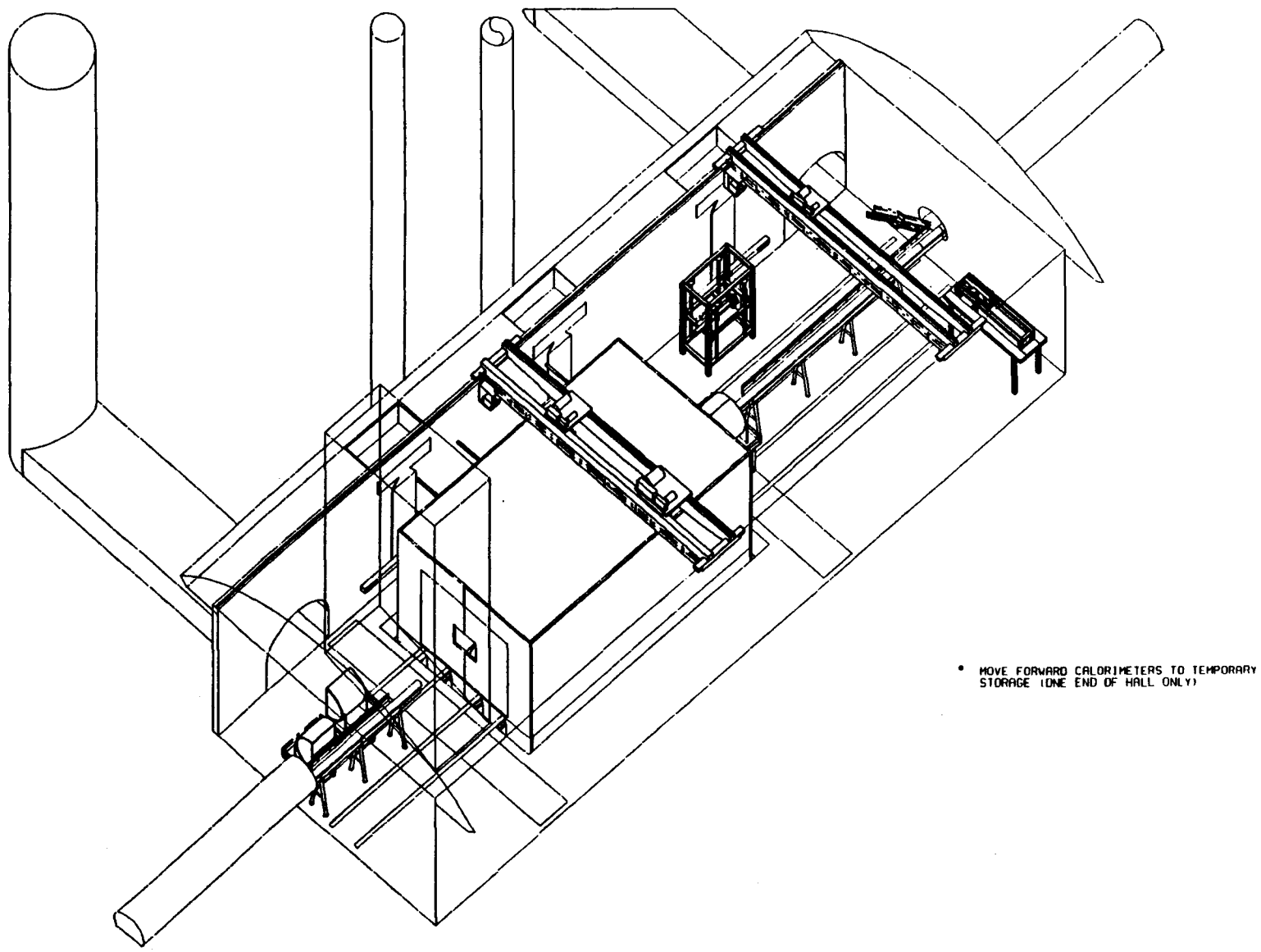

Figure 3.45. Baseline Detector—Endcap Calorimeter Module Replacement (Step 1)

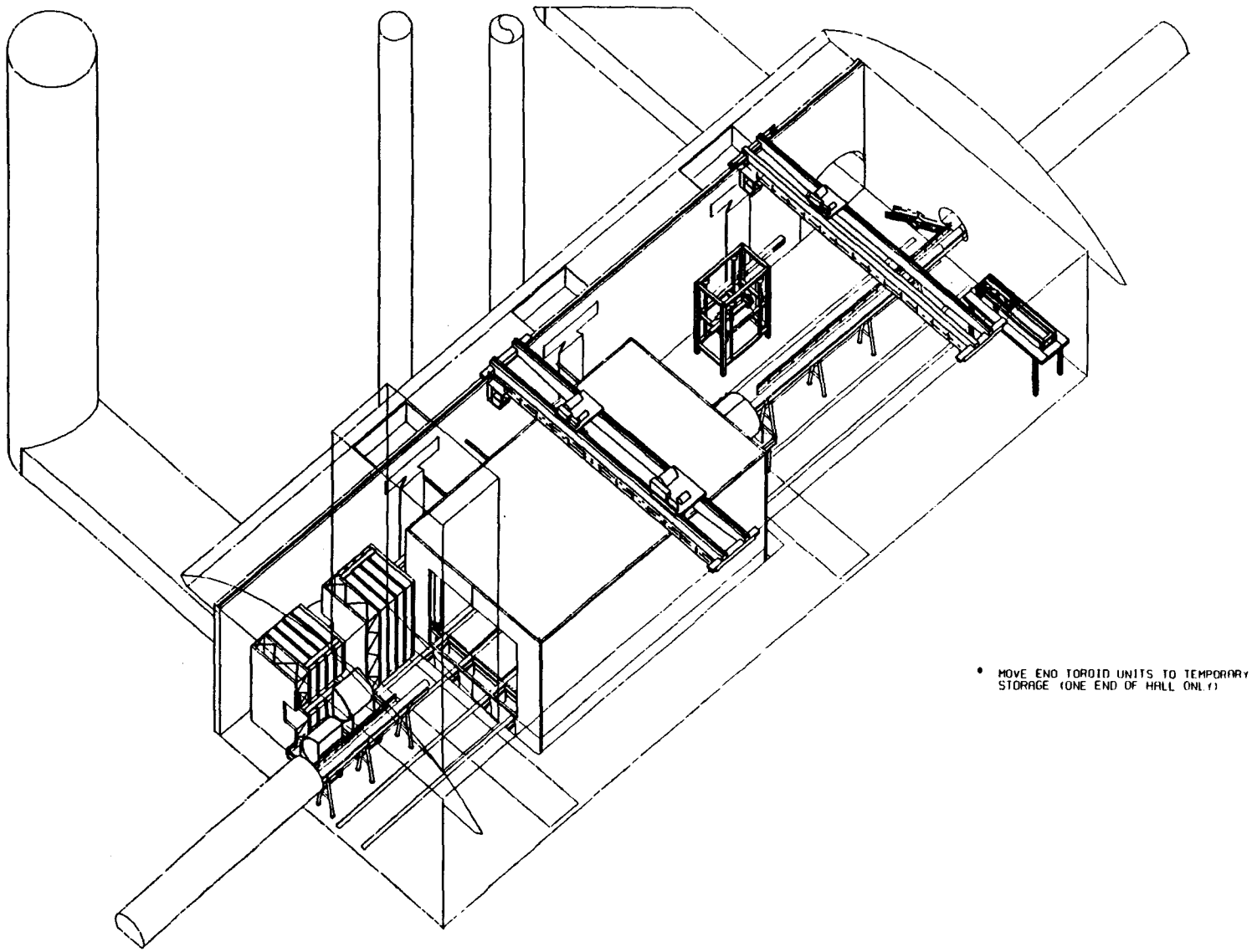

Figure 3.46. Baseline Detector—Endcap Calorimeter Module Replacement (Step 2)

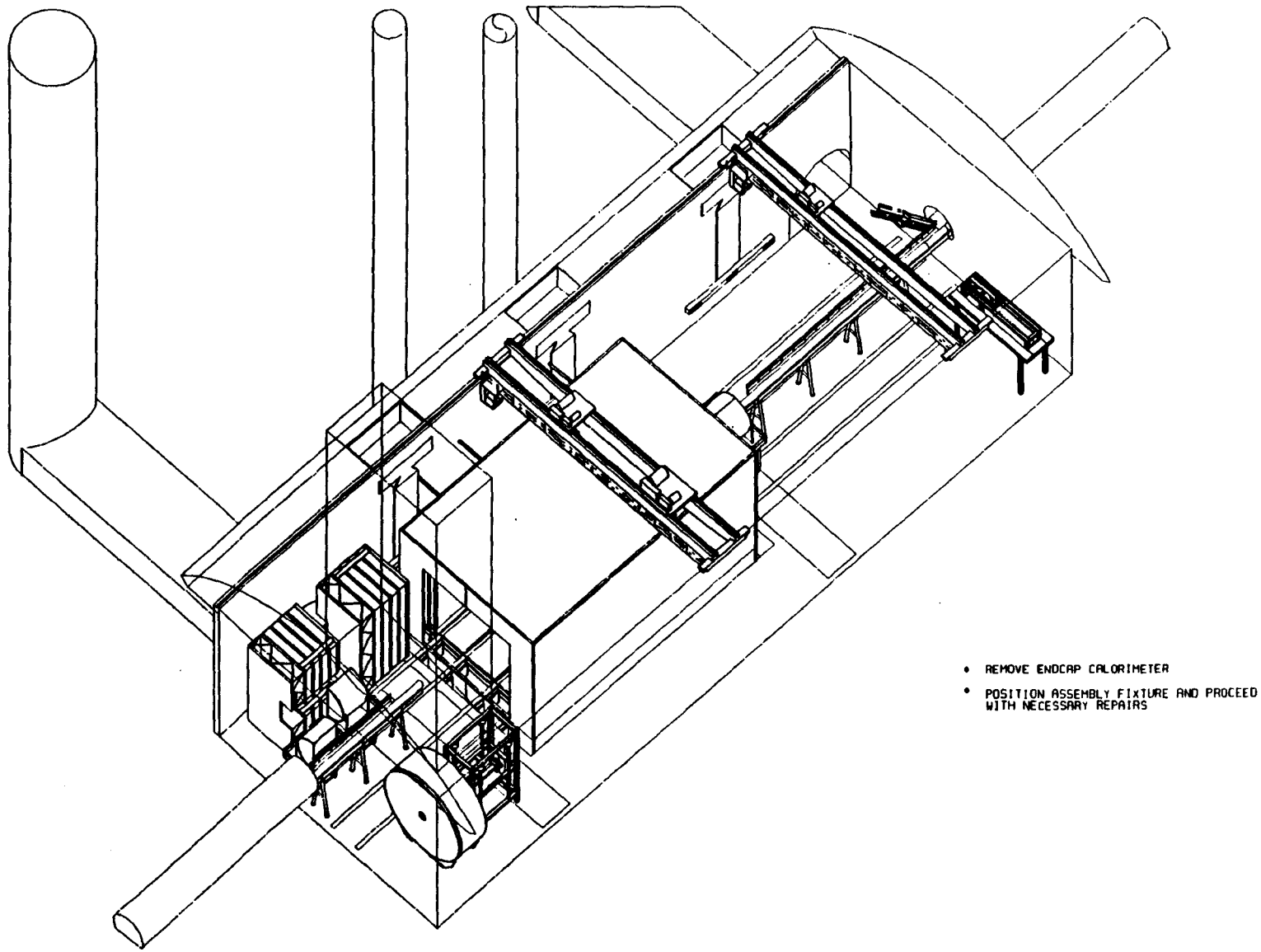

Figure 3.47. Baseline Detector—Endcap Calorimeter Module Replacement (Step 3)

the construction shaft (which area is available). The forward calorimeters and end toroids are moved to one side of the accelerator magnets, and the endcap is then brought into the hall. The disassembly fixture can now be positioned on either side of the calorimeter and the faulty module removed. Reassembly proceeds in the reverse manner.

3.5.3 Silicon Tracking Repair

Silicon repair is depicted in Figures 3.48 through 3.51. The first step is to remove the forward calorimeters off the beamline and to pull the end toroids out and move them to the sides. The endcap calorimeters are then pulled back as far as the accelerator magnets will allow. Sufficient room is now available between the endcaps and the outermost muon chambers to allow the transport of necessary equipment into the detector. This also provides enough clearance between the outer muon chambers and the endcap to make some crane coverage possible. The next step is to position a fixture (a monorail has been used in this study) to remove the tracking devices. The intermediate tracking units are removed first. The silicon tracker can then be extracted. Since the tracking device weighs only about 270 kg, it can be lowered onto a cart and rolled out into the hall if necessary. Reassembly proceeds in the reverse manner.

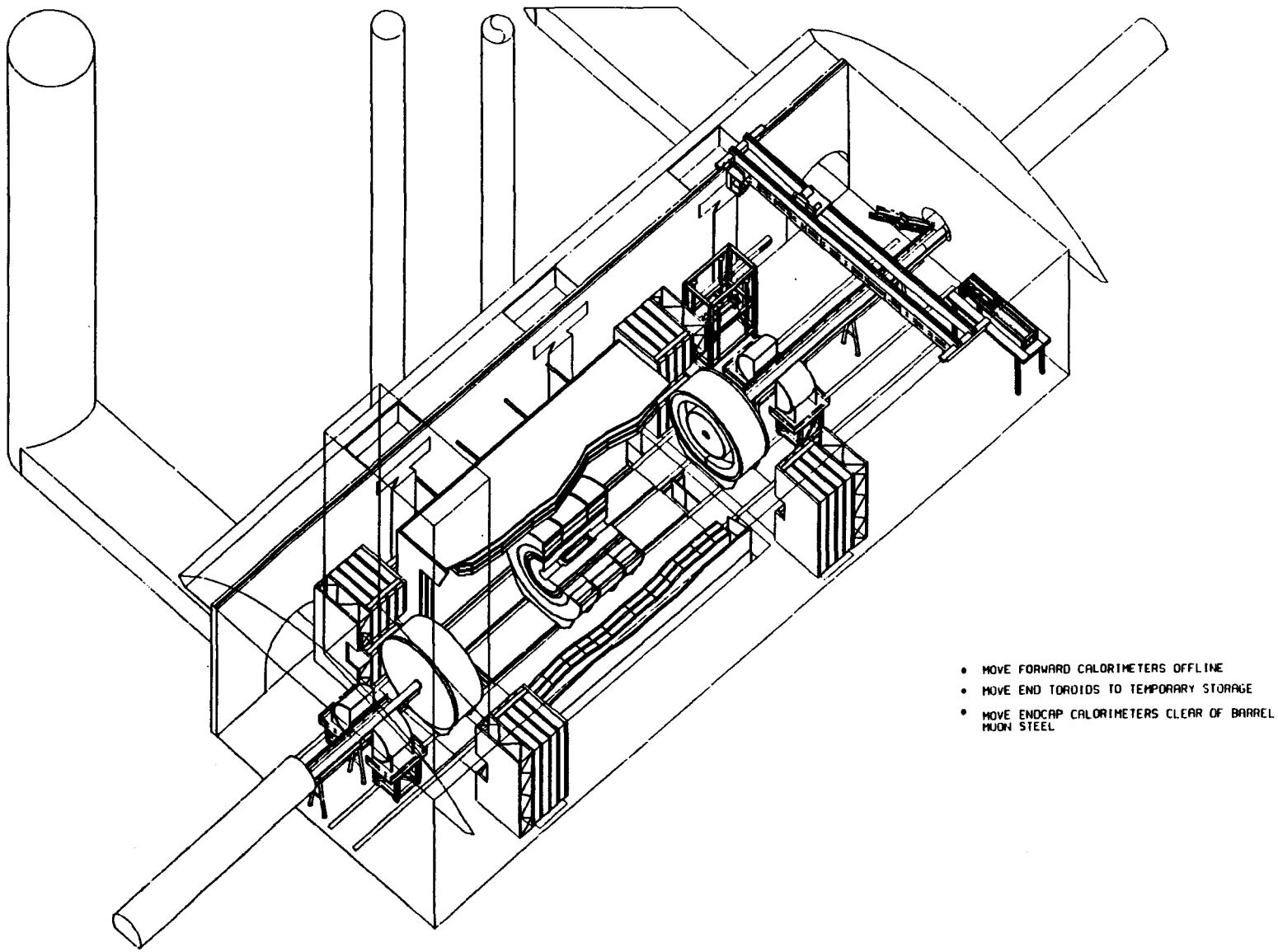

Figure 3.48. Baseline Detector—Silicon Tracking Repair (Step 1)

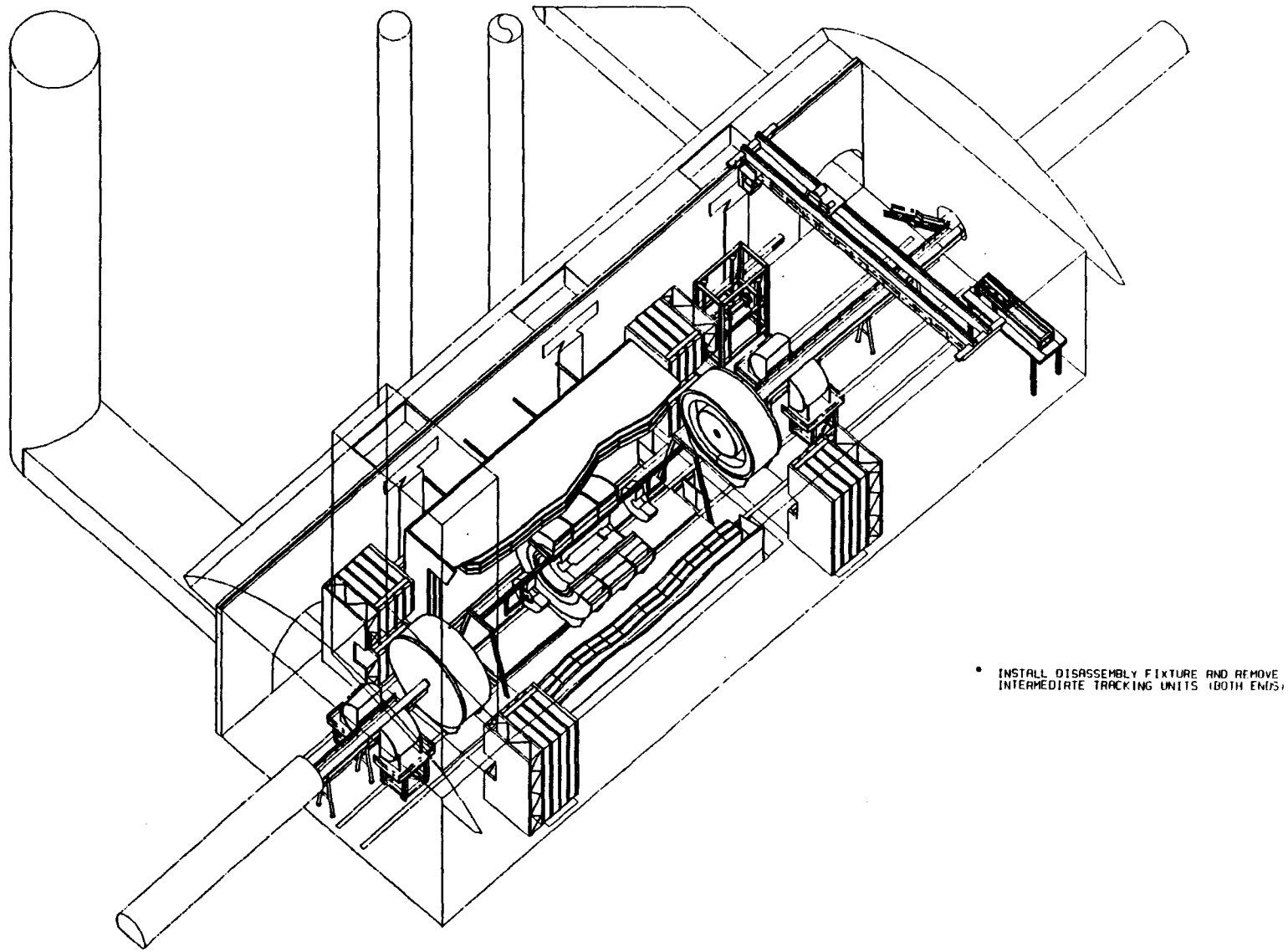

Figure 3.49. Baseline Detector—Silicon Tracking Repair (Step 2)

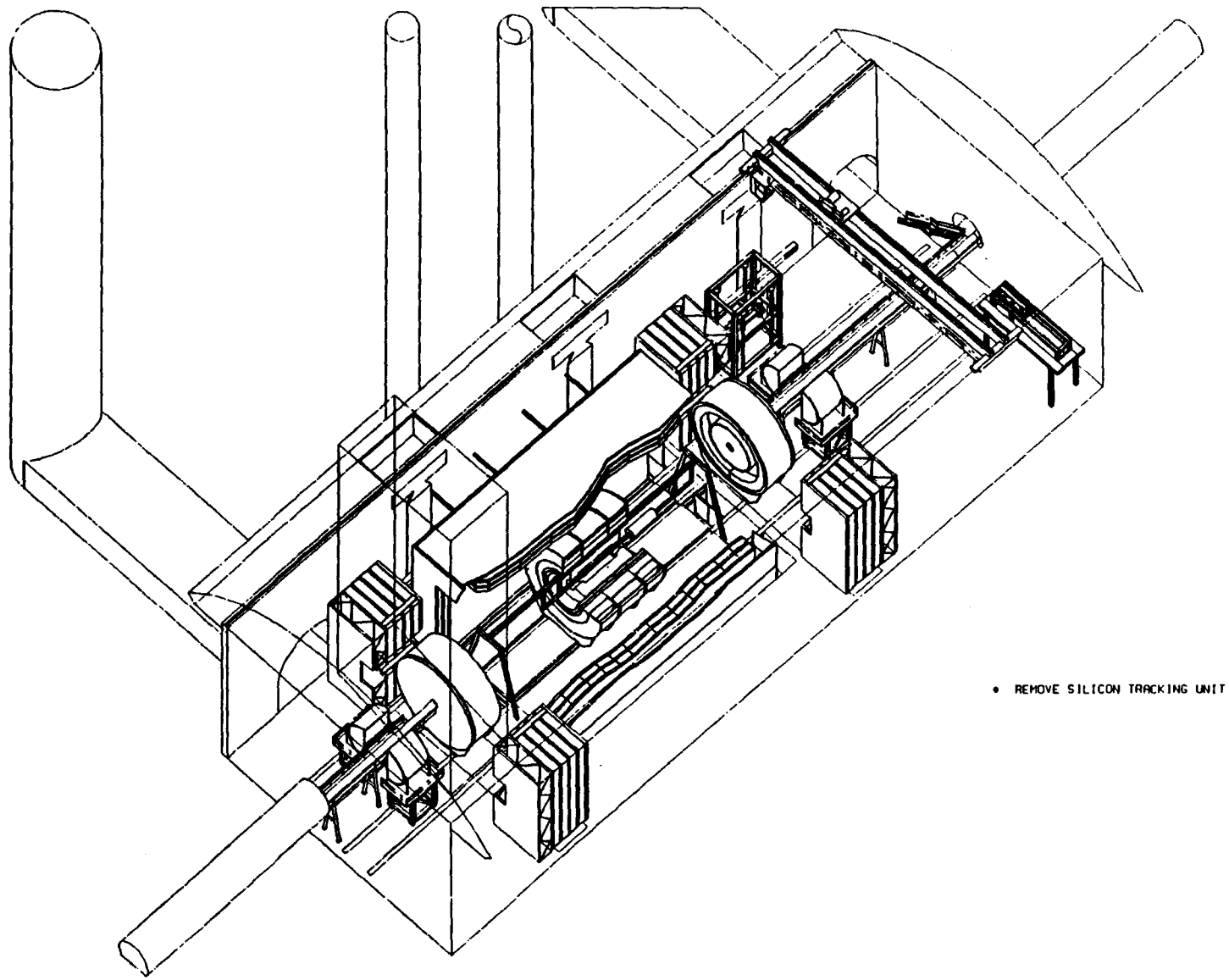

Figure 3.50. Baseline Detector—Silicon Tracking Repair (Step 3)

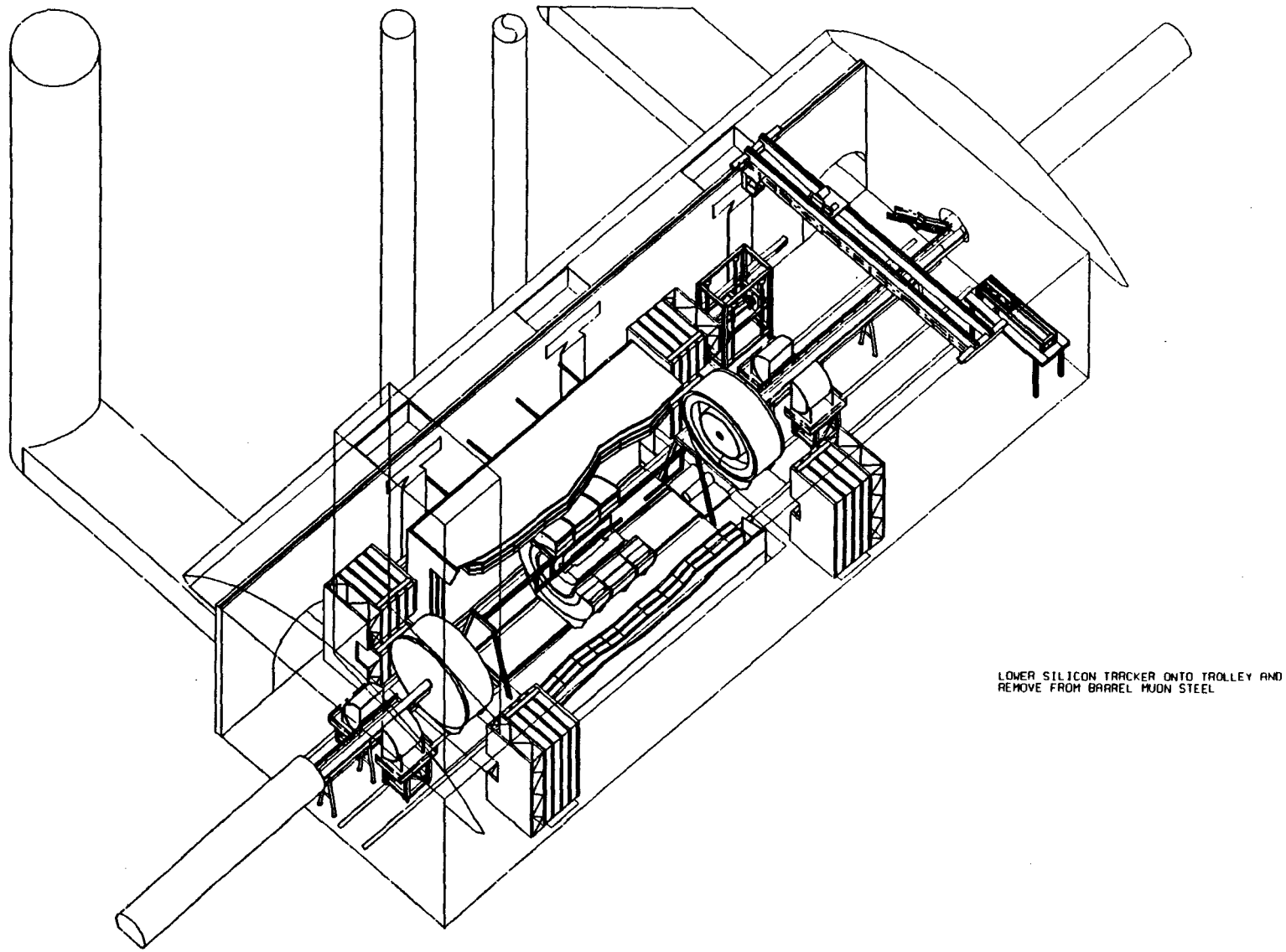

Figure 3.51. Baseline Detector—Silicon Tracking Repair (Step 4)

4.0 AIR CORE TOROID DETECTOR

4.1 Air Core Toroid Detector Description

In this chapter we discuss the Air Core Toroid (ACT) detector, so named because of a pair of superconducting toroids in the endcap region. A three-dimensional view of the detector is shown in Figure 4.1, and a cross-section and elevation view are shown in Figures 4.2 and 4.3, respectively.

We describe this detector starting with the tracking system and working outward. The tracking system is divided into a silicon inner tracker and an outer tracker. The outer tracker is further divided into central and intermediate regions. These three elements arrive as an assembled subsystem; we consider them only from the point of view of installation, testing, and maintenance. The solenoidal coil design is based on an "air-core" or short solenoid design.[1] This magnet does not use iron near the ends of the coil, and hence the external forces on the coil cryostat and the calorimeter are dominated by gravity. Any electromagnetic forces between the calorimeter and coil have been ignored.

The calorimeter is loosely based on the Warm Liquid design by EG&G;[2] however, the studies described here apply equally to any self-supporting calorimeter built from "modules" of 20 to 50 tonnes. The calorimeter modules are assembled into five cylindrical bays: three central bays and two endcap bays. Each bay extends about 3 m along the beam line and weighs about 1200 tonnes. One essential ingredient of the calorimeter bays is the inclusion of return iron in the individual calorimeter modules to create a field-free region for electronics or photomultiplier tubes (PMT) on the outside of the calorimeter. About 65% of the flux is returned through the volume of the non-magnetic calorimeter, and the remaining 35% is returned through the steel at the outside of the calorimeter. There are small forward ($5 > |\eta| > 3$) calorimeters for missing energy measurements. These are located just in front of the interaction region quadrupoles.

The calorimeter is surrounded by magnetized iron muon toroids, 1.5 m thick in the barrel region ($|\eta| < 1.5$). The octagonal barrel iron toroid has 2 coils located near each corner, for a total of 16 coils. There are four planes of muon chambers in the barrel region, with two on the outside and two on the inside of the iron. The momentum resolution of the exterior muon system is limited by the position resolution of the chambers and the 1.5-m gap between the two exterior chambers. Charge determination is possible to momenta well in excess of 1 TeV/c. In order to maintain the electronics at the back of the central calorimeter, the innermost muon chamber layer must be moved. This chamber layer is mounted on rails similar to a closet door, so that alternate panels can be moved as necessary to gain access to the back of the calorimeter.

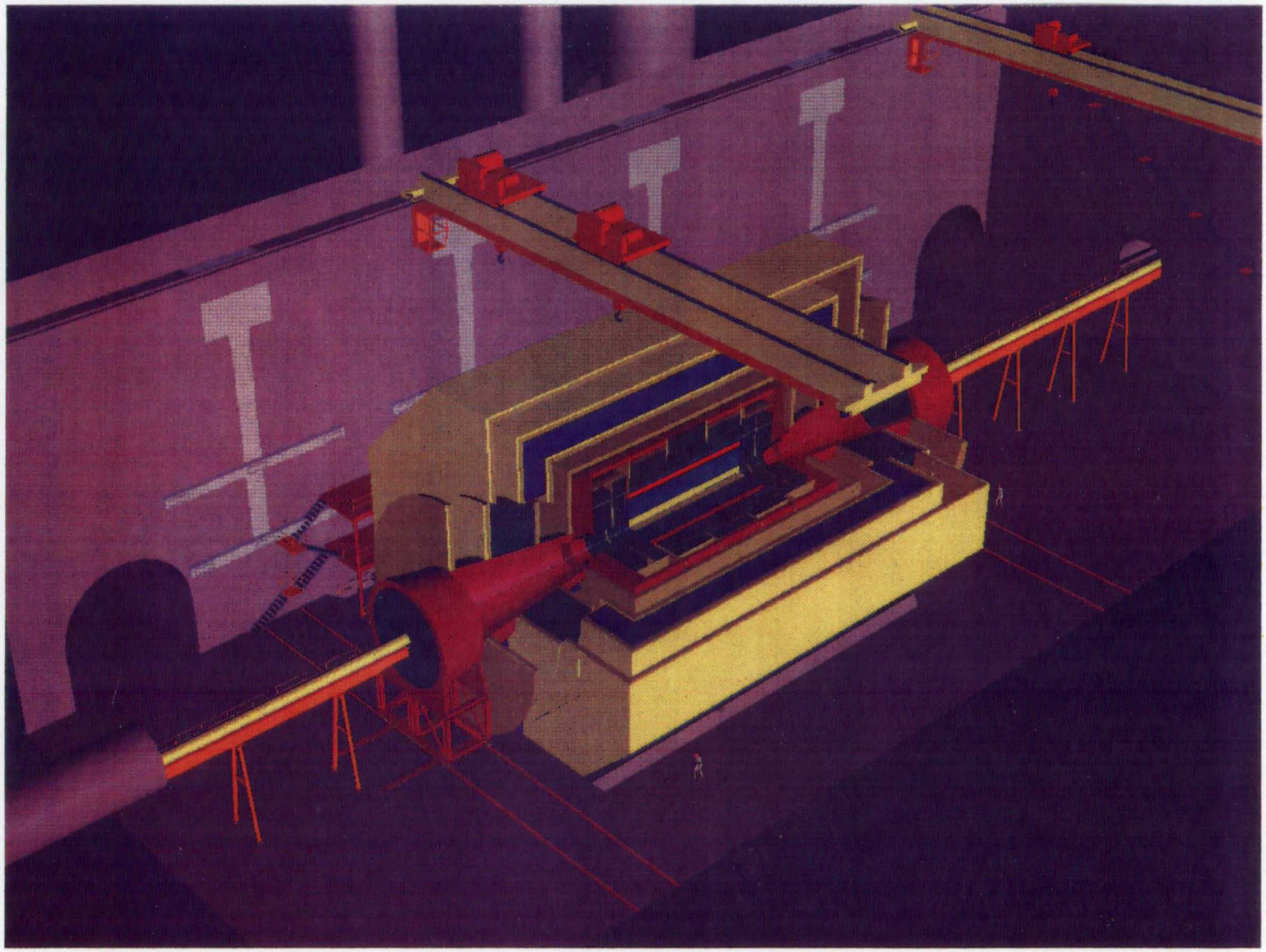

Figure 4.1.Overall ACT Detector Layout (3-D View)

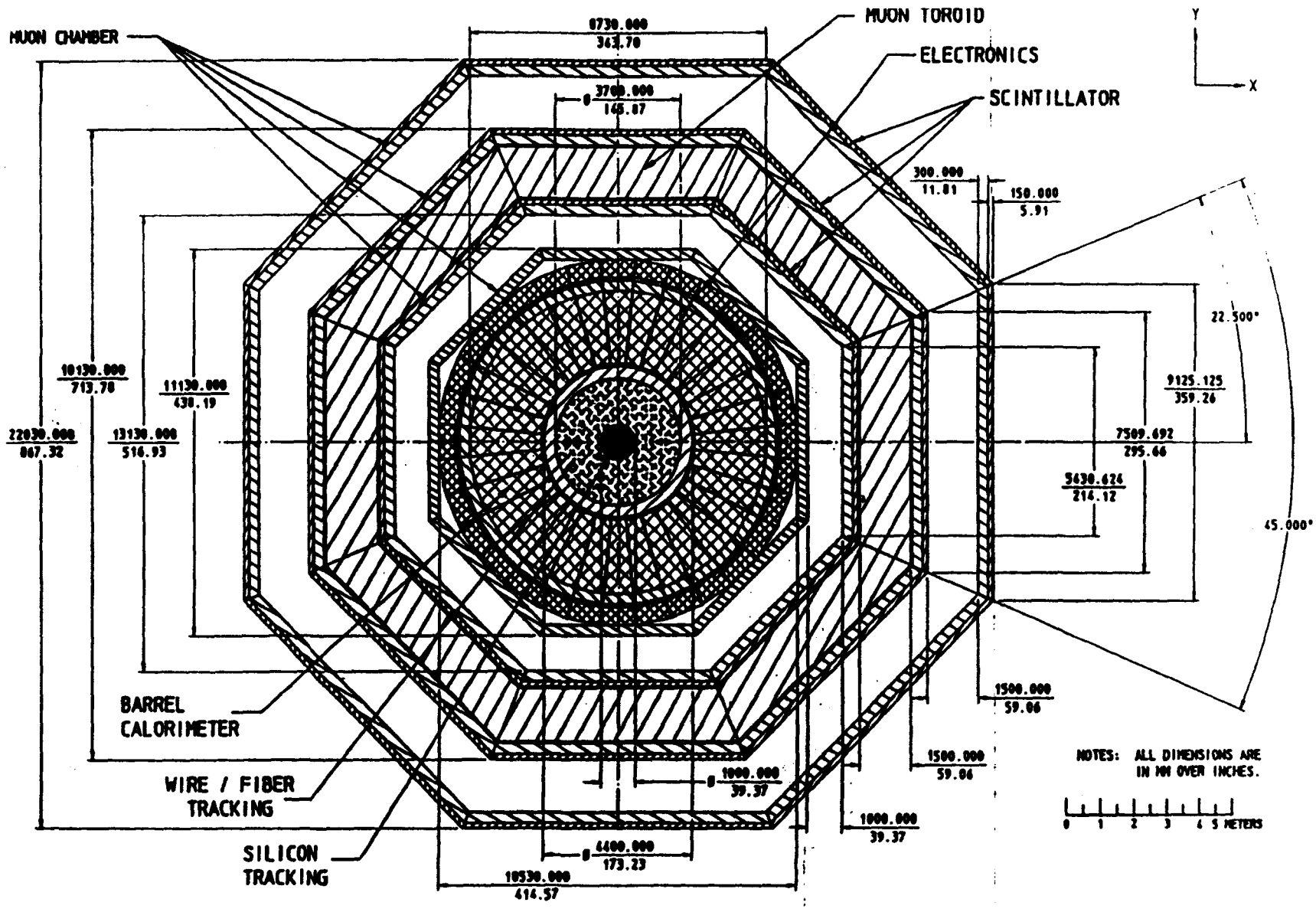

Figure 4.2. Cross-Section of Air Core Toroid Detector

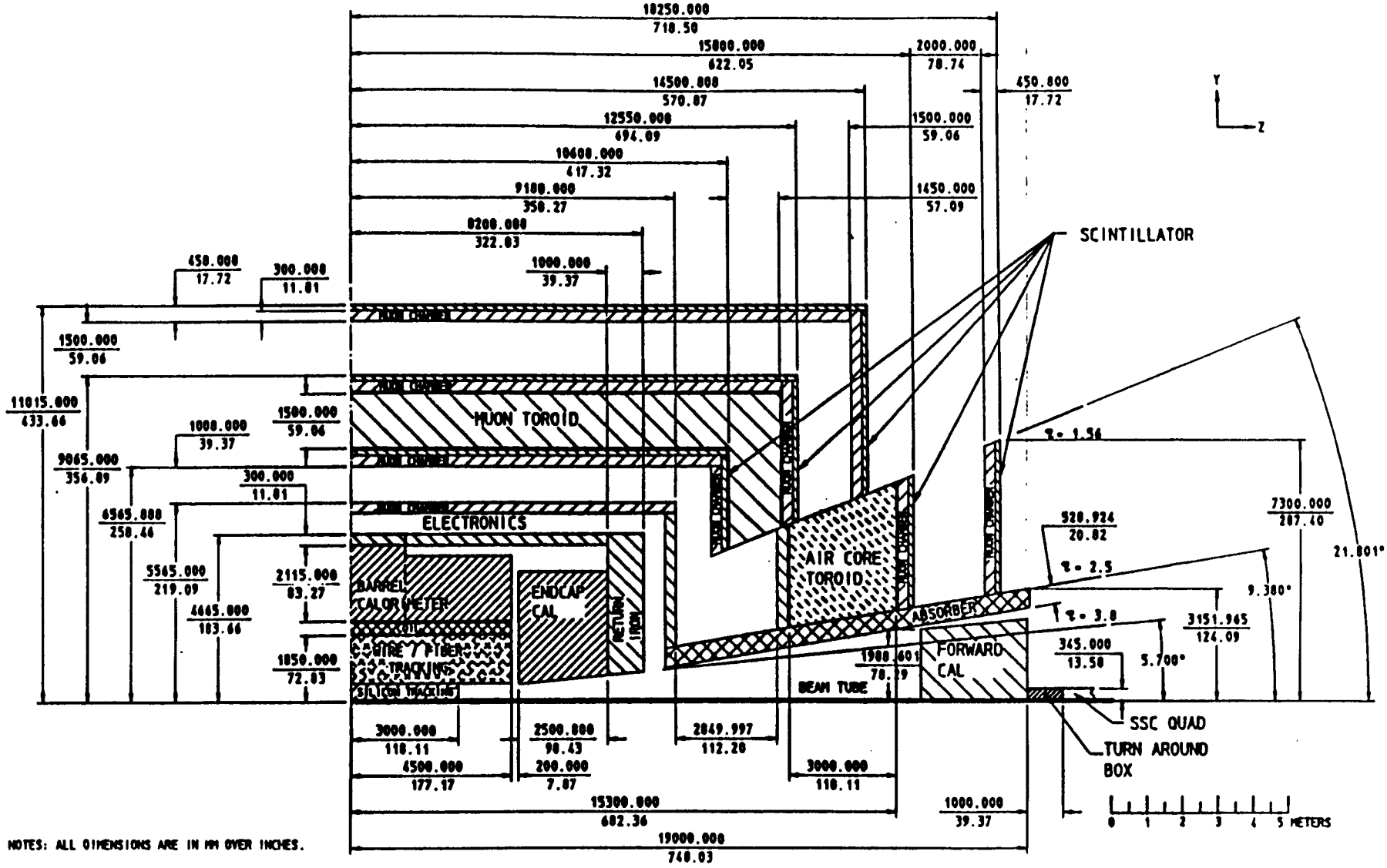

Figure 4.3. Elevation View of Air Core Toroid Detector

The momentum resolution of the central tracking device deteriorates at small angles with respect to the beam line; it is in these forward/backward directions that the most accurate momentum measurement for muons is achieved by the ACTs. In these superconducting magnets, the magnetic field circulates around the beam line, and muon chambers must measure the angle of the track before and after the toroids in the θ direction. Analogous to the barrel region, there are four chamber stations associated with the ACT: two chamber stations in front of the ACTs and two chambers following. These measure the bend angle of muons as they pass through the magnetic field of the toroids.

Three layers of trigger scintillators in the barrel (ACT) region provide a fast trigger for muons. These scintillators crudely measure the bend angle of muons exiting the steel or ACTs.

We anticipate a large flux of low-momentum particles in the forward direction from beam spray, particles escaping from the inside surface of the endcap calorimeters, and albedo from the forward calorimeters. To protect the muon chambers in this area from these low-energy particles, we add a conical absorber layer approximately 50-cm-thick between the ACT and the beam line. The absorber must be designed to intercept both charged and neutral particles, including neutrons. For the purposes of this study we assume the absorber is solid steel, but we expect it will consist of several layers of different materials to provide the optimum neutron absorption.

The ACT detector is logically equivalent to the baseline detector but has slightly different dimensions, capabilities, and technology. The differences are summarized as follows:

- The length of the tracking volume is increased from 8 m to 9 m, to obtain better tracking coverage at small angles with respect to the beam line.
- The barrel iron muon toroids are changed in shape from a square to an octagon. In this configuration the tracking chambers of the muon system more closely approximate ideal cylinders. This improves their position resolution for high-energy (i.e., radial) tracks. Due to maintenance and access considerations, the chamber midway through the steel is eliminated. The separation between the pairs of muon chambers inside and outside the iron toroids is increased to improve the angular resolution, and hence, the momentum resolution of the system.
- Superconducting ACTs replace the endcap iron toroids in order to improve the momentum resolution for muons in the forward direction. This magnet has better analyzing power than the iron magnets, and the lever arms of the chambers are increased to further improve the resolution.
- New muon trigger scintillator layers provide an indication of a penetrating particle early in the trigger logic.

Approximate dimensions and some overall mechanical parameters of the ACT detector are listed in Table 4.1.

Table 4.1. ACT Detector Mechanical Parameters

Detector	Size	Units	Comments
Tracking Volume	3.7 × 9.0	m^2	od × length
Total Channels	200	K	incl. inter & central
Silicon Tracking	1.0 × 6.0	m^2	diameter × length
Silicon Tracking Weight	0.6	tonne	
Coil	3.7 × 4.4 × 9.0	m^3	id × od × length
Barrel Calorimeter	4.5 × 9.3* × 8.0	m^3	id × od × length
Weight	4400	tonne	includes return steel
Total Channels	120	K	includes endcaps
Endcap Calorimeter	1.0 × 9.3* × 3.5	m^3	id × od × length
Weight	3000	tonne	both ends
Muon Barrel Toroids	17.1 × 17.1 × 24.6	m^3	w × h × length
Weight	15,580	tonne	
Muon ACT Toroids	4.0 × 12.2 × 3	m^3	id × od × length
Weight	160	tonne	both ends
Muon Barrel Chambers	22.0 × 22.0 × 36.5	m^3	w × h × length
Total Channels	60	K	
Muon ACT Chambers	12.6 × 12.6 × 5.5	m^3	w × h × length
Total Channels	40	K	includes both ends

* includes return steel

Each subsystem in the detector will require a variety of connections for proper operation and to meet safety requirements. The connections to each subsystems consist of:

- Mechanical supports
- Trigger and data acquisition cables
- Power, including low and high voltage connections.
- Cooling fluids or gases
- Sub-system speciality fluids or gases
- Alignment monitoring and adjustment
- Environmental monitoring (temperature, oxygen concentration , explosive gas concentrations, smoke detectors, etc).

The details of these connections will depend critically on technology chosen for each subsystem, and planning will have to consider the interactions between subsystems as well as the needs of individual detector elements. However, the general strategy for the "hookup" of the detector to external systems is as follows.

For all detector subsystems, the front-end electronics, level 1 trigger electronics, and temporary data storage for about 100 crossings (including data buffering between the level 1 and level 2

trigger decisions) are mounted directly on the mechanical structure of the subsystem. These electronics are connected via flexible cable trays to global trigger and data acquisition electronics located in a multi-story gallery next to the detector inside the collision hall. The flexible cable trays allow motion of detector subsystems to provide access to the internal portions of the detector without disconnecting cables or utilities. This includes the cryogenic fluids and power leads necessary for the ACTs.

The layout of the hall currently allocates the second and third floors for trigger and data acquisition areas. Each floor of the gallery is approximately 4 m wide by 30 m long. These two floors are fully air-conditioned enclosures and are provided with computer (false) floors for routing of cables between electronics racks. Data acquisition and trigger signals are communicated to the surface via the 3-m-diameter cable shaft located 8 m inside the wall next to the gallery. Floors above the third level of the gallery (as well as the basement below the first floor) are reserved for mechanical systems, gas and fluid handling, and cryogenics systems for the superconducting solenoid and ACTs. These floors do not have separate air-conditioning or computer floors. Utilities for these areas, as well as any heavy-duty power lines, are connected to the surface via a separate utility shaft to avoid pickup of switching noise from the heavy-duty power cables on the data acquisition cables.

4.2 Air Core Toroid Detector Hall Design

4.2.1 Overview and General Hall Plan

The ACT detector collision hall is 33.0 m wide and 82.0 m long, constructed with its long axis parallel to the collider beam line as shown in Figure 4.4. To best utilize the floor areas reserved for muon steel and calorimeter assembly, the center of the detector is offset by 1.5 m and 5.5 m from the long and short axes of the hall, respectively. Dimensions of the hall are based on access around the completed detector, space requirements for assembly and checkout of the calorimeters and end muon toroids, and clearance requirements for retracting the detector components for maintenance access. In-place upgrading of the detector has also been considered. A temporary air-tight partition between the muon steel assembly and the calorimeter assembly areas of the hall is erected to provide a clean area for calorimeter assembly.

As shown in Figure 4.5, the top of the main operating floor is set level with the top of the roller tracks in the barrel muon steel, and the basement under the detector is about 5 m below that. A 3-m-wide passage for moving small equipment on the operating floor and a 7-m-wide passage for transporting large items by the hall crane from one end of the hall to the other are provided.

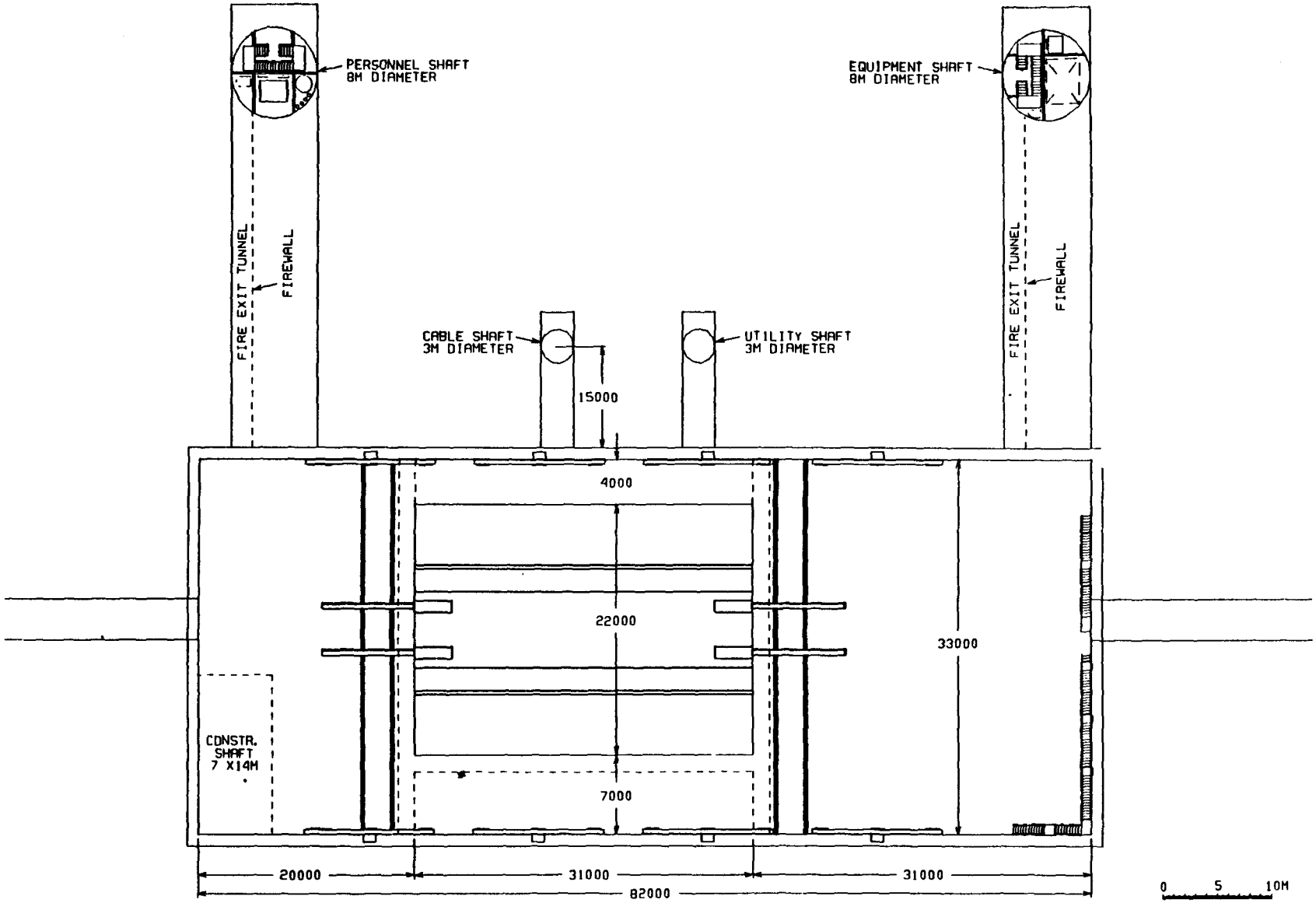

Figure 4.4. ACT Detector—Hall Floor Plan

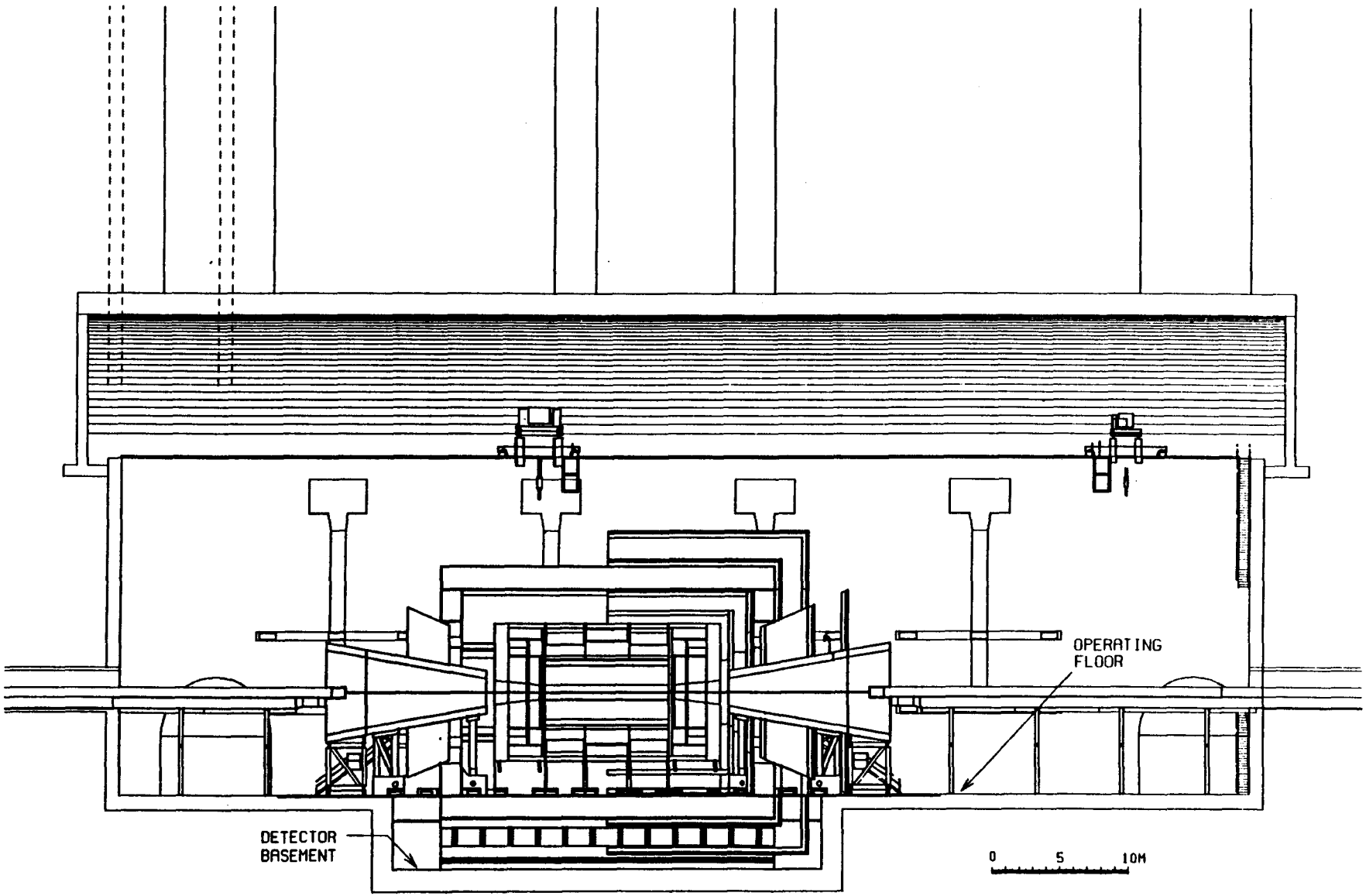

Figure 4.5. ACT Detector—Section at Beam Line

The basement is extended to the side wall of the hall under the 4-m-wide passage to provide room for pumps, compressors, utility distribution and other equipment, and structural requirements.

The walls of the hall are tied to the rock behind by rock anchors. The walls extend about 23 m above the operating floor, as shown in Figure 4.6. The crane runways rest directly on the top of the side walls, which are provided with vertical recesses for the flush-mounted air-conditioning ductwork.

The roof of the collision hall is a parabolic concrete arch supported on independent foundations just behind the top of the side walls (Figure 4.6). This low-rise arch imposes an outward force on the rock mass behind the side walls of the hall, thereby reducing the heave forces on the side walls. The arch foundations are not tied to the walls, so that any change in the overburden or surface loading above the arch will not affect the walls or the floors of the hall. Placing the roof of the hall on top of the walls would impose a high vertical load on the walls, and in turn on the edge of the hall floor slabs, which may be just above the weak Eagle Ford Shale if the hall is located at the west cluster. The resulting immediate and long-term floor movements would be significant and could be influenced by changes in the overburden pressure on the roof.

The space between the top of the wall and the base of the arch can be used for distribution of some of the hall utilities, and for servicing of the cranes, the fans of the air-conditioning system, and the roof drainage sumps.

The proposed hall configuration may be constructed by conventional open excavation, or by excavating to the top of the walls and constructing the roof arch while the excavation proceeds to the hall floor. The latter arrangement will permit an earlier start of the backfill operation, and therefore, reduce construction time of the hall.

4.2.2 Detector Basement and Support

The adopted maximum floor movement is 2.5 mm for short duration (one week) loading and 25 mm for long duration (one year or more) loading after all components of the detector are in place. These floor movement specifications require a very rigid concrete basemat under the detector. The floor movement during erection of the muon steel and after the central calorimeters are installed is also restricted to 25 mm; however, this could be compensated for by pre-setting the main steel barrel supports before erection of the muon steel begins. Weight calculations indicate that the detector loading on the basement floor is about the same as the present vertical rock pressure at this elevation. This means that deflection of the floor due to the weight of the detector will be very small; therefore, floor movement will be largely controlled by the heaving pressure of the underlying rock. In the operating floor areas the floor loading is very low—less than 10% of

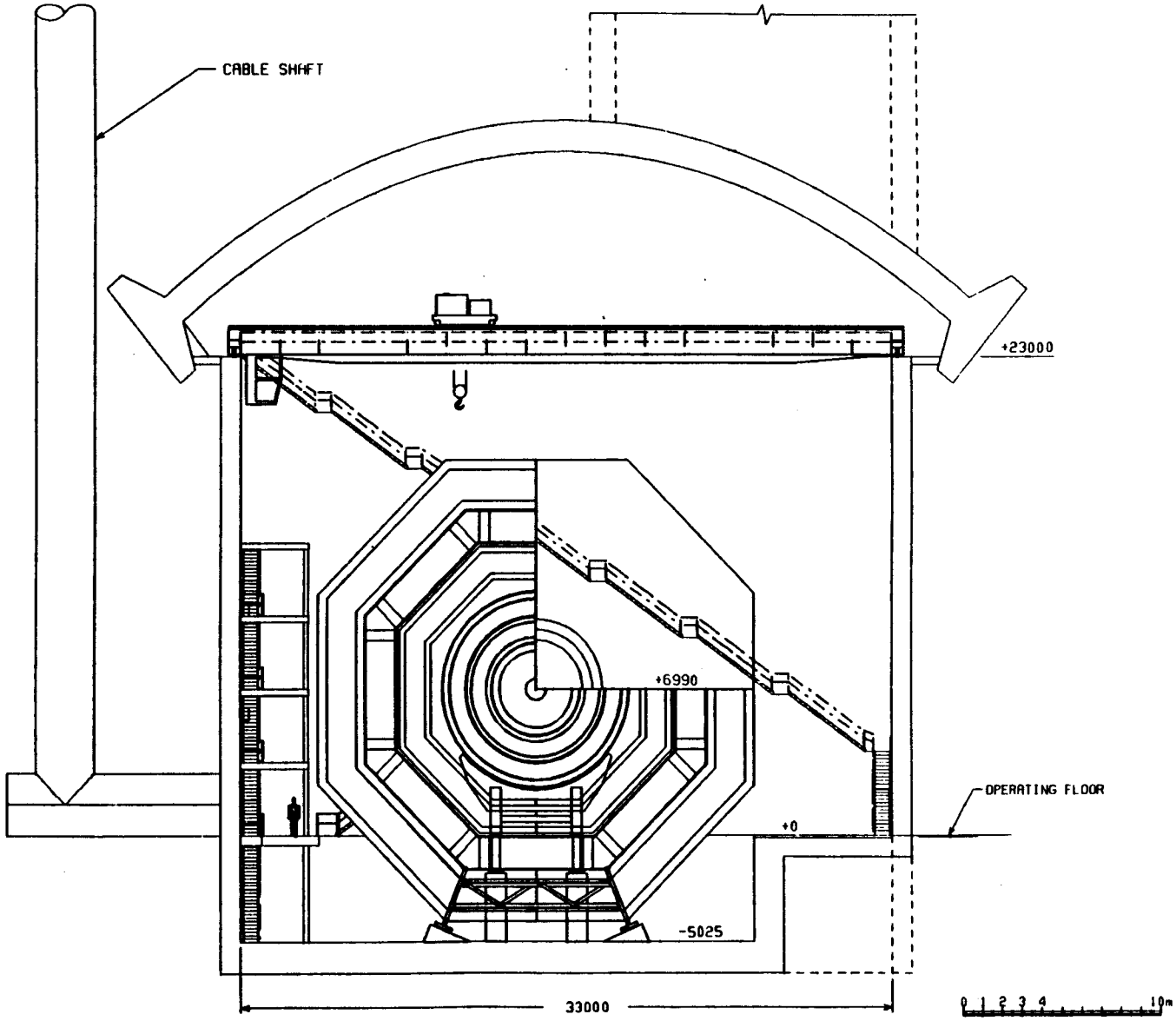

Figure 4.6. ACT Detector—Section through Interaction Point

the present rock pressure—and, therefore, the upward floor movement due to the unopposed heave could be significant.

To reduce floor movements, the detector basement must be made very rigid. The stiffness of the basemat depends on the thickness and uncracked moment of inertia and modules of elasticity of the concrete, as well as on the length and aspect ratio of the floor spans. The vertical restraint of the perimeter walls will also effect the deflection of the slab.

To construct a basement slab to be as rigid as possible, the edge of the detector floor is restrained by the stiff walls of the hall on two sides and by the heavily reinforced retaining walls at the ends of the detector. Using a higher strength (and Young's modulus) concrete also reduces deflections. Our preliminary finite element calculations indicate that floor deflections caused by the stationary and moving components of the detector will not exceed the adopted maximum floor movements. Floor movement caused by heaving of the underlying rock mass may be large, however, and could require special design considerations as outlined below.

Detailed design of floor will be based on the actual detector loadings and deflection limitations, and on the results of a geotechnical investigation of the physical properties of the underlying rock at the selected hall location. However, if the hall is located at the west cluster, the detector support floor will rest on or directly above the Eagle Ford Shale, and will, therefore, be subjected to the long-term heave forces of the shale. Assuming that the excavation is stable, the immediate (elastic) heave of the rock is not a problem until the concrete floor has hardened. After that, swelling due to the migration of the moisture in the rock and to creep and redistribution of stresses caused by the uneven overburden pressure may cause a slow upward floor movement. The magnitude and duration of this movement would be difficult to estimate. However, there are several ways to overcome the heave problem. A simple solution is to provide the means to adjust the height of the base plates of the four barrel support beams. This may be accomplished by supporting the base plate on a sole plate and shims, as shown in Figure 4.7. To adjust the elevation of the detector, low-height hydraulic jacks placed under the base plate are used to unload the shim plates; after the shim thickness is adjusted, the jacks lower the detector to the required elevation. After the nuts are locked to the base plates the jacks are removed.

A more direct solution to the heave problem is to post-tension the floor slab to the underlying rock. This is be done by drilling into the rock through several rows of blockouts near the midspan of the floor and installing rock bolts to a depth of approximately 1.5 times the width of the hall. The lower 1/3 of the bolt length is grouted into the rock, while the upper 2/3 is sleeved to permit slippage. The bolts are initially tensioned for the weight of the detector and, if required, further tensioned to reduce heave. The floor movements are continuously monitored by lasers; if required, the bolts may be retensioned or slackened to adjust the floor elevation.

MOVEMENT OF TRACK DUE TO WEIGHT OF:	MOVEMENT (mm) VERT.	HORIZ.
1. BARREL STEEL	0.325	0.018
2. CALORIMETER (CENTERED)	0.22	0.008
3. CALORIMETER (1" OFFSET)	0.24	0.05
4. LATERAL FORCE (10% OF 1+2)	0.084	3.30
5. BARREL + CALORIMETERS	0.055	0.025

NOTE: ABOVE DISPLACEMENTS EXCLUDE MOVEMENTS OF CONCRETE FLOOR

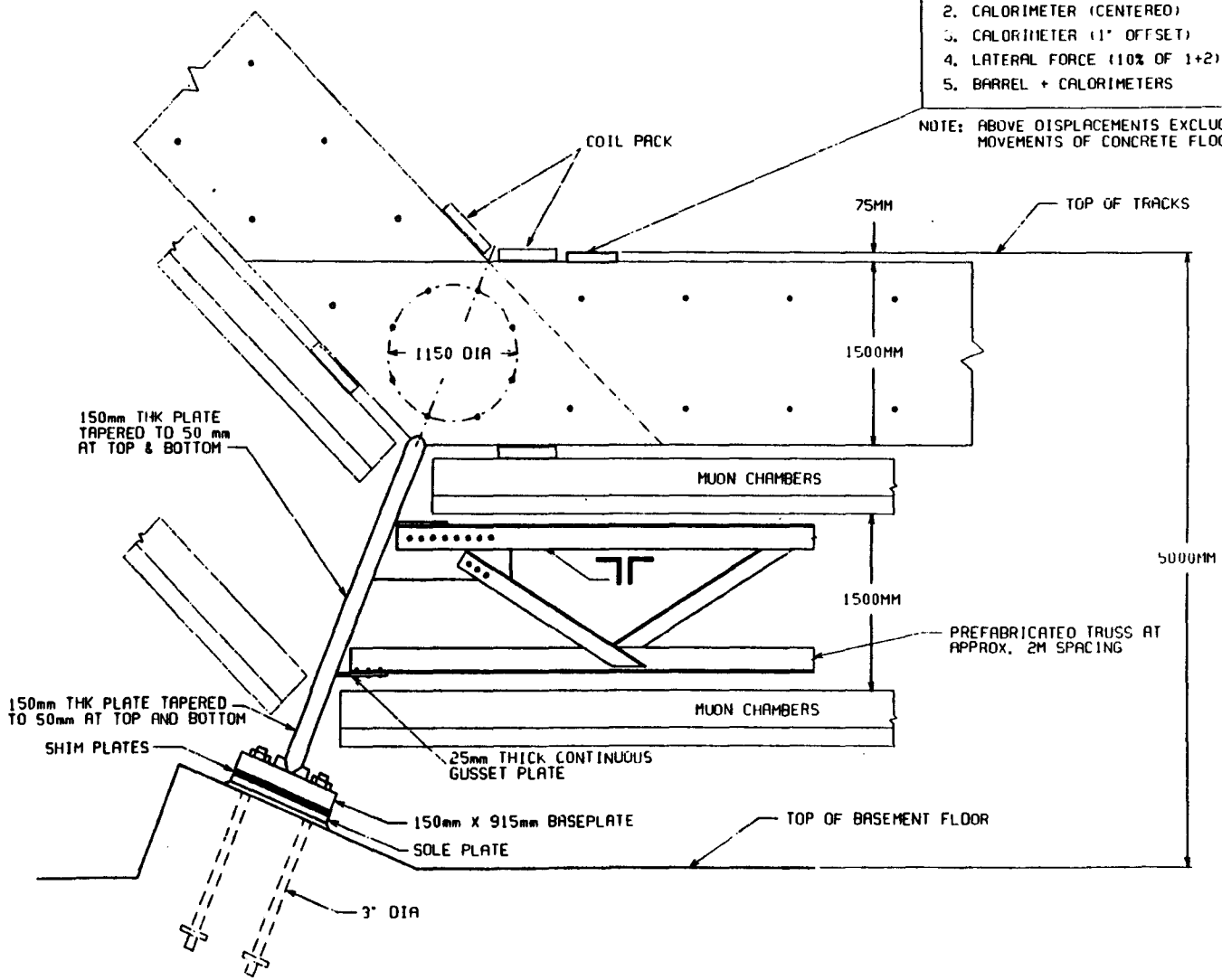

Figure 4.7. ACT Detector—Inclined Plate Barrel Support

4.2.3 Operating Floor Construction

To facilitate disassembly of the detector components and access to the detector, the top of the operating floor is set level with the top of the roller tracks in the barrel. Unlike the detector basement floor, the operating floor will be loaded to less than 10% of the present vertical rock pressure at this elevation. This means that to reduce floor movement to acceptable levels, the heave pressure from the underlying rock will have to be restrained by the floor slab. Excessive floor heaving could slow down disassembly operations of the detector because rolling the heavy components on a sloping floor will require special procedures to insure safety. The supports of the forward calorimeter and of the acceleration magnets must be adjustable to maintain proper alignment.

Floor heave could be reduced by post-tensioning the floor slab to the underlying rock, as described in Section 4.2.2, or by separating the floor slab from the rock by a layer of compressible materials. This problem should be studied further as soon as the results of the geotechnical investigation become available.

4.2.4 Access and Utility Shafts

Access to the hall is provided by a rectangular construction shaft penetrating the hall roof in the southeast corner of the hall and by two circular shafts, both with stairs and one equipped with an elevator. Separate shafts for utilities, cabling, and air-conditioning ducts are also provided. The location of these shafts is shown on Figure 4.4 ; shaft information is summarized in Table 4.2.

Table 4.2. Hall Shafts.

Name or Use	Size	Cross-section	Access
Construction Shaft	7 m × 14 m	rectangular	crane only
Equipment Shaft	8 m	round	stairwell/crane
Personnel Shaft	8 m	round	stairwell/elevator
Cable Shaft	3 m	round	stairwell
Utility Shaft	3 m	round	stairwell/dumbwaiter

The construction shaft provides a 14-m by 7-m access into the hall for lowering all steel used in constructing the muon barrel and the end toroids; the support beams and erection rigs of the barrel; and the saddles, washers, and return flux steel of the endcap calorimeters. The air core toroids, solenoidal coil, central tracking device, and the muon chamber panels are also brought down through the construction shaft. To maximize the usable floor area for detector assembly and for possible major repair or modification work on the detector in the future, the construction shaft is located in the corner of the detector hall. Placing the shaft on the center line of the hall would require a longer hall for detector assembly and would locate the shaft over the beam line. Location

of the construction shaft over the beam line would inhibit the use of the shaft after beam line components are in place. Once the detector assembly has been completed, this shaft is closed at the top by overlapping precast concrete slabs to block radiation. These slabs may be removed later to regain access to the hall for lowering large objects.

The equipment shaft is 8 m in diameter and is located away from the northwest corner of the detector hall so that at the surface the shaft is outside the area excavated for the hall construction. This allows the shaft to be built earlier to provide access to the hall before the hall roof is constructed and backfilled. The bottom of the shaft is connected to the operating floor by an 8-m-wide concrete-lined tunnel. The equipment shaft and tunnel are partitioned by a fire wall to enclose the fire escape stairs and egress route from the hall (Figure 4.8). The stairwell and egress route in the tunnel are slightly pressurized to prevent smoke from entering this region in the event of a fire. The equipment shaft also incorporates a 3-m by 4-m hoisting well for lowering calorimeter modules, electronics, and other equipment. Space for a 900 kg capacity construction elevator and for the ductwork of the hall ventilation system is also provided.

The personnel shaft is located a distance from the southwest wall of the detector hall. For the reasons given above, this shaft is also situated outside of the region excavated during hall construction. As shown in Figure 4.8, this 8-m-diameter shaft and the connecting tunnel house the second fire escape stairwell and egress route. The personnel shaft contains the passenger/light-freight elevator connecting the operations center on the surface to the main hall floor, the ductwork for the hall ventilation system, and the piping and power supply for the conventional hall services (e.g., lighting, power outlets, cranes, and sumps).

The cable shaft is 3 m in diameter and is located approximately 15 m from the west wall of the hall in line with the center of the detector. This shaft will carry all signal cables from the hall to the data acquisition and control rooms of the operations center on the surface. As shown in Figure 4.9, the shaft is equipped with vertical cable trays—60 cm. by 15 cm (24 in. by 6 in.) and 90 cm by 15 cm (36 in. by 6 in.)—and a 1.5-m-diameter spiral staircase to provide access to the cables. The cable trays are arranged to be within arm's reach of the staircase. The bottom of the cable shaft is at the operating floor level of the hall; however, additional cable passages from the shaft to the floors supporting the electronics cabinets are also provided.

The utility shaft, also 3 m in diameter, is located at least 9 m away from the west wall of the hall in order to bypass the hall roof foundation. The location of this shaft is coordinated with the layout of the surface facilities. The bottom of the shaft is at the floor level of the detector support. As shown in Figure 4.9, the utility shaft will have several compartments for the 400 Hz, 60 Hz, and DC power lines, the tracking chamber gases and helium and nitrogen gases, and the cryogenics and safety systems. A 1.5-m-diameter spiral staircase with frequent landings and a 250-

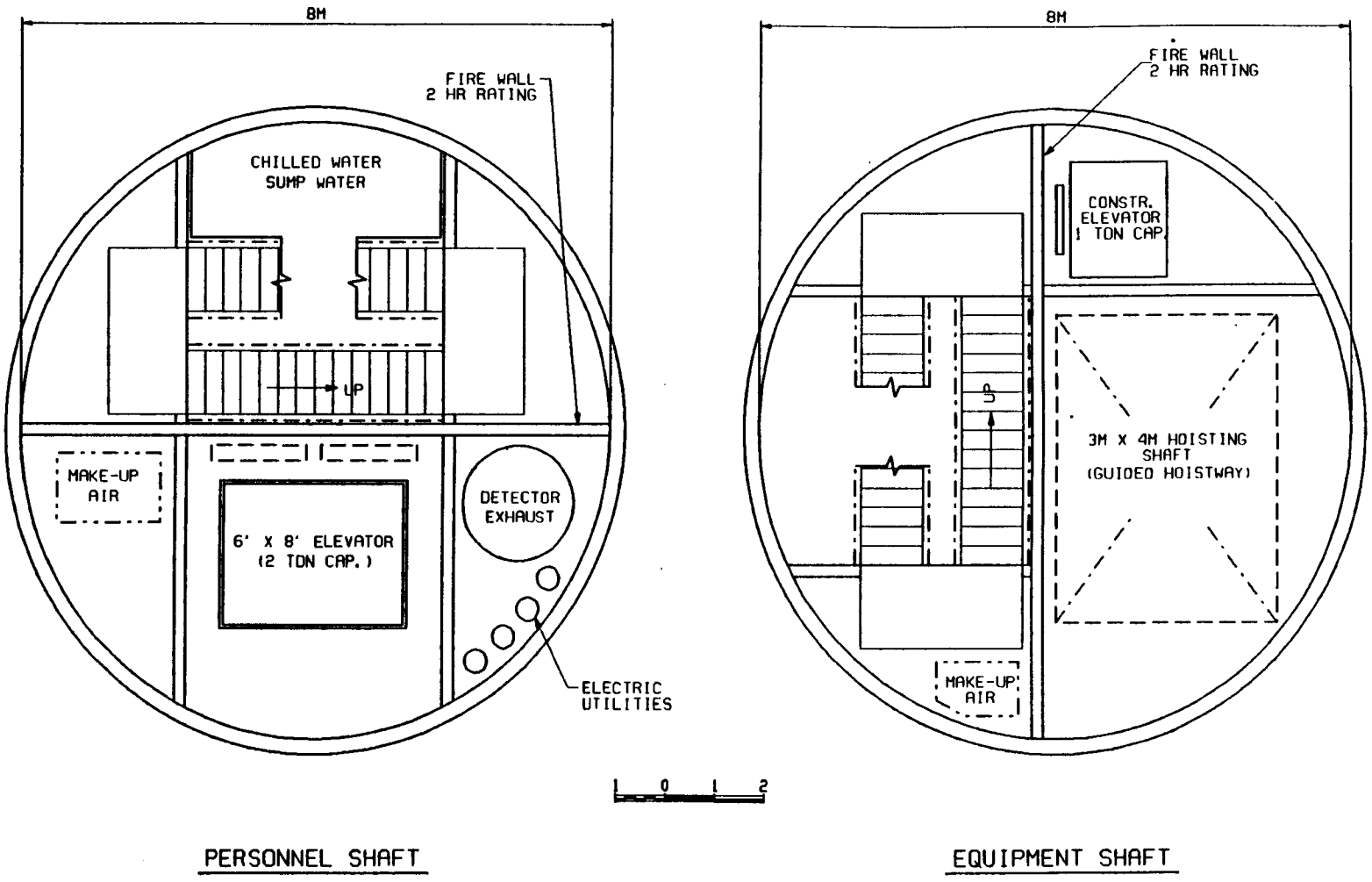

Figure 4.8. ACT Detector—Personnel and Equipment Shaft Profiles

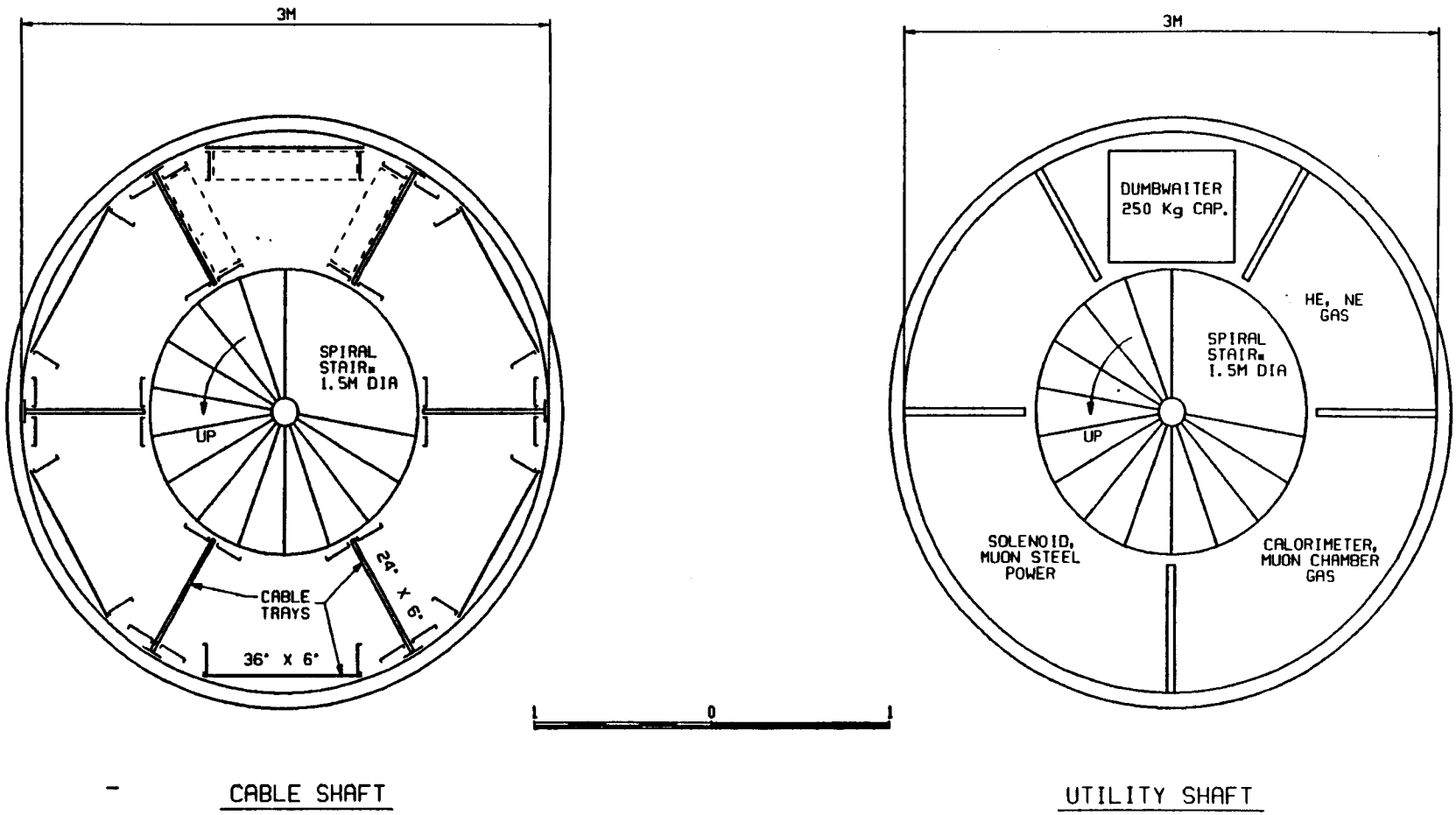

Figure 4.9. ACT Detector—Cable and Utility Shaft Plans

kg-capacity dumbwaiter to carry maintenance tools and equipment for servicing these utilities are also provided.

4.3 Air Core Toroid Detector Assembly

4.3.1 Muon Steel Barrel Assembly

The configuration and construction of the octagonal muon steel barrel is shown in Figure 4.10, and some general specifications are listed in Table 4.3

Table 4.3. Mechanical Specification for ACT Detector Muon Toroids.

Thickness of steel at 90°	1.5 m
Magnetic field	1.8 T
Maximum allowed gap in steel	3 mm
Minimum fraction of steel along any radial path	98 %
Field at inner radius of ACT	1.8 T
Field integral in ACT projected along $\theta = 0^{o}$	4.5 T-m

The barrel steel will be assembled from 1500-mm (59 in.)-wide trapezoid-shaped plates (Figure 4.11). The plates are arranged to lay in the X-Y plane, parallel to the flux lines. The plate thickness is 198 mm (7.75 in.), except for the three 380-mm (15 in.)-thick plates centered at the interaction point, and a 194-mm (7.5 in.)-thick plate at each end of the barrel. The reason for the three thick plates at the interaction point is to meet the 98% minimum solid material ray penetration criterion. As shown on the side view in Figure 4.10, a total of 119 layers make up the 24,100 mm length of the barrel.

Except for the three 380-mm (15 in.)-thick central layers, the plates are ordered from the steel mills in one piece. The length of the 380 mm plates exceeds the maximum rolling length available from U.S. mills, so these plates must be spliced by partial penetration butt-welding. The plates may be gas-cut from standard rolling widths; however, the sloping edge of the "short" plates, and about 2200 mm (86 in.) at each end of the "long" plates are milled for bearing on each other. Except for two grooves for the radial support plates of the barrel, no other machining is required.

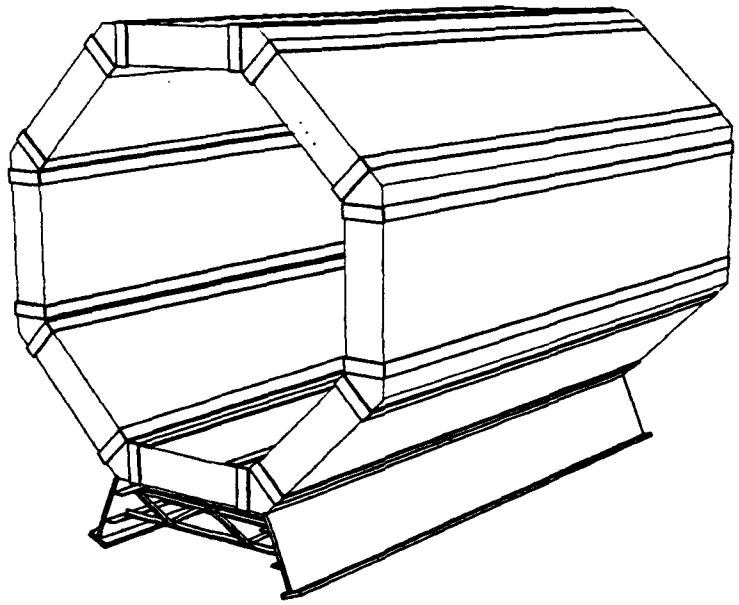

MUON STEEL BARREL PERSPECTIVE

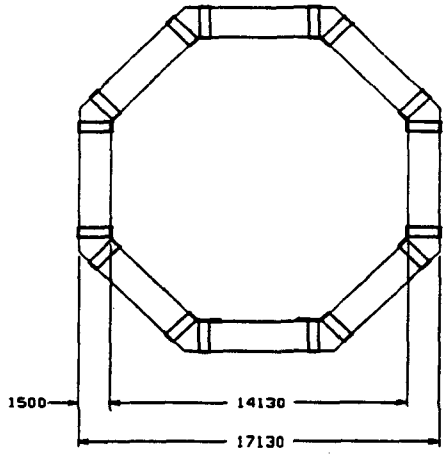

END VIEW

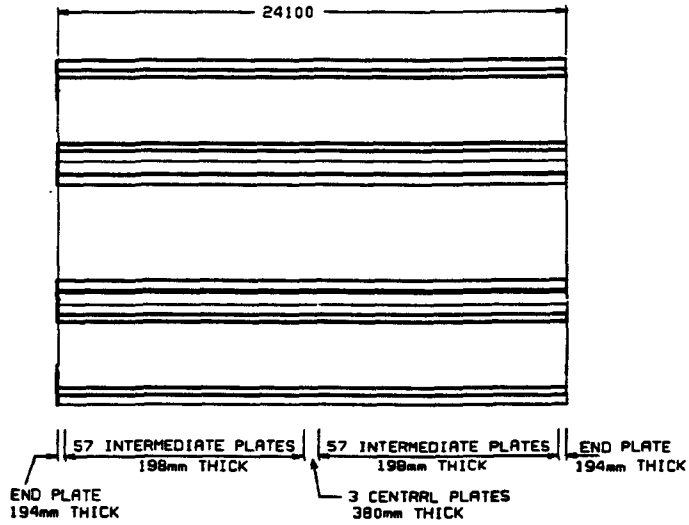

SIDE VIEW

Figure 4.10 ACT Detector—Muon Steel Barrel Dimensions

The strength of the barrel is provided by the overlapping long plates tied together by the eight 38-mm (1.5 in.)-diameter, high-strength bolts located on a 1150-mm (40 in.)-diameter bolt circle, as shown in Figure 4.11. These bolts provide a slip-critical connection between the long plates, thereby preventing rotation at the corners of the octagonal-shaped barrel. (Slip-critical joints are defined by the codes as joints in which slip would be detrimental to the serviceability of the detector.) Our finite element calculations indicate that the deflection at the top of the barrel is 3 mm (1/8 in.) due to self weight. However, as described below, the gravitational load can be compensated by appropriate adjustment of the erection frame before tightening of the corner bolts. The bolts away from the corners are used to pull the plates together so that the gap between the plates does not exceed 3 mm anywhere in the barrel. Thus, the 98% minimum solid material ray penetration criterion is achieved.

We have also investigated the feasibility of using thicker plates, plates in different orientation and arrangement, and plates secured with high-strength bolts tapped into the muon steel. Using thicker plates for the barrel would reduce the number of plates to be installed, but this is not considered an advantage because the plates may be handled in groups of four or more during shipping and installation. Thicker plates would require larger diameter and/or more bolts in order to pull them together and to provide the required strength at the corners of the barrel. Thicker plates will also cost more to buy, and the machining and general handling costs are higher.

Plates arranged with mitered ends pointing toward the interaction point would not meet the ray penetration criterion and would require bolts installed in machined pockets and tapped into the muon steel. Longitudinal bolts or plug welds to pull the plates together would also be required. A brief investigation of tapping-high strength bolts (ASTM A490 or Grade 8) into the soft muon steel (Fy = 28 ksi) was also made. Theoretically, the length of thread engagement should be about four times the bolt diameter; however, because of shear lag, there will be some yielding of the first few threads of the hole. Normally, the strength of the nut (or tapped material) is equal to or higher than the bolt strength, but in this case the yield strength of the bolt is about four times that of the tapped material. Consultations with experts in the field indicate that this type of connection is very unusual and should be tested for pull-out strength in a laboratory.

Concerning a plate arrangement where the moment and shear force are transferred through the machined joints by compression on the steel and combined tension and shear of the bolt, we have found that such a joint will have to be machined to a very close angular tolerance. This is because after tightening of the bolts, the joint will close tight and the angular deviation of the machined surfaces from the true will determine the actual shape of the barrel after assembly. Any errors in machining will be hard to correct in the field, so all components of this type of design should be preassembled in the fabrication shop.

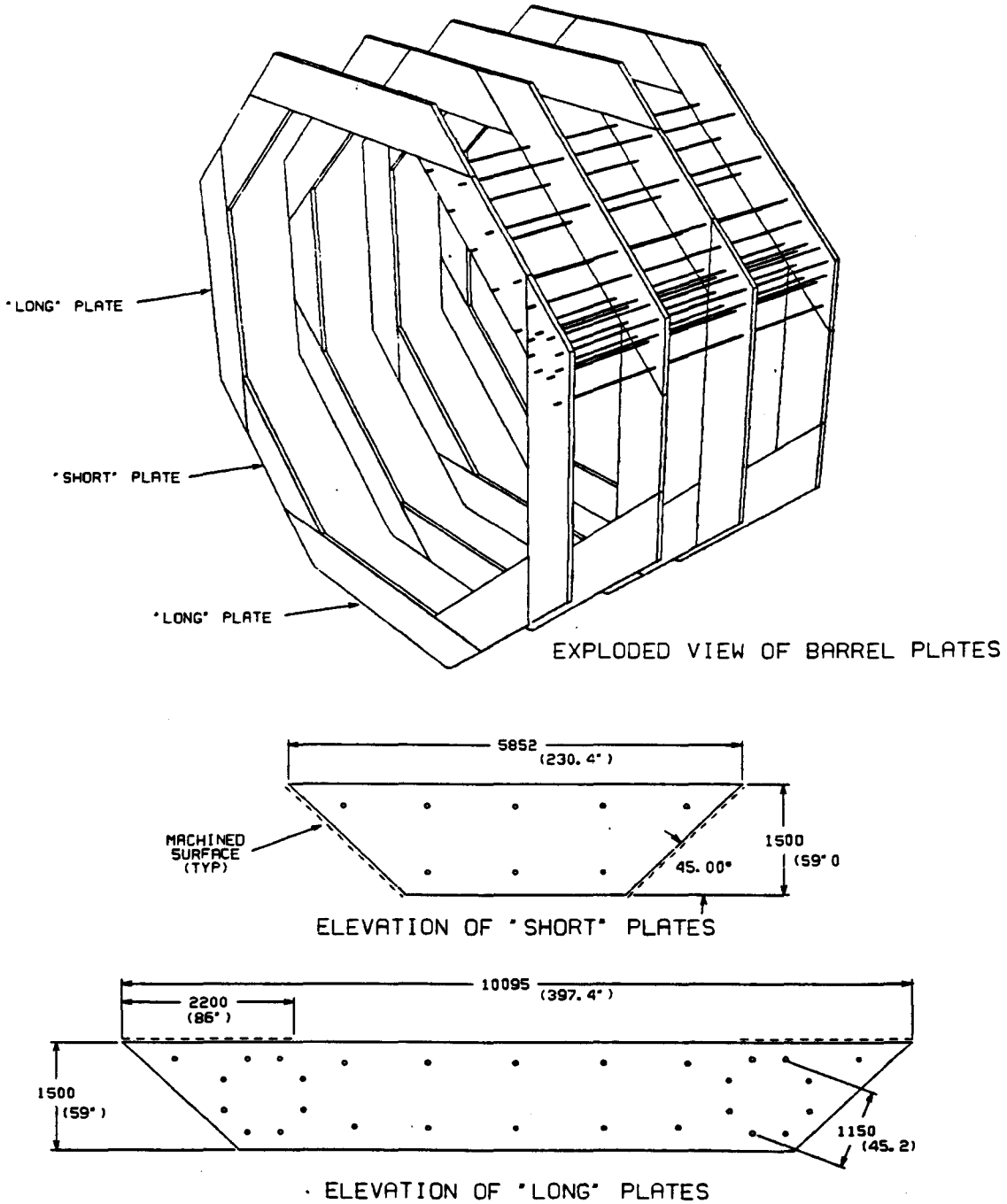

Figure 4.11 ACT Detector—Muon Steel Barrel Construction

The plates of the barrel are drilled with oversized holes to facilitate installation of the longitudinal bolts and to permit adjustments of the barrel shape during assembly. To reduce bolt length the plates will be pulled together in groups of eight. The outermost plates of each group will have recessed holes on both sides to receive the bolts from the adjacent group of plates. The length of the plates depends on their position in the barrel. The number of each plate type required for the barrel is shown in Table 4.4.

Table 4.4. Plate Count for Muon Barrel Steel Toroid.

Plate Location	Length ¥ Thickness (mm)	Number Required	Weight of Each Plate (tonnes)
Central Short Plates	5852 × 380	12	19.47
Central Long Plates	10095 × 380	12	38.45
Interm. Short Plates	5852 × 198	456	10.15
Interm. Long Plates	10095 × 198	456	20.04
Short End Plates	5852 × 194	8	9.94
Long End Plates	10095 × 194	8	19.63

Note: All plates are 1500 mm wide. Length is the overall length of each plate.

To provide maximum chamber coverage, the barrel muon steel is supported on two inclined longitudinal plates resting on the concrete floor (Figure 4.12). The plates are braced together at about 2-m-longitudinal intervals to resist buckling and any lateral force on the barrel. As shown in Figure 4.7, the bracings are located between the two outer layers of the muon chambers to avoid interference. The base of these supports is designed to facilitate vertical adjustment of the barrel elevation to compensate for the floor movements described in Section 4.2.2.

Prior to the muon steel barrel assembly, the two inclined plate supports of the barrel are installed. The muon steel erection rig and the temporary supports of the lower inclined plates of the barrel are also installed at this time. See Figures 4.13 and 4.14.

The barrel steel assembly proceeds as follows. The pre-drilled and painted steel plates are assembled into jigs on the surface and are lowered into the hall through the construction shaft by the yard crane in groups of four. From the construction shaft laydown area in the hall, the plates are moved to the muon steel staging area by winched carts. After final checkout the plates are lifted into place in groups of four by the hall crane. One or two erection crews construct the barrel, beginning in the middle of the detector and working out toward opposite ends.

Beginning with the bottom segment of the barrel, four long plates, separated temporarily by 200-mm-wide wood spacers, are placed on the supports. Next, the four inclined long plates are installed on both sides of the barrel. Finally, the four short plates are placed between the long plates of the bottom three segments of the barrel. The above procedure is repeated until about 3 m of the bottom segments of the barrel is assembled (Figure 4.15). Note that the number of plates to

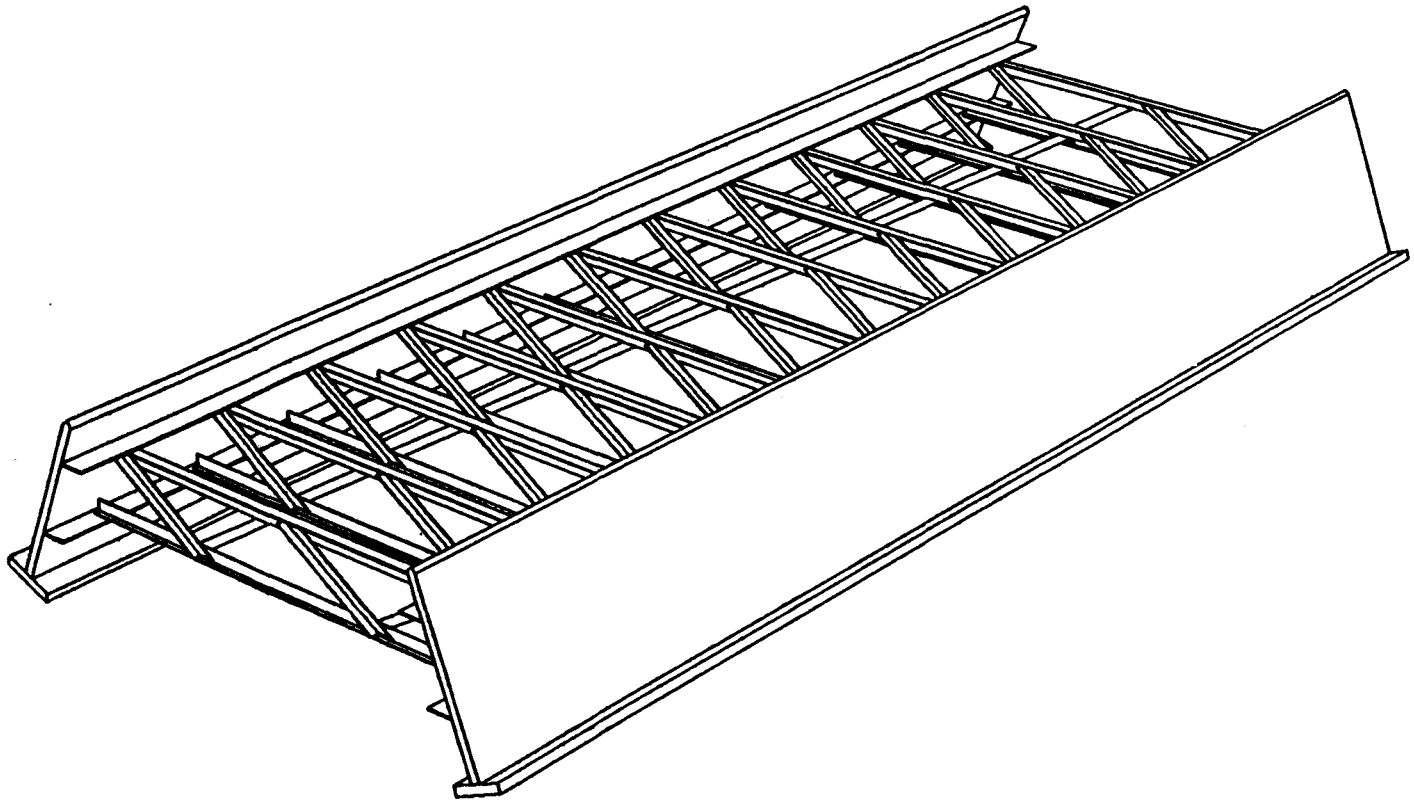

Figure 4.12. ACT Detector—Muon Steel Barrel Supports

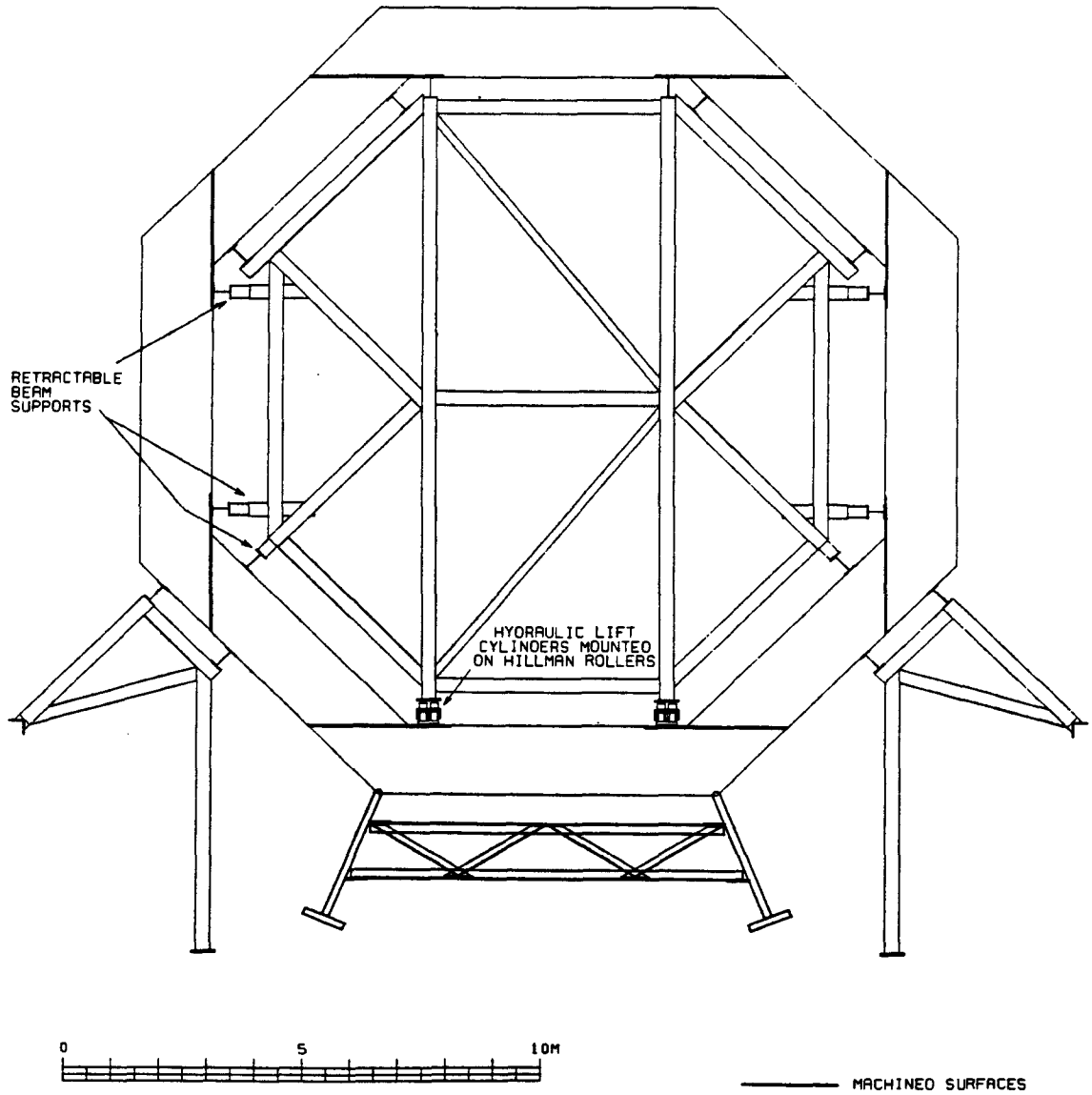

Figure 4.13 ACT Detector—Muon Steel Assembly Frame

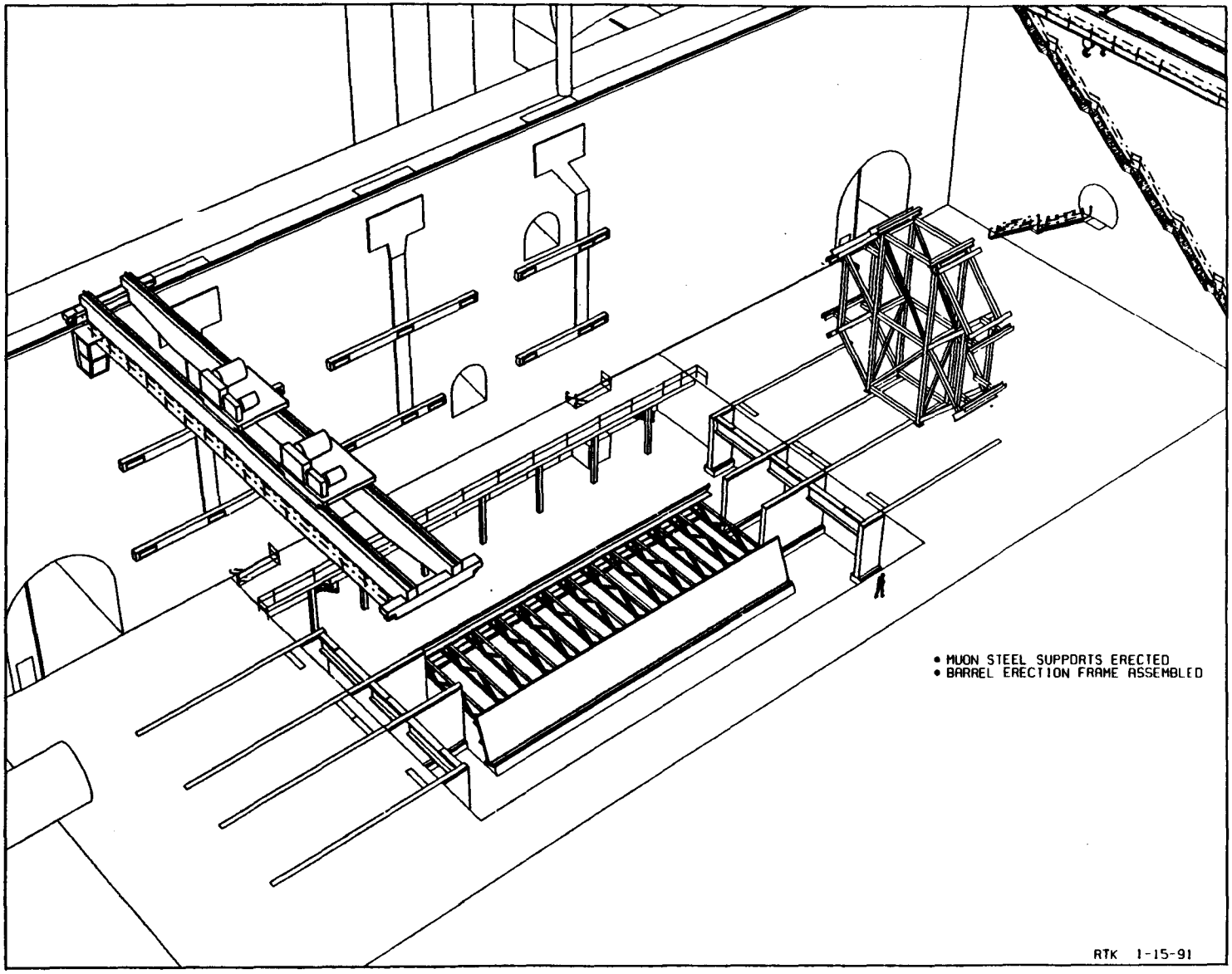

Figure 4.14. ACT Detector—Muon Toroid Construction

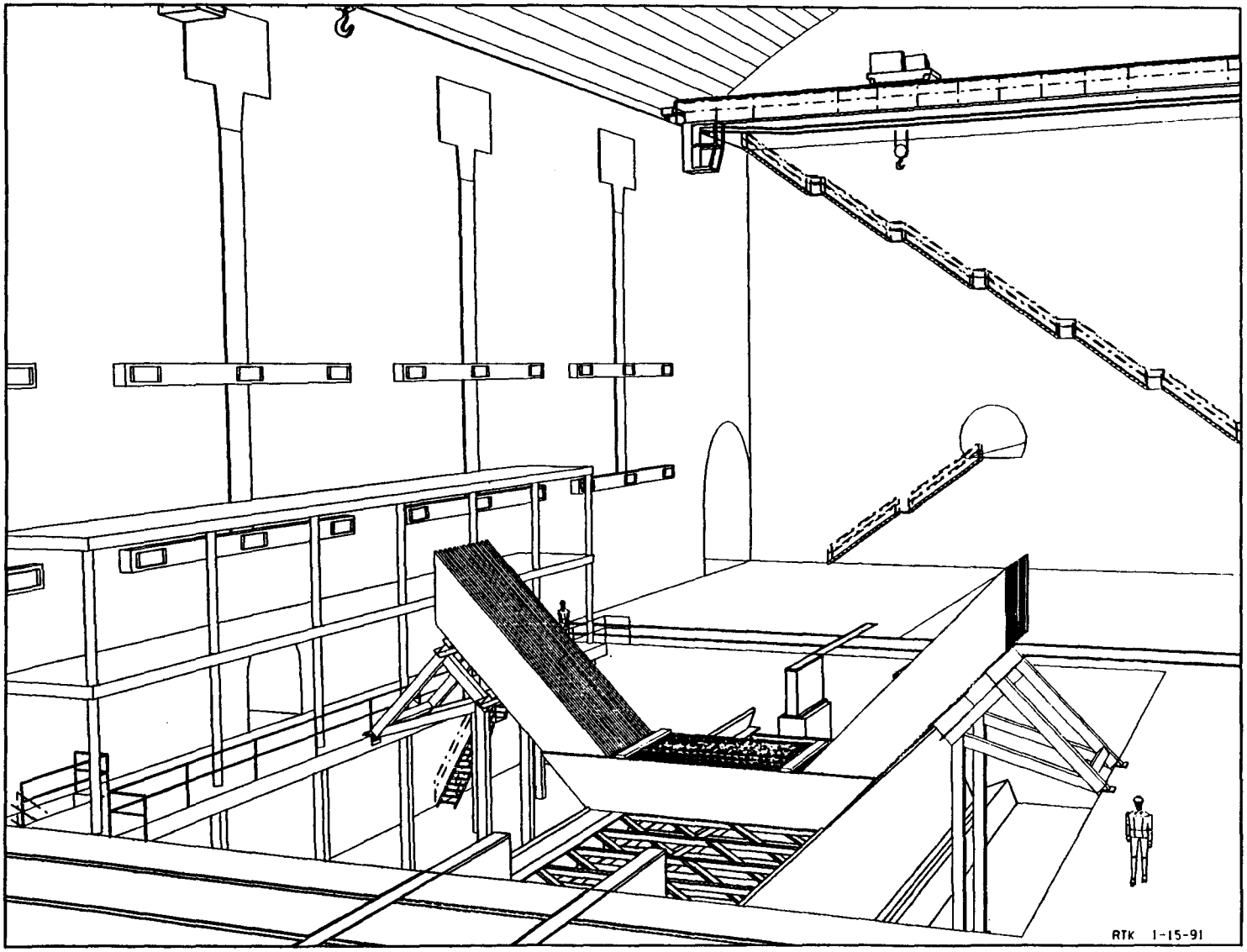

Figure 4.15. ACT Detector—Muon Steel Barrel Assembly (Step 1)

be lifted by the hall crane at one time does not affect the assembly procedures and may be varied by the assembly contractor.

After the above steps are completed, temporary tracks are installed on the bottom plates, and the assembly frame shown in Figure 4.16 is rolled onto the bottom segment of the barrel. The assembly frame is equipped with adjustable longitudinal beams to support the upper segments of the barrel and to align the plates before tightening of the longitudinal bolts.

In the next step, using the procedures described for the bottom segments, a 3-m length of the vertical and the top three segments of the barrel plates are assembled (Figure 4.17).

After installing all plates in a 3-m-long portion of the barrel, the plates are pulled together by hydraulic jacks. The longitudinal bolts are installed next, and after the final alignment check of the barrel is completed the longitudinal bolts are tightened to the required tension in a predetermined sequence. The bolt tension is checked with an ultrasonic device prior to assembly of the next group of plates.

The proposed plate arrangement and assembly procedures permit full adjustment of the barrel shape to the required tolerances, including compensations for dead load deflection, without shimming or grinding to correct for fabrication errors.

The magnetic field is powered by 16 coils symmetrically located at each corner of the octagonal muon steel. After the construction of the barrel steel is complete, 32 half-coil packages are lowered into the hall via the construction shaft. These half-coils are pre-assembled modules approximately 24 m long, slightly longer than the full length of the barrel. Each half-coil on the outside of the steel is mechanically and electrically joined at the north and south ends of the barrel toroid to its mate on the inside surface of the steel. Water circuits are completed using flexible tubing.

4.3.2 Muon Air Core Toroid Assembly

The air core toroid assembly includes the muon steel toroid, the air core toroid, the absorber, and several layers of muon chambers, as shown in Figure 4.18. The whole assembly is supported on a single structural frame equipped with rollers to permit movement when opening the detector for inspection or repair.

As shown in Figure 4.19, the muon steel toroids are assembled with two alternating shapes of 145-mm (5.75 in.)-thick plates in ten layers. The selected combination of plate size and thickness is available from most domestic mills in a single piece. Larger or thicker plates would require butt-welding, which is costly and could be difficult when small flatness tolerances must be maintained. Each layer of the toroid plates is offset by 45° to provide an overlap of the crescent-shaped plates. The nine high-strength bolts in this overlap will be able to resist the gravity and magnetic forces acting on the toroid.

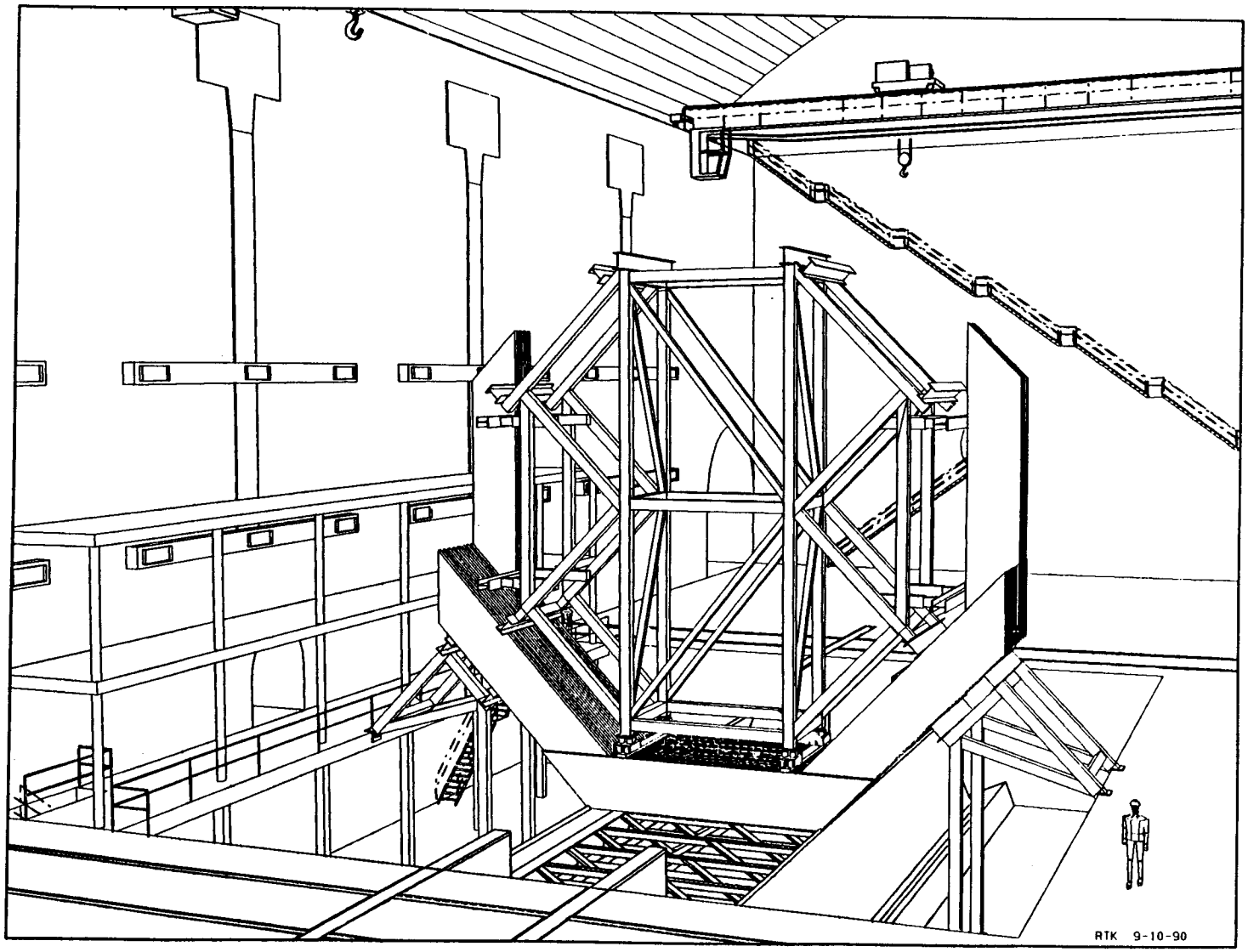

Figure 4.16. ACT Detector—Muon Steel Barrel Assembly (Step 2)

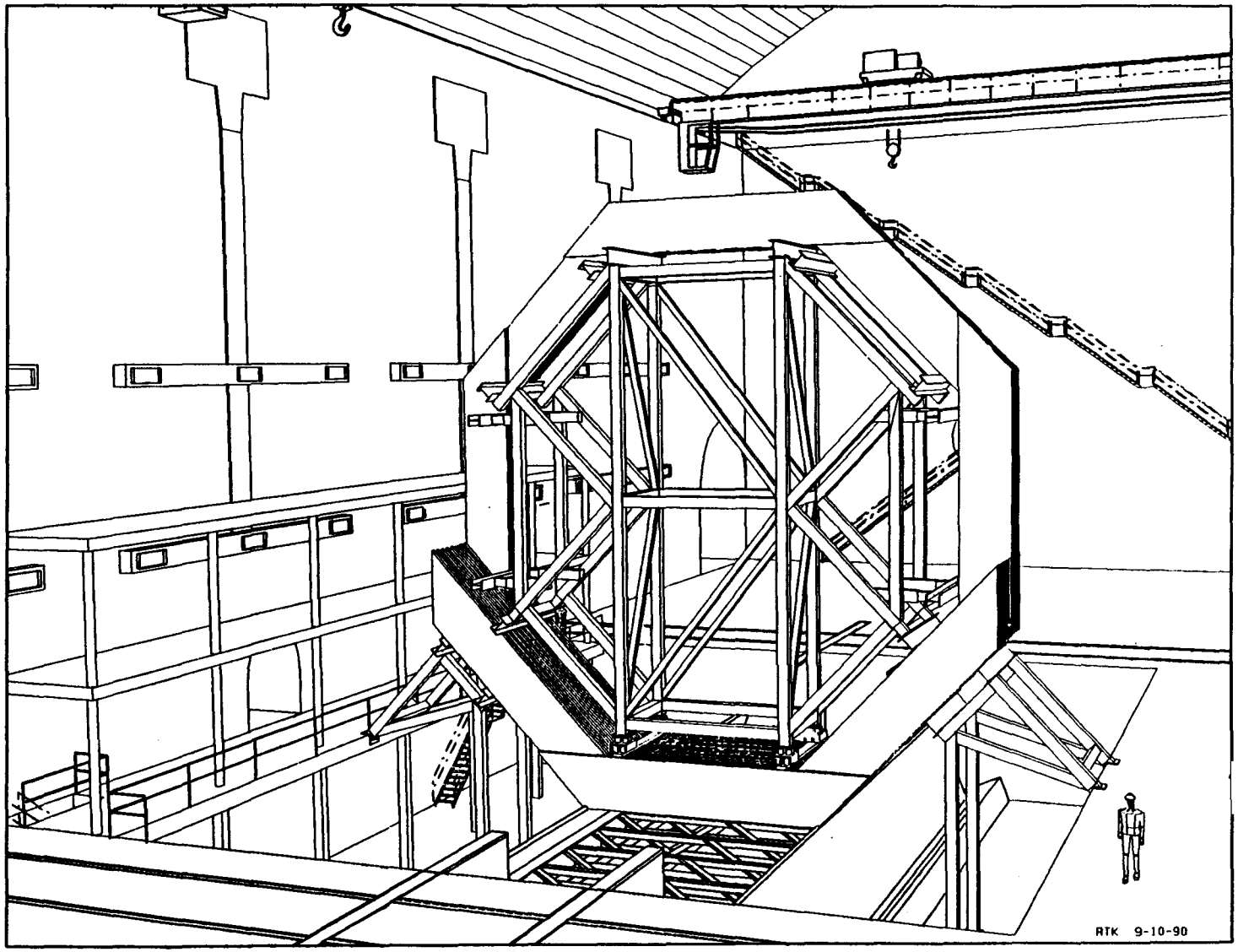

Figure 4.17. ACT Detector—Muon Steel Barrel Assembly (Step 3)

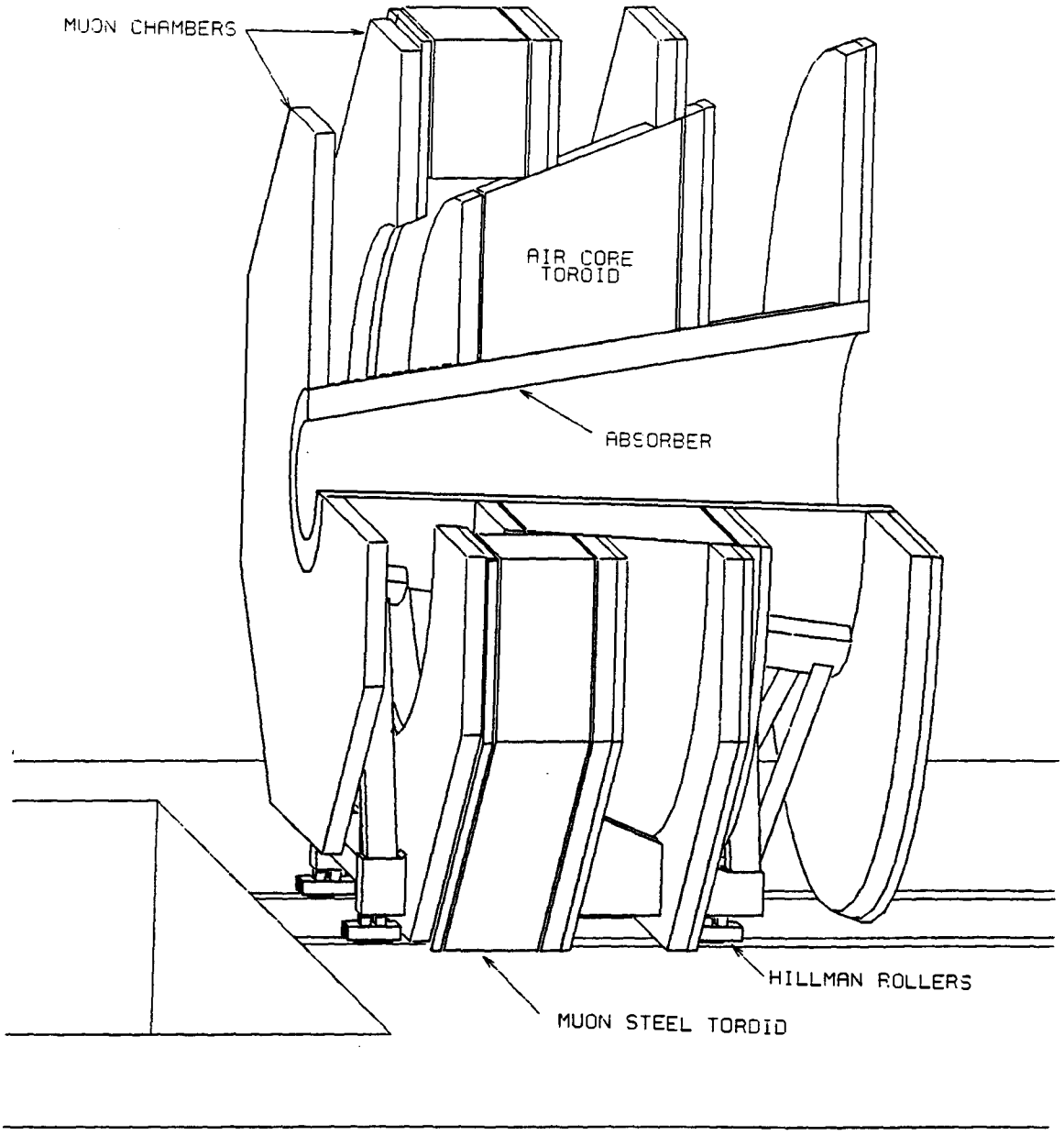

Figure 4.18 ACT Detector—Air Core Toroid Assembly

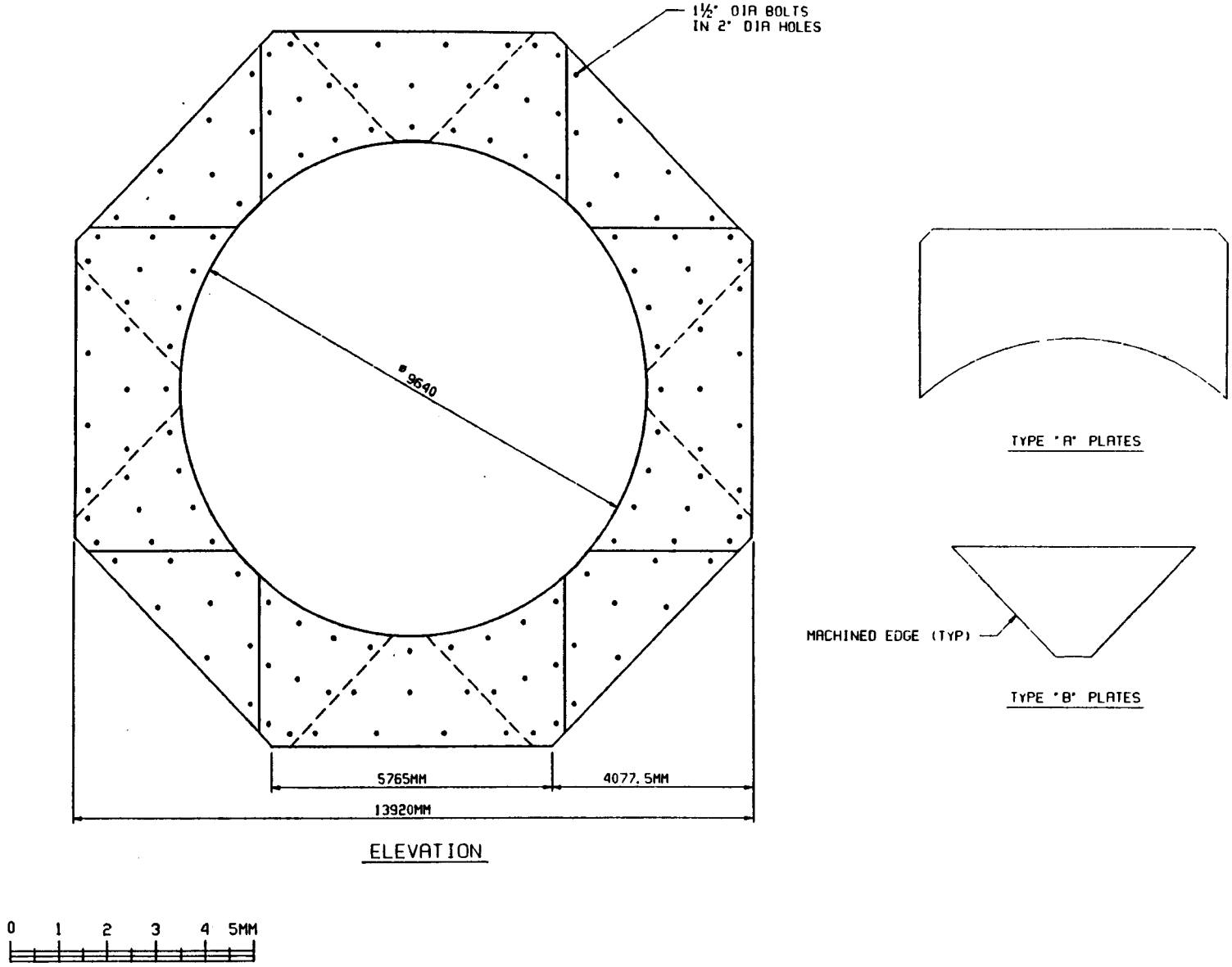

Figure 4.19. ACT Detector—Muon Steel End Toroid (Elevation)

A vertical jig frame, as shown in Figure 4.20, will be used to support and align the plates during assembly. The first set of plates is bolted temporarily to the jig while the remaining plates are clamped and/or bolted to the first set and to the core of the jig. During assembly the bottom plates are supported on temporary steel sleepers that have been shimmed to provide a perfectly horizontal surface at the correct height above the floor. After all ten layers of the muon steel toroids are assembled, the permanent high-strength bolts are installed through the oversized holes and are fully tightened after final alignment of the plates.

Once the toroid is completed, steel outriggers designed to support the toroid and the absorber are installed. In the next step the hydraulic jacks and Hillman rollers are installed under the outriggers so that the hydraulic cylinders can lift the whole assembly for moving. The completed toroid is shown in Figure 4.21.

The absorbers are assembled from eight cast steel sections on permanent saddles, supported on temporary rollers (Figure 4.22). The eight sections are held together by bolting them to heavy plate rings at each end.

We assume that the air core toroids are delivered to the site as a single unit, or that they are assembled on the surface. The air core toroids are then mounted on temporary frames supported on Hillman rollers in a building near the construction shaft on the surface. After completion and checkouts, the air core toroid is rolled onto a jacking frame at the top of the construction shaft and is lowered to the hall floor.

The jacking frame will serve as a slow, heavy-capacity freight elevator that may be used to lower the air core toroids as well as the calorimeter bays and the endcap calorimeters. The maximum weight to be lowered is approximately 200 tonnes, as determined by the endcap calorimeter. The size of the frame is determined by the air core toroids.

As shown in Figure 4.23, the jacking frame assembly consists of four hollow-core hydraulic jacks provided with multiple wedges that clamp onto a series of lowering cables which hold the jacking frame. The frame is constructed from rigid box members onto which the air core toroids or calorimeters can be rolled. The jacks are mounted on two cross beams that straddle the construction shaft. Note that for simplicity only one cable has been shown on each jack. We anticipate about 40 cables per jack. These bundles of cables are laid along the muon steel yard on wood guides or held on large diameter reels. (By the time the jacking frames are needed the muon steel assembly is complete.)

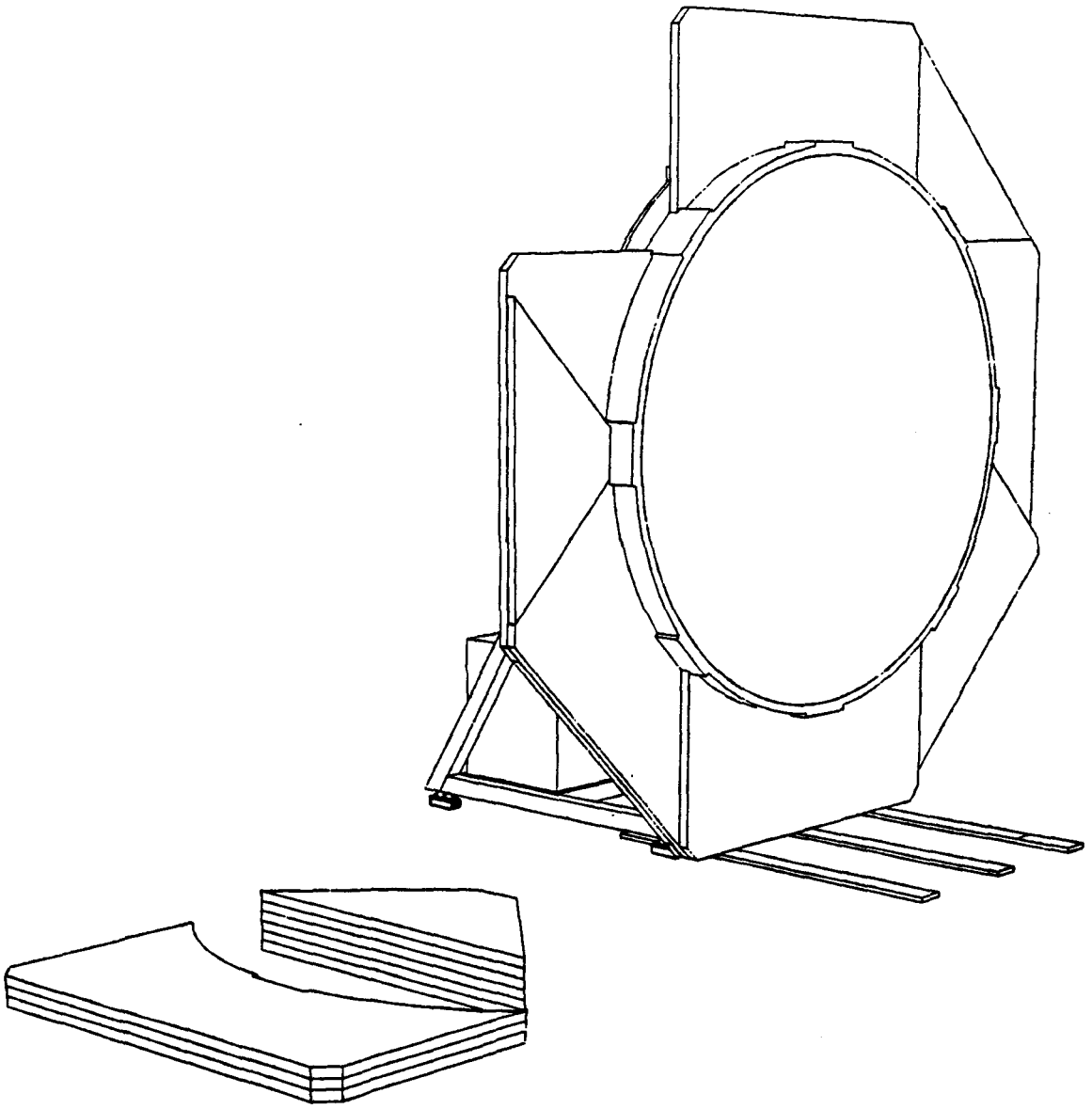

Figure 4.20 ACT Detector—Muon Steel End Toroid (Under Construction)

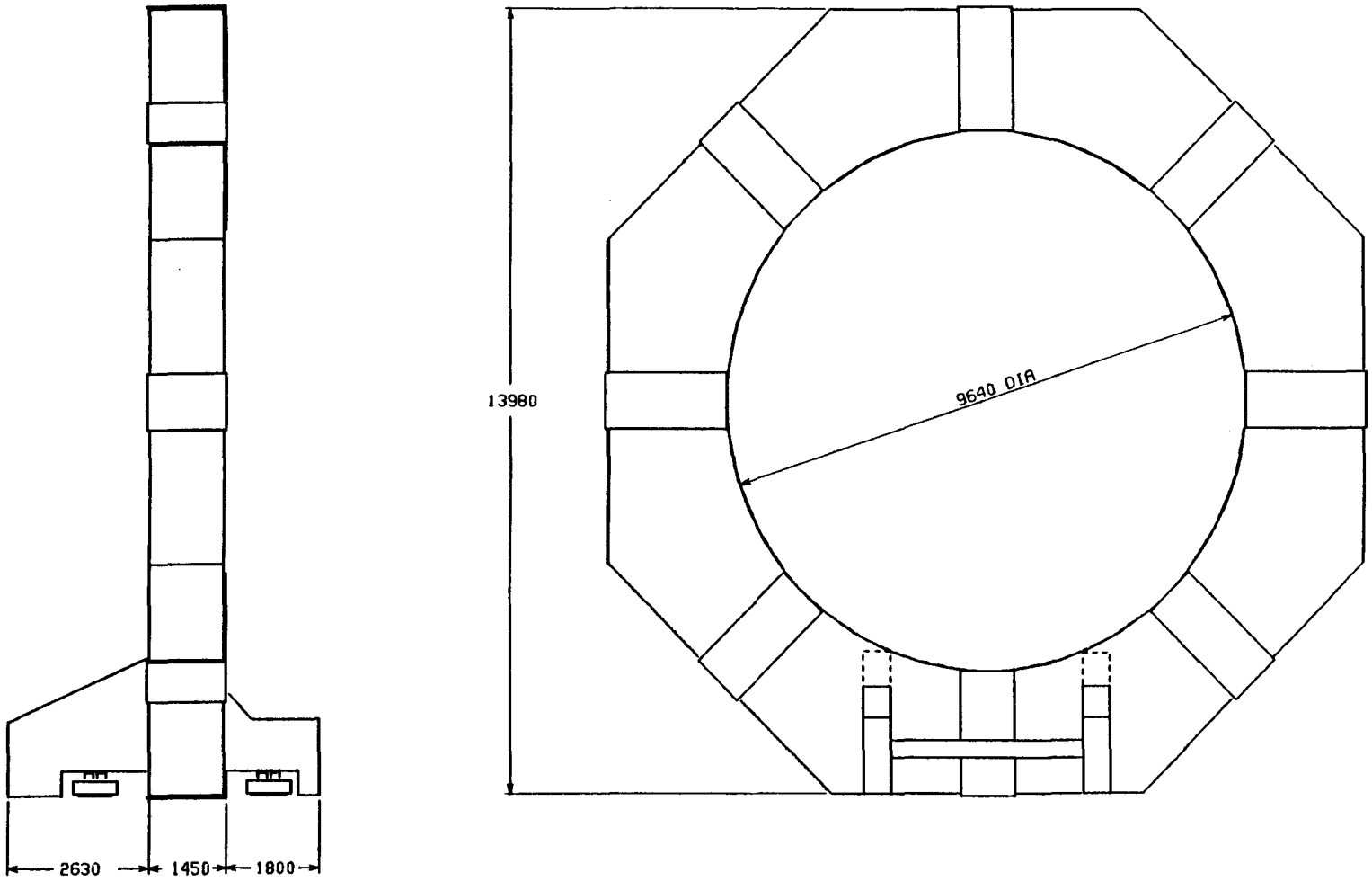

Figure 4.21. ACT Detector—Muon Steel End Toroid

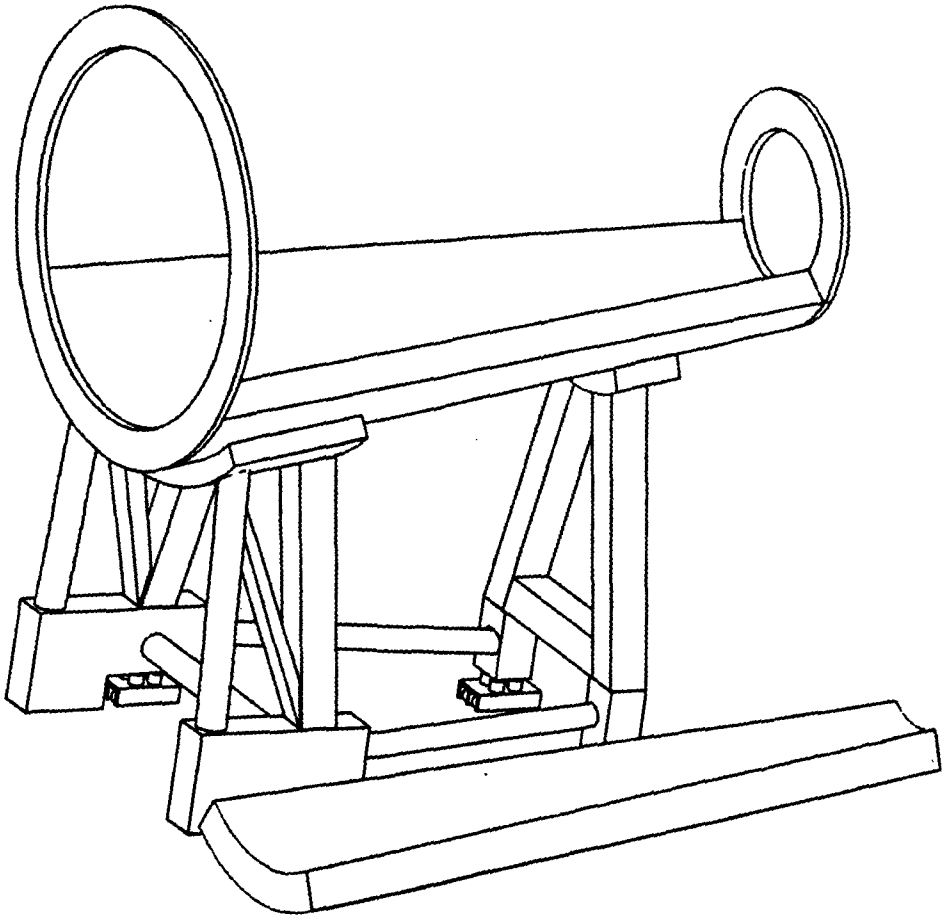

Figure 4.22 ACT Detector—Absorber Under Construction

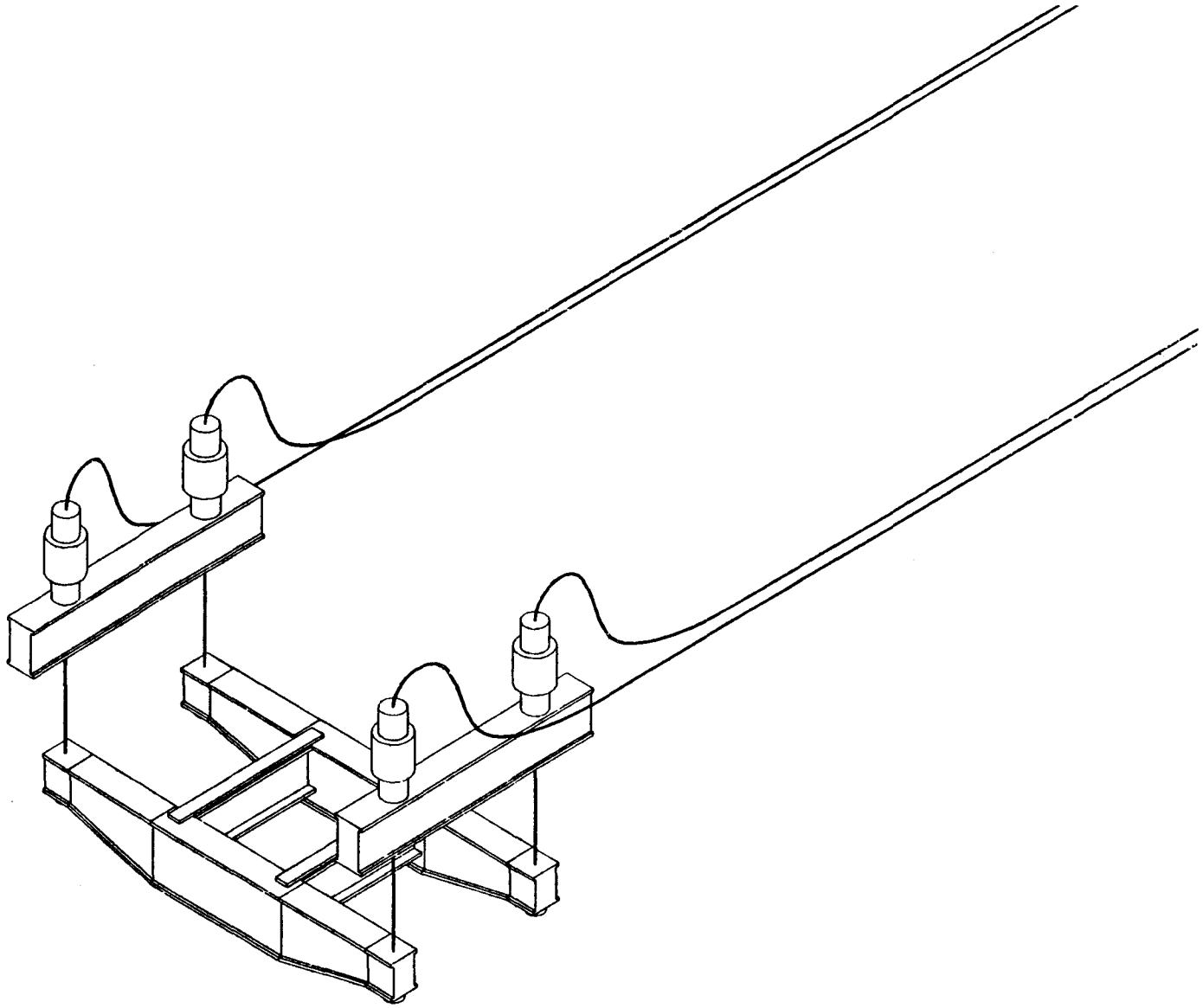

Figure 4.23. ACT Detector—Jacking Frame

The jacking frame weighs around 50 tonnes and is stored beside the construction shaft, as shown in Figure 4.24. When needed, the overhead crane installs the facing frame on the top of the construction shaft, and the air core toroid is rolled onto the frame. When it reaches the hall floor, the jacking frame enters an approximately 2-m-deep depression so that the top of the frame is level with the operating floor. This depression is covered with a heavy, removable platform when the jacking frame is not in use.

Based on a nominal operating speed of the jacking system of 4.8 m/h, it takes approximately 13 hours to lower the ACT to the hall floor. Allowing time for rolling onto the frame, lowering, and rolling off the frame, we estimate three days are required to move an air core toroid or calorimeter bay from the surface to the hall floor. We recommend that the design of the jacking frame and the lowering operation be entrusted to experienced professional companies specializing in heavy lifts.

For this study we have obtained from such a company the very rough cost estimates for leasing the system described (Table 4.5). Note that this type of jacking equipment is generally leased and may not be purchased.

Table 4.5. Unit Labor and Rental Costs for Hydraulic Jacking System.

Move-in and Assembly	$125,000
Dismantling	$75,000
Equipment Rental	$25,000 per month
Equipment Operation	$4,000 per day

Assuming that both air core toroids are ready for lowering in one month, the total cost of moving them into the hall is shown in Table 4.6.

Table 4.6. ACT Jacking Frame Cost Summary.

Equipment Mobilization and Dismantling	$200,000
Equipment Rental	$125,000
Equipment Operation	$24,000
TOTAL COST	$349,000

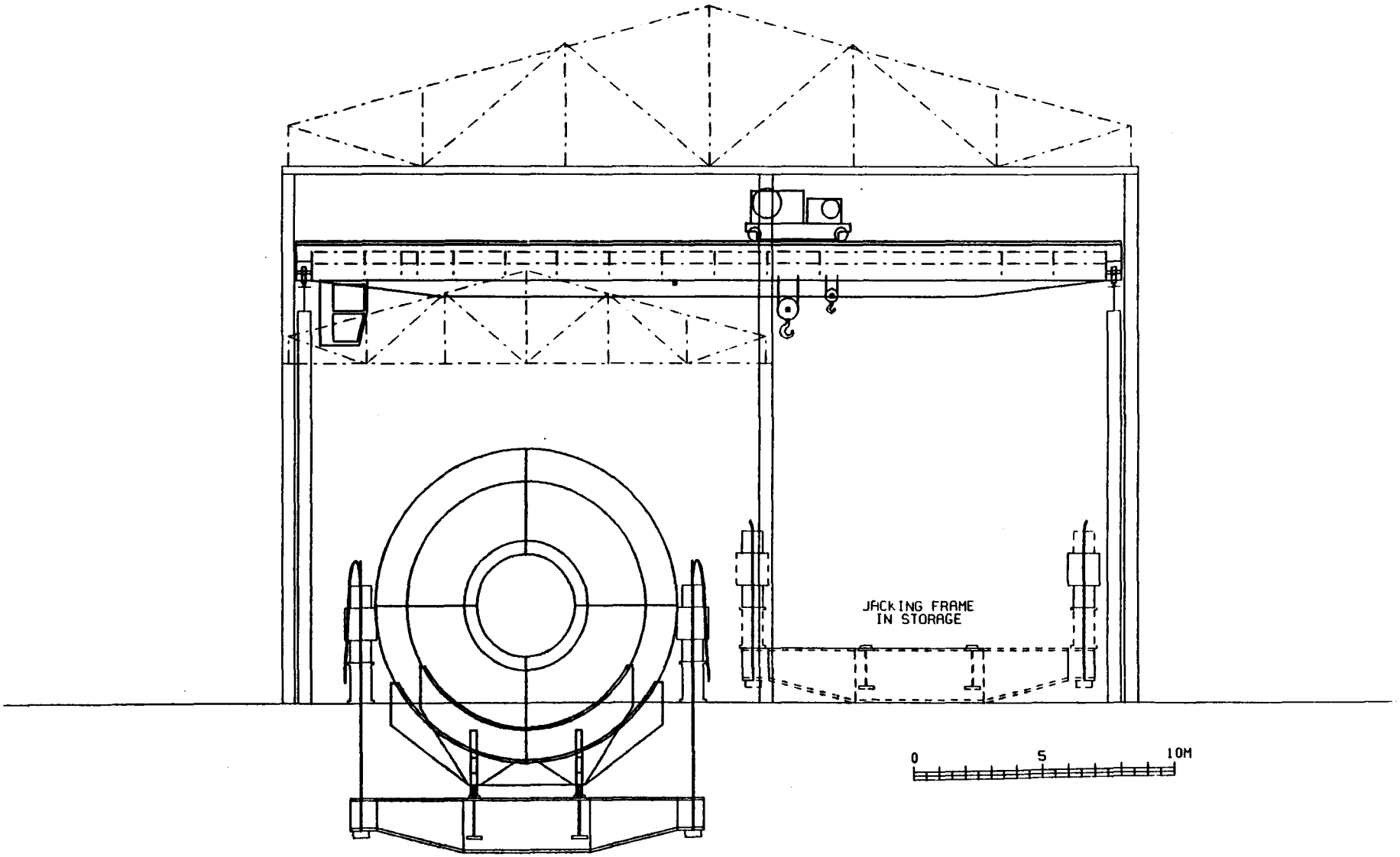

Figure 4.24. ACT Detector—Jacking Frame Lowering an Air Core Toroid

After an air core toroid has been lowered into the hall, assembly of the absorber, the air core, and the muon steel end toroids into a single movable unit proceeds as follows. As the weight of the air core toroid and absorber exceeds the capacity of the overhead hall crane by several times, the assembly procedures of these components rely entirely on using hydraulic jacks and Hillman rollers. As shown in Figures 4.25 and 4.26, the air core and steel toroids and the absorber are assembled in eight steps.

First, the absorber is moved into the air core toroid with the help of an assembly tool. At this point the air core toroid is bolted to the absorber, and the temporary frame of the air core toroid is removed. Next, the absorber/air core toroid assembly is moved into the muon steel toroid using the assembly tool, and the support frames of the two are bolted together to complete the assembly. Finally, the prefabricated muon chambers are lowered to the hall floor and installed on the completed assembly.

4.3.3 Calorimeter Assembly

The central and endcap calorimeters of the baseline detector are assembled in the north end of the hall. As shown in Figure 4.27, this area of the hall is sealed off from the rest of the hall by a temporary, air-tight partition. The HVAC system of the hall is temporarily adjusted to maintain a slight overpressure in the calorimeter assembly area. This overpressure will prevent entry of dust and fumes generated by the muon steel assembly and other work. A total area of about 25.5 m by 15 m is provided for calorimeter assembly. (Note that this area does not include the space set aside for the clean room.) This area allows the construction of one calorimeter bay at a time, while still providing room for the mobility of all construction equipment as well as access to the equipment shaft. The calorimetry of the baseline detector consists of three central and two endcap calorimeter bays, shown in Figures 4.28 and 4.29.

Testing of the assembled calorimeter bays is performed in a clean room constructed to the east of the calorimeter assembly area, as shown in Figure 4.27. The clean room is separated from the assembly area by strip doors (overlapping flexible strips of heavy plastic) to allow unrestricted movement of the bays. The room has a steel deck roof to provide support and working area for a self-contained pumping/filtration unit used to fill the modules of a bay with an ionization liquid, such as TMP. The clean room is also pressurized by filtered air. The clean room is sized to hold up to four calorimeter bays with an allowance of 3 m of clearance between them. This clearance permits mobility of the telescoping work platforms used to reach any area of the calorimeter assemblies during checkouts and filling of the modules.

Each calorimeter bay is constructed from preassembled modules weighing on the order of 20 tonnes. These modules are delivered to the calorimeter storage and staging building at the surface. From the staging area the modules are lowered to the hall through the equipment shaft and

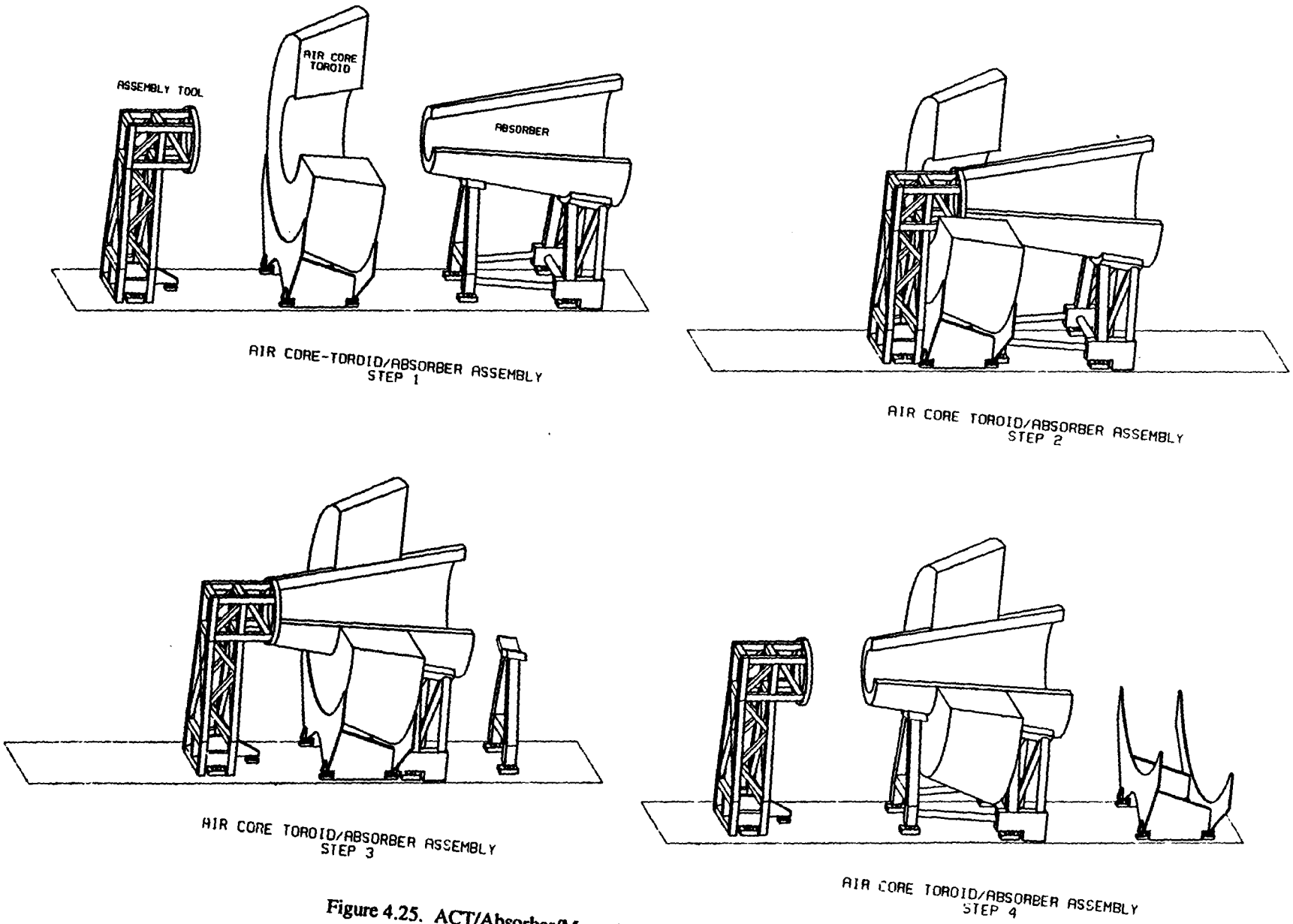

Figure 4.25. ACT/Absorber/Muon Steel Assembly (Steps 1-4)

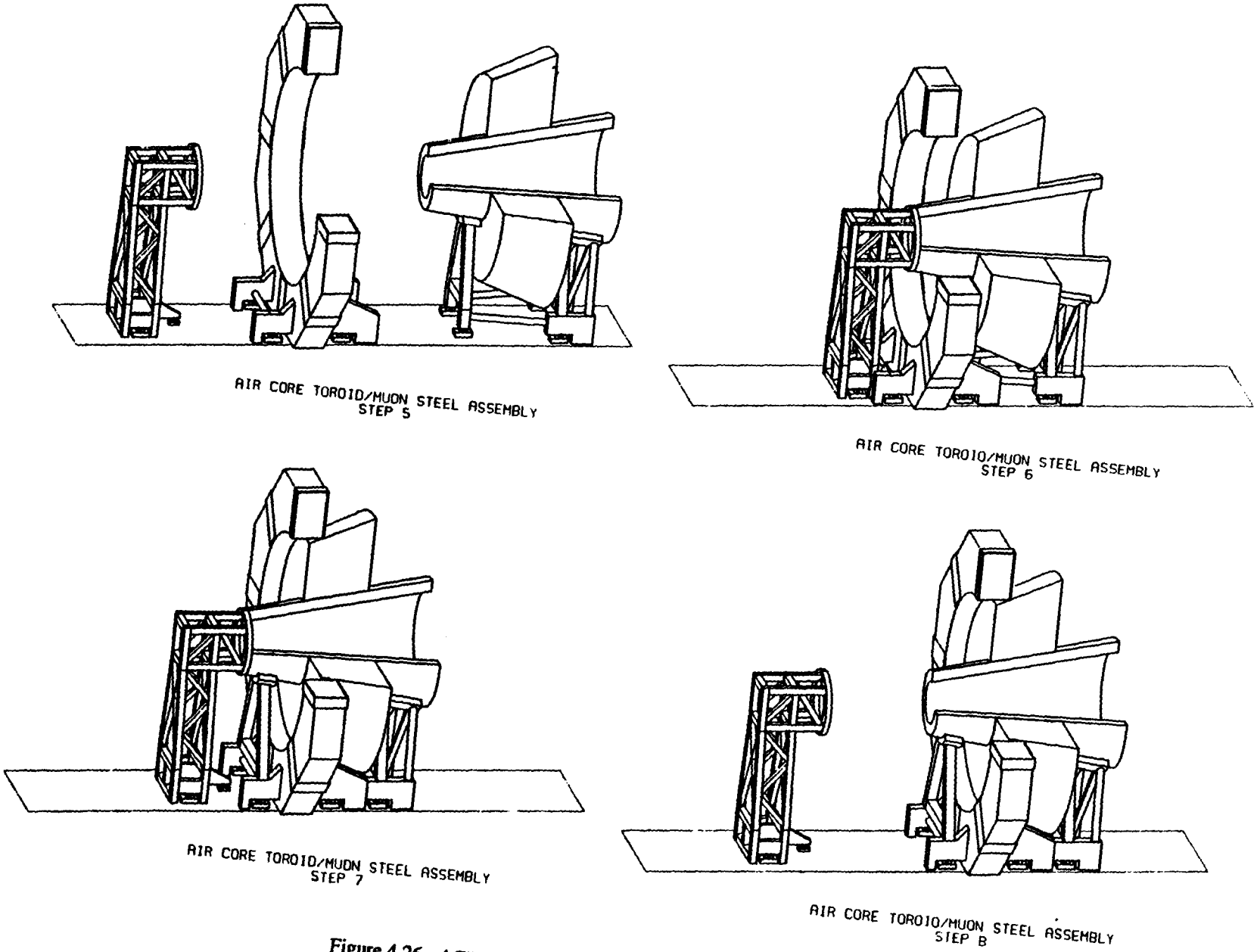

Figure 4.26. ACT/Absorber/Muon Steel Assembly (Steps 5-8)

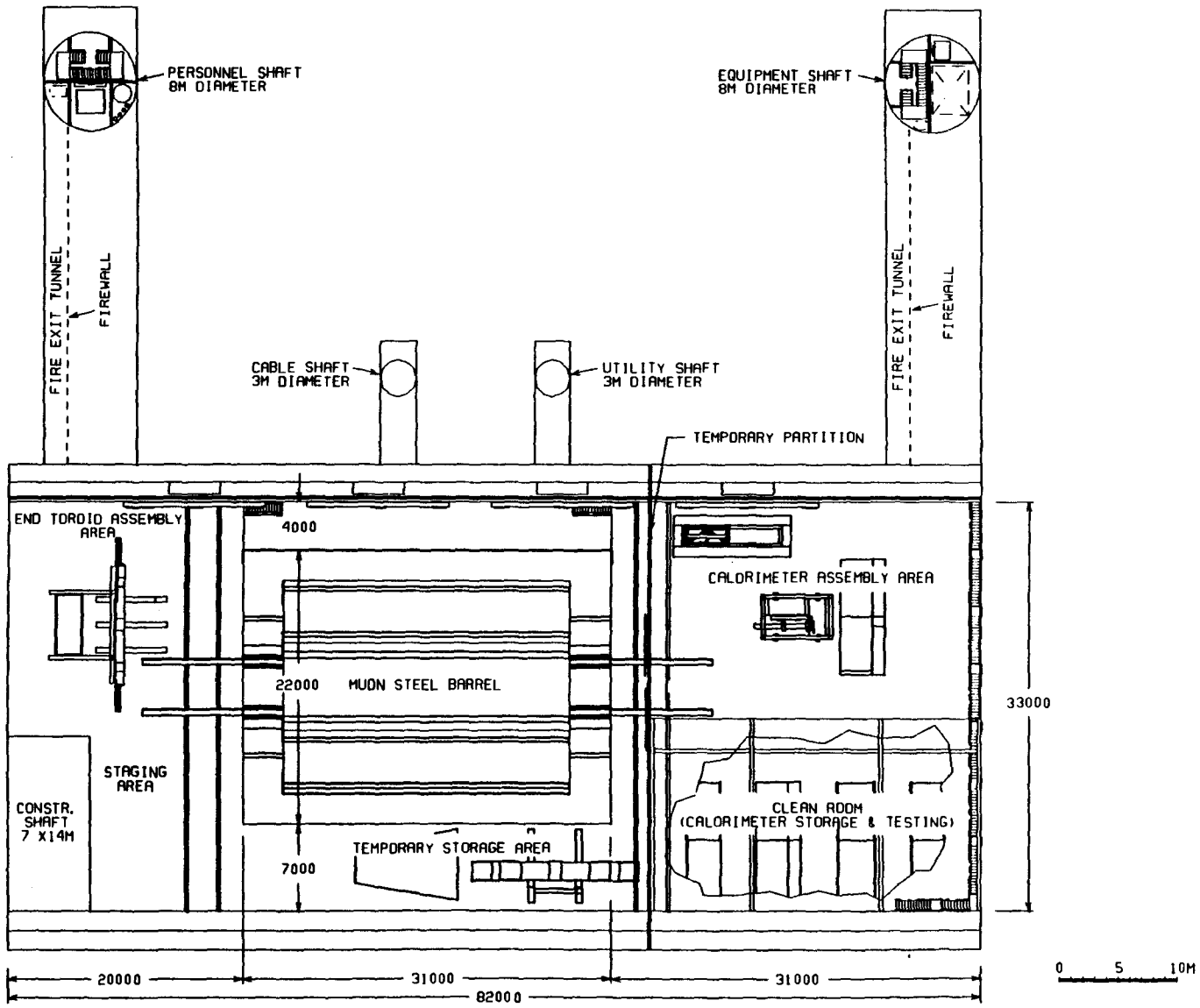

Figure 4.27. ACT Detector—Detector Assembly Layout

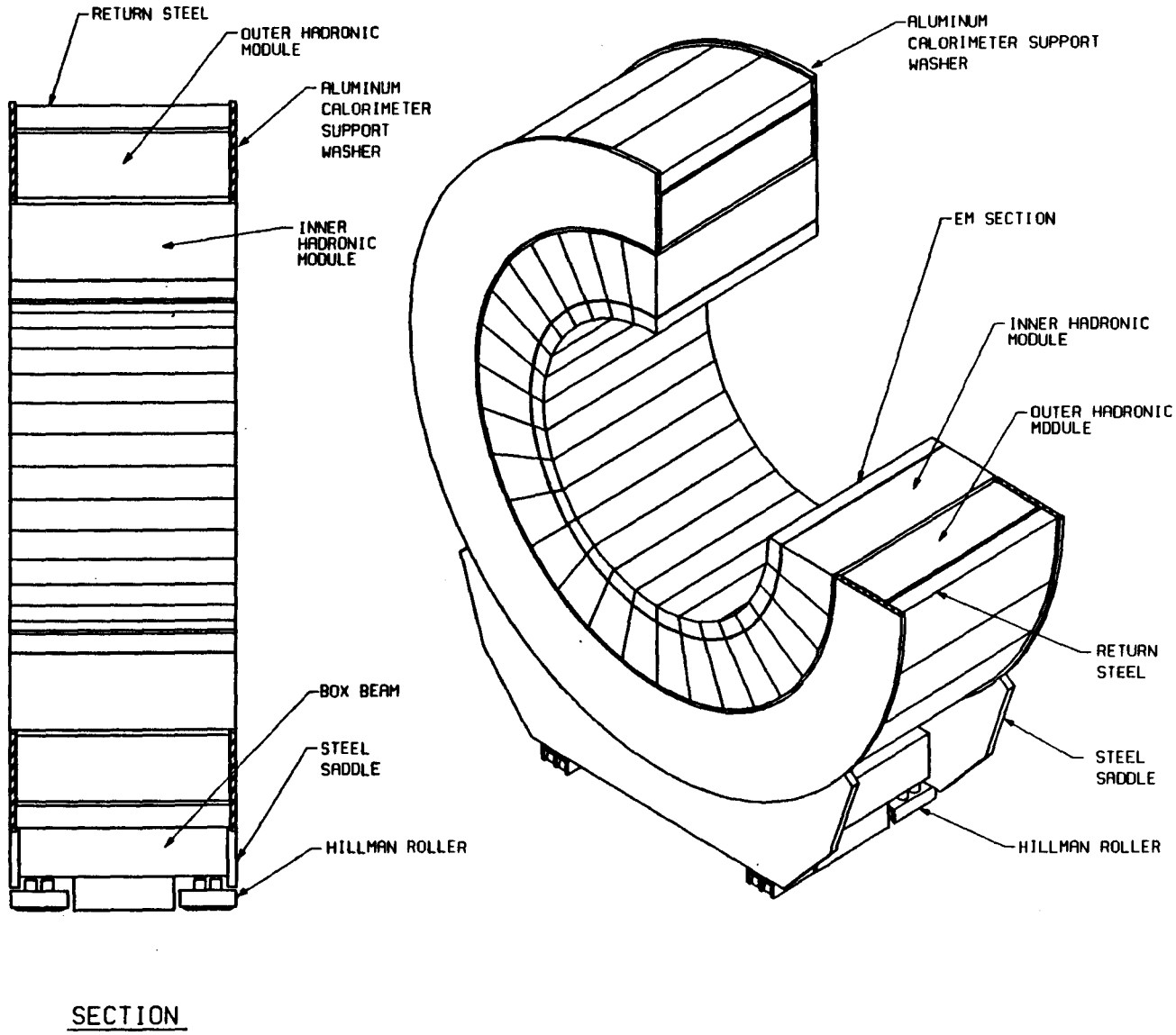

Figure 4.28. ACT Detector—Central Calorimeter

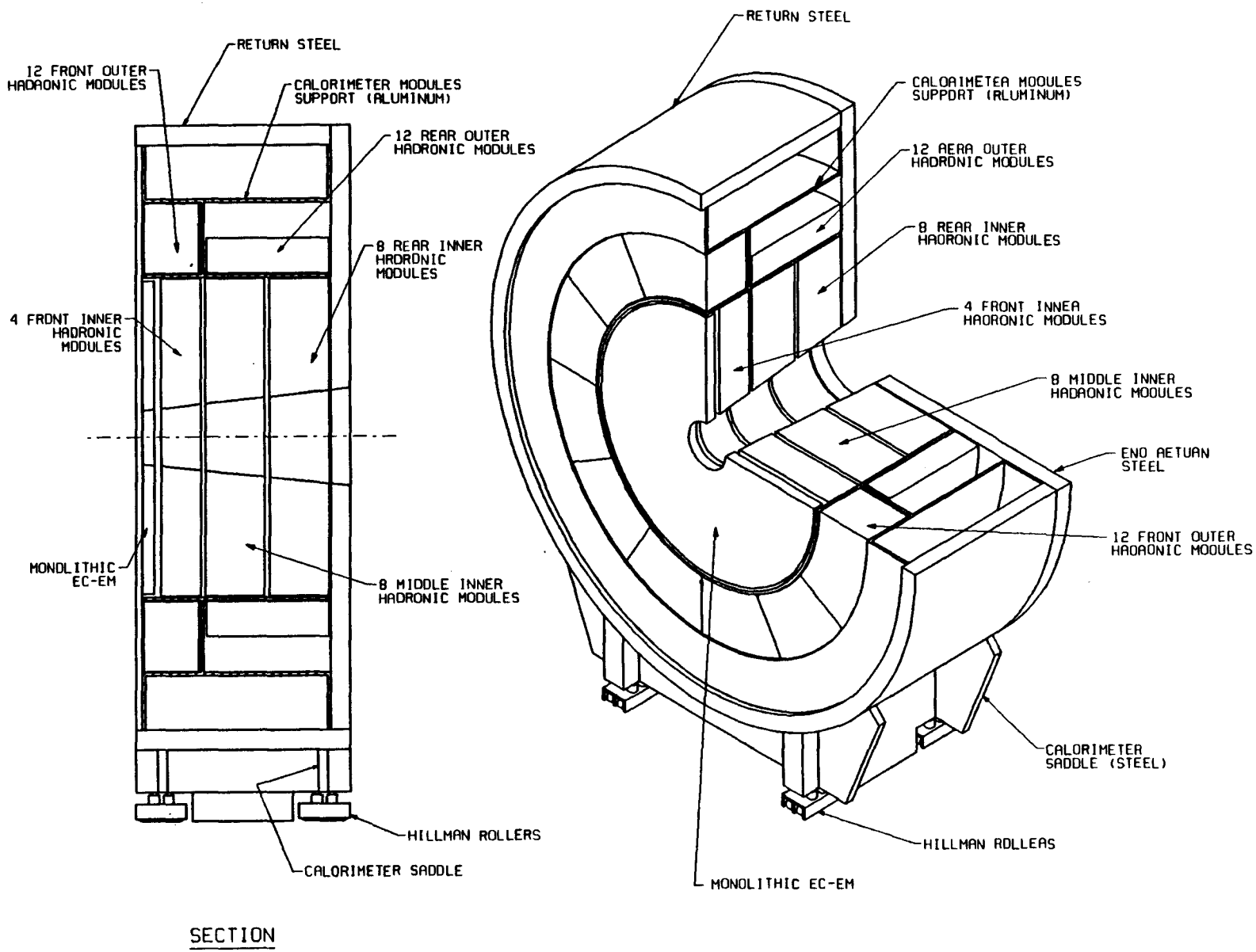

Figure 4.29. ACT Detector—Endcap Calorimeter

are moved to the assembly area on carts. The steel saddles and aluminum washers and frames of the calorimeter bays are lowered to the hall through the construction shaft and are moved to the calorimeter assembly area by the hall crane.

The support saddles are interconnected by box members equipped with four sets of Hillman rollers and hydraulic jacks. Normally, the weight of the calorimeter bay is carried by the box beam resting on steel blockage on the roller tracks. When the calorimeter bay needs to be moved, the rollers are lowered by the hydraulic cylinders, and the entire bay is rolled on steel tracks laid on the operating floor or installed in the muon steel barrel. The rollers can pivot through 360°, allowing the movement of the calorimeter bays in any direction required.

The central calorimeter bays are constructed of 32 inner modules and 32 outer modules bolted to two aluminum washers supported on steel saddles, as shown in Figure 4.28.

Assembly of a central calorimeter bay (Figure 4.30) proceeds as follows:

1. Assemble the steel saddles and box beams onto the four rollers and anchor the assembly to the floor.
2. Install temporary spacer struts between two washers and lift this subassembly onto the saddles. The top of the saddles are fitted with lubricated bronze bearing bars to facilitate rolling of the washers during assembly of the modules.
3. Install brackets and hydraulic cylinders to the washers and saddle. These cylinders provide the rotational motion needed during the assembly process.
4. Lift in four inner calorimeter modules and bolt to the inside edge of the washers in the topmost position. Since the inner calorimeter modules are longer (along the beam line) than the clearance between the two washers, they are lifted through the washers perpendicular to the position they will assume once installed.
5. Lift in four outer modules with flux return steel and install in topmost position, using bolts recessed in the outside face of the washers.
6. Rotate the washer/module assembly 45° clockwise using the hydraulic cylinders, remove the temporary spacer struts at the top of the washers, and repeat the above two steps until all but the last five inner modules are installed. Because of the limited space between the two washers, the last five inner modules are installed with the fixture used for the installation of the end calorimeter modules.
7. After all modules of a central calorimeter bay are installed, lock the saddle to the washer with bolts tapped into the washer, remove the hydraulic cylinders, and move the completed bay into the clean room.

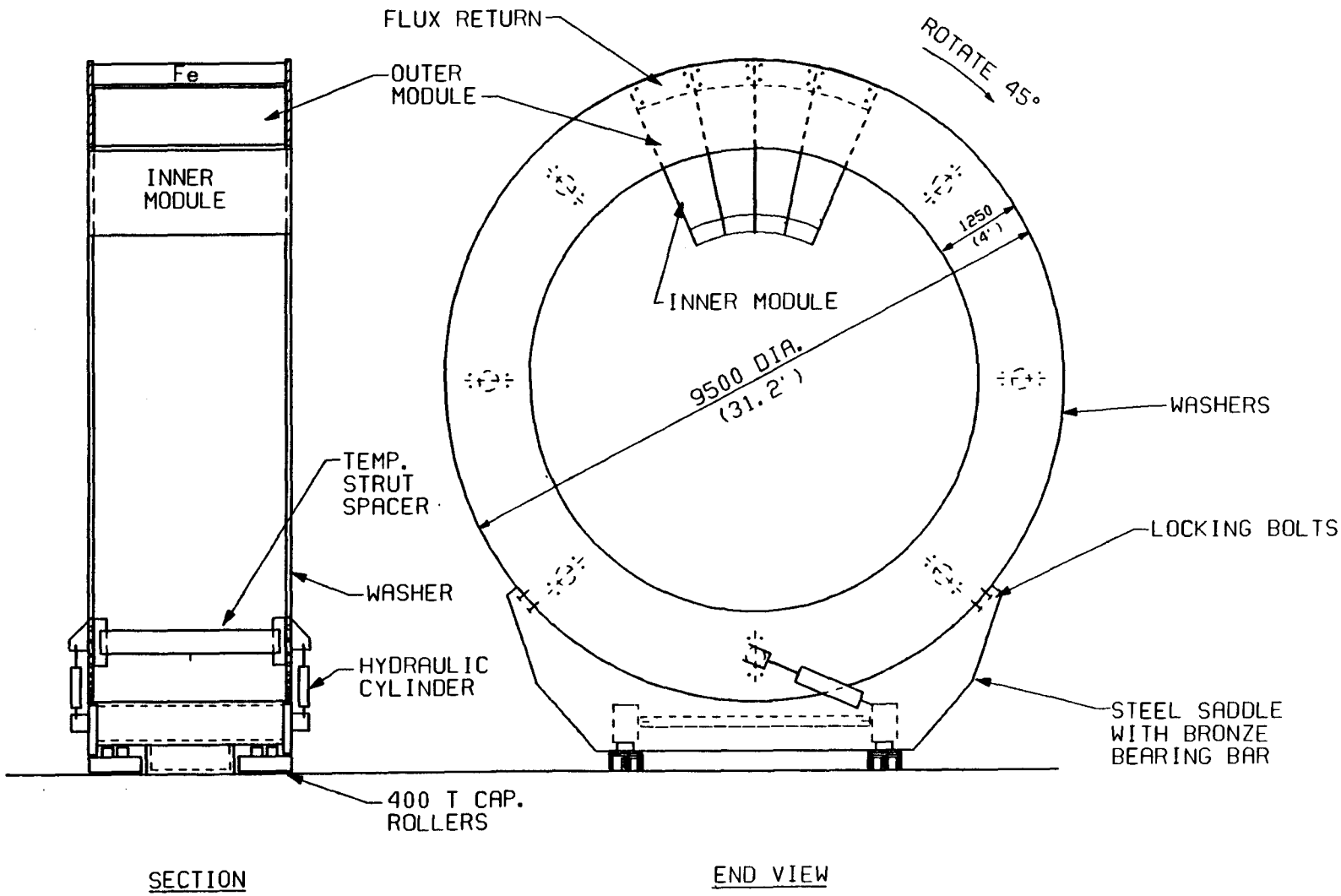

Figure 4.30. ACT Detector—Central Calorimeter Bay Assembly

We have performed several finite-element computer analyses to insure that deformation of the washer will not interfere with the installation of the modules during assembly. As shown in Figures 4.31 and 4.32, the maximum stress and deflection of the 100-mm (4 in.)-thick aluminum washers during and after assembly of the modules are acceptable.

The endcap calorimeter bays are made up of 20 inner hadronic modules and 24 outer hadronic modules, plus a monolithic EM module (Figure 4.29). The modules are bolted to a welded aluminum frame consisting of an inner and outer shell and three washers. The aluminum frame is supported by the lower portion of the flux return steel, which is welded to the support saddle to form a rigid cradle. The module support frame, the lower half of the return steel and saddle assembly, and the top half of the return steel are lowered to the floor through the construction shaft. The two halves of the return steel are field-welded, and the rollers and hydraulic jacks are installed under the saddle. The completed return steel and saddle assembly is moved to the calorimeter assembly area.

Assembly of the endcap calorimeter bays will proceed as follows:

1. Install the module support frame inside the return steel barrel and lock in.
2. Position the special assembly fixture shown in Figure 4.33 and fasten it to the end of the return steel by temporary bolts. This prevents any movement between the fixture and the module support frame which would interfere with the installation of the modules.
3. Install the 8 middle and 8 rear inner calorimeter modules, then the 12 rear outer modules. The assembly fixture is repositioned periodically to access the full face of the calorimeter assembly.
4. Move the assembly fixture to the opposite face of the endcap calorimeter bay, bolt to the return steel, and install the 4 front inner and the 12 front outer hadronic modules.
5. Install the monolithic EM module and move the assembled endcap to the clean room for the final electrical checkouts and filling of the modules.

The flat end return steel of the endcap calorimeters is installed by bolting the steel plates to the machined rear face of the curved return steel. The end return steel will be assembled from three to five segments to facilitate removal for servicing the rear face of the endcap.

As previously noted, the calorimeters are moved about the detector hall on Hillman rollers running on steel tracks. The bays are moved from the assembly area to the clean room and to their operating positions in the barrel muon steel on portable steel tracks welded to the floor plate. However, as described in Section 4.2.3, permanent tracks will be provided in certain areas of the hall. The calorimeters will be pulled along the tracks by hydraulic jacks bolted to the steel tracks.

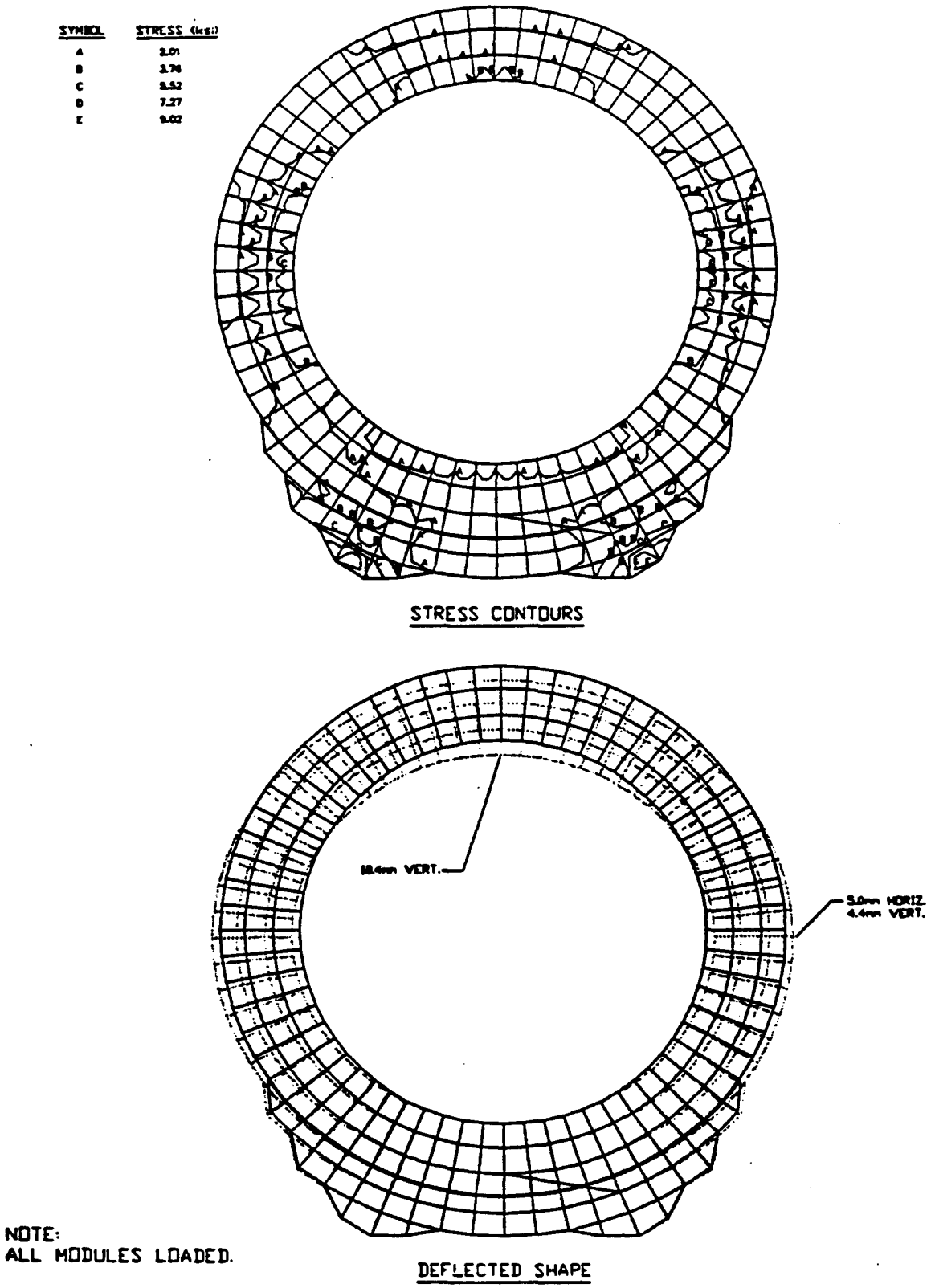

Figure 4.31. ACT Detector—Central Calorimeter Washer Analysis (All Modules Inserted)

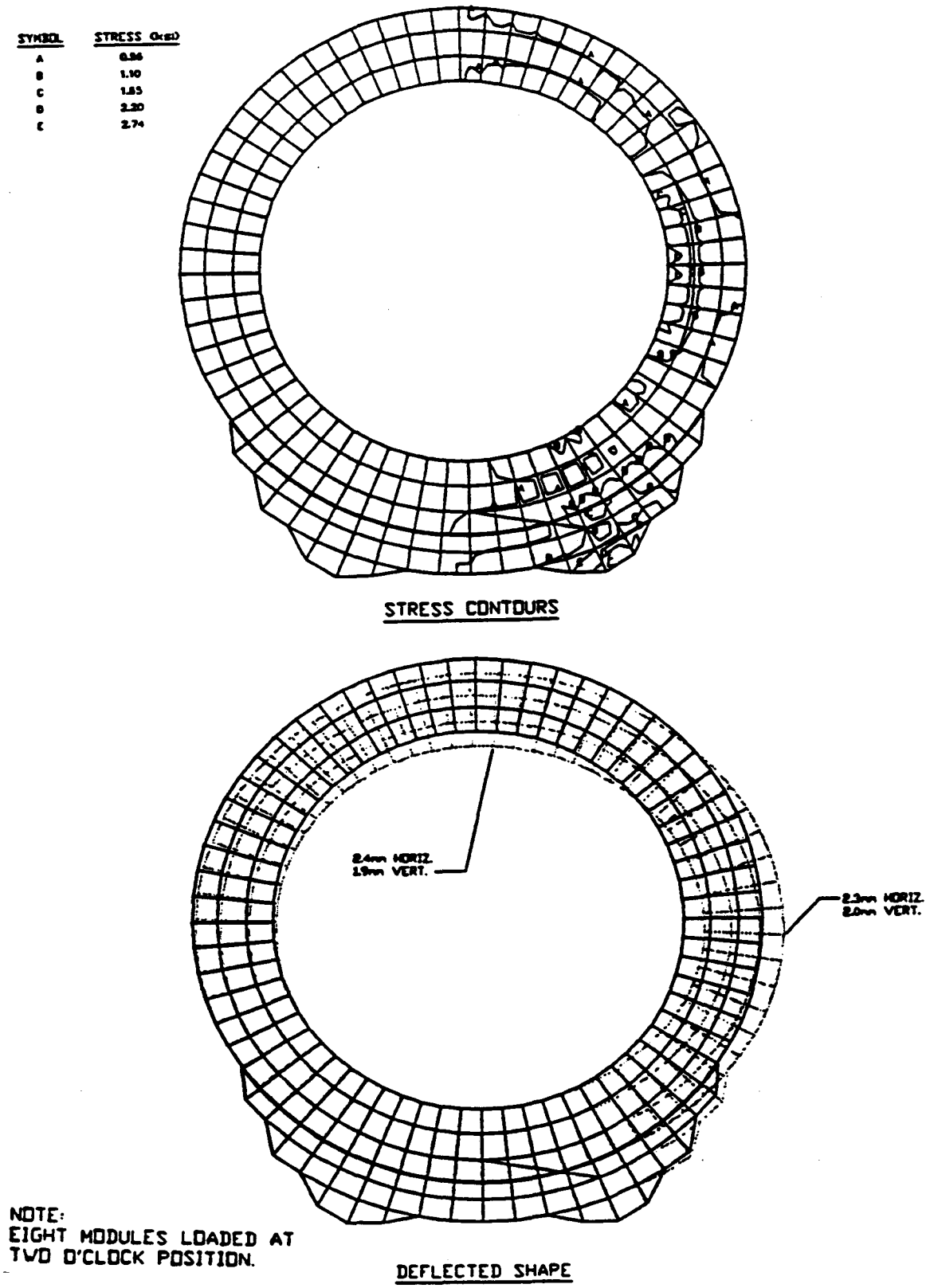

Figure 4.32 ACT Detector—Central Calorimeter Washer Analysis (8 Modules Inserted)

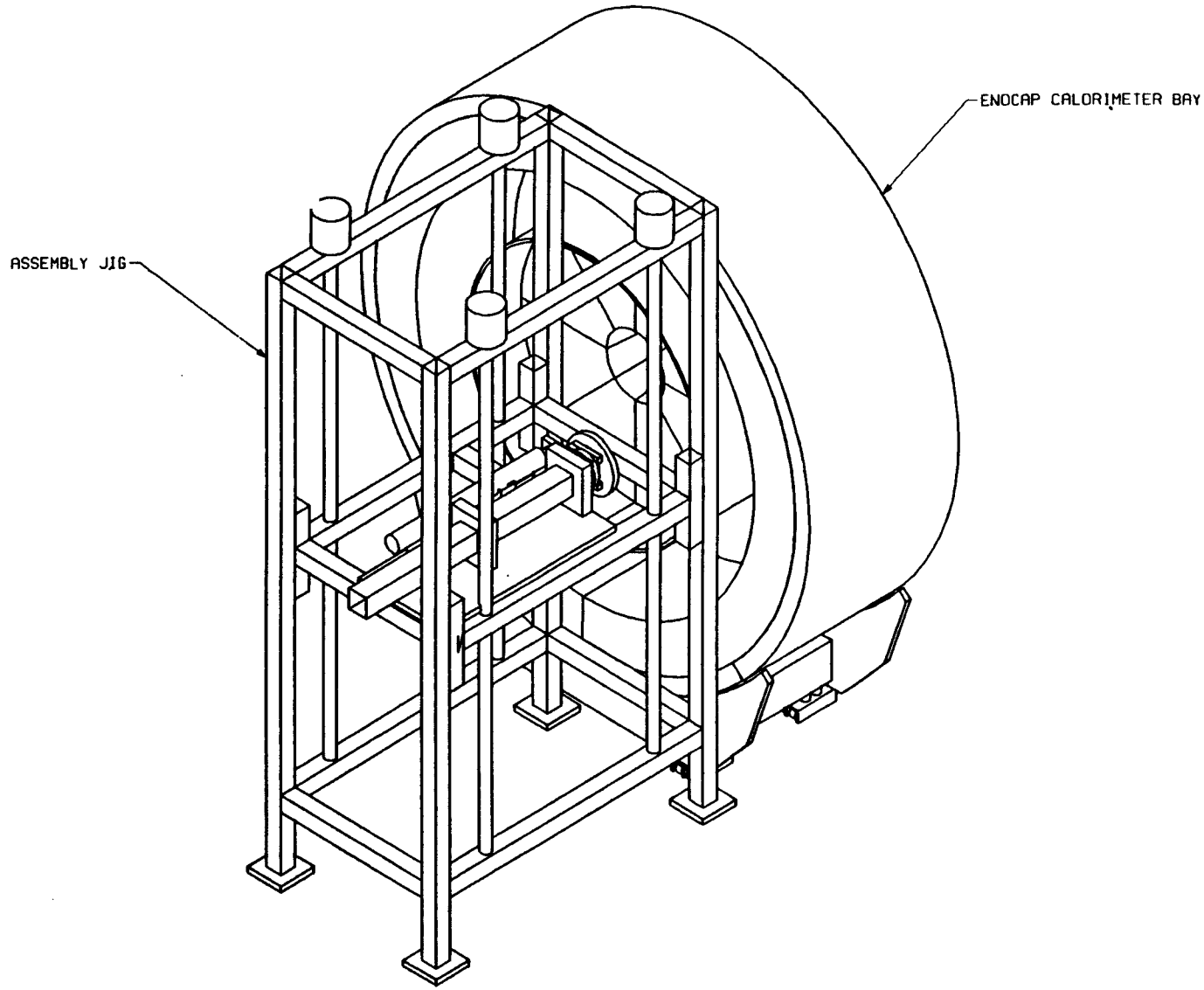

Figure 4.33. ACT Detector—Endcap Calorimeter Assembly Frame

The estimated manpower requirement for assembling the calorimeters is as follows:

- Receiving, unloading, unpacking, and staging the modules at topside; lowering modules to hall—8 men.
- Receiving modules at bottom, moving to assembly area—4 men.
- Module installation—6 men.

The estimated rate of installation using the above manpower is two modules per 8-hour shift. After two modules are installed, they are tested in a second shift before installation of the next two modules. Additional physicist manpower to checkout modules after installation is required.

4.3.4 Muon Chambers

We assume that the muon chambers arrive in the hall as panels, several meters on a side, ready to be installed. Support and alignment frames are attached to the muon steel to accept the panels. Transport of the panels is by hall crane. The problems of muon chamber support and alignment have been greatly simplified in this study and need to be addressed in future studies.

4.3.5 Solenoidal Coil

The superconducting solenoidal coil arrives at the detector hall fully assembled and ready to be installed. It is assumed that the coil arrives at the hall mounted on a mandrel which is designed to support the coil during transportation to the site and during installation. The coil is lowered into the hall via the construction shaft and is carried by the overhead hall crane to the area previously used for calorimeter assembly. Mounting the coil on its temporary support trolleys, and any other pre-installation work, is done in this area. During the coil installation, all muon steel work and calorimetry assembly will have been completed, leaving sufficient space available for coil work.

After unpacking and inspection, the coil is installed in the following steps:

1. The coil is first lifted by its mandrel onto the saddles of the temporary supports located at each end of the coil. These temporary supports will hold the coil on the beam line; they are designed to roll on calorimeter tracks.
2. After the shipping mandrel is extended by bolting an approximately 12-m-long beam to one end, the coil is rolled into the barrel calorimeter until the end of the cantilever mandrel extension has emerged from the calorimeter, as shown in Figure 4.34. A third movable support stand is bolted to the free end of the mandrel extension, and the middle temporary support stand is removed.

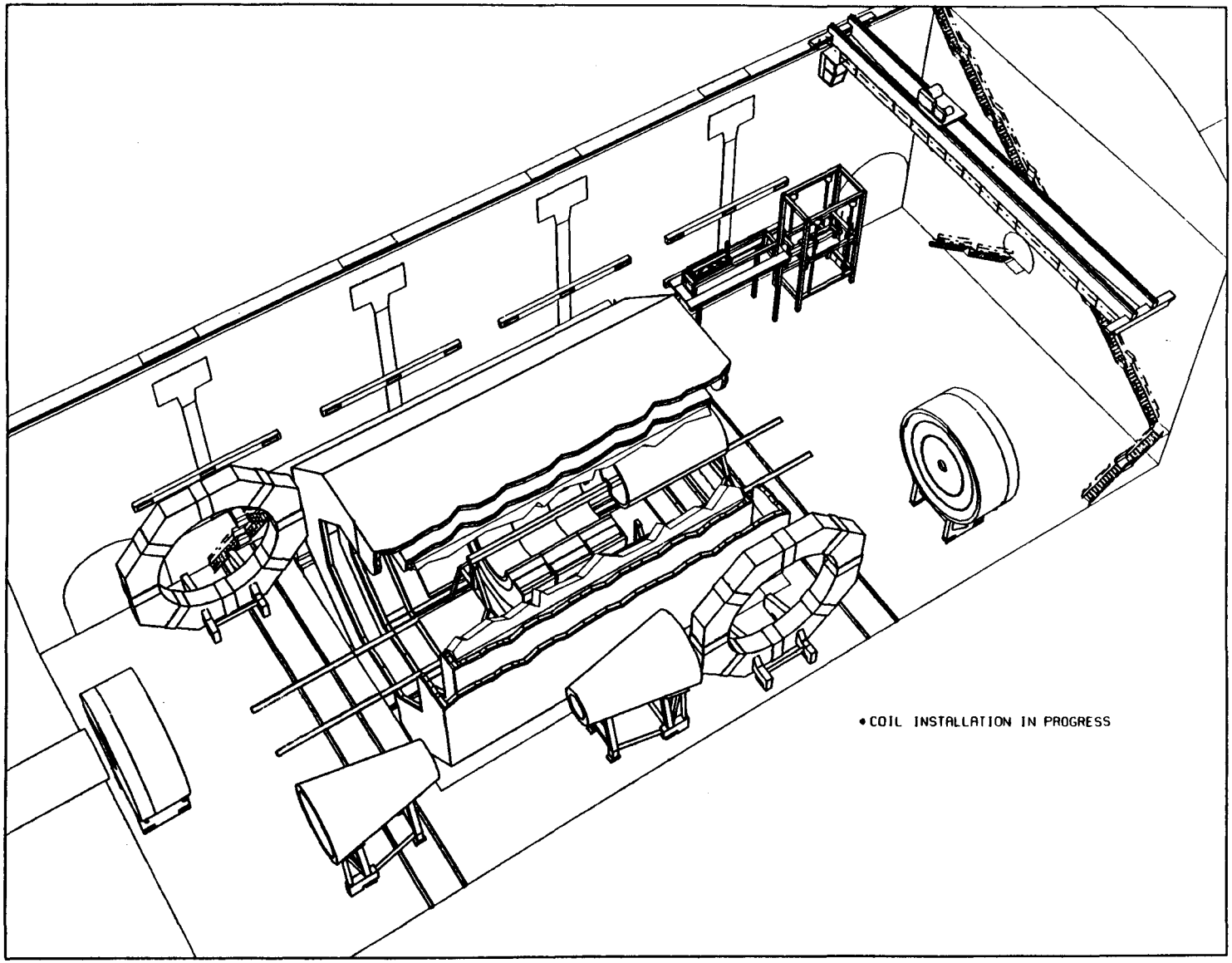

Figure 4.34. ACT Detector—Solenoid Coil Installation

3. The coil is now moved into the barrel calorimeter. After installation of the permanent support links to the calorimeter and removal of the shipping ties, the mandrel is rolled out from the coil.
4. Cryogenic and power connections are made.
5. Field mapping takes place after the coil has been cooled and the endcap calorimeters have been temporarily moved into their operating positions.

The superconducting solenoidal coil operates at a cryogenic temperature of 4.5 K by boiling liquid helium in the magnet and liquid nitrogen in shield. The cryogenic valve box is located on top of the north end of the detector. Cryo pipes and electric power are connected to the magnet via an approximately 30-cm^2-diameter chimney. Figure 4.35 shows a schematic layout of the required cryogenic cooling system in the hall and at the surface. As shown in the figure, the cryogenic and vacuum equipment, such as local dewars and pumps, is located on the gallery at the side of the detector. A walkway from the gallery to the top of the detector is included to facilitate access to the cryogenic valve box.

4.3.6 Central Tracking Device

We assume that the central tracking unit, including the silicon tracking device, arrives at the hall fully assembled on a mandrel and ready to be installed. The central tracking device is lowered into the hall through the construction shaft and is carried to the calorimeter assembly area by a hall crane. This area is used for any necessary pre-installation work . After checkout, the tracking unit is installed using the temporary support stands of the coil, in a manner similar to the installation of the coil.

4.3.7 Beam Pipe

The beam pipe arrives at the hall in segments and is assembled on site. These segments are lowered into the hall through the construction shaft and are either rolled to their installation sites on trolleys or carried by the hall crane. Any preparatory work done on the beam pipe can be done in any area adjacent to the barrel muon steel or in the barrel itself.

4.3.8 Forward Calorimeters

We assume that the forward calorimeters arrive at the detector hall in halves, each half fully assembled. They are brought into the detector hall through the construction shaft, carried to their installation sites, and lifted onto their support cradles by the hall crane. Any work required on the forward calorimeters is accomplished *in situ* once they have been installed. Sufficient room is available for this work.

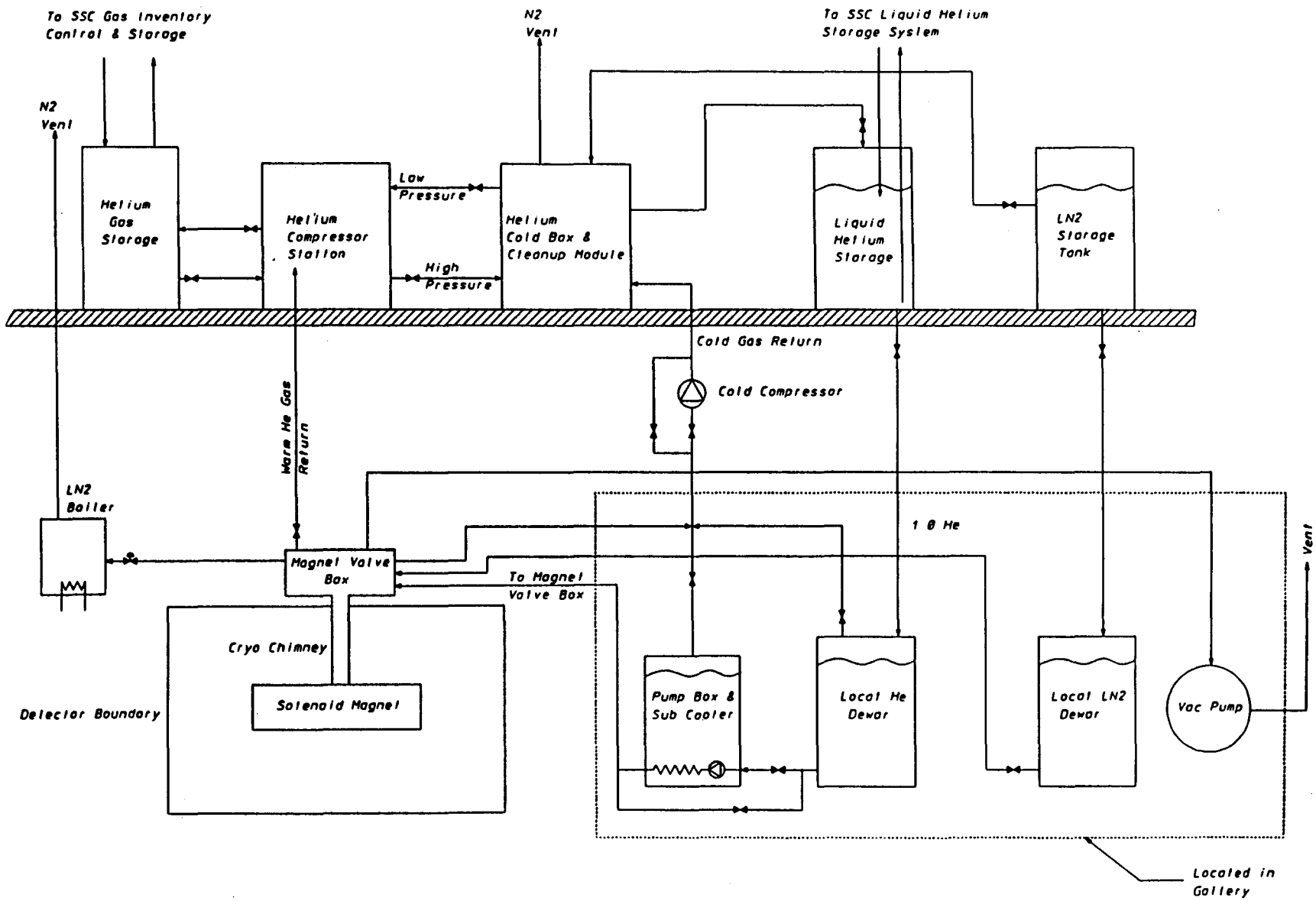

Figure 4.35. Solenoid Cryogenic System Schematic

4.3.9 Electronics/Triggering

We have not studied the assembly of the readout and triggering electronics needed for this detector. We have provided space for the electronic and its cables. The cables to the surface for the electronics and triggering are carried by the cable shaft, which has been provided specifically for this purpose.

4.3.10 Accelerator Components

The assembly of accelerator components is carried out in coordination with the SSC Laboratory. We assume that the accelerator components are brought into the hall through the construction shaft and are carried to their installation sites by either of the two cranes in the detector hall. There is space available adjacent to their installation sites for any necessary preassembly work.

4.3.11 Calorimeter Assembly Above Ground

This section examines the concept of assembling the calorimeter sections above ground and lowering the completed bays into the hall after testing. Surface construction may be more efficient and safer. It permits greater and more flexible calorimeter movement. It also allows for the detector hall to be reduced in size, although probably not enough to compensate for the duplication of equipment required. This duplication arises from the need to be able to disassemble the calorimeters underground in case of malfunction after installation. Figures 4.36 and 4.37 show the above-ground facilities for the concept being studied. Figures 4.38 and 4.39 show a cross section and an elevation of the surface facilities in relation to the detector hall.

The muon steel is handled in a yard covered by an 80-tonne gantry crane. The gantry crane and a portion of the yard rail tracks are built ahead of beneficial occupancy in the area away from the hall excavation, as seen in Figure 4.36. This gantry crane is equipped with a trolley, a 65-tonne hook and a 15-tonne auxiliary hook, both capable of lowering loads up to 64 m below the surface via the construction shaft.

The yard (Figure 4.36) is capable of storing 25% of the plates required for the muon steel barrel. We assume it is acceptable to store short plates on top of long plates. The yard is covered with roofing for about 30 m; the rest of the yard is uncovered. The roofed portion will allow operation during foul weather. The muon steel plates are stored on edge, on 4 × 4 logs. They are stored and moved in groups of four by the gantry crane.

The calorimeter modules are received, tested, and calibrated in the calorimeter module staging building provided with a 40-tonne bridge crane. Once the modules are ready for assembly, they are

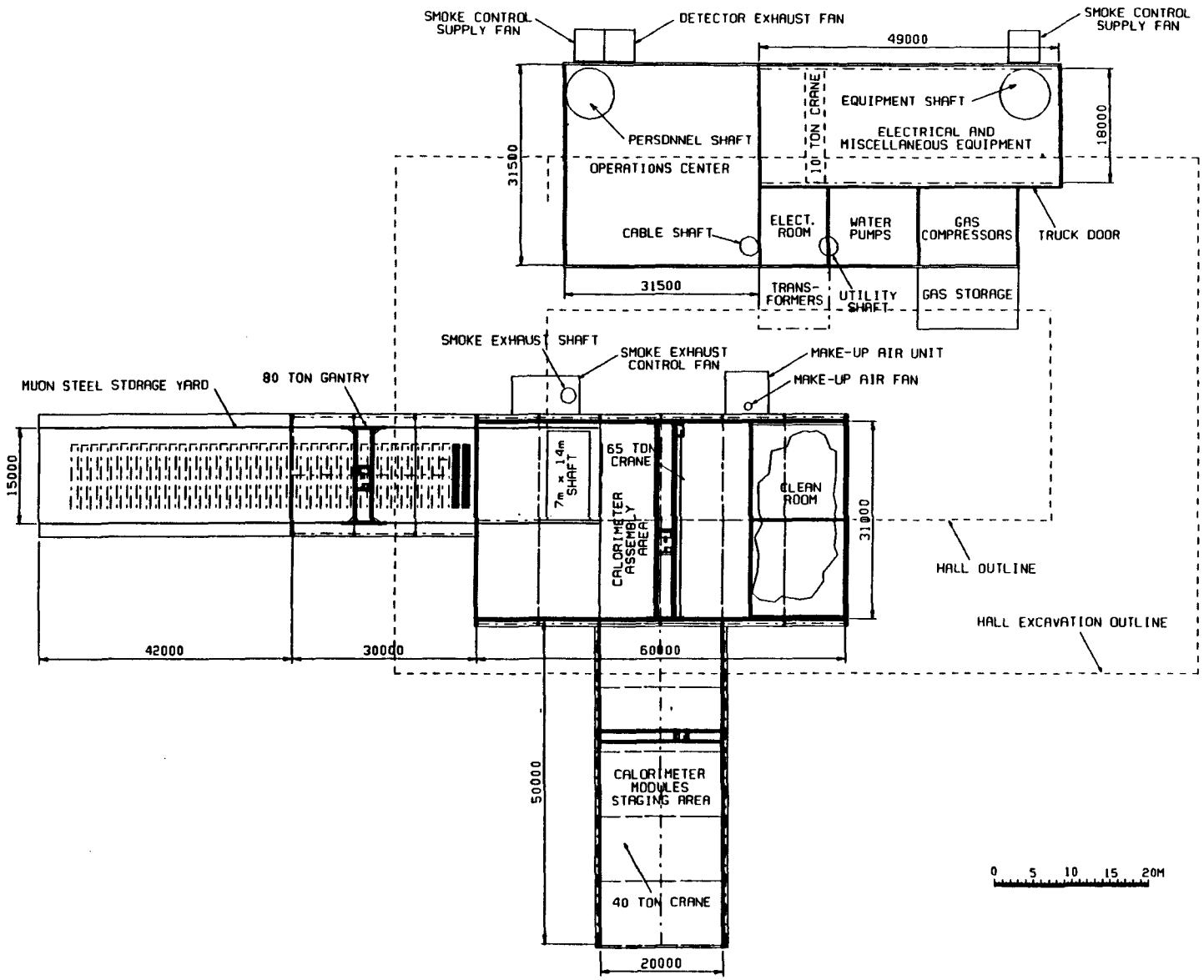

Figure 4.36. ACT Detector—Surface Facilities—Calorimeter Assembly Above Ground (Plan View)

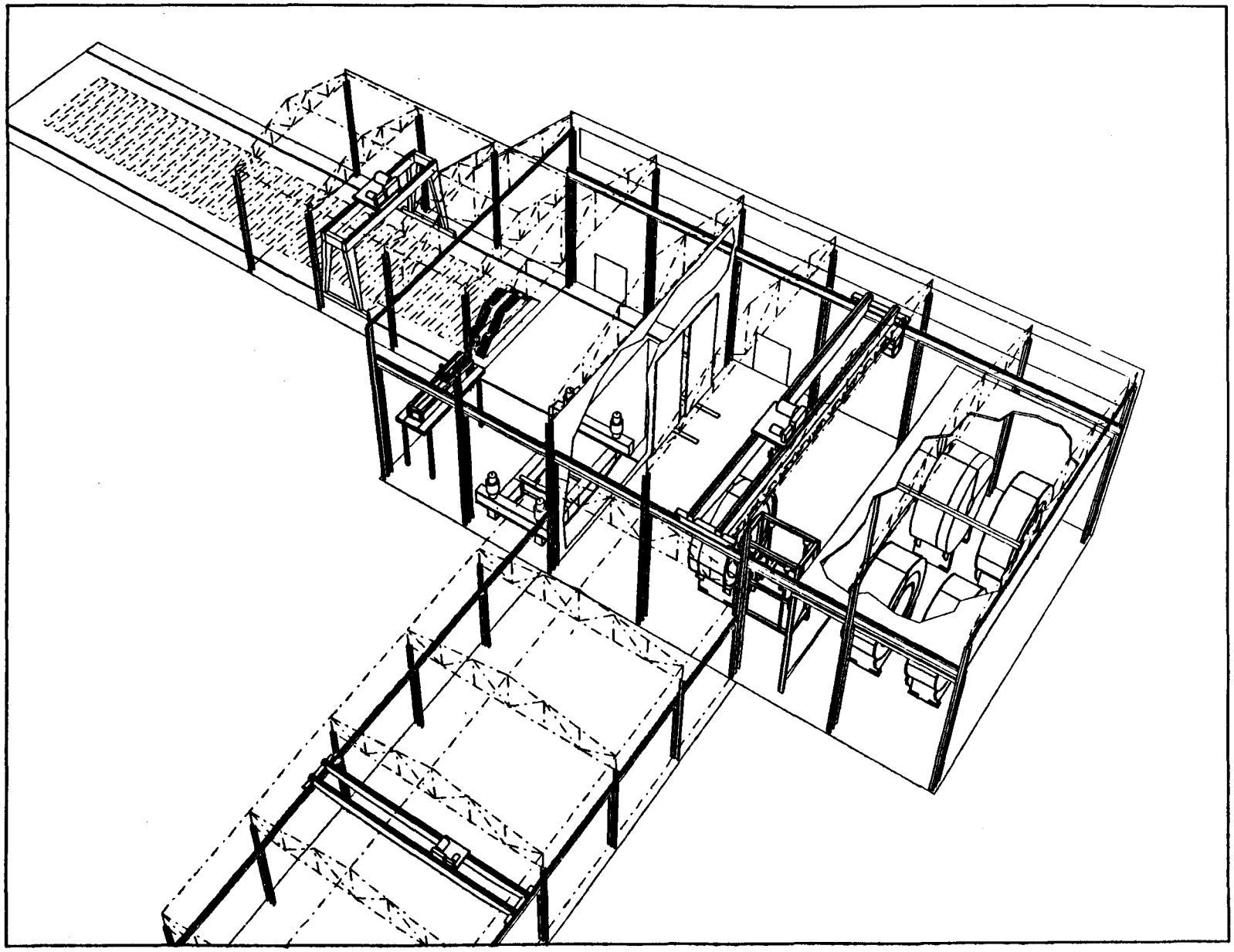

Figure 4.37. ACT Detector—Surface Facilities—Calorimeter Assembly Above Ground (3-D View)

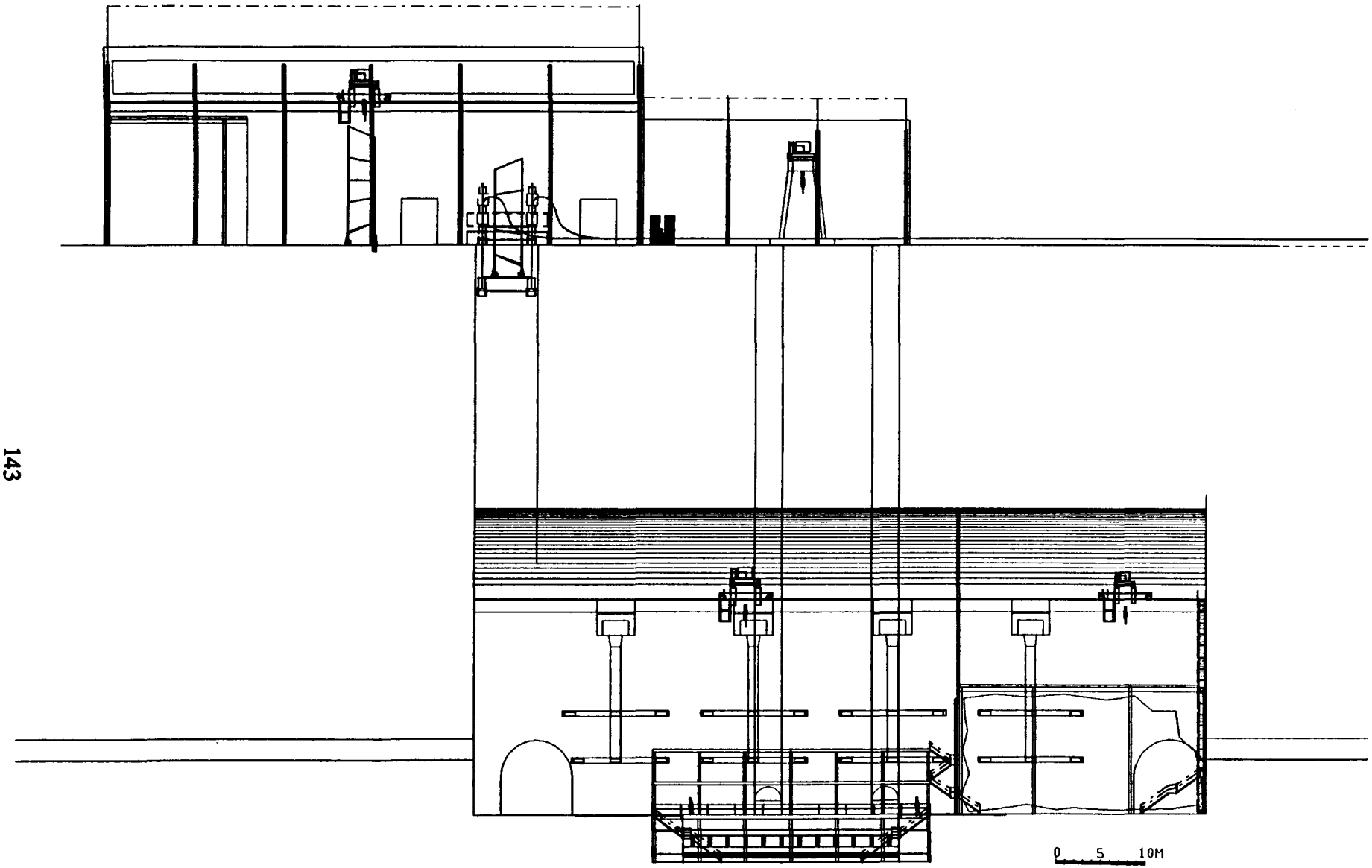

Figure 4.38. ACT Detector—Surface Construction Facilities (Front Section)

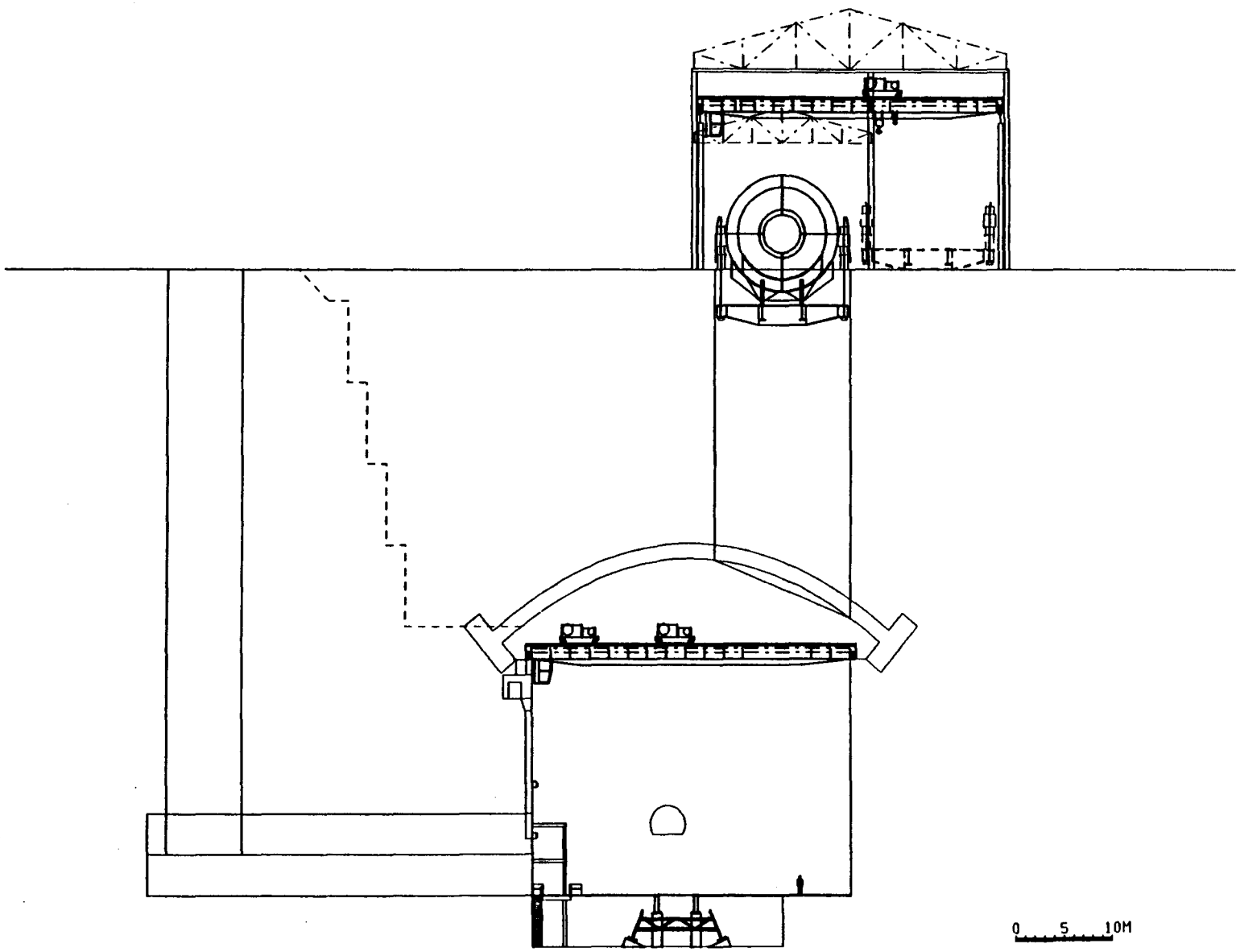

Figure 4.39. ACT Detector—Surface Construction Facilities (End Section)

lifted by the bridge crane onto a transfer car, which carries them to the assembly building next door. This building is air-conditioned.

The calorimeter assembly building is provided with a 65-tonne bridge crane and with hook height sufficient to lift the air core toroids. This crane will not be able to handle loads down the shaft. When this is needed, the gentry crane will be used. The bridge crane can however move loads to within reach of the gantry crane.

The calorimeter assembly building is subdivided into three separate rooms. Proceeding from south to north they are: 1) the head house for the construction shaft, 2) the calorimeter assembly room, and 3) a clean room for storage and testing of completed calorimeter bays.

The head house encloses the construction shaft, with access for the muon gantry crane. This room also provides a "laydown" and a temporary, covered storage area for equipment that must be lowered into the hall via the construction shaft. Examples are ventilation equipment, fork lifts, and assembly fixtures, or sub-system assemblies such as the central tracking chamber device or the muon tracking chambers.

The central air-conditioned room is the calorimeter assembly room, which is provided with large doors that communicate to the room housing the construction shaft. It is in this room that the calorimeter modules are loaded into their support frames to create the finished calorimeter bays. Large doors connect this room with the module staging building described above.

At the north end of the calorimeter assembly building is a large, relatively clean room sized to store four completed calorimeter bays during testing. Clearance of 3 m between the bays permits mobility of the telescoping work platforms used to reach any area of the calorimeter assemblies during checkout.

Above-ground subsystem assembly is achieved in four phases. During Phase 1, the muon steel is lowered by the gantry crane, while calorimeter modules are tested in the staging building. Figure 4.40 shows the status of the construction at the end of Phase 1. The construction buildings are ready to receive calorimeter modules for assembly from the staging building next door. Note that a partition has been installed to separate the calorimeter assembly area from the area surrounding the construction shaft. A clean room for testing calorimeter sections has also been completed.

During Phase 2, the muon steel continues to be lowered while the calorimeter sections are being assembled and tested (Figure 4.41).

At the end of Phase 3, the muon steel has all been lowered, and the calorimeter sections are lowered to the underground hall floor while the air core toroids are being assembled and tested (Figure 4.42).

At the end of Phase 4, the air core toroids are lowered to the hall floor (Figure 4.43).

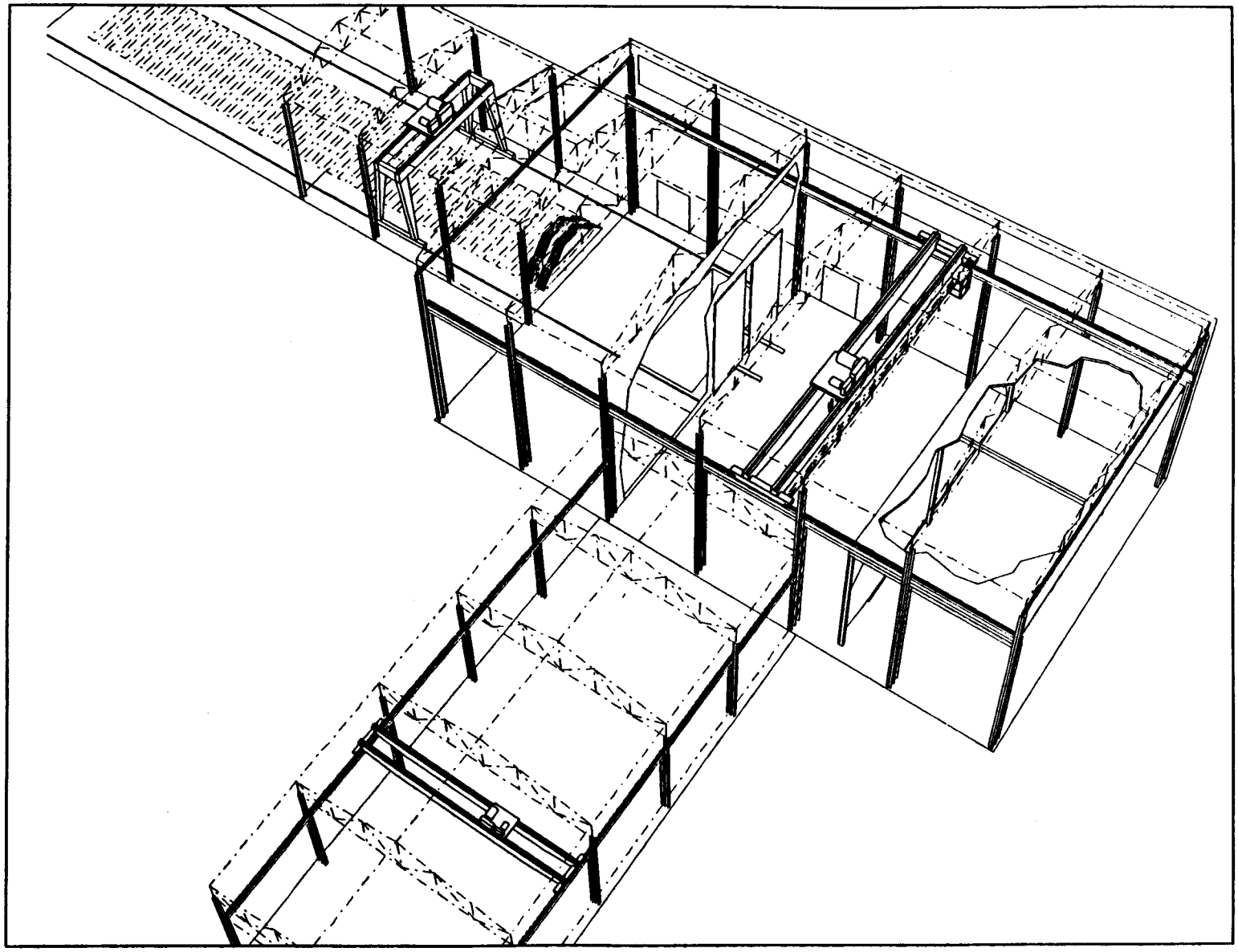

Figure 4.40. ACT Detector—Surface Construction Facilities (Phase 1)

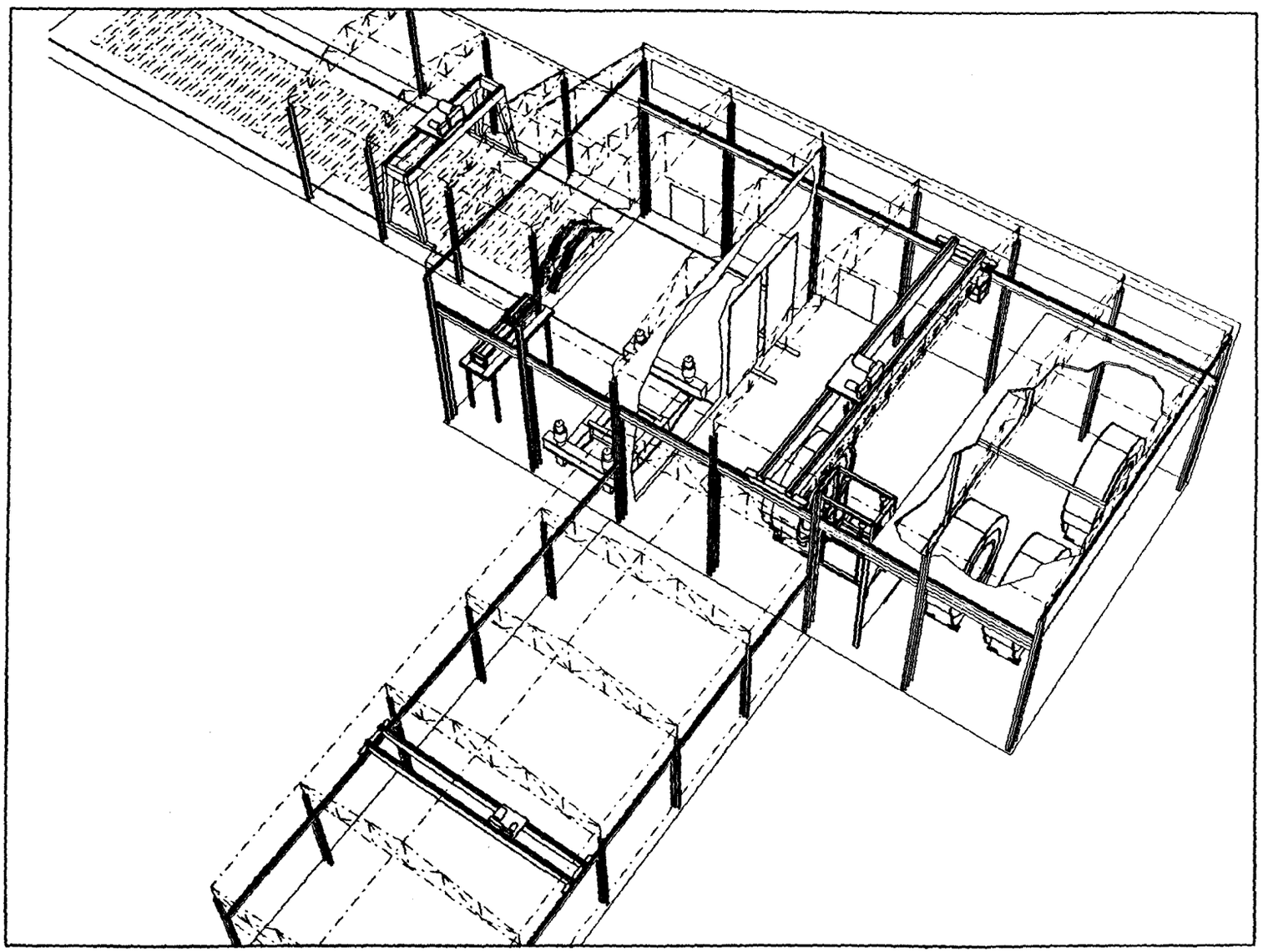

Figure 4.41. ACT Detector—Surface Construction Facilities (Phase 2)

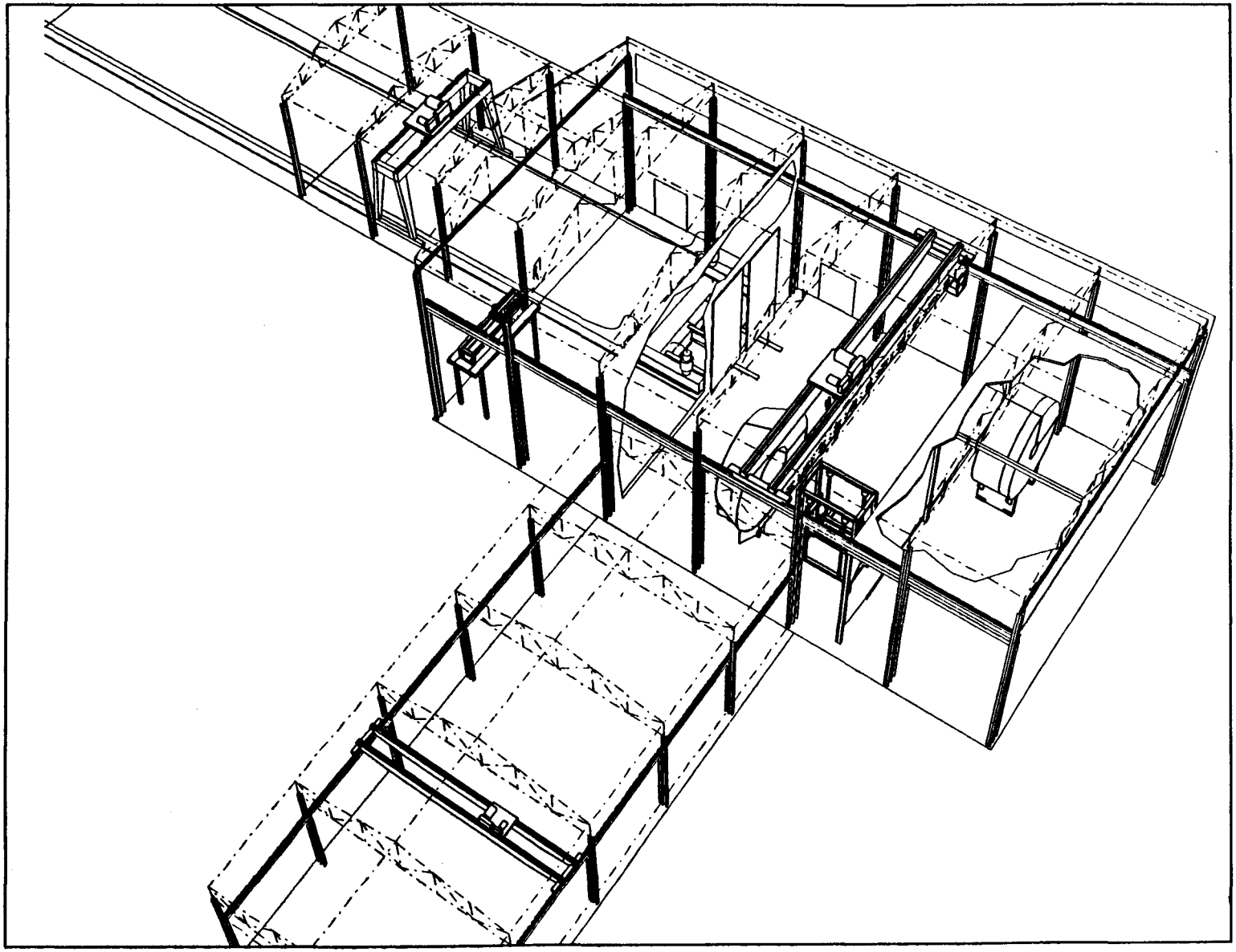

Figure 4.42. ACT Detector—Surface Construction Facilities (Phase 3)

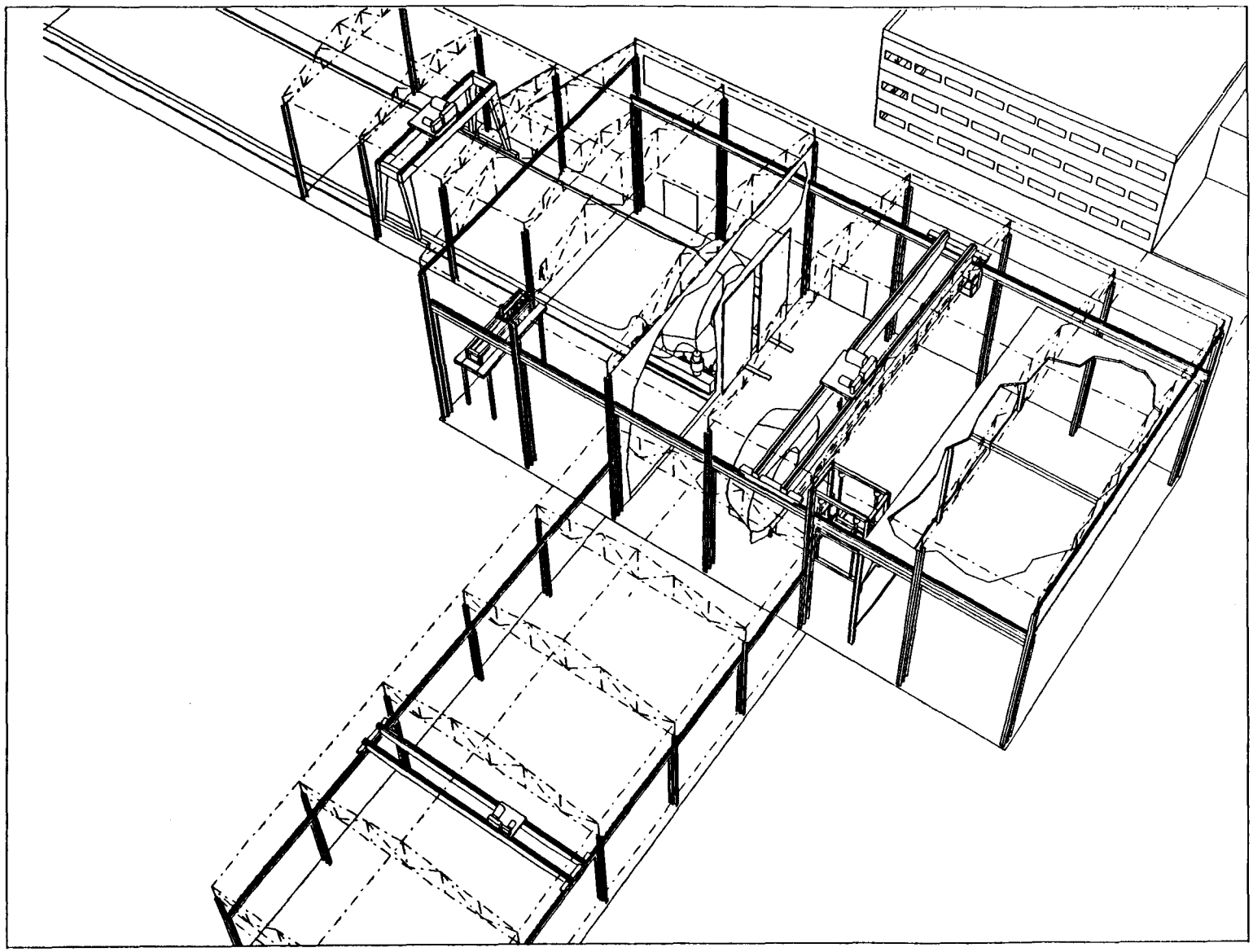

Figure 4.43. ACT Detector—Surface Construction Facilities (Phase 4)

4.4 Schedule and Sequential Construction Drawings

4.4.1 ACT Detector Schedule

The estimated schedule for construction of the ACT detector is shown in Figure 4.44. Estimates for the assembly of the muon steel have assumed that two crews are involved and that work proceeds from the middle outward in two directions. Assembly of the endcap toroid steel is done by the same crews during the periods when the coils for the barrel toroids are being connected to power and to Low Conductivity Water (LCW), and are being tested for electrical continuity and integrity of the electrical insulation and cooling system. We consider the Air Core Toroids to be high-tech devices that are delivered late in construction of the project. We schedule their introduction into the hall as late as possible to be consistent with data acquisition at the end of 42 months. The width of the hall permits the ACTs to be installed even after the rest of the detector is largely in place, because they can be moved from one end of the hall to the other using the 7-m-wide corridor at one side of the detector.

Both the barrel and the endcap calorimetry assembly schedules assume that one calorimeter module is installed and tested per day. We foresee the calorimeter installation occupying two shifts per day: the day shift to install, and the evening shift to test and calibrate the installed modules. We allow five months contingency at the end of the calorimeter schedule; a third shift per day may also be employed as additional contingency time. The overall scheduling for the detector is easiest if at least one endcap calorimeter is completed prior to installation of the barrel system. This simplifies motion of the heavy objects inside the collision hall.

The superconducting coil cannot be installed until the barrel calorimeter is complete and has been placed in its final position on the beam line. From the argument in the previous paragraph, this would imply that at least one endcap calorimeter has also been fabricated. Prior to installation of the central tracking device, the magnetic field of the solenoid must be measured. This requires installation of the endcap calorimeters, since they provide part of the return yoke of the magnet. Initial testing of the field-mapping instrumentation can take place simultaneously with the installation and testing of the coil, but the final mapping must wait until all of the magnetic elements are installed and operational.

After the magnetic field has been mapped, the endcap calorimeters are withdrawn and installation of the central tracking device (including the silicon tracker) can proceed. The central tracking is assumed to arrive in the hall as a single, pre-tested unit that requires minimal debugging inside the collision hall prior to installation in the detector.

Installation of the muon chambers begins with completion of the barrel iron toroids and their coils. The exterior chambers are installed first, followed by the chambers on the inside of the steel

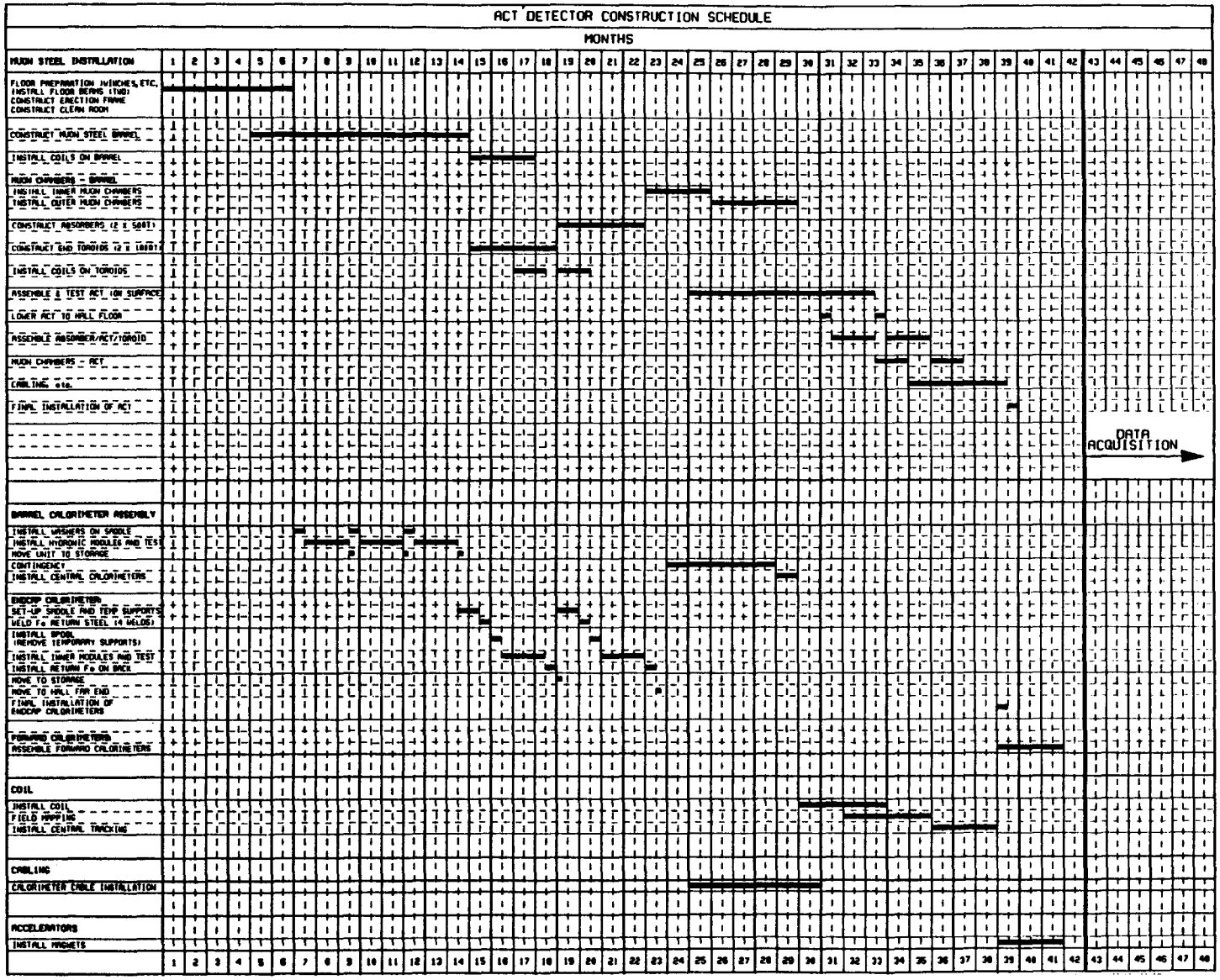

Figure 4.44. Air Core Toroid Detector Construction Schedule

(except for those on the bottom, which are installed with the barrel calorimeter). The endcap muon chambers are installed as soon as the endcap iron toroids, their coils, the ACT, and the steel absorber are assembled.

Estimating the schedule for the installation of the electronics is more problematical; we have not considered this schedule in detail. We assume that large scale-testing of the data acquisition system and pathways begins with the assembly of the first calorimeter bay. Some of this testing could provisionally be done using the electronics gallery in the hall as a temporary data acquisition location. However, prudent planning implies that beneficial occupancy of the operations center should be no later than one year after beneficial occupancy of the collision hall.

4.4.2 Detector Assembly Sequence

A three-dimensional computer model of the detector construction sequence has been created (Figures 4.45 to 4.59). The construction steps are depicted at three-month intervals beginning with the hall at beneficial occupancy (month 0, Figure 4.45).

The detector assembly begins with installation of the barrel muon steel supports and construction of an erection frame. The necessary materials are brought into the hall via the construction shaft. Any preparatory work can be accomplished in the staging area adjacent to the erection sites.

The state of the hall after three months is seen in Figure 4.46. At this time the muon steel support is complete, and construction of the hall partition and clean room is ready to begin.

Figure 4.47 shows the hall during the sixth month of construction. The hall partition and clean room are complete. The muon steel construction is underway, and construction is about to begin on the central calorimeter bay. Materials for the muon steel barrel are brought into the hall via the construction shaft. The calorimeter support shells and washers are also brought into the hall through the construction shaft. The calorimeter modules are brought into the hall through the equipment shaft.

At nine months (Figure 4.48), the muon steel construction continues and is roughly half-finished. The central calorimeter bay is complete and has been moved to the clean room for electrical checkouts. Construction begins on the first end calorimeter bay.

The hall at 12 months is seen in Figure 4.49. Work on the muon steel barrel continues. The first end calorimeter is complete and has been moved to the clean room for electrical checkouts. Construction begins on the second end calorimeter.

Figure 4.50 shows the hall during month 15 of construction. The muon steel barrel is complete, and installation of the barrel coils is in progress. The second end calorimeter is complete and is undergoing electrical checkouts in the clean room. Construction is begun on the first endcap calorimeter. Construction is also begun on the muon steel end toroids.

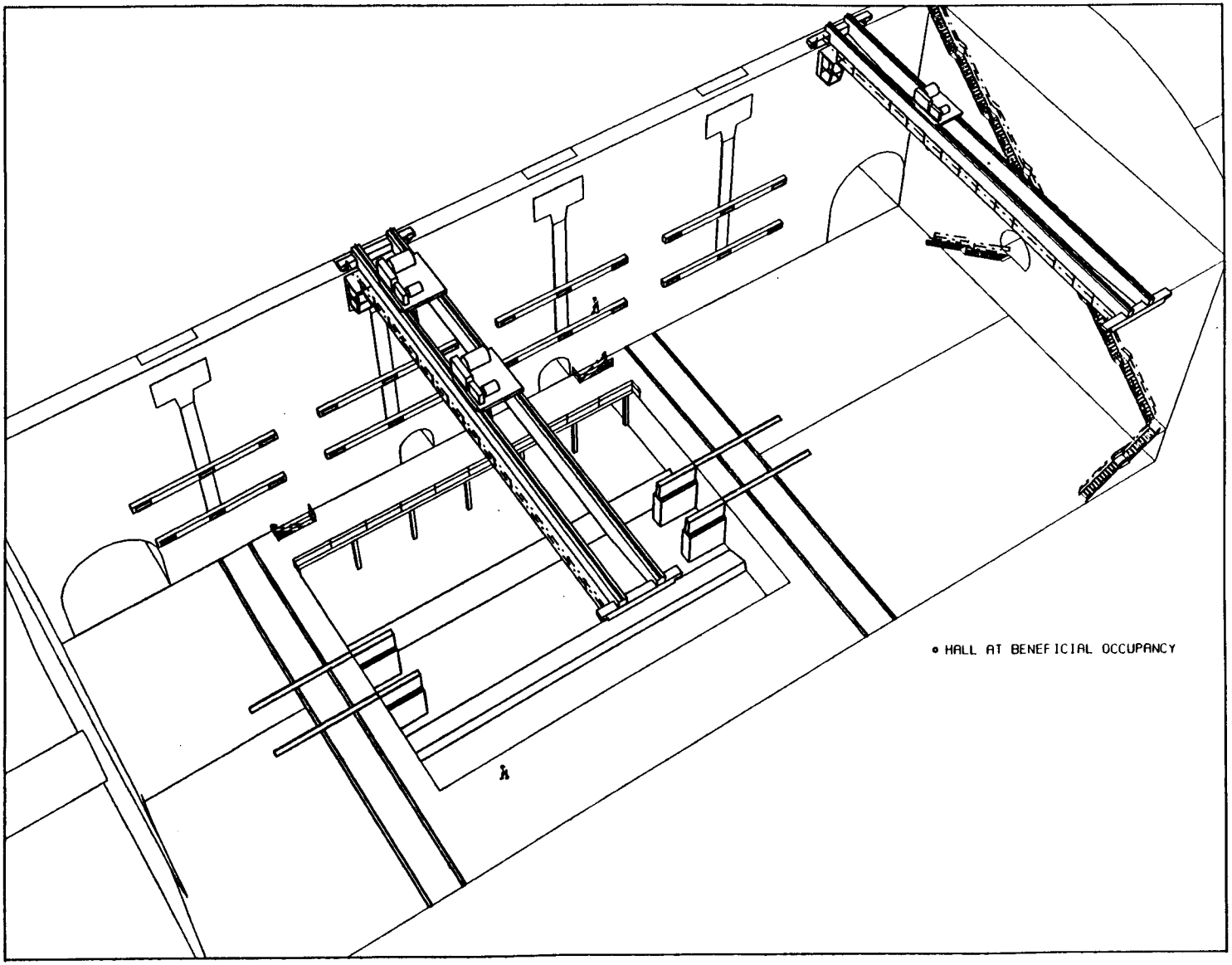

Figure 4.45. ACT Detector Construction Sequence (Month 0)

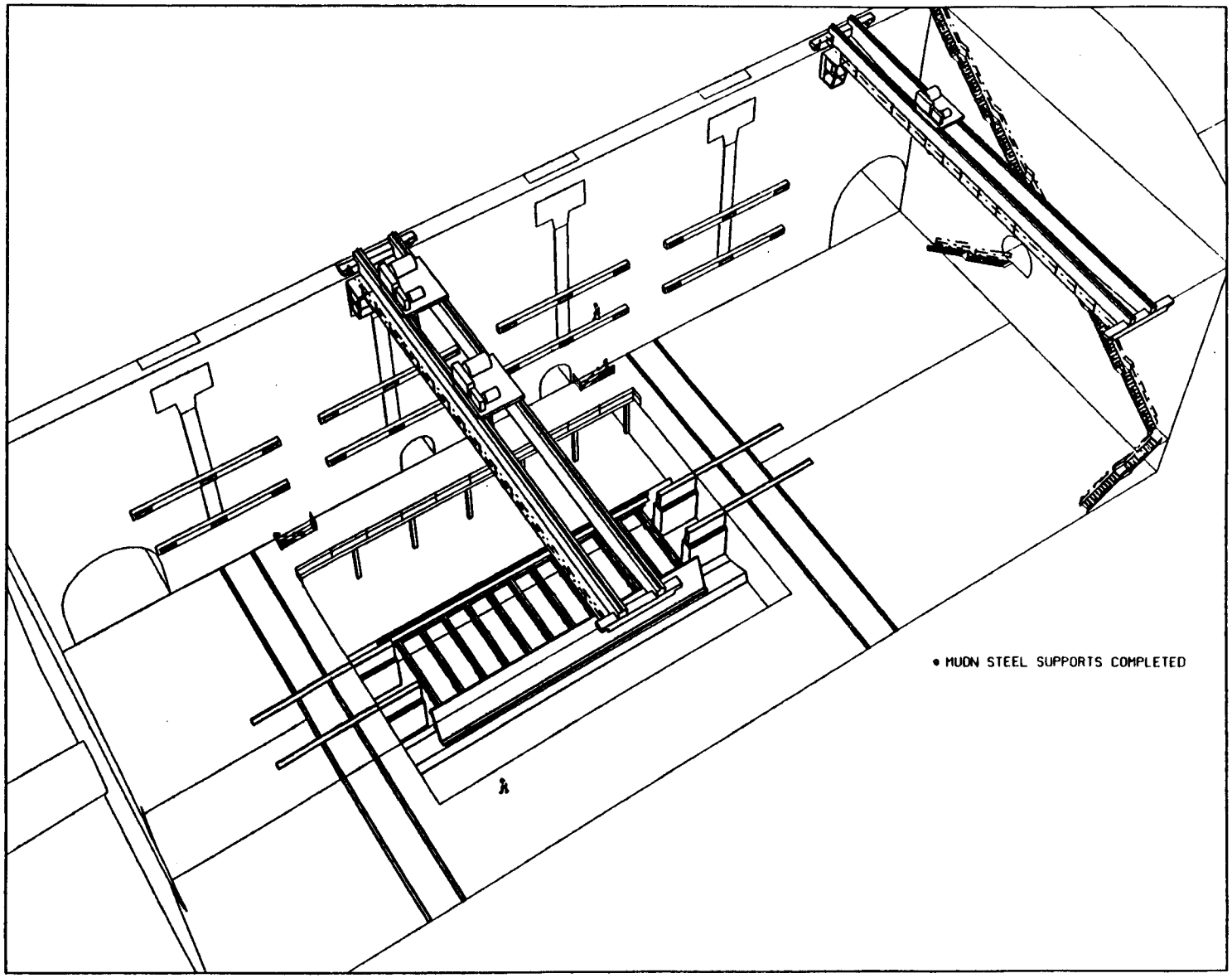

Figure 4.46. ACT Detector Construction Sequence (Month 3)

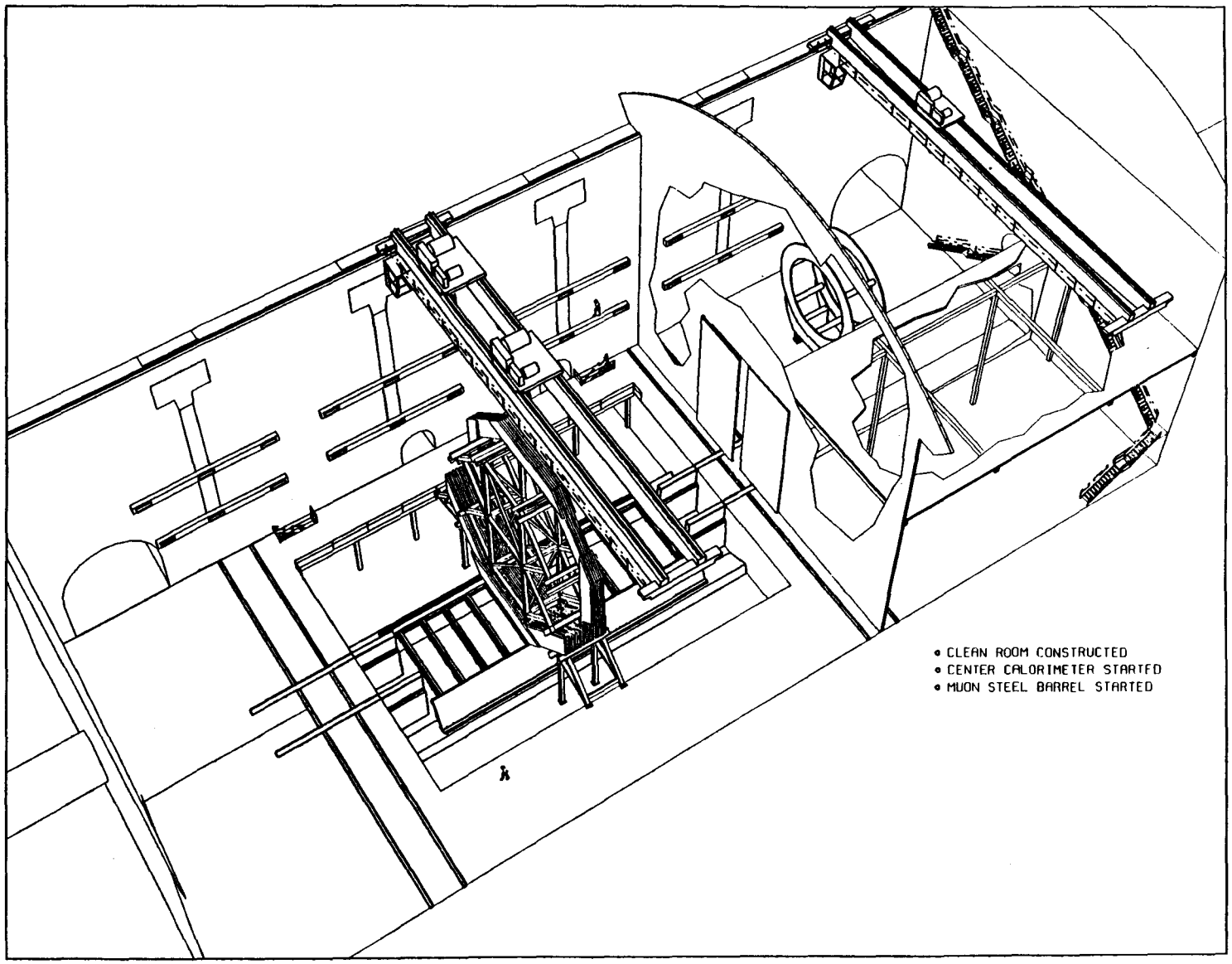

Figure 4.47. ACT Detector Construction Sequence (Month 6)

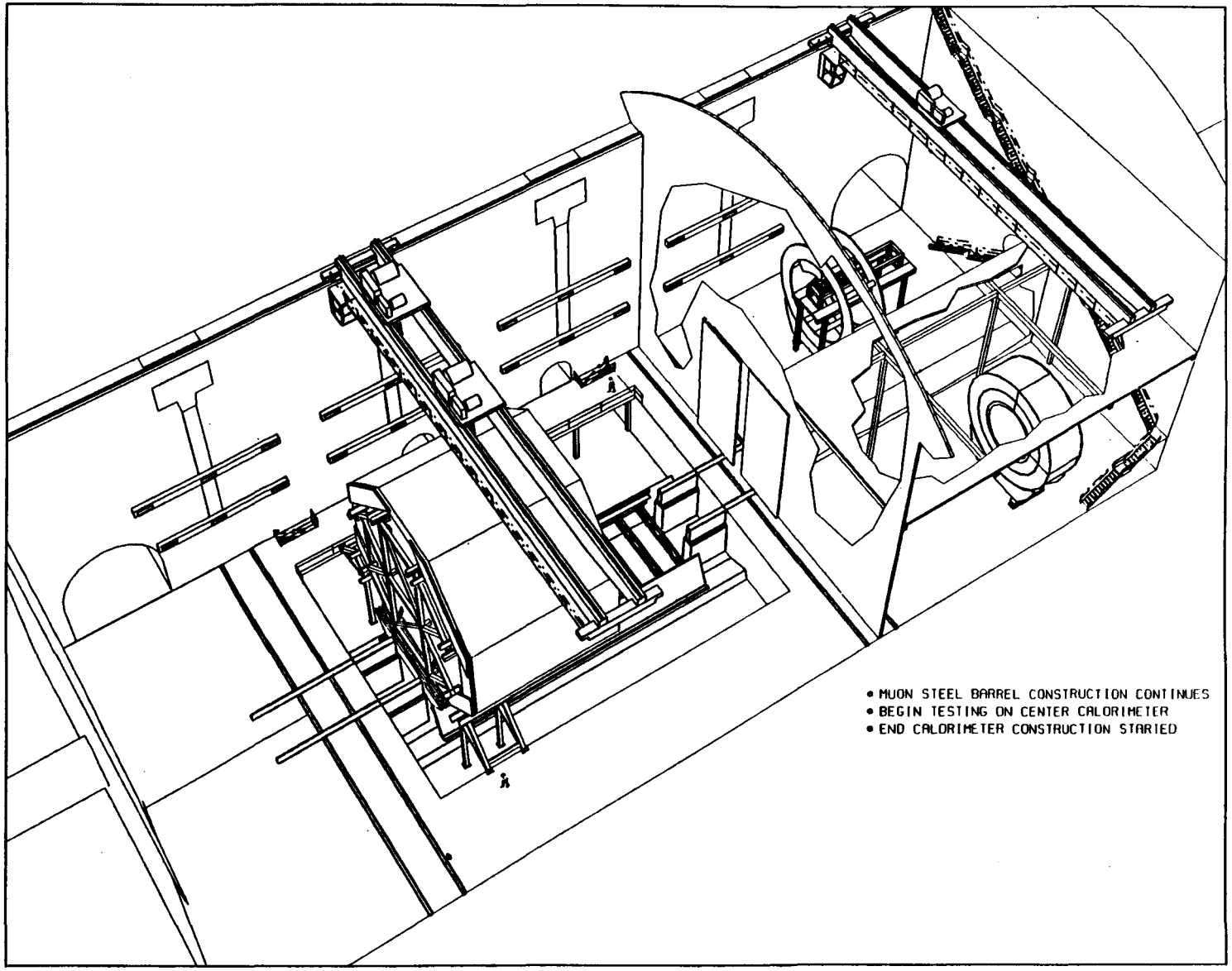

Figure 4.48. ACT Detector Construction Sequence (Month 9)

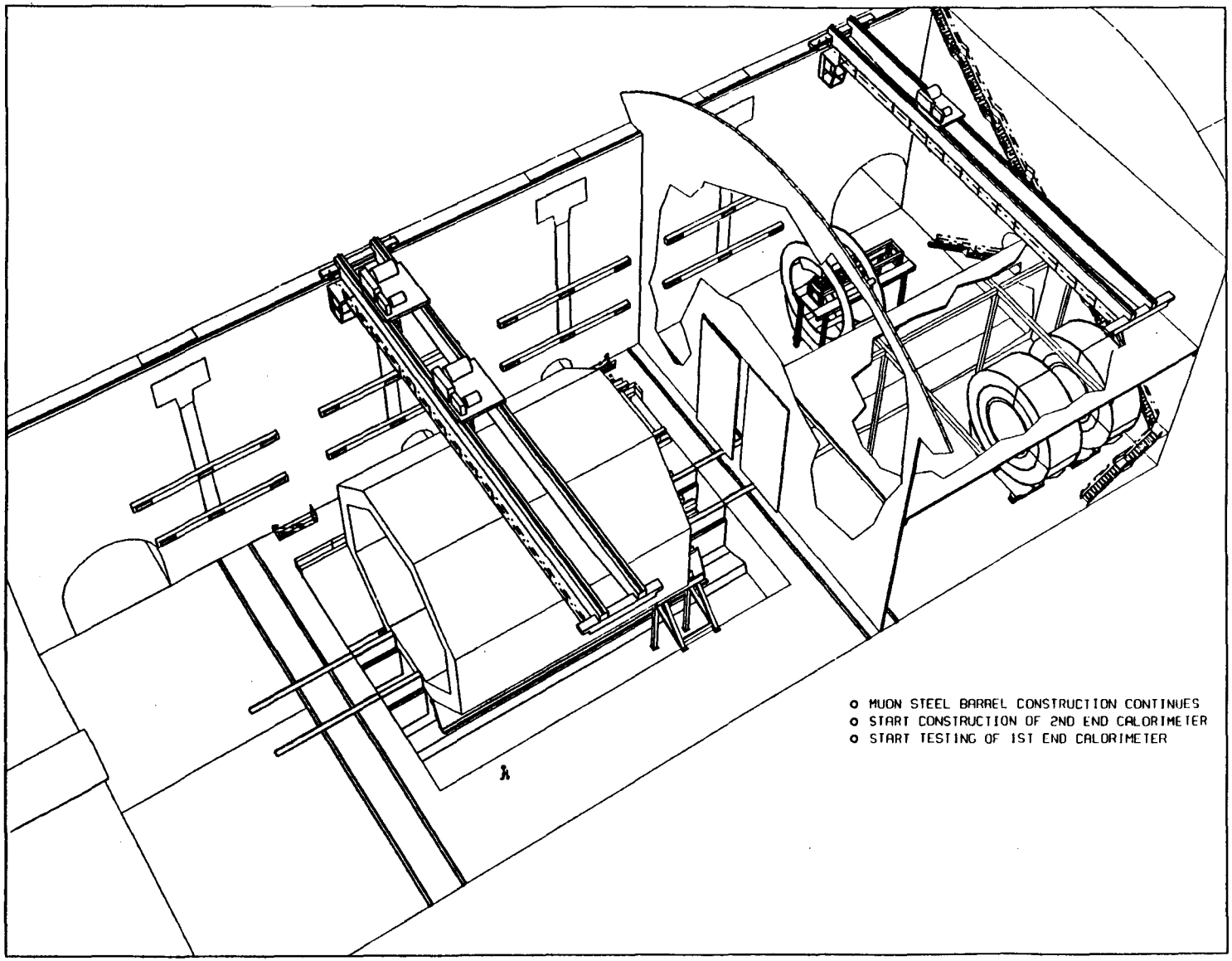

Figure 4.49. ACT Detector Construction Sequence (Month 12)

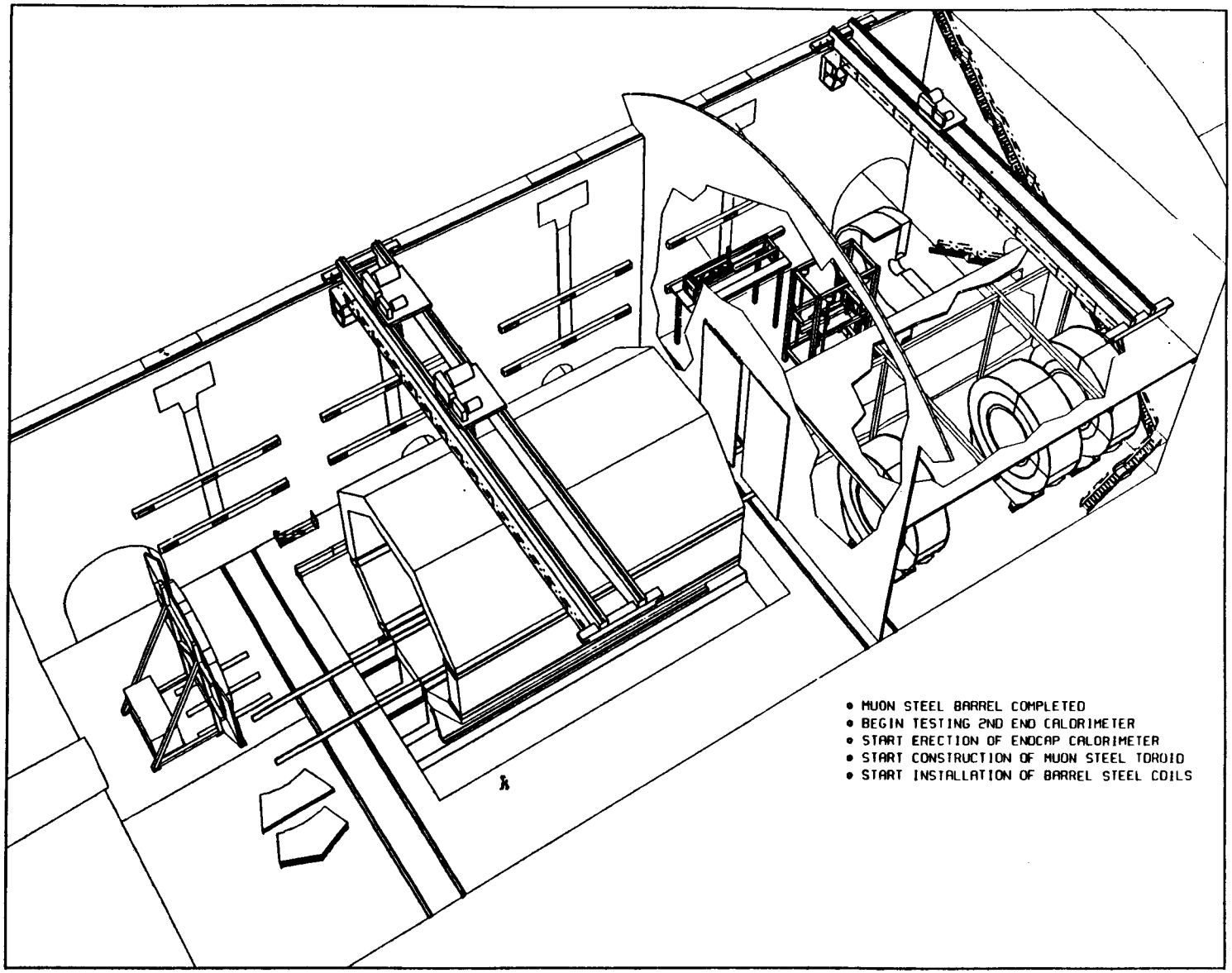

Figure 4.50. ACT Detector Construction Sequence (Month 15)

During month 18 (Figure 4.51), the installation of the muon steel barrel coils is complete. The construction of the muon steel toroids is also completed during this period. The end toroids coil installation is in progress. The first endcap calorimeter assembly is complete and awaits transport to the clean room.

The state of the hall after 21 months is shown in Figure 4.52. The first endcap calorimeter has been moved to the clean room and is undergoing electrical checkouts. Construction has begun on the second endcap calorimeter. Installation of the end toroid coils is complete. The first absorber cone is complete, and assembly of the second absorber cone is in progress.

Figure 4.53 shows the hall at 24 months. The last endcap calorimeter has been moved to the opposite end of the hall and is undergoing electrical checkouts. The construction of the second absorber is complete. The installation of the barrel steel inner muon chambers is in progress. A platform for housing electronics and utilities has been erected on the side of the detector hall containing the narrow gallery.

During month 27 (Figure 4.54), installation of the outer muon chambers is in progress on the muon steel barrel.

The hall at month 30 is seen in Figure 4.55. At this time the installation of the outer muon chambers is complete, and the central calorimeters have been installed. The hall partition and the clean room have been dismantled. Installation of the coil is underway.

At month 33 (Figure 4.56), the coil has been installed, and the process of mapping the coil field is in progress. The first air core toroid has been lowered into the hall and has been assembled into an integral unit with an absorber and a muon toroid. Installation of the muon chambers of this assembly will begin at this time. The second air core toroid will also be lowered into the hall at this time.

By the month 36 (Figure 4.57), the second absorber/ACT/muon toroid assembly is complete, and installation of its muon chambers is underway. The muon chamber installation is complete on the first absorber/ACT/muon toroid unit. Installation of the central tracking device begins at this time. The endcap calorimeters have been previously moved offline in preparation for this activity.

The state of the hall at month 39 is seen in Figure 4.58. At this time the final installation of the endcap calorimeters has taken place, along with the installation of the absorber/ACT/toroid units. Assembly of the forward calorimeter and the accelerator components begins at this time. Figure 4.59 shows the hall at completion.

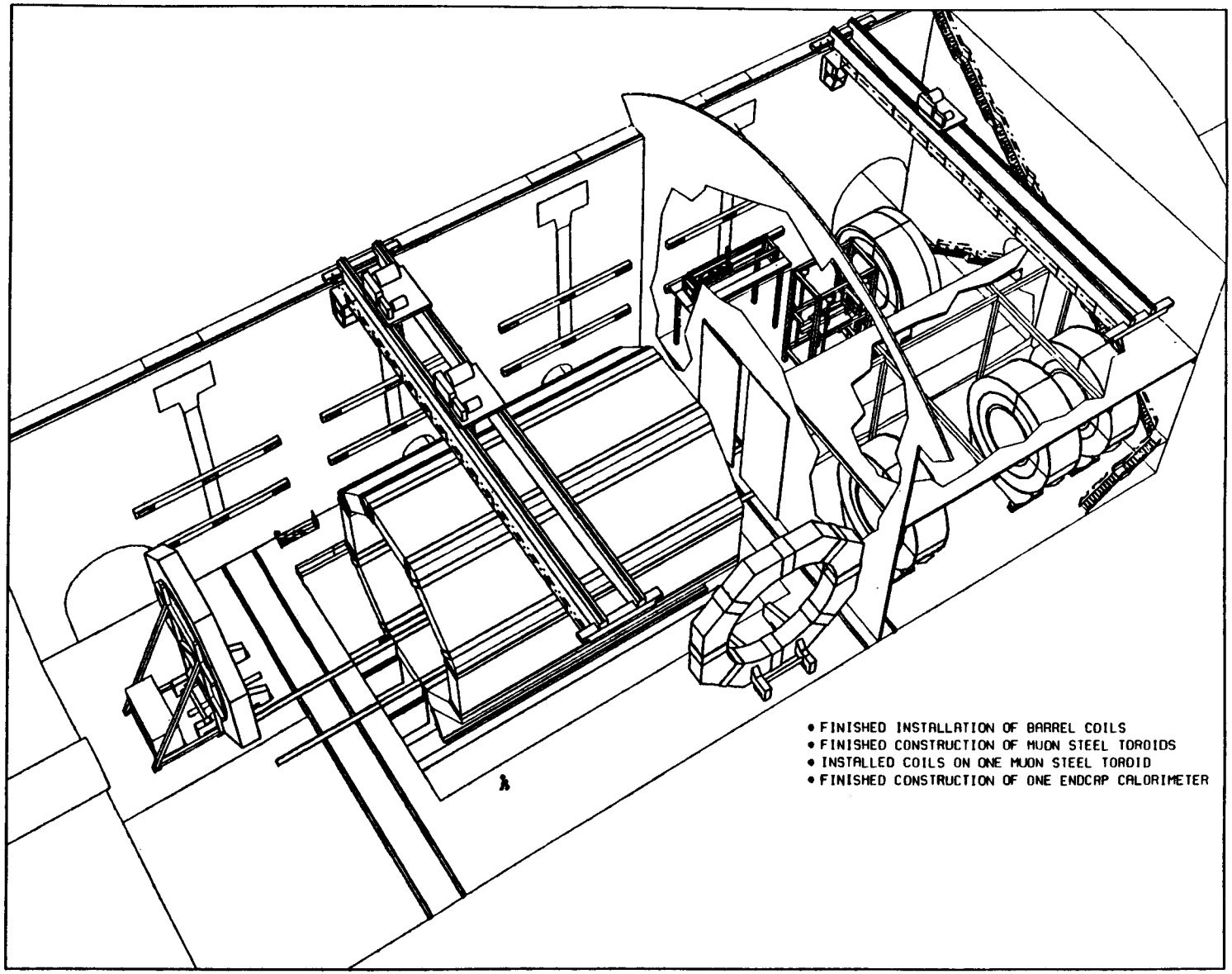

Figure 4.51. ACT Detector Construction Sequence (Month 18)

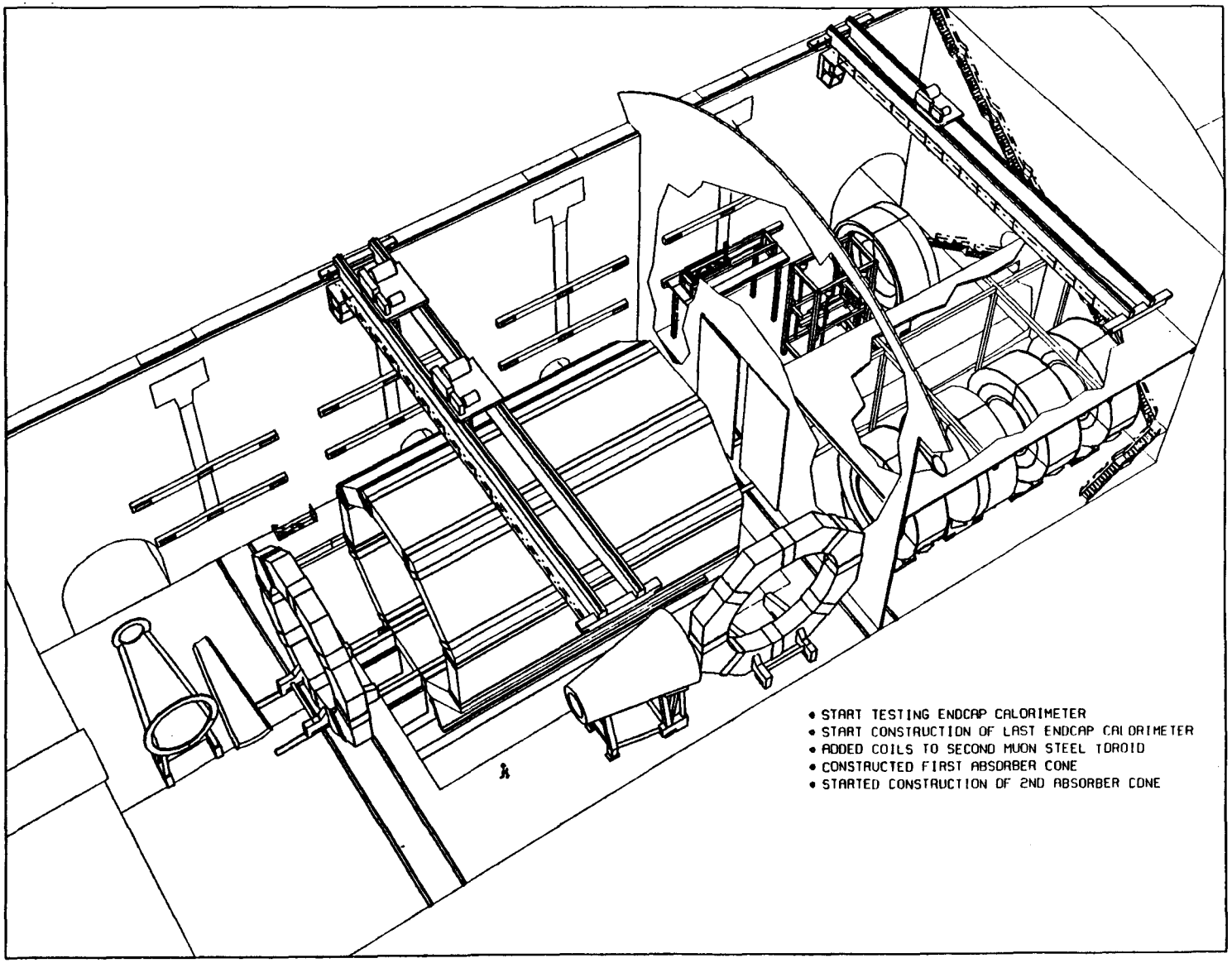

Figure 4.52. ACT Detector Construction Sequence (Month 21)

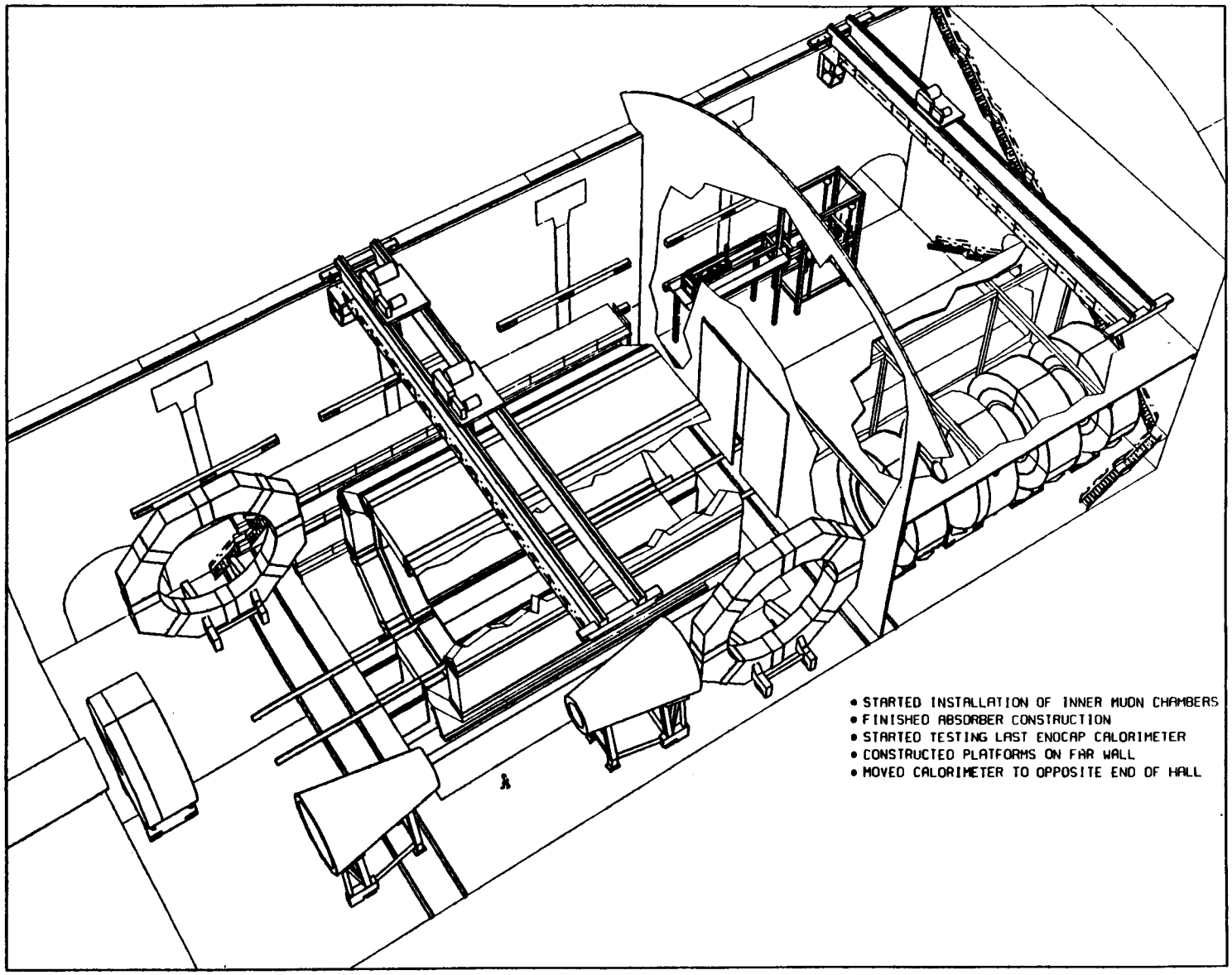

Figure 4.53. ACT Detector Construction Sequence (Month 24)

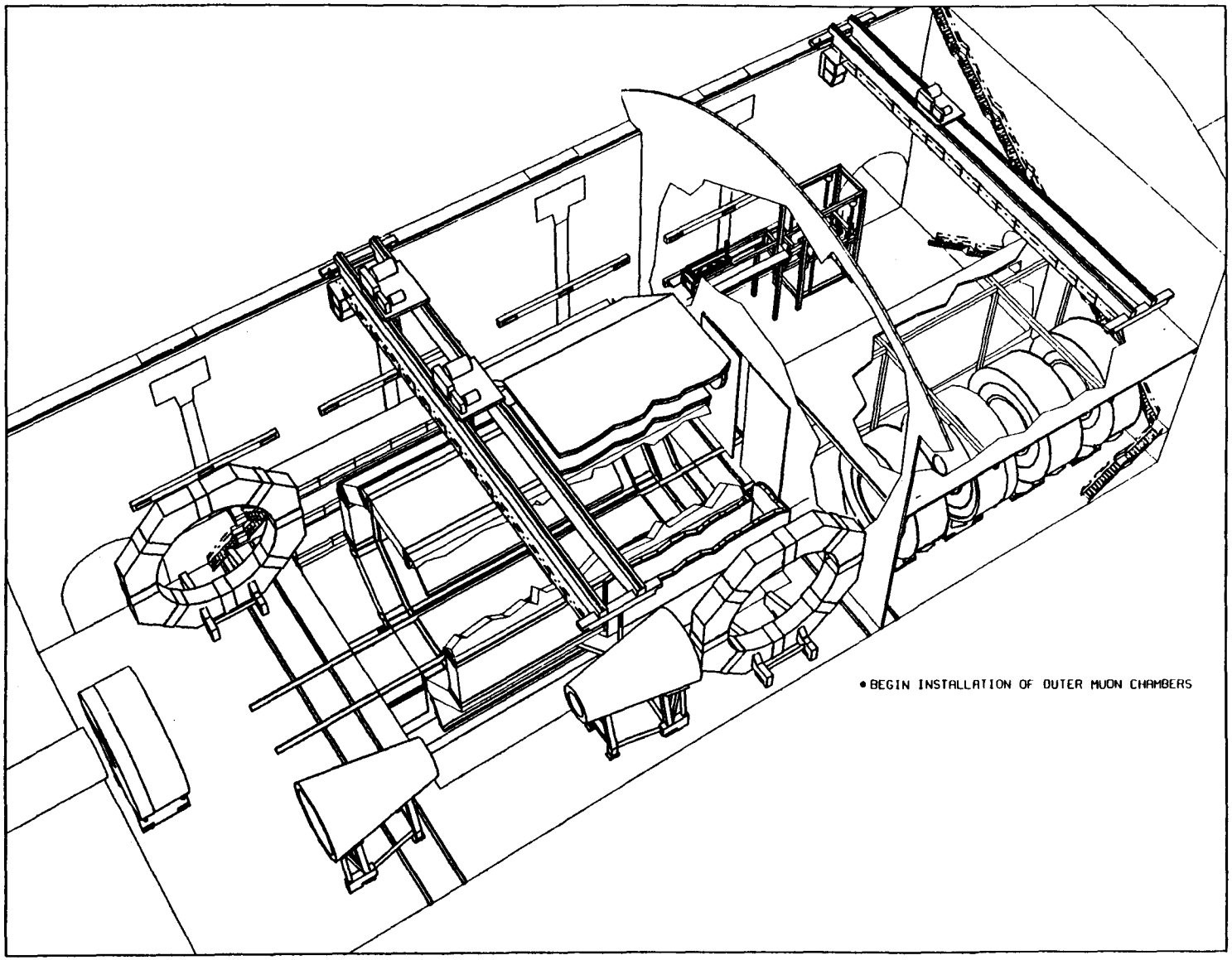

Figure 4.54. ACT Detector Construction Sequence (Month 27)

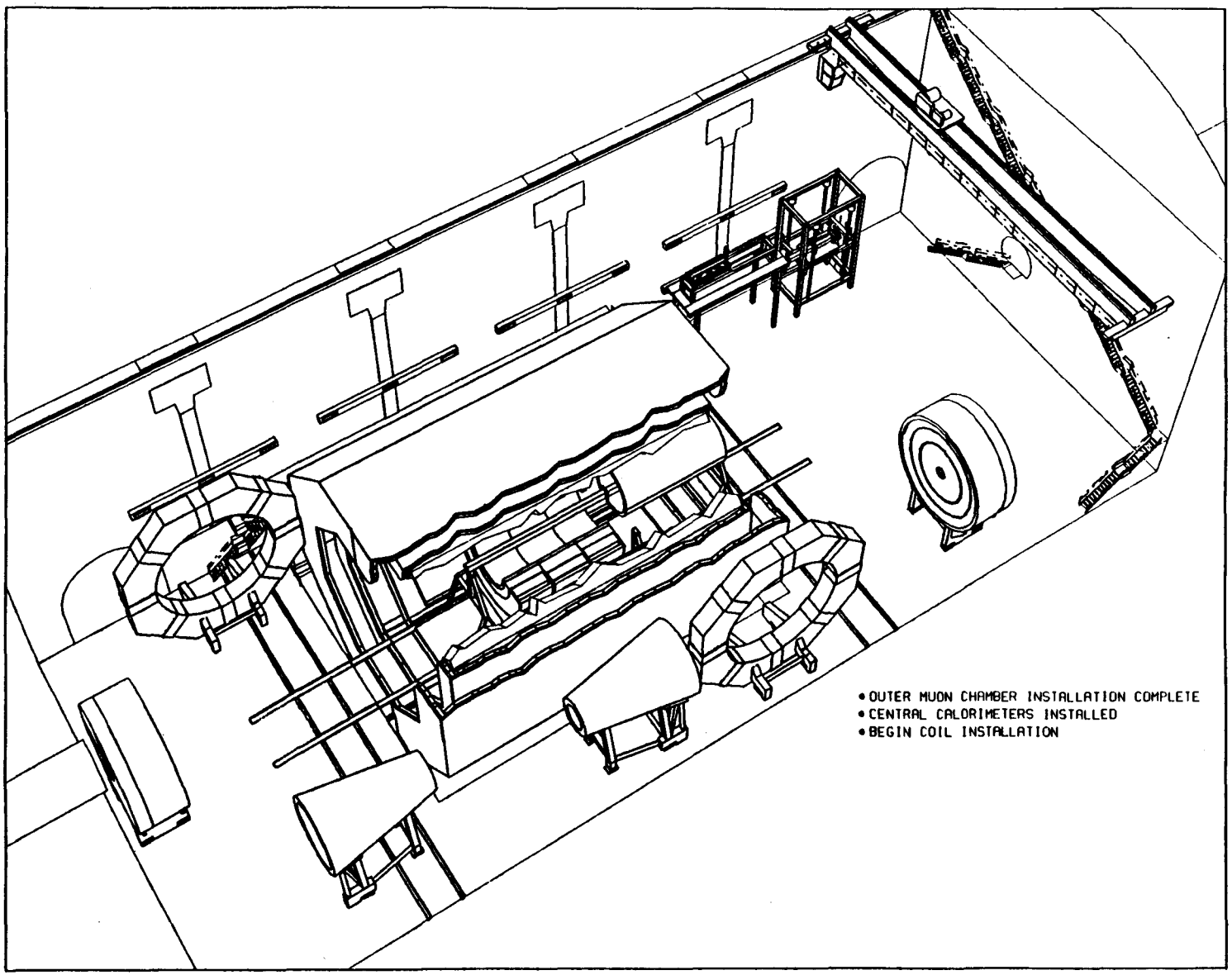

Figure 4.55. ACT Detector Construction Sequence (Month 30)

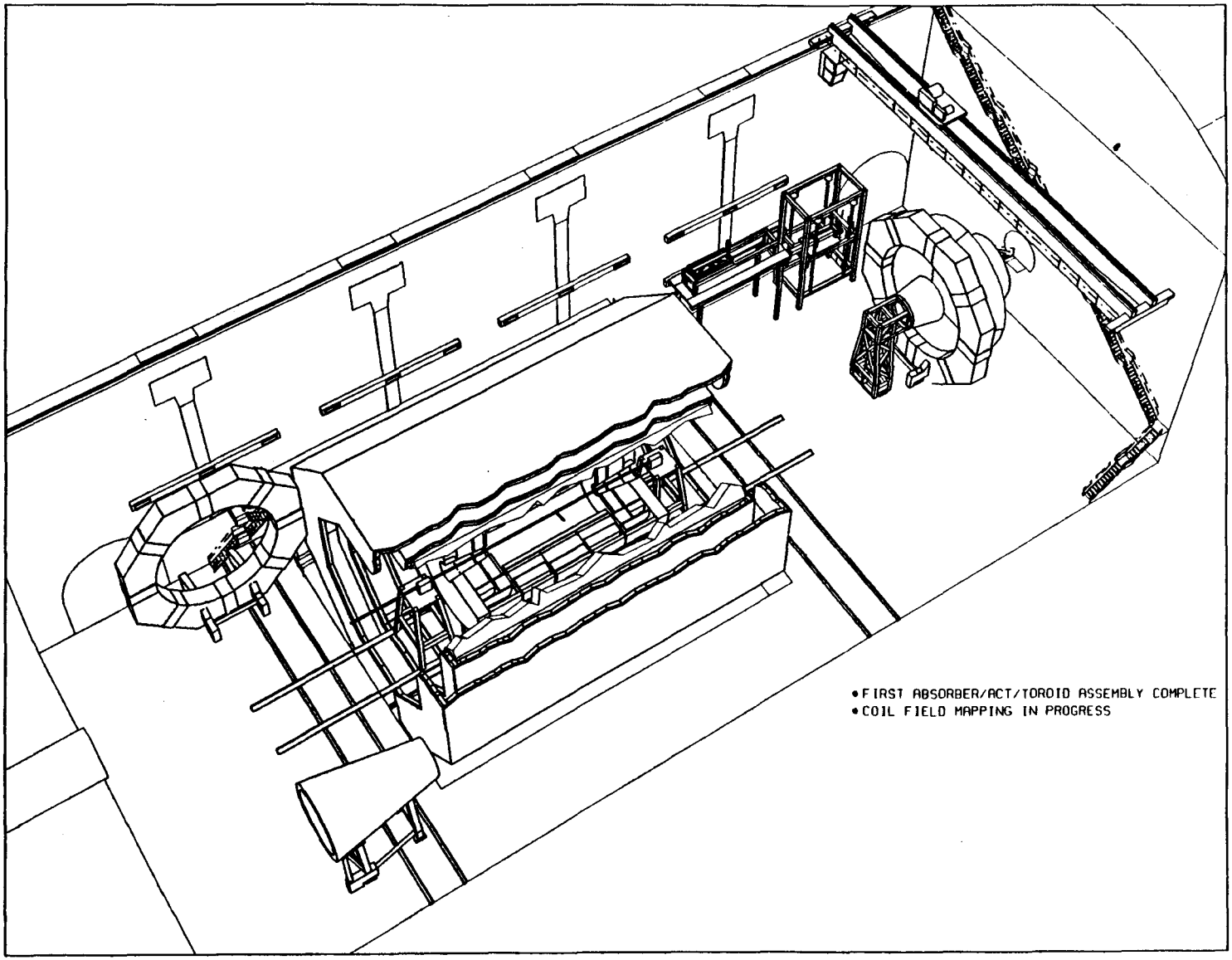

Figure 4.56. ACT Detector Construction Sequence (Month 33)

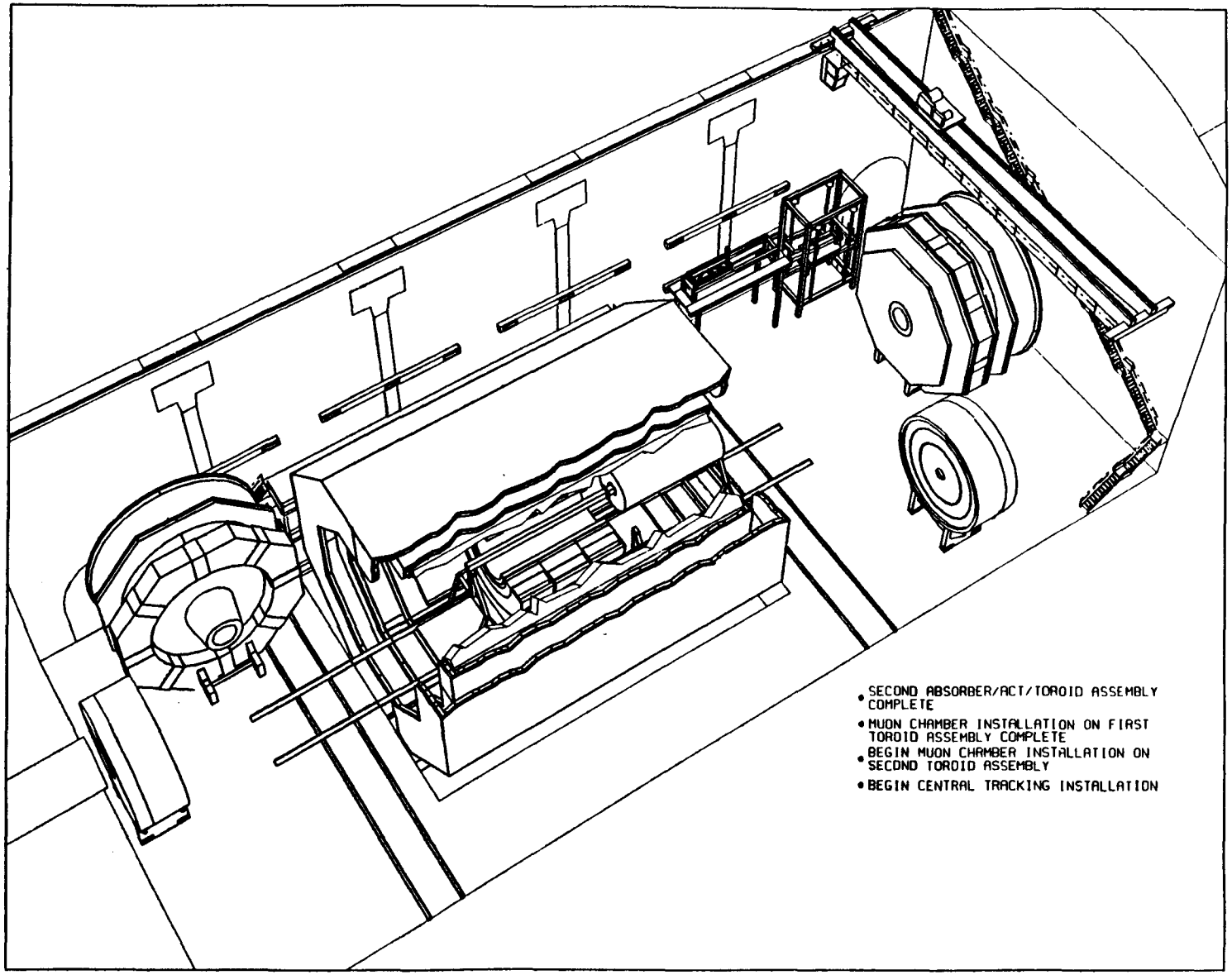

Figure 4.57. ACT Detector Construction Sequence (Month 36)

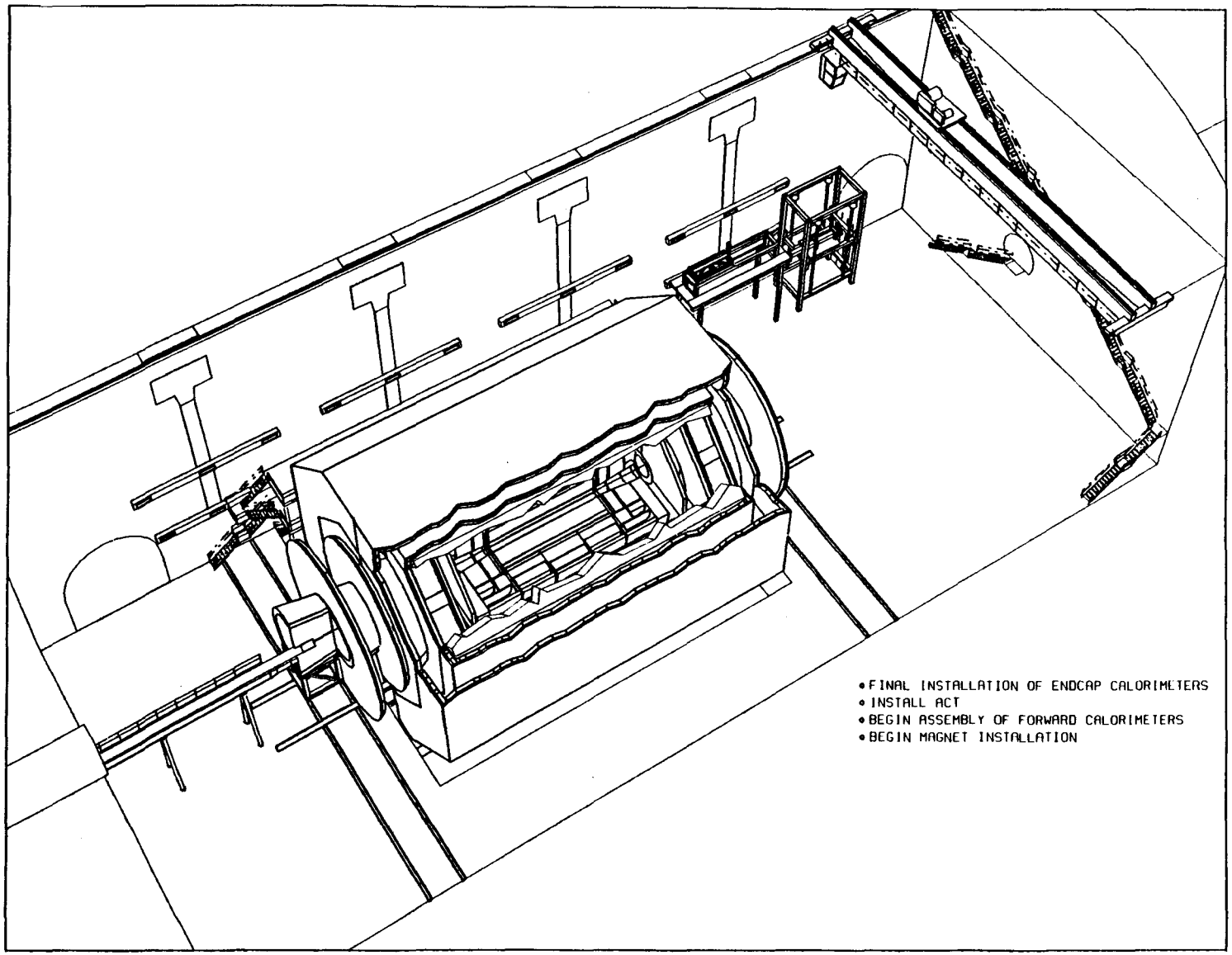

Figure 4.58. ACT Detector Construction Sequence (Month 39)

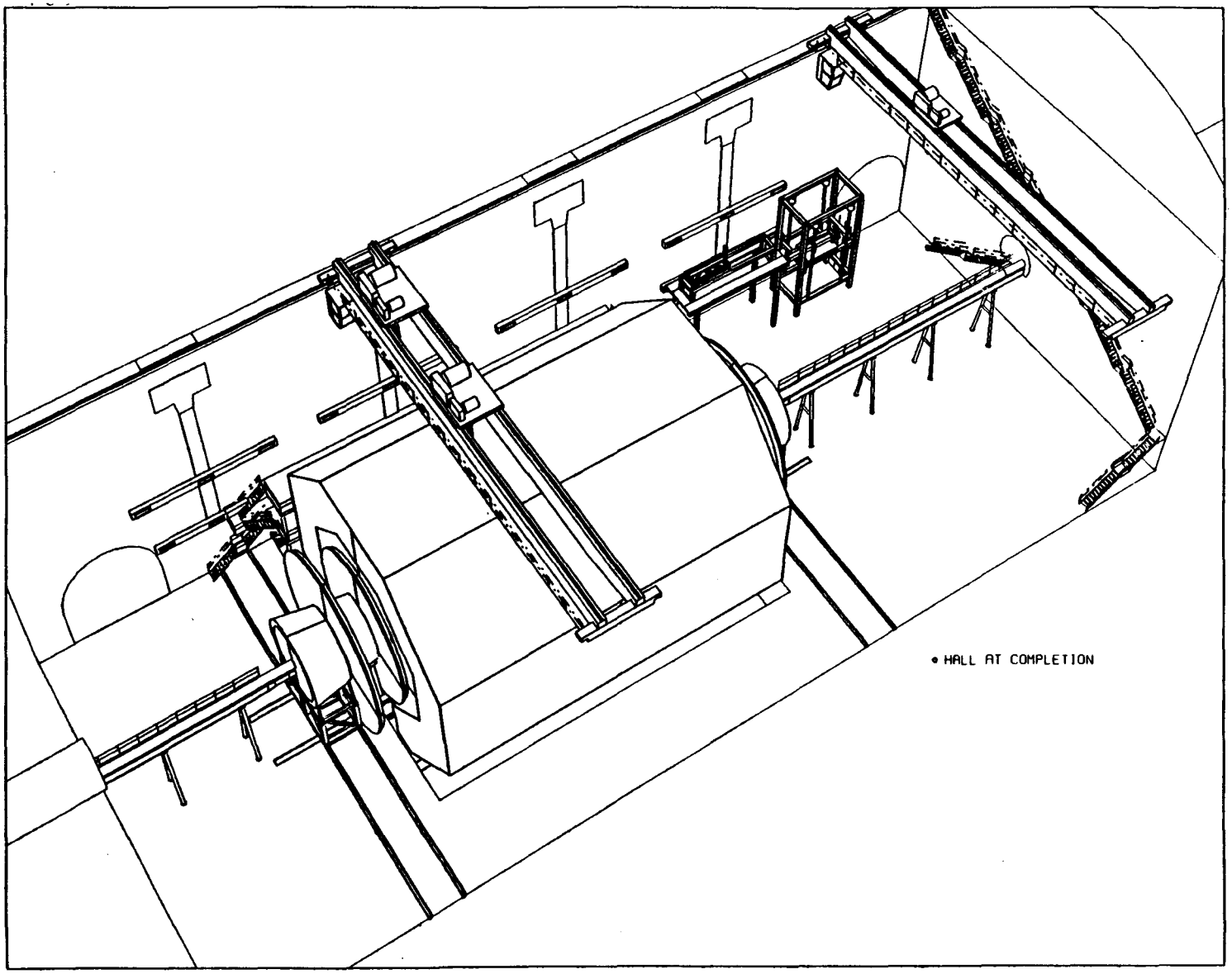

Figure 4.59. ACT Detector Construction Sequence (Month 42)

4.5 Disassembly and Repair Sequences

4.5.1 Minor Repairs

The detector has been conceptualized so that minor repairs can be made without having to break the beam tube. Figure 4.60 shows the detector open for minor repairs. The procedure is as follows: First, the forward calorimeter opens in two halves and moves out of the way. Second, the muon toroids move back as far as possible without interfering with the magnet support system. Third, the calorimeters move back 1 m or more. This will allow access to most electronics in the detector.

4.5.2 Endcap Calorimeter Module Repair

The repair of a calorimeter module entails a major operation of disassembly of the detector. As shown in Figure 4.61, the calorimeters are temporarily moved out of the way. It is then necessary to interrupt and remove the beam tube, dipoles and magnets, which will be stored at the south end of the hall. The muon toroid is then moved and stored at the southeast end of the hall, and the forward calorimeters are brought over to the side of the hall to provide working space for the next step.

Figure 4.62 shows the endcap calorimeter removed from the barrel and placed in a working position. The assembly fixture is positioned by the crane in front of the calorimeter for module removal and replacement.

4.5.3 Silicon Tracking Repair

In order to repair the silicon tracking device, it must be removed from the detector. The removal procedure is depicted in Figures 4.63 through 4.65. As shown in Figure 4.63, the procedure starts with the displacement of the forward calorimeters laterally to allow space for retraction of the muon toroids. The toroids and endcap calorimeters can retract approximately 7 m, creating a 7-m working space at each side of the barrel calorimeter to allow for tools and equipment to operate during the removal.

The beam tube needs to be removed at this point. The intermediate tracking units are now removed and can be stored temporarily inside the detector, as shown in Figure 4.64.

As Figure 4.65 shows, an extraction device is installed and the silicon tracking device is removed and transported outside the detector by a light monorail temporarily assembled for this purpose.

Replacement of the silicon tracking device proceeds in the reverse manner as above.

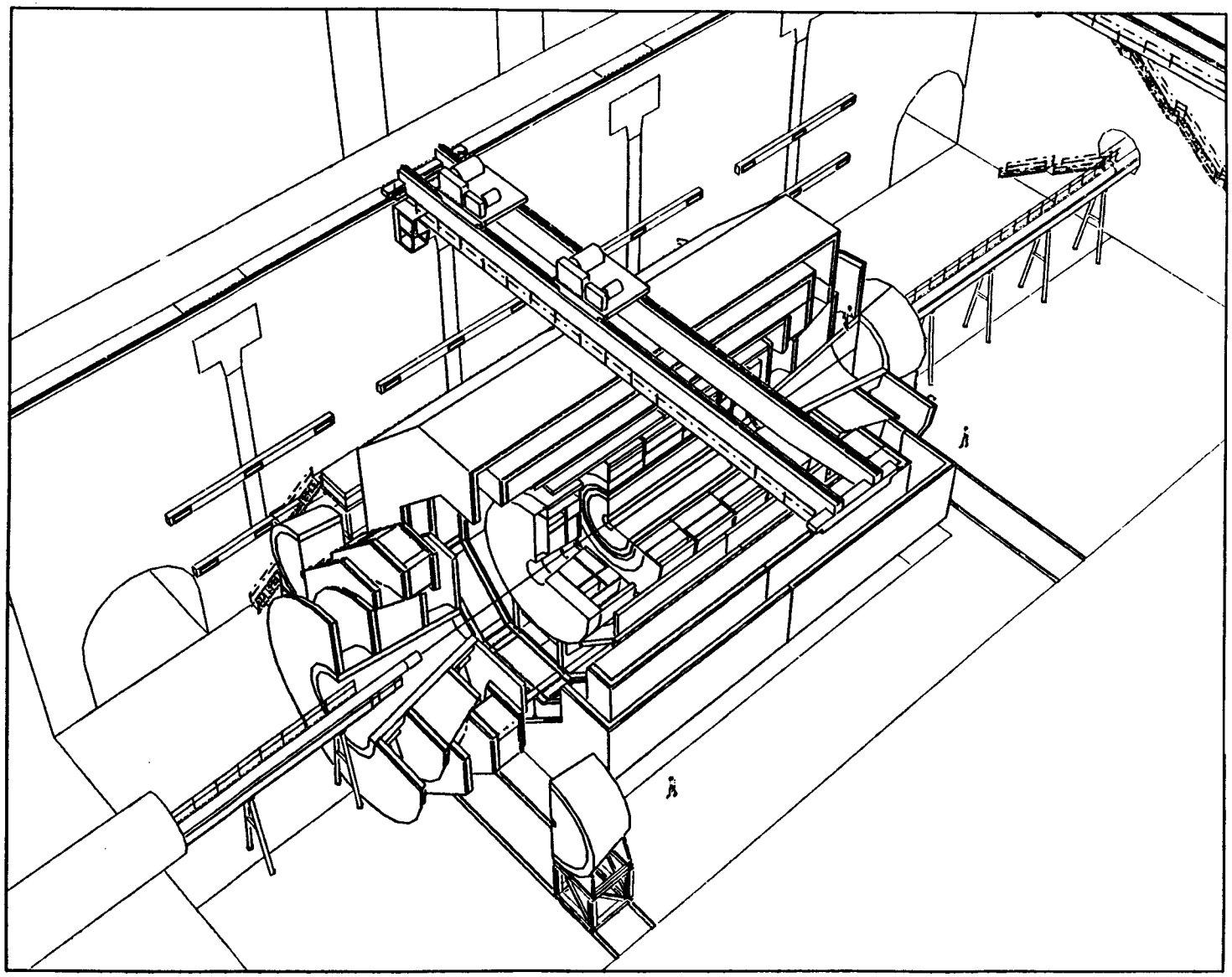

Figure 4.60. ACT Detector Open for Minor Repairs

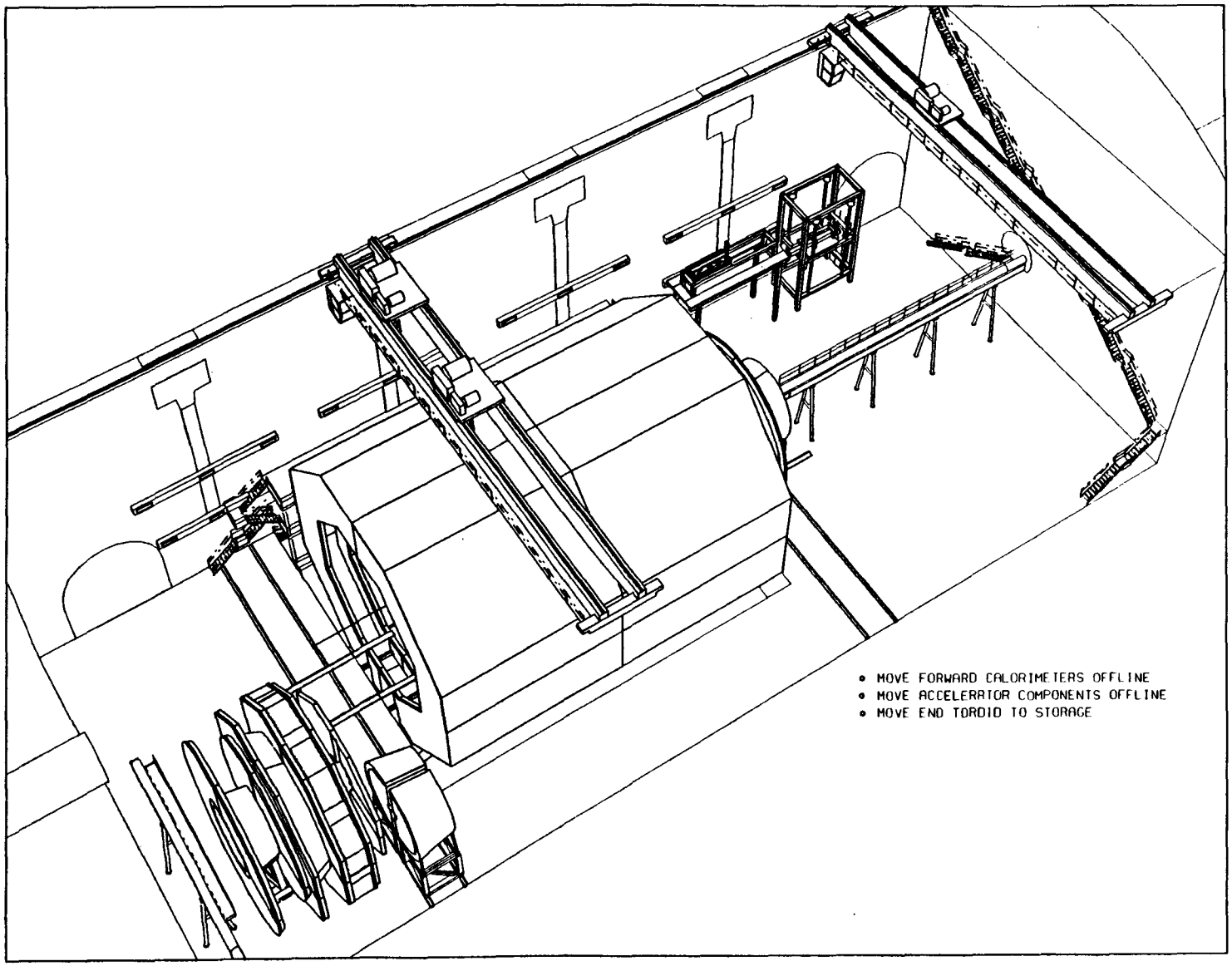

Figure 4.61. ACT Detector—Endcap Calorimeter Module Replacement (Step 1)

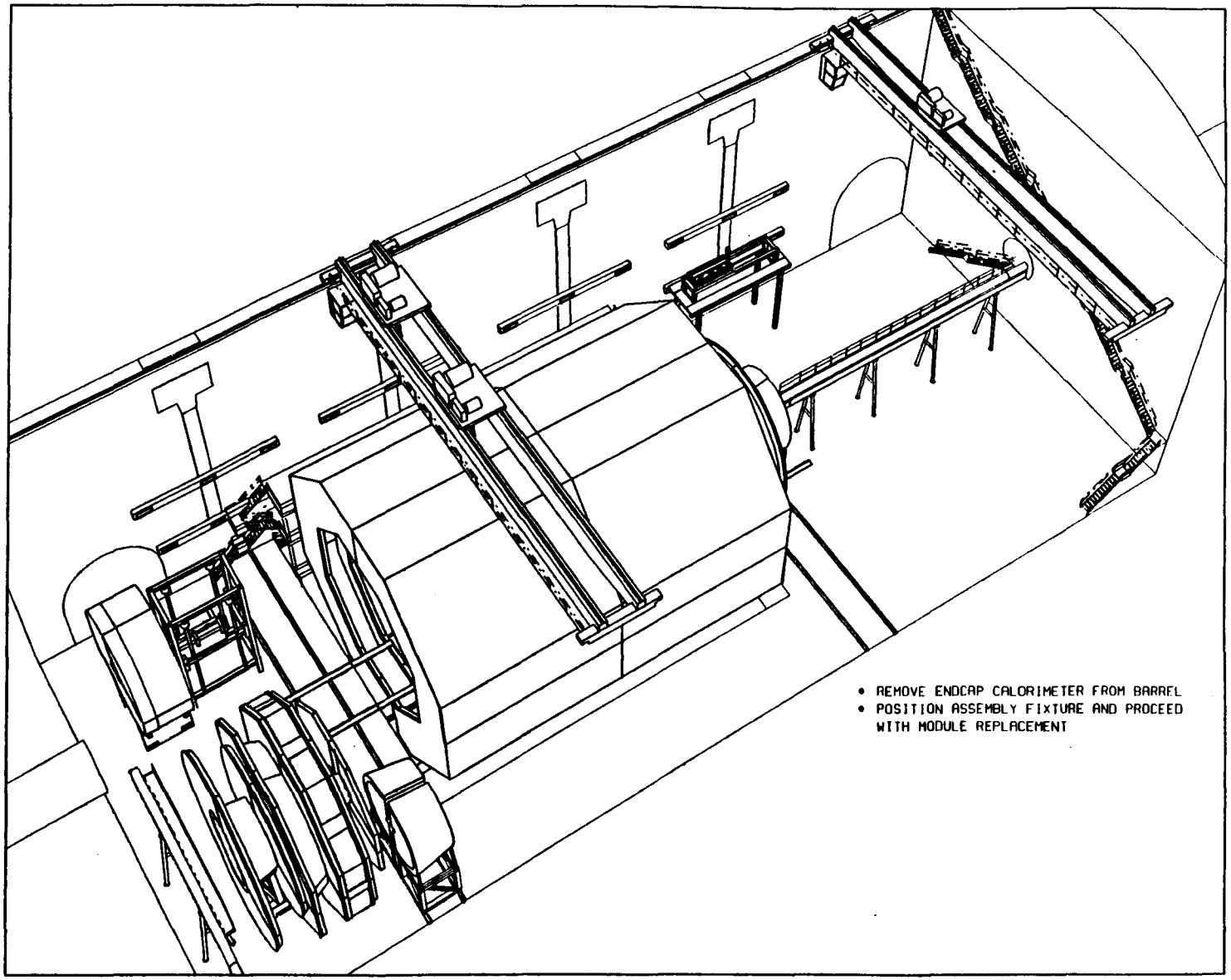

Figure 4.62. ACT Detector—Endcap Calorimeter Module Replacement (Step 2)

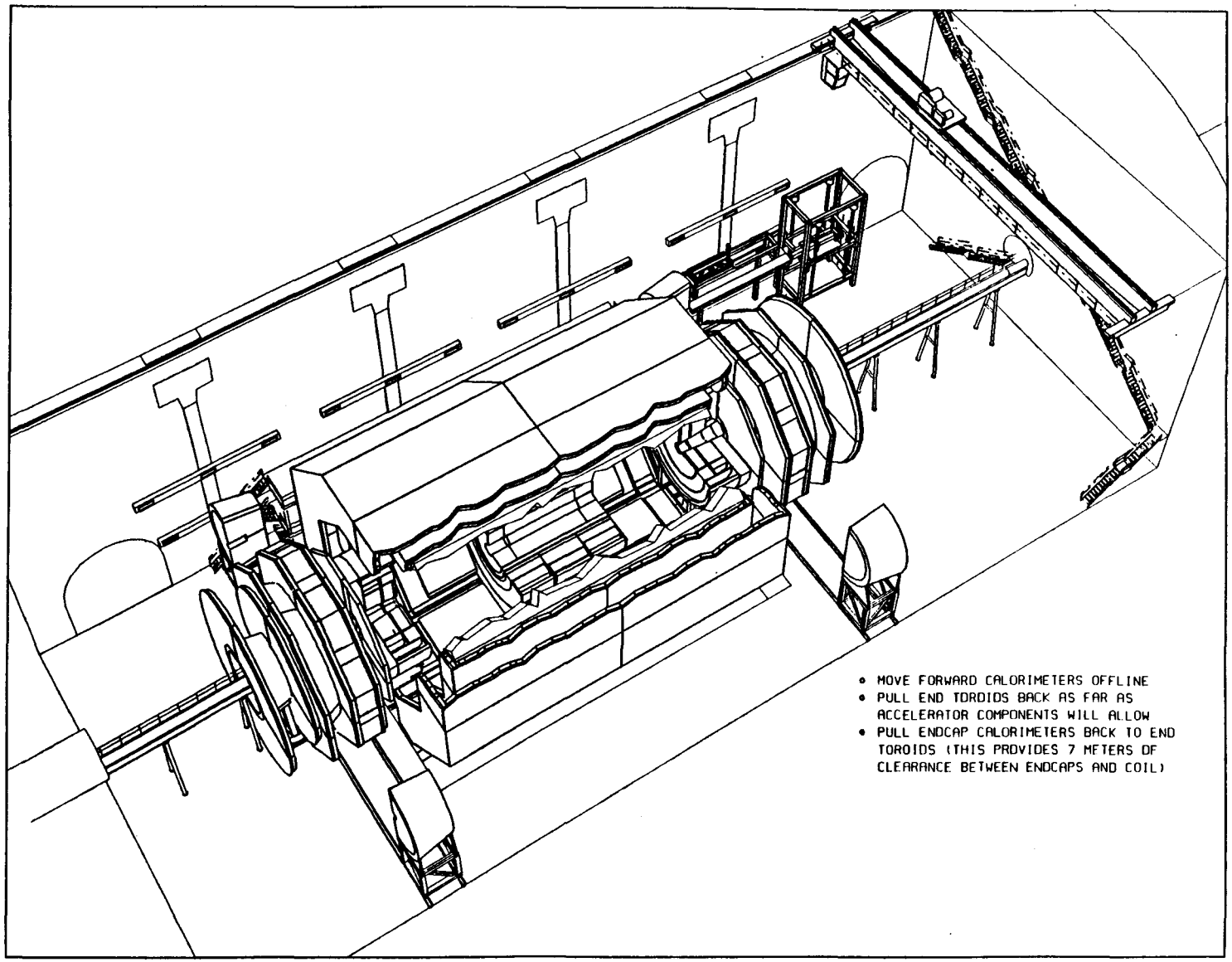

Figure 4.63. ACT Detector—Silicon Tracking Replacement (Step 1)

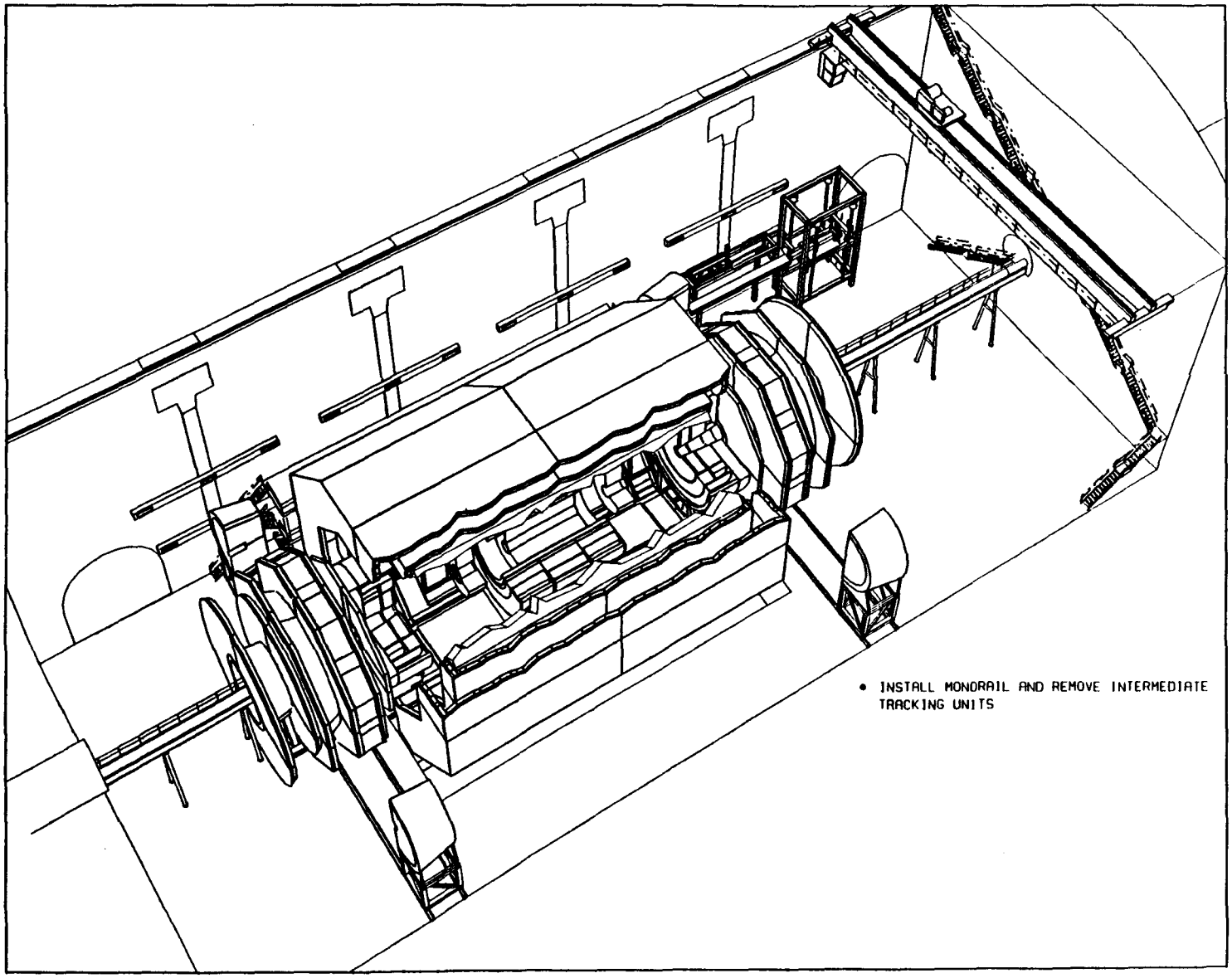

Figure 4.64. ACT Detector—Silicon Tracking Replacement (Step 2)

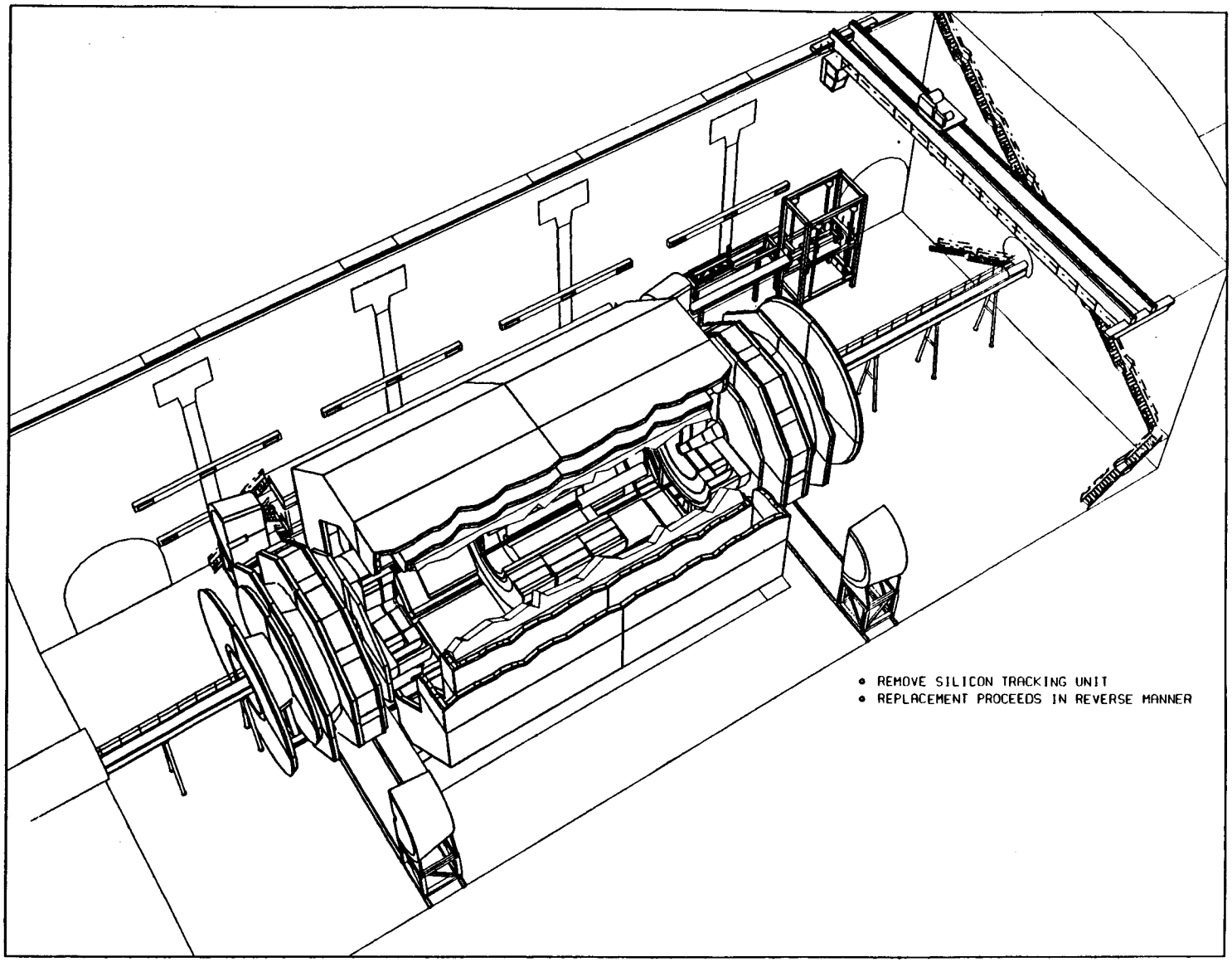

Figure 4.65. ACT Detector—Silicon Tracking Replacement (Step 3)

5.0 LIQUID ARGON CALORIMETER DETECTOR

5.1 Liquid Argon Calorimeter Detector Description

The Liquid Argon Calorimeter (LAC) detector design is developed around a calorimeter in which the active medium for detecting energy is liquid argon, a cryogenic fluid that must be maintained at 89 K. As showers develop in the calorimeter, ionization is left in the liquid argon. The number of ions produced is proportional to the total energy deposited in the calorimeter. A liquid argon calorimeter has the advantage of being radiation-resistant. The LAC Detector, however, presents new problems in the design of the detector and the hall because it introduces a large volume (180,000 l) of liquid argon which must be maintained at cryogenic temperatures. The general hall and detector design philosophy addresses safety concerns associated with a leak within the hall due either to damage to a liquid argon cryostat or to one of the liquid transfer lines. The major hazards resulting from these accidents are asphyxiation, cryogenic burns, reduced visibility, and damage to structural members due to low temperature exposure. A special insulated sump, with insulated transfer lines between the detector and the sump, has been added to reduce the amount of liquid argon evaporated into the hall in the event of a leak. This sump has a separate vent line to the surface, where the cold argon gas can be safely vented.

Safety considerations have also played a major part in the overall design philosophy of the detector. In previous designs, we maintained an access space between the outside of the calorimeter and the inside of the muon steel for maintenance of electronics in this area. In the LAC detector this access space has been eliminated for two reasons:

1. The LAC is less dense on average than equivalent calorimeters based on other technologies. For the same total thickness of absorber as measured in nuclear interaction lengths, the LAC is physically about 1 m thicker. This increases the cost of the detector. Eliminating the access space reduces the overall size of the detector and, therefore, the overall cost.

2. The annular space between the calorimeter and the muon steel represents an extremely confined space with limited egress in case of a catastrophic loss of liquid argon. Hence, we have chosen to achieve access to this space, when the calorimeter is filled with liquid argon, by moving the end toroids about 8 m axially, rather than by providing an annular access space.

The logic of the LAC detector remains the same as in previous detector designs: a tracking system in a solenoidal magnetic field surrounded by a calorimeter. The calorimeter is, in turn, surrounded by an extensive system of iron toroids, tracking chambers, and trigger scintillators for muon detection. A three-dimensional view of the detector is shown in Figure 5.1, and a cross-section and elevation of the detector are shown in Figure 5.2.

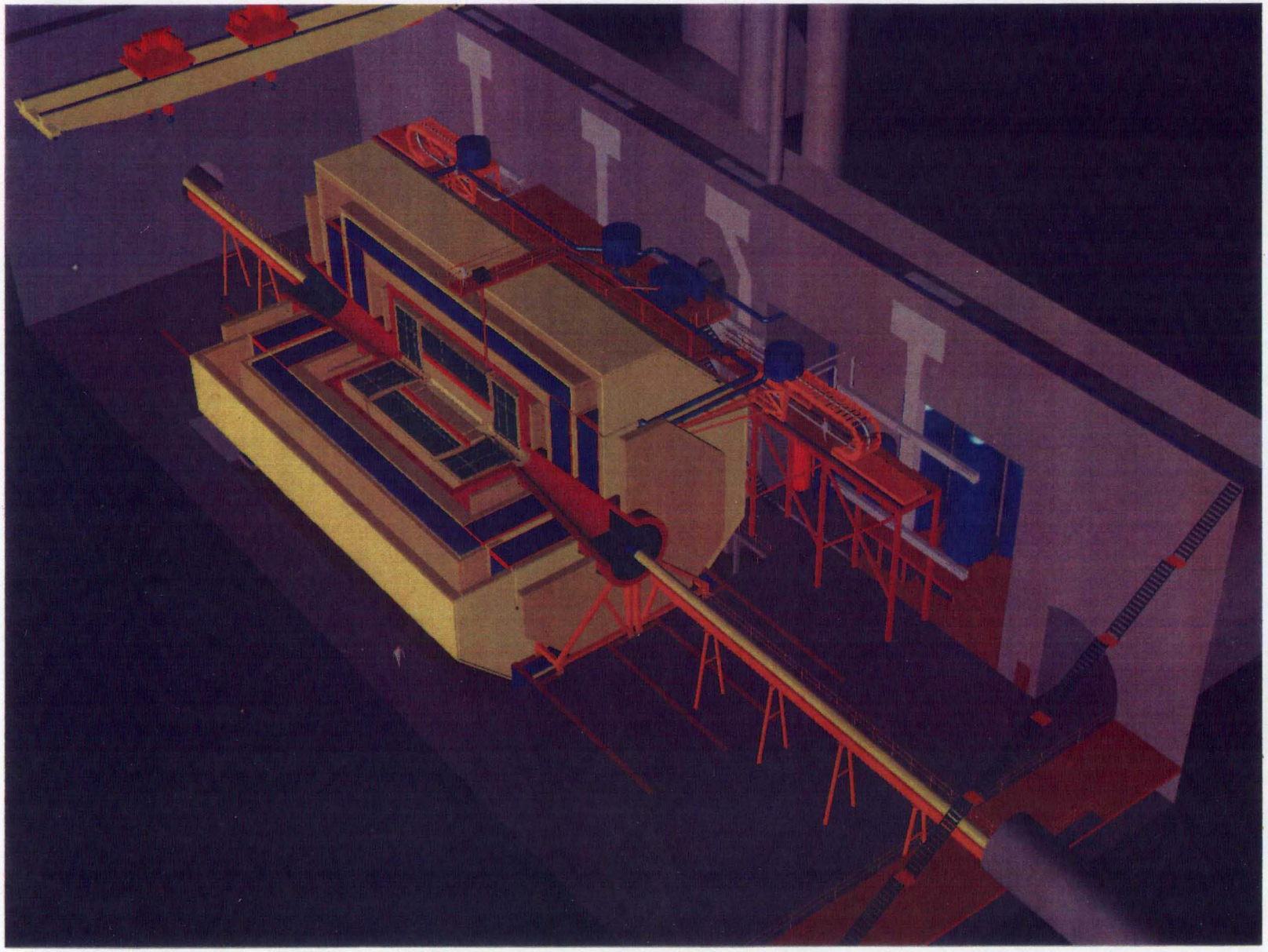

Figure 5.1.Overall LAC Detector Layout (3-D View)

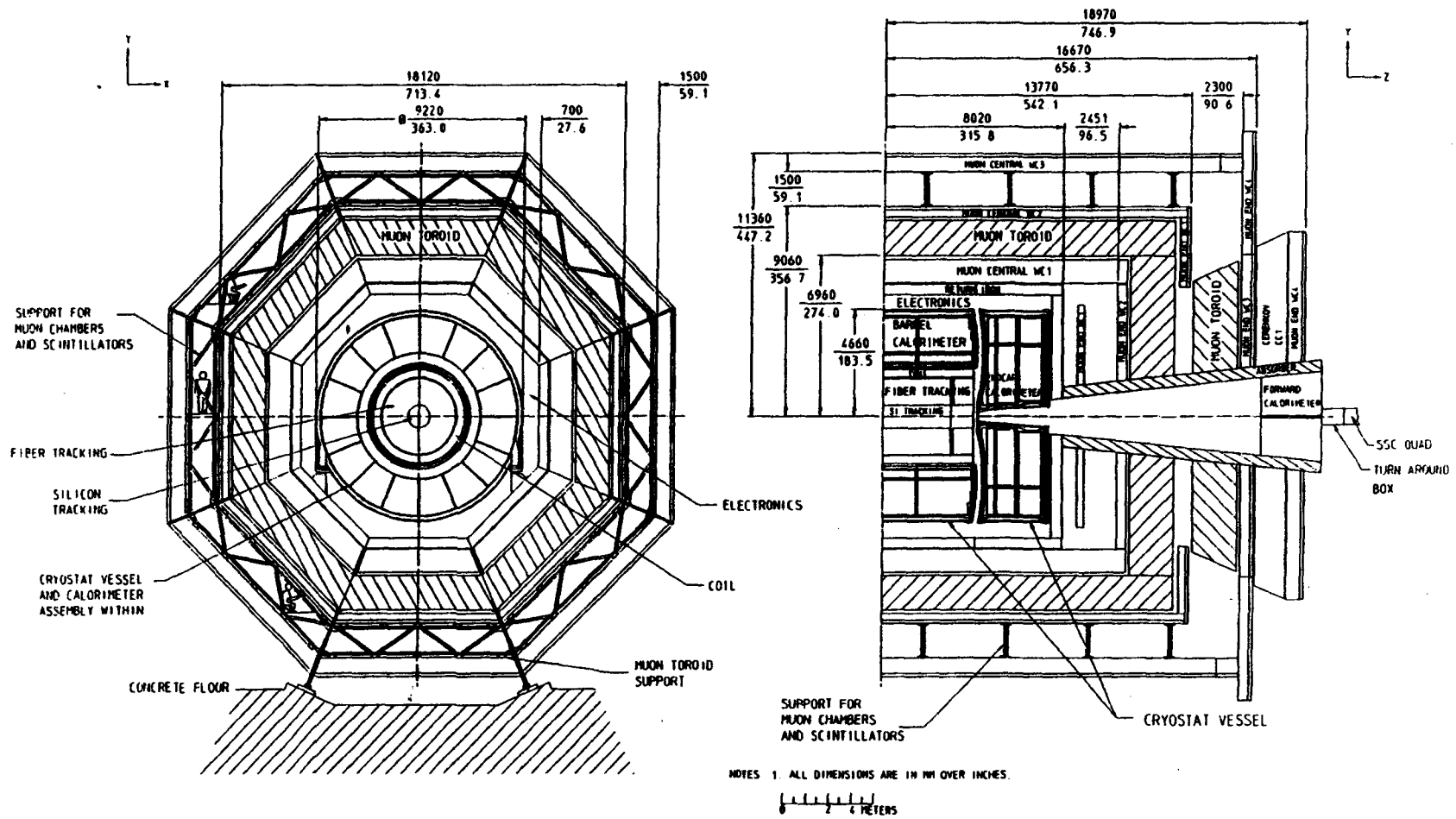

Figure 5.2. Cross-Section and Plan View of LAC Detector.

We describe this detector in detail starting with the tracking system and working outward. The tracking system is a silicon inner tracker with an outer tracker. The outer tracker is further divided into a central and intermediate region, and both trackers are assumed to be fabricated using scintillating fiber technology. These three elements arrive as assembled sub-systems, and we consider them only from the point of view of installation, testing, and maintenance. The solenoidal coil design is based on an "air-core" or short solenoid design.[1] This magnet does not use iron near the ends of the coil; hence, the external forces on the coil cryostat and the calorimeter are dominated by gravity. Any electromagnetic forces between the calorimeter and coil have been ignored.

The calorimeter is based on a design produced by KEK Laboratory in Japan, Kawasaki Heavy Industries, the SSC Laboratory, and Lawrence Berkeley Laboratory. We have specifically considered the routing of pipes and locations of cryogenic services for the calorimeter. The entire calorimeter is composed of three cylindrical sections: a barrel calorimeter and two endcap calorimeters. The barrel is about 9 m long. Each endcap calorimeter extends about 3 m along the beam line and weighs about 1200 tons. The electronics for the calorimeter and tracking lie in two annular spaces directly outside the calorimeter at each end of the barrel. The central part of this space is occupied by the feed-throughs which transport the calorimeter signals from cryogenic to room temperature. Electronics for the endcap calorimeters are mounted either in the analogous space on the outside diameter of the endcap calorimeter or just outside the endwall of the calorimeter.

Outside the electronics space is the return yoke for the magnet. About 65% of the flux is returned through the volume of the non-magnetic calorimeter, and the remaining 35% is returned through the steel at the outside of the calorimeter. Note that there is no access to the electronics space without moving the endcap calorimeters.

There are small forward ($5 > |\eta| > 3$) calorimeters for missing energy measurements. These are located directly in front of the interaction region quadrupoles.

The calorimeter is surrounded by magnetized iron muon toroids. In the barrel region ($|\eta| < 1.5$) the toroid is 1.5 m thick. The octagonal barrel iron toroid has 2 coils located near each corner, for a total of 16 coils. There are three stations of muon chambers in the barrel region, two on the outside and one on the inside of the iron. The momentum resolution of the exterior muon system is limited by the position resolution of the chambers and the 1.5 m gap between the two exterior chambers. Charge determination is possible to momenta well in excess of 1 TeV/c. The chambers on the inside of the steel are 1 m thick and are inserted on rails parallel to the long (z) axis of the detector. Access to the chambers at the middle of the detector is achieved by removing an endcap calorimeter, then removing as many muon chambers as necessary to reach the chamber desired.

At small angles with respect to the beam line the momentum resolution of the central tracking device deteriorates. In these forward directions the most accurate momentum measurement for muons comes from the intermediate iron toroids. These toroids are 4 m thick and are energized to 1.8 T. In analogy to the barrel region, there are chamber stations on both sides of the iron to measure the incoming and outgoing muon trajectory. For mechanical reasons we have divided the equivalent inner chamber into two separate chambers. Hence, there are four chamber stations in the intermediate muon system: two chamber stations in front of the toroids and two stations following the toroids. Two layers of trigger scintillators in the barrel and endcap regions provide a fast trigger for muons. These scintillators crudely measure the bend angle of muons exiting the steel.

We anticipate a large flux of low-momentum particles in the forward directions from beam spray, particles escaping from the inside surface of the endcap calorimeters, and albedo from the forward calorimeters. To protect the muon chambers in this area from these low-energy particles, we add a conical absorber layer approximately 50 cm thick between the intermediate muon system and the beam line. The absorber must be designed to intercept both charged and neutral particles, including neutrons. For the purposes of this study we assume the absorber is solid steel, but we expect it will consist of several layers of different materials to provide the optimum neutron absorption.

Other than elimination of the access space just outside the calorimeter, the major differences between the LAC and the ACT detector are as follows:

1. The size of the muon system has been adjusted to allow for the different size of the LAC.
2. The two internal barrel muon chambers have been combined into a single structure of equivalent thickness.
3. We have replaced the endcap Air Core Toroids of the previous design with iron toroids.
4. The size of the tracking volume is reduced to 3.4 m diameter by 8 m long.

Table 5.1 lists some major mechanical properties of the LAC detector.

Table 5.1. LAC Detector Mechanical Parameters.

Detector	Size	Units	Comments
Tracking Volume	3.4 × 8.0	m	diameter × length
total channels	1195	K	Fiber, incl. inter & central
Silicon Tracking	1.0 × 5.6	m	diameter × length
Silicon Tracking Weight	0.6	tonne	
Coil	3.4 × 4.1 × 8.0	m	id × od × length
Barrel Calorimeter	4.2 × 11.6* × 8.0	m	id × od × length
weight	4900	tonne	includes return steel
Total channels	93	K	Includes endcaps
Endcap Calorimeter	1.0 × 11.6* × 4.0	m	id × od × length
weight	3130	tonne	both ends
Muon Barrel. Toroids	17.0 × 17.0 × 26.1	m	w × h × length
weight	15,770	tonne	
Muon Endcap Toroids	12.2 × 12.2 × 4	m	w × h × length
weight	8320	tonne	both ends
Muon Barrel Chambers	22.4 × 22.4 × 33.0	m	w × h × length
Total Channels	66	K	
Muon Endcap Chambers	16.0 × 16.0 × 10.3	m	w × h × length
Total Channels	42	K	including both ends

* includes return steel

Each subsystem in the detector will require a variety of connections for proper operation and to meet safety requirements. The connections to each subsystems consist of:

- Mechanical supports
- Trigger and data acquisition cables
- Power, including low and high voltage connections
- Cooling fluids or gases
- Sub-system speciality fluids or gases
- Alignment monitoring and adjustment
- Environmental monitoring (temperature, oxygen concentration, explosive gas concentrations, smoke detectors, etc.)

The details of these connections depend critically on the technology chosen for each subsystem. Planning must consider the interactions between subsystems as well as the needs of an individual detector element. However, the general strategy for the "hookup" of the detector to external systems is as follows.

For all detector subsystems the front-end electronics, level 1 trigger electronics, and temporary data storage for about 100 beam bunch crossings (including data buffering between the level 1 and level 2 trigger decisions) are mounted directly on the mechanical structure of the subsystem. These electronics are in turn connected via flexible cable trays to global trigger and data acquisition electronics located in a multi-story gallery next to the detector inside the collision hall. The flexible cable trays allow motion of detector subsystems to provide access to the internal portions of the detector without disconnecting cables or utilities. This includes the cryogenic fluids necessary for the endcap calorimeters, which must move 8 m to access the central detector.

The layout of the hall currently allocates the second and third floors of this gallery for trigger and data acquisition areas. Each floor of the gallery is approximately 4 m wide by 30 m long. These two floors are fully air-conditioned enclosures and are provided with computer (false) floors for routing of cables between electronics racks. Data acquisition and trigger signals are communicated to the surface via the 3-m-diameter cable shaft, located 8 m inside the wall next to the gallery. Floors above the third level of the gallery are reserved primarily for the cryogenics systems of the superconducting solenoid and calorimeter. These levels, as well as the basement below the first floor, do not have separate air-conditioning or computer floors. Utilities for these areas, as well as any heavy-duty power lines, are connected to the surface via a separate utility shaft to avoid pickup of switching noise from the heavy-duty power cables to the data acquisition cables.

The fourth and fifth levels of the gallery hold LAC cryogenic and vacuum equipment such as argon conditioners, valve boxes, and turbomolecular pumps. Figure 5.3 shows the layout of the endcap cryogenic equipment on the level 4 platform. Level 5 has the barrel cryogenic equipment and the solenoidal magnet helium cryogenic equipment. As shown in Figure 5.4, there are two flexible piping carriages, one on each end of the fourth level of the gallery, to allow the end caps to move up to 8 m from the operating position without breaking the vacuum or cryogenic lines. The elevation of the cryogenic equipment ensures that cryogenic lines will always point upward to avoid possible vapor traps. By placing the dewars at approximately the same elevation as the detector, pressure due to the argon liquid head in the conditioners remains within acceptable limits.

5.2 Liquid Argon Calorimeter Detector Hall Design

5.2.1 Overview and General Hall Plan

The LAC detector collision hall is 31.0 m wide and 88.0 m long, constructed with its long axis parallel to the collider beam line, as shown in Figure 5.5. Dimensions of the hall are based on access around the completed detector, space requirements for assembly and checkout of the calorimeters and end muon toroids, and clearance requirements for retracting the detector

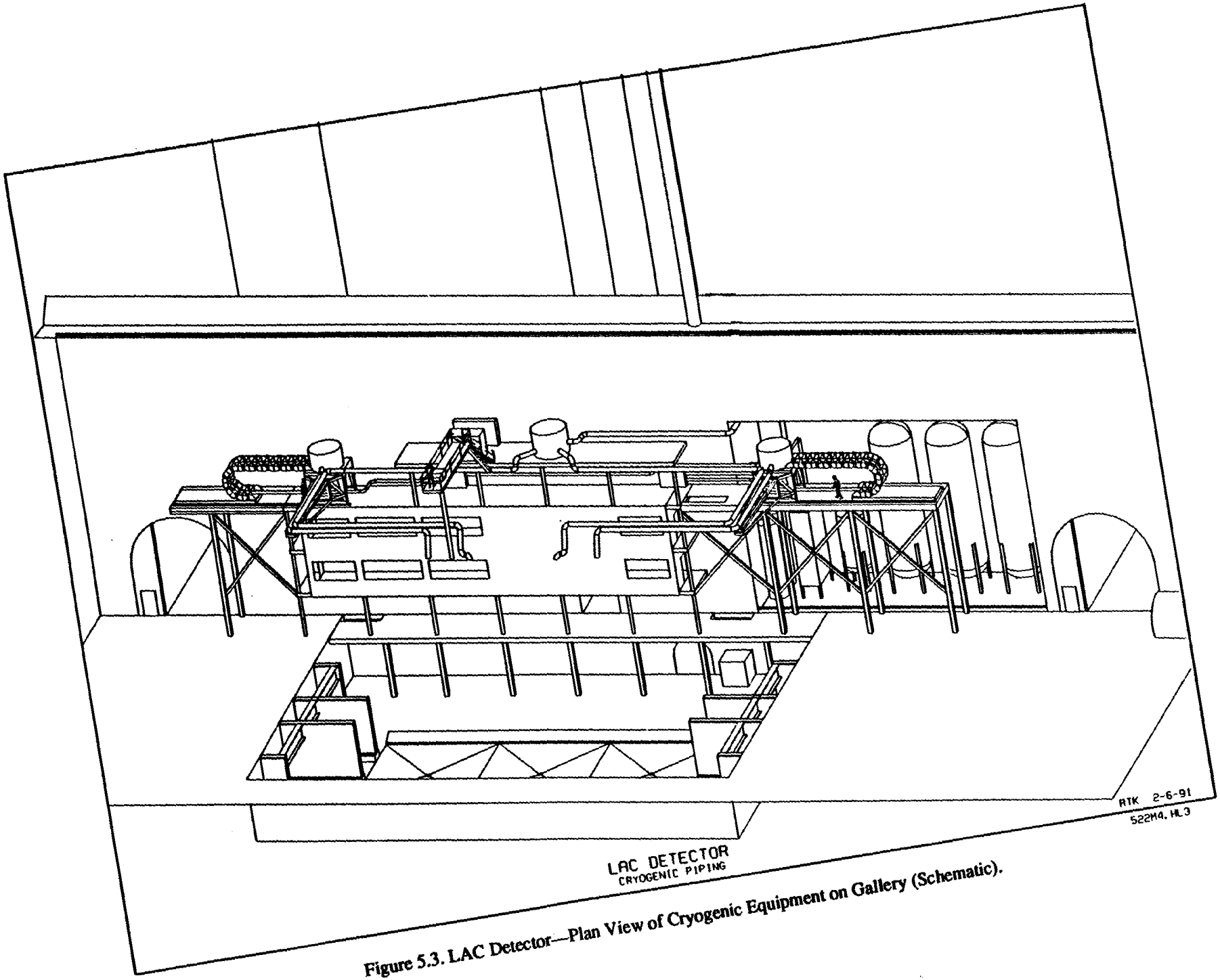

Figure 5.3. LAC Detector—Plan View of Cryogenic Equipment on Gallery (Schematic).

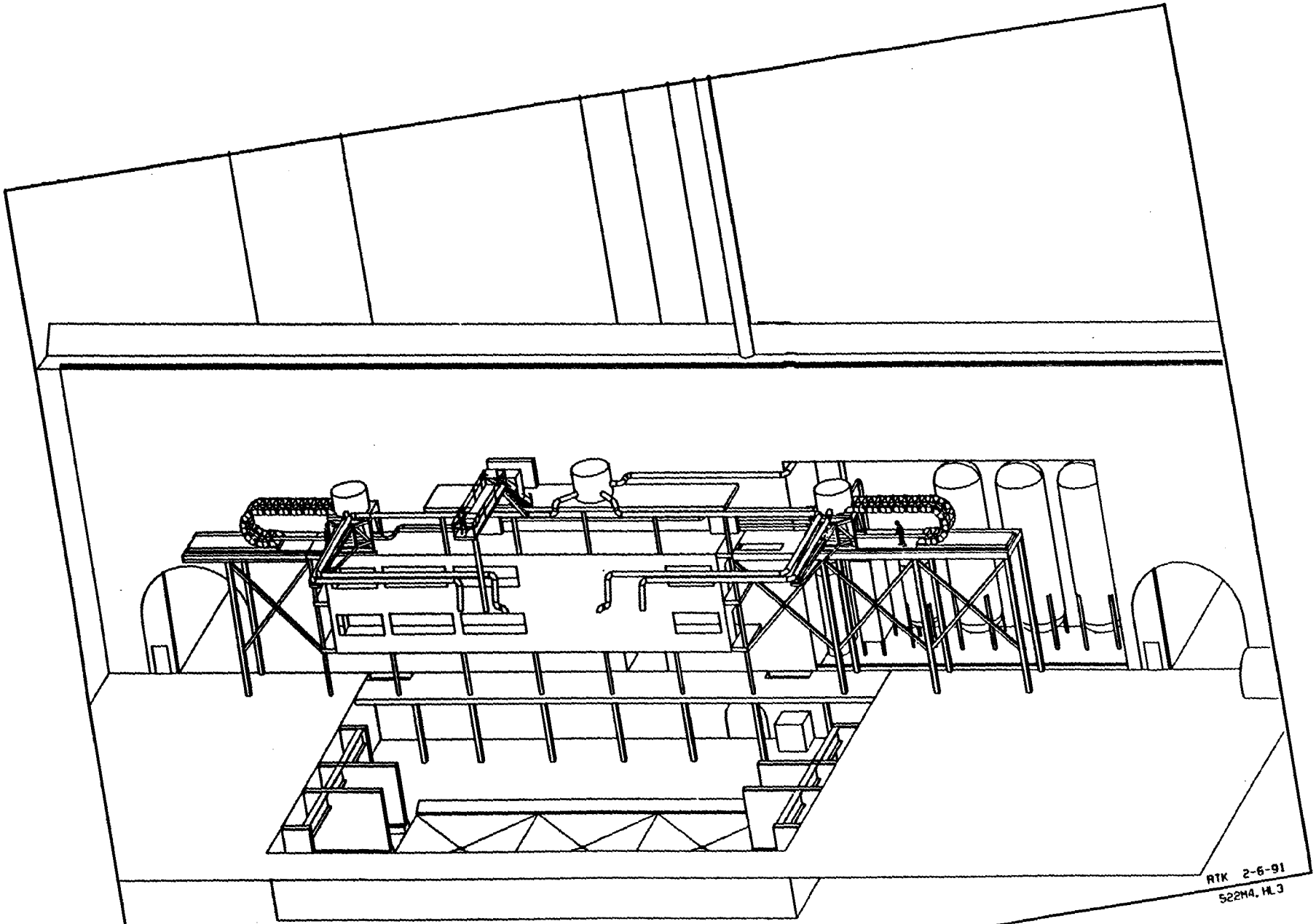

Figure 5.4. LAC Detector Shown Without Muon Barrel.

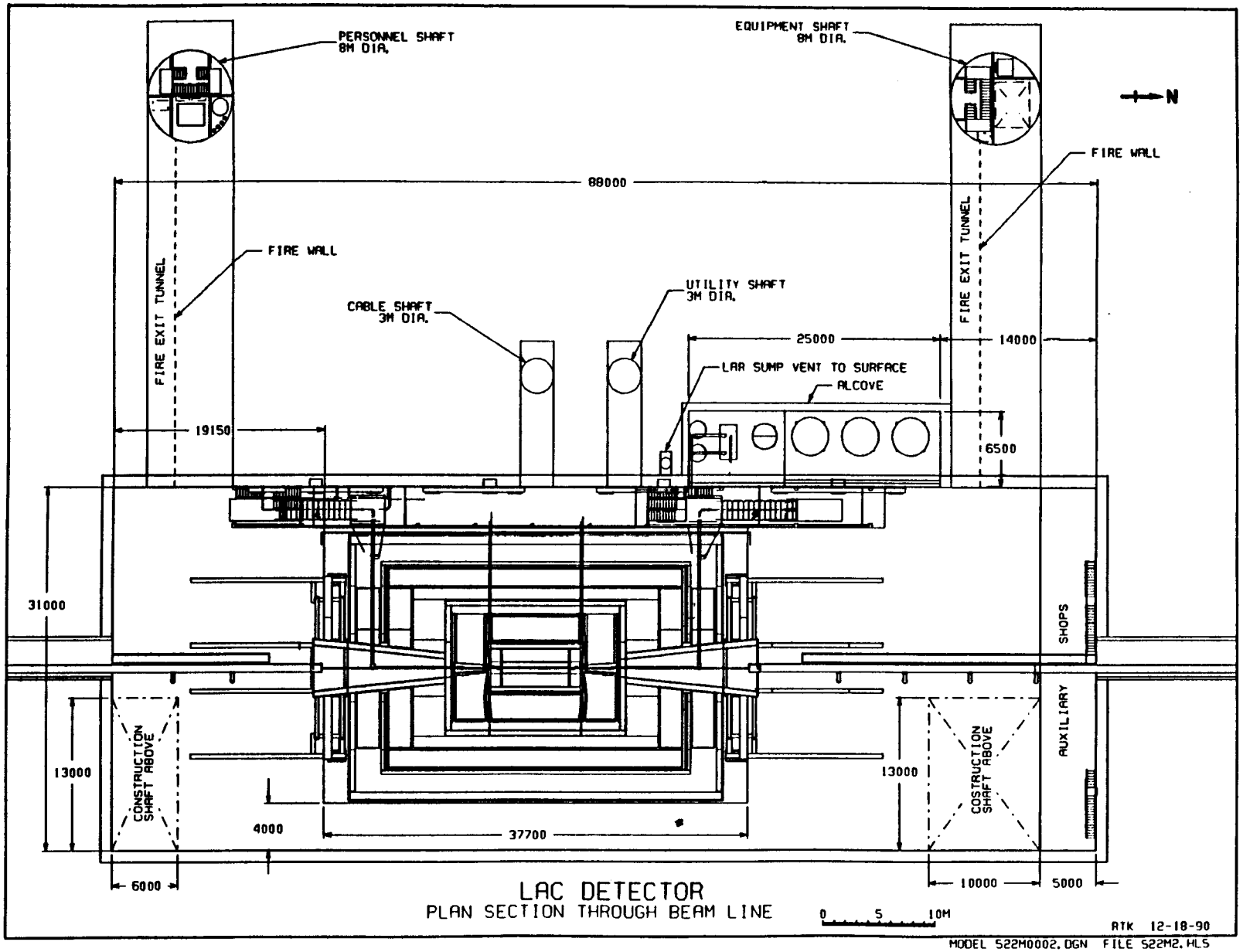

Figure 5.5. LAC Detector—Plan Section of Detector Hall.

components for maintenance access. In-place upgrading of the detector has also been considered. A temporary air-tight partition between the muon steel assembly and the calorimeter assembly areas of the hall is erected during calorimeter assembly to provide a clean area . As shown in Figure 5.3, a 5-m-wide area at the north end of the hall is reserved for the auxiliary shops required during calorimeter assembly and general maintenance. Table 5.2 lists the cryogenic equipment of the LAC detector that would be installed in a 6.5-m-deep and 25.0-m-wide alcove located in the west wall of the hall.

Table 5.2. Liquid Argon Cryogenic Equipment.

Item	Number	Capacity	Size
Dewars			
Liquid argon	3	60,000 l	4.0 m$^{\phi}$ × 9 m
Liquid nitrogen	1	20,000 l	3.0 m$^{\phi}$ × 6 m
Boilers			
Liquid argon	1	3 stage × 50 kW = 150 kW	1.5 m$^{\phi}$ × 10 m
Liquid nitrogen	1	3 stage × 50 kW = 150 kW	1.5 m$^{\phi}$ × 10 m
Valve boxes and Distribution headers	N/A	N/A	1 × 2 × 1 m^3

The alcove is sealed from the hall by removable concrete panels and is drained to a sump under the detector basement by several insulated floor drains. These large-diameter floor drains are designed to remove any argon gas in the alcove. Suction fans are provided to maintain the alcove space at a slightly lower pressure than that of the main hall. We have estimated the extra cost of the alcove and the removable concrete wall at $700,000.

As shown on Figures 5.6 and 5.7, the top of the main operating floor is set level with the top of the roller tracks in the barrel muon steel, and the basement under the detector is about 5.0 m below that. A 3-m-wide clear passage for moving small equipment along the west side of the detector on the operating floor is provided, as is a 4-m-wide passage along the east side of the detector for transporting large items by the hall crane from one end of the hall to the other.

The basement is extended to the side wall of the hall under the west passage to provide room for pumps, compressors, utility distribution, and other equipment, and for structural requirements. Under the west side of the detector basement is a large insulated sump to collect liquid argon spills and vapors in the hall and in the alcove. The sump is evacuated to the surface by a 1-m-diameter insulated vent line.

The walls extend about 22.8 m above the operating floor, as shown in Figure 5.6. The crane runways rest directly on the top of the side walls, which are provided with vertical recesses for the

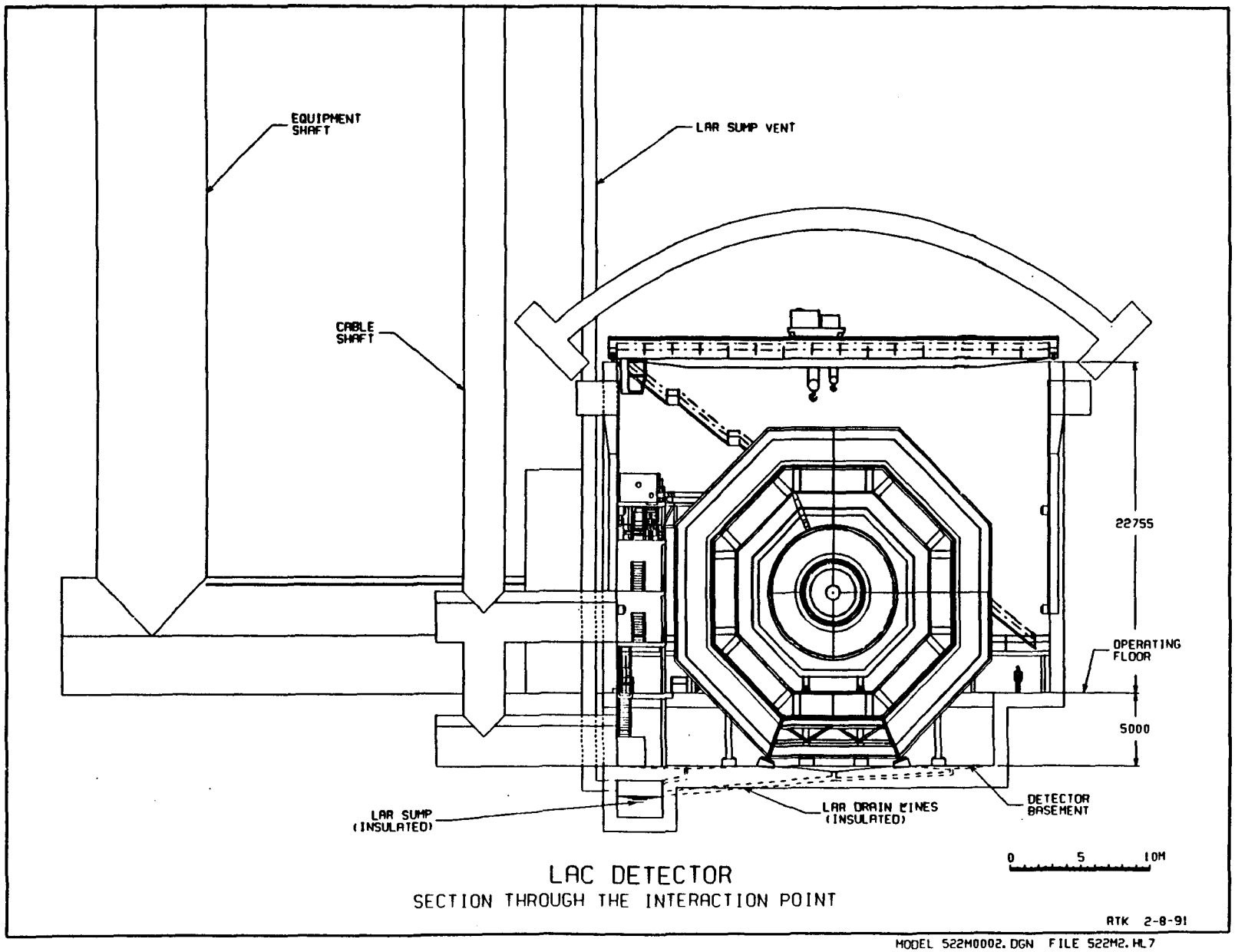

Figure 5.6. LAC Detector—Section through Interaction Point.

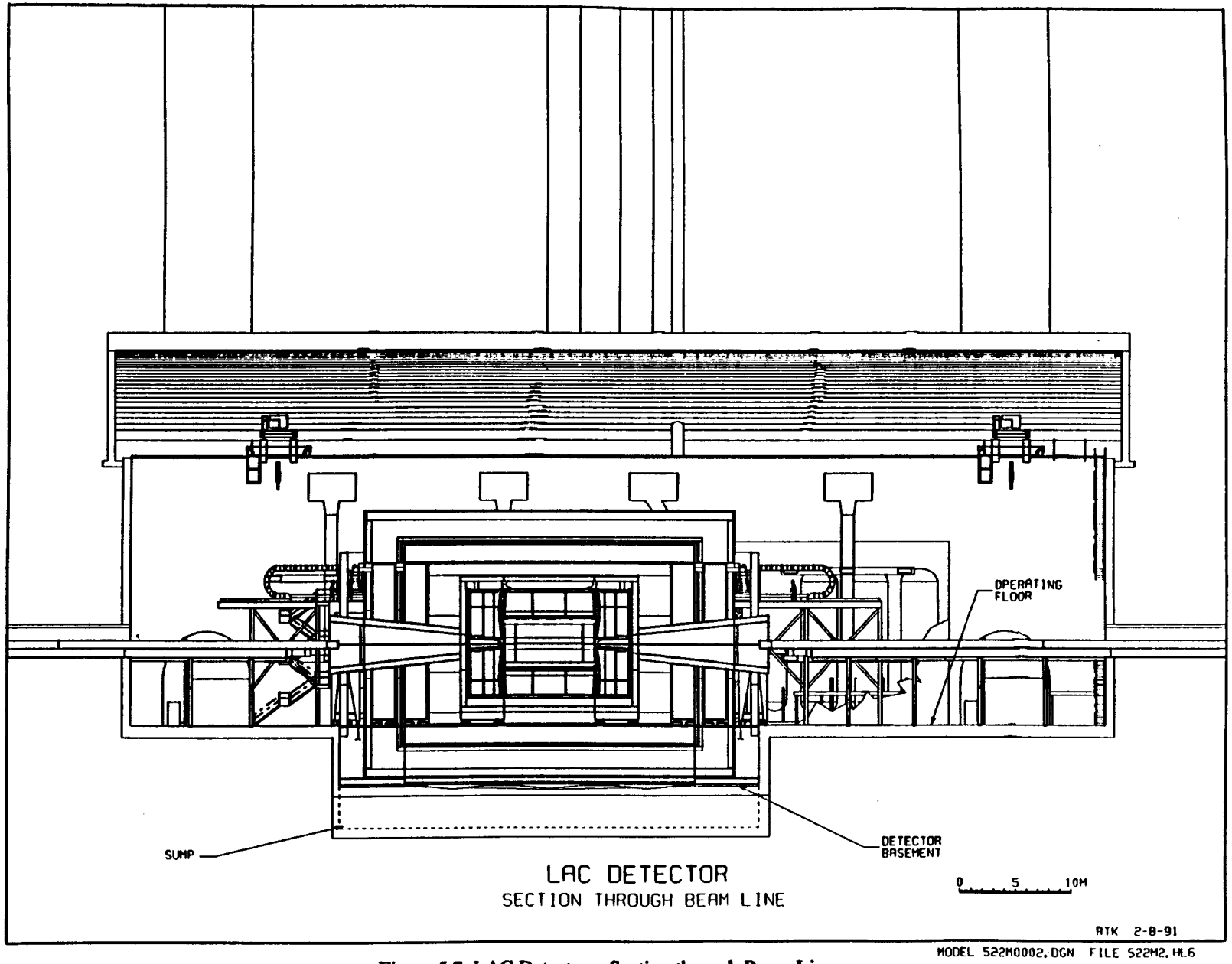

Figure 5.7. LAC Detector—Section through Beam Line.

flush-mounted air-conditioning ductwork. The walls of the hall are tied to the rock behind by rock anchors.

The roof of the collision hall is a parabolic concrete arch supported on independent foundations just behind the top of the side walls, as shown in Figure 5.6. This low-rise arch imposes an outward force on the rock mass behind the side walls of the hall, thereby reducing the heave forces on the side walls. The arch foundations are not tied to the walls, so that any change in the overburden or surface loading above the arch will not affect the walls or the floors of the hall. Placing the roof of the hall on top of the walls would impose a high vertical load on the walls and, in turn, on the edge of the hall floor slabs, which may be just above the weak Eagle Ford Shale if the hall is located at the west cluster. The resulting immediate and long-term floor movements would be large and could be influenced by changes in the overburden pressure on the roof.

The space between the top of the wall and the base of the arch can be used for distribution of some of the hall utilities and to service the cranes, the fans of the air-conditioning system, and the roof drainage sumps.

The proposed hall configuration may be constructed by conventional open excavation or by excavating to the top of the walls and constructing the roof arch while the excavation proceeds to the hall floor. This arrangement will permit an earlier start of the backfill operation, and will, therefore, reduce construction time of the hall.

5.2.2 Safety Considerations

The LAC detector contains approximately 180,000 l of liquid argon, which is maintained at 89 K by boiling liquid nitrogen. Due to the large volume of liquid argon in the LAC detector, the hall has been designed to achieve maximum possible safety during installation, operation, and disassembly procedures.

The alcove area in the hall provides space for large argon storage tanks to facilitate transfer of liquid argon to and from the cryostats without the risk of subjecting the cryostats to the large liquid head that exists between the surface and the hall. Similarly, the platform containing most of the cryogenic equipment is located at the desired elevation on the west wall nearest the detector. This minimizes the risk of damage to cryogenic lines due to movement of cranes or forklifts.

To facilitate disassembly of the detector, the cryogenic piping system incorporates flexible carriages, which allow the end caps to move up to eight m without disconnecting any vacuum or cryogenic lines. The size of the carriage is based on the 10-in.-diameter vacuum vent line and an axial stroke of 8 m. Special mounting platforms are installed in the hall for supporting the carriages.

Spills are collected by insulated trays directly under all cryogenic equipment, valve boxes, and distribution headers. These trays are connected by insulated piping to intermediate sumps or

directly to the main sump. The variable-speed fans of the main sump remove the liquid and some of the gaseous argon collected by the trays. The connecting lines may be isolated by valves controlled by the argon spill sensors so that suction in the lines affected by a spill can be maximized.

To address large spills of liquid argon, a thermally insulated subfloor sump with a liquid argon capacity of 300,000 l is placed under the detector basement. The sump serves as a holding volume in case of a catastrophic accident that would lead to a large liquid argon spill. Any spill in the detector area is collected by the depressed basement floor, which is sloped to several rows of large-diameter floor drains connected to the sump by insulated lines embedded in the floor (Figure 5.6). These drain lines are designed for rapid collection of liquid and gaseous argon. (Argon is heavier than air, and, therefore, will tend to remain on the floor.) Floor drains rather than trenches are used so the spill can be disposed into a totally insulated area as quickly as possible, thereby reducing evaporation of the spill. Floor drains and piping are also less expensive and less obstructive to traffic on the floor. Any reduction in floor stiffness (so important to minimize the floor movement) caused by the pipes can be compensated for by extra reinforcements. To remove argon gas from the high points of the floor, additional suction ducts located around the perimeter of the detector basement and certain areas of the operating floor are provided.

The sump is connected to the surface via a 1-m-diameter vent line designed to evacuate argon gas at a maximum rate of 20,000 cfm, the worst-case rate of argon gas boil-off. The suction fans can be sized for twice the worst-case rate to permit mixing of the argon gas with ambient air, thereby reducing the concentration of argon in the discharge flue. The fans are activated by gas sensors placed at critical locations in the hall. The mechanism of dispersing the discharged argon into the atmosphere is not addressed in this design report; it should be studied after the layout of surface buildings is completed.

The impact of liquid argon leaks on the hall ventilation system is not addressed. Gaseous argon is heavier than air and will tend to stay near the bottom of the hall. Therefore, smoke evacuation vents which are located at the ceiling will not be helpful and may be counterproductive if they are activated during a liquid argon spill in the hall.

5.2.3 Detector Basement and Support

The adopted maximum floor movement is 2.5 mm for short duration (one week) loading and 25 mm for long duration (one year or more) loading after all components of the detector are in place. These floor movement specifications require a very rigid concrete basemat under the detector. Floor movement during erection of the muon steel and after the calorimeters are installed is also restricted to 25 mm; however, this could be compensated for by presetting the main steel barrel supports before erection of the muon steel begins. Weight calculations indicate that the

detector loading on the basement floor is about 105% of the present vertical rock pressure at this elevation. This means that deflection of the floor due to the weight of the detector could be very small, and, therefore, the floor movement will be largely controlled by the heaving pressure of the underlying rock. In the operating floor areas, floor loading is very low (less than 10% of the present rock pressure); therefore, the upward floor movement due to the unopposed heave could be large.

To reduce floor movements the detector basement must be made very rigid. The stiffness of the basemat depends on the thickness and uncracked moment of inertia and modulus of elasticity of the concrete, as well as on the length and aspect ratio of the floor spans. The vertical restraint of the perimeter walls will also affect the deflection of the slab.

To construct a basement slab to be as rigid as possible, the edge of the detector floor is restrained by the stiff walls of the hall on two sides, and by the heavily reinforced retaining walls at the ends of the detector. Using a higher strength (and Young's modulus) concrete also reduces deflections. Our preliminary finite element calculations indicate that floor deflections caused by the stationary and moving components of the detector will not exceed the adopted maximum floor movements. However, floor movement caused by heaving of the underlying rock mass may be large and could require special design considerations as outlined below.

Detailed design of floor will be based on the actual detector loadings and deflection limitations, and on the results of a geotechnical investigation of the physical properties of the underlying rock at the selected hall location. However, if the hall is located at the west cluster, the detector support floor will rest on or directly above the Eagle Ford Shale, where it will be subjected to the long-term heave forces of the shale. Assuming that the excavation is stable, the immediate (elastic) heave of the rock is not a problem until the concrete floor has hardened. After that, swelling due to migration of the moisture in the rock and to creep and redistribution of stresses caused by the uneven overburden pressure may cause a slow upward floor movement. The magnitude and duration of this movement would be difficult to estimate. However, there are several ways to overcome the heave problem. A simple solution is to provide the means to adjust the height of the base plates of the barrel supports. This may be accomplished by supporting the base plate on a sole plate and shims, as shown in Figure 5.8 To adjust the elevation of the detector, low-height hydraulic jacks placed under the base plate would be used to unload the shim plates. After the shim thickness has been adjusted, the jacks would lower the detector to the required elevation. The jacks may be removed after the nuts are locked to the base plates.

A more direct solution to the heave problem is to post-tension the floor slab to the underlying rock. This is done by drilling into the rock through several rows of blockouts near the midspan of the floor and installing rock bolts to a depth of approximately 1.5 times the width of the hall. The lower 1/3 of the bolt length is grouted into the rock, while the upper 2/3 is sleeved to permit

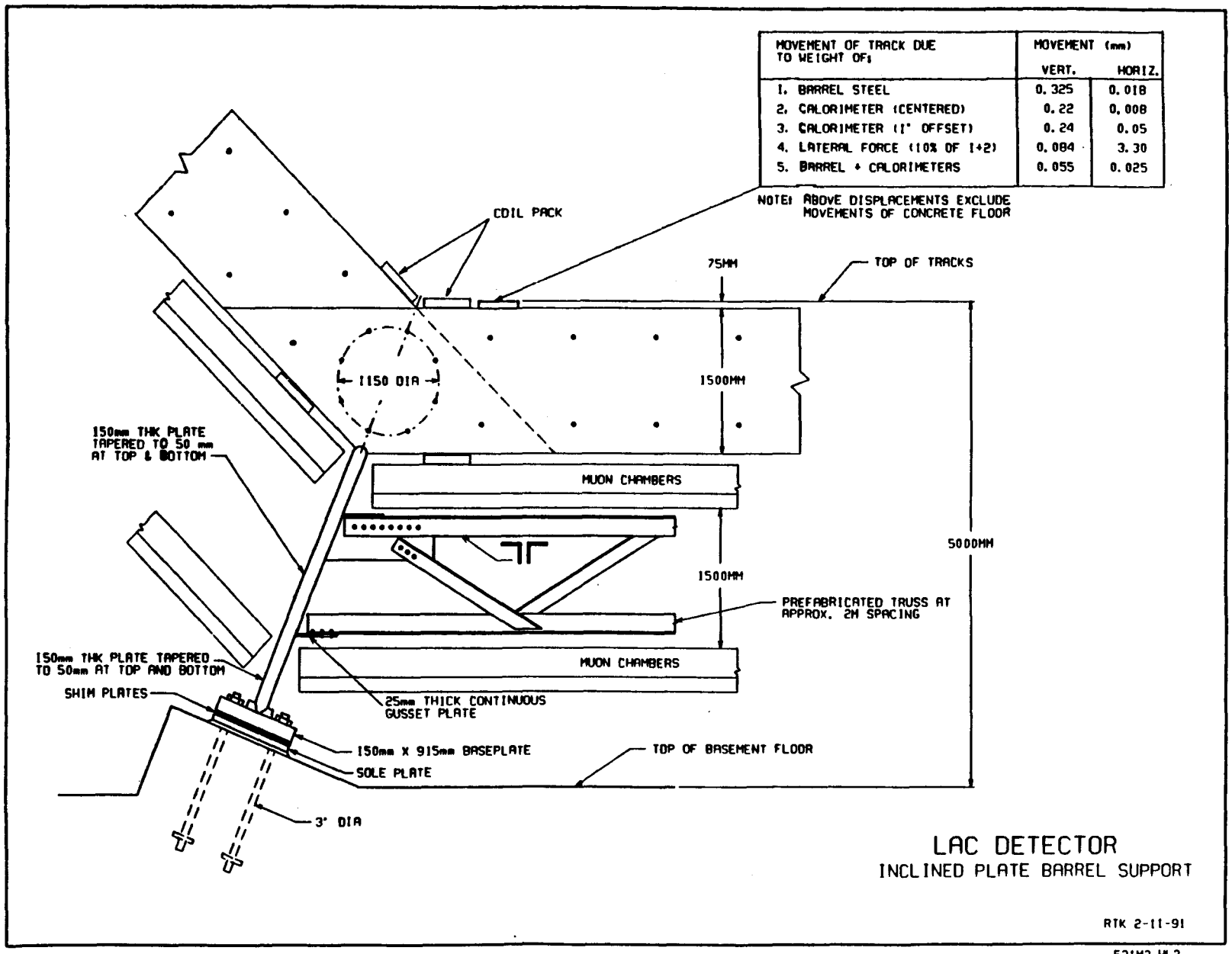

Figure 5.8. LAC Detector—Inclined Plate Barrel Support.

slippage. The bolts are initially tensioned for the weight of the detector and, if required, further tensioned to reduce heave. The floor movements are continuously monitored by lasers, and, if required, the bolts may be retensioned or slackened to adjust the floor elevation.

5.2.4 Operating Floor Construction

To facilitate disassembly of the detector components and access to the detector, the top of the operating floor is set level with the top of the roller tracks in the barrel. Unlike the detector basement floor, the operating floor will be loaded to less than 10% of the present vertical rock pressure at this elevation. This means that to reduce floor movement to acceptable levels, the heave pressure from the underlying rock will have to be restrained by the floor slab. Excessive floor heaving could slow down disassembly operations of the detector because rolling the heavy components on a sloping floor will require special procedures to insure safety. The supports of the forward calorimeter and of the acceleration magnets will have to be made adjustable to maintain proper alignment.

Floor heave could be reduced by post-tensioning the floor slab to the underlying rock, as described in Section 5.2.3, or by separating the floor slab from the rock by a layer of compressible materials. This problem should be further studied as soon as the results of the geotechnical investigation are available.

To facilitate movement of the detector components during construction and major disassembly, the entire floor area north and south of the detector basement is covered by a 12-mm-thick steel plate. The plate is leveled before anchoring to the floor slab by high-strength grout. This arrangement provides the proper rolling surface and distributes the high rolling pressures of the rollers under the end toroids and calorimeters. Some components of the detector are moved to predetermined areas via guided paths to provide access to the central tracking device and calorimeters for testing and maintenance. To facilitate this work, the floor plate in these areas is thickened to about 36 mm and is machined flat to reduce rolling resistance. Tapped holes for anchoring the push/pull jacks are provided in these areas.

5.2.5 Access and Utility Shafts

Access to the hall is provided by two rectangular construction shafts penetrating the hall roof in the northeast and southeast corners of the hall, and by two circular shafts, both with stairs and one equipped with an elevator. Separate shafts for utilities, cabling, and for the air-conditioning ducts are also provided. Figure 5.5 shows the location of these shafts; Table 5.3 provides additional information about the shafts.

Table 5.3. Hall Shafts.

Name or Use	Size	Cross-section	Access
Construction Shaft #1	10 m × 13m	rectangular	crane only
Construction Shaft #2	6 m × 13m	rectangular	crane only
Equipment Shaft	8 m	round	stairwell/crane
Personnel Shaft	8 m	round	stairwell/elevator
Cable Shaft	3 m	round	stairwell
Utility Shaft	3 m	round	stairwell/dumbwaiter

Construction Shaft #1 is located near the northeast corner of the hall and provides a 10 by 13 m access into the hall for lowering the barrel calorimeter jackets, the completed endcap calorimeter, and the forward calorimeters and the central tracking device. Some of the muon chamber panels may also be brought down through this shaft. Construction Shaft #2 provides a 6 by 13 m access into the hall for lowering all steel used in constructing the muon barrel, the end toroids,and the support beams and erection rigs of the barrel. When the muon steel assembly is finished, the completed endcap calorimeter and forward calorimeter and the majority of the muon chamber panels are also brought down through this construction shaft.

To maximize the usable floor area for detector assembly and for possible major repair and/or modification work on the detector in the future, the construction shafts are located in the corners of the detector hall. Placing the shafts on the center line of the hall would require a longer hall for detector assembly and would locate the shaft over the beam line. Location of the construction shaft over the beam line would inhibit the use of the shaft after beam line components are in place. Once the detector assembly has been completed, both construction shafts are closed at the top by overlapping precast concrete slabs to block radiation. These slabs may be removed later to regain access to the hall for lowering large objects.

The equipment shaft is 8 m in diameter and is located away from the northwest corner of the detector hall so that at the surface the shaft is outside the area excavated for hall construction. This allows the shaft to be built earlier to provide access to the hall before the hall roof is constructed and backfilled. The bottom of the shaft is connected to the operating floor by an 8-m-wide, concrete-lined tunnel. The equipment shaft and tunnel are partitioned by a fire wall that encloses the fire escape stairs and egress route (Figure 5.9). The stairwell and egress route in the tunnel are slightly pressurized to prevent smoke from entering this region in the event of a fire. The equipment shaft also incorporates a 3 m by 4 m hoisting well for lowering calorimeter modules, electronics, and other equipment. Space for a 2000-lb-capacity construction elevator and for the ductwork of the hall ventilation system is also provided.

The personnel shaft is located a distance from the southwest wall of the detector hall. For the reasons given above, this shaft is also situated outside the region excavated during hall

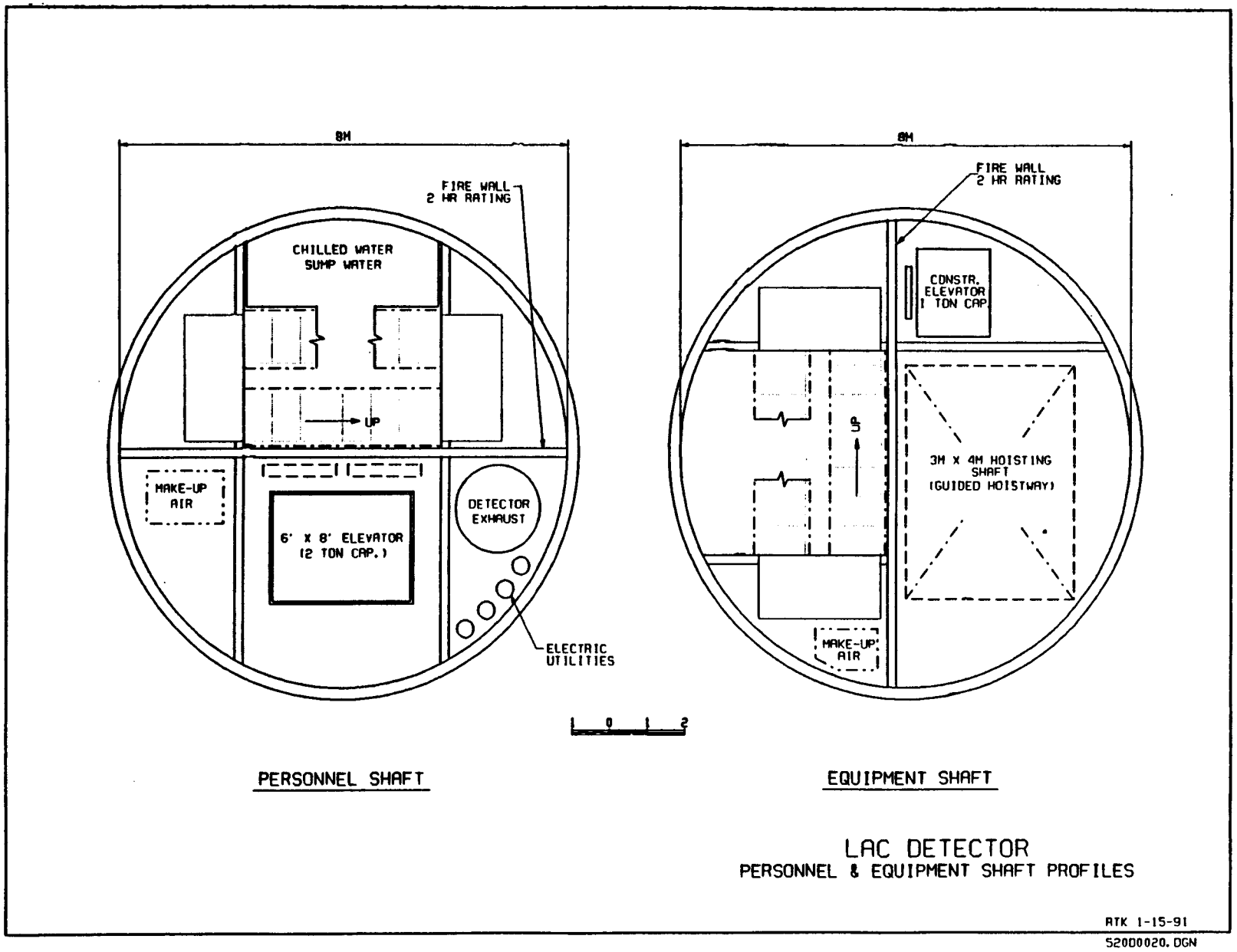

Figure 5.9. LAC Detector—Personnel and Equipment Shaft Profiles.

construction. As shown in Figure 5.9, this 8-m-diameter shaft and the connecting tunnel house the second fire escape stairwell and egress route. The personnel shaft contains the passenger/light freight elevator connecting the operations center on the surface to the main hall floor, the ductwork for the hall ventilation system, and the piping and power supply for the conventional hall services, such as lighting, power outlets, cranes, and sumps.

The cable shaft is 3 m in diameter and is located approximately 15 m from the west wall of the hall in line with the center of the detector. This shaft will carry all signal cables from the hall to the data acquisition and control rooms of the operations center on the surface. As shown in Figure 5.10, the shaft is equipped with 60 cm × 15 cm (24 in. × 6 in.) and 90 cm × 15 cm (36 in. × 6 in.) vertical cable trays and a 1.5-m-diameter spiral staircase to provide access to the cables. The cable trays are arranged to be within arm's reach from the staircase. The bottom of the cable shaft is at the operating floor level of the hall; however, additional cable passages from the shaft to the floors supporting the electronics cabinets are also provided.

The utility shaft, also 3 m in diameter, is located at least 9 m away from the west wall of the hall to bypass the hall roof foundation. The location of this shaft is coordinated with the layout of the surface facilities. The bottom of the shaft is at the detector support floor level; additional access to the top equipment floor is also provided. As shown in Figure 5.10, the utility shaft will have several compartments for the 400 Hz, 60 Hz, and DC power lines, the tracking chamber gasses and helium and nitrogen gasses, and the cryogenics and safety systems. Also provided are a 1.5-m-diameter spiral staircase with frequent landings and a 250-kg-capacity dumbwaiter to carry maintenance tools and equipment for servicing these utilities.

5.3 Liquid Argon Calorimeter Detector Assembly

5.3.1 Muon Steel Barrel Assembly

The configuration and construction of the octagonal muon steel barrel is shown in Figure 5.11, and some general specifications are listed in Table 5.4.

Table 5.4. Mechanical Specification for LAC Detector Muon Toroids.

Thickness of steel at 90°	1.5 m
Magnetic field	1.8 T
Maximum allowed gap in steel	3 mm
Minimum fraction of steel along any radial path	98 %
Thickness of steel in endcaps parallel to beam	4.0 m

The barrel steel will be assembled from 1500 mm (59 in.)-wide, trapezoid-shaped plates as shown in Figure 5.12. The plates are arranged to lie in the X–Y plane, parallel to the flux lines. The plate thickness is 190 mm (7.5 in.), except for the three 380 mm (15 in.)-thick plates centered

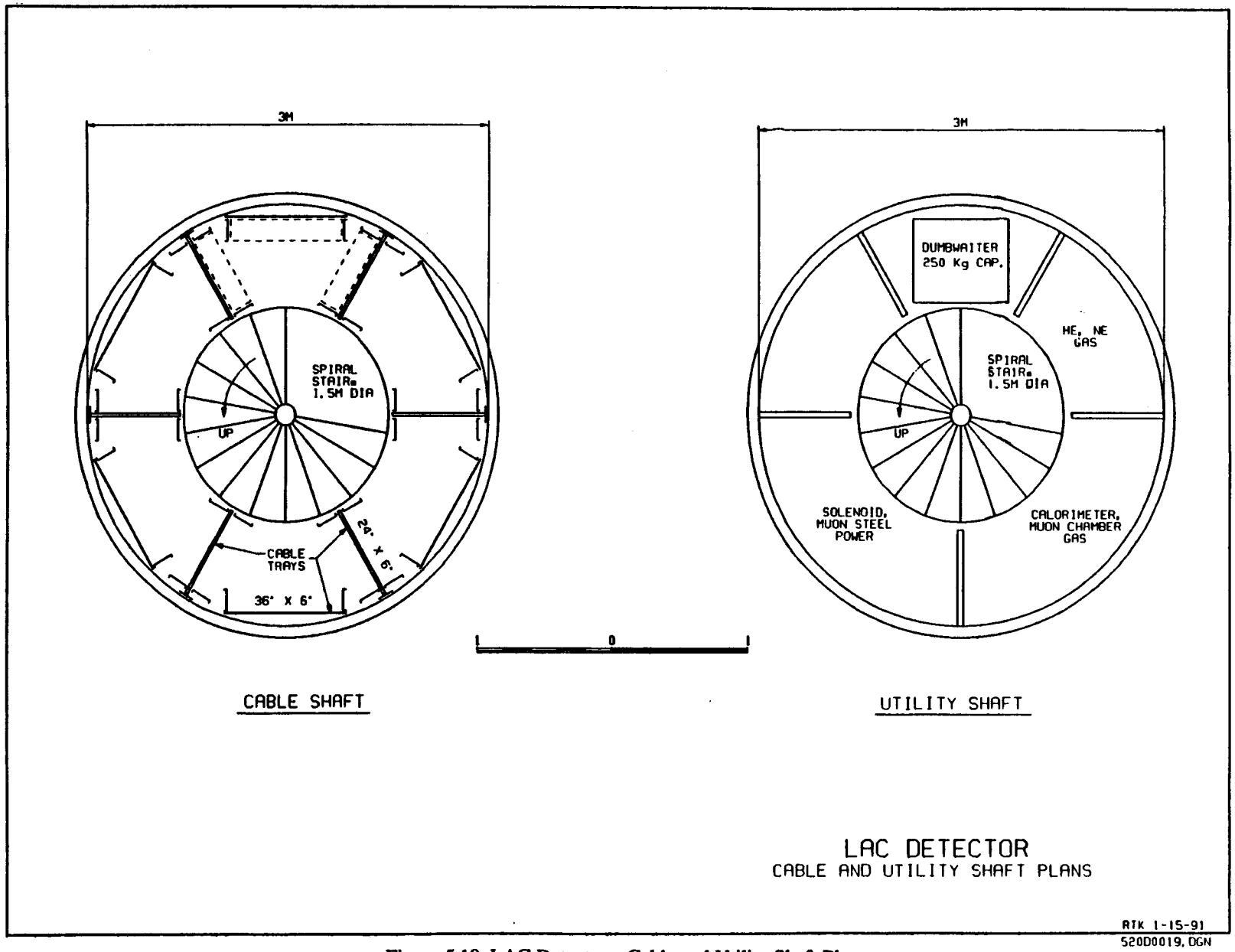

Figure 5.10. LAC Detector—Cable and Utility Shaft Plans.

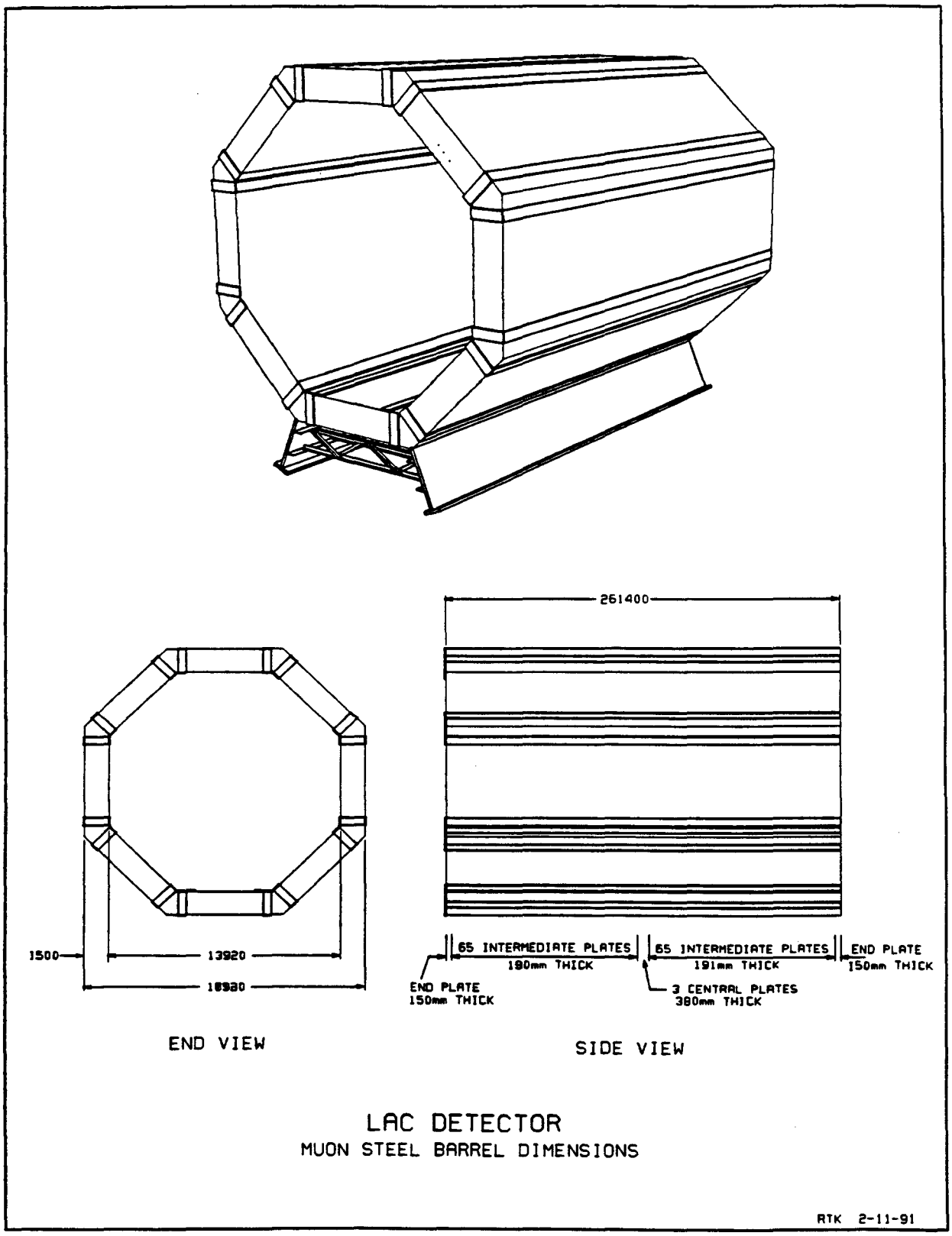

Figure 5.11. LAC Detector—Muon Steel Barrel Dimensions.

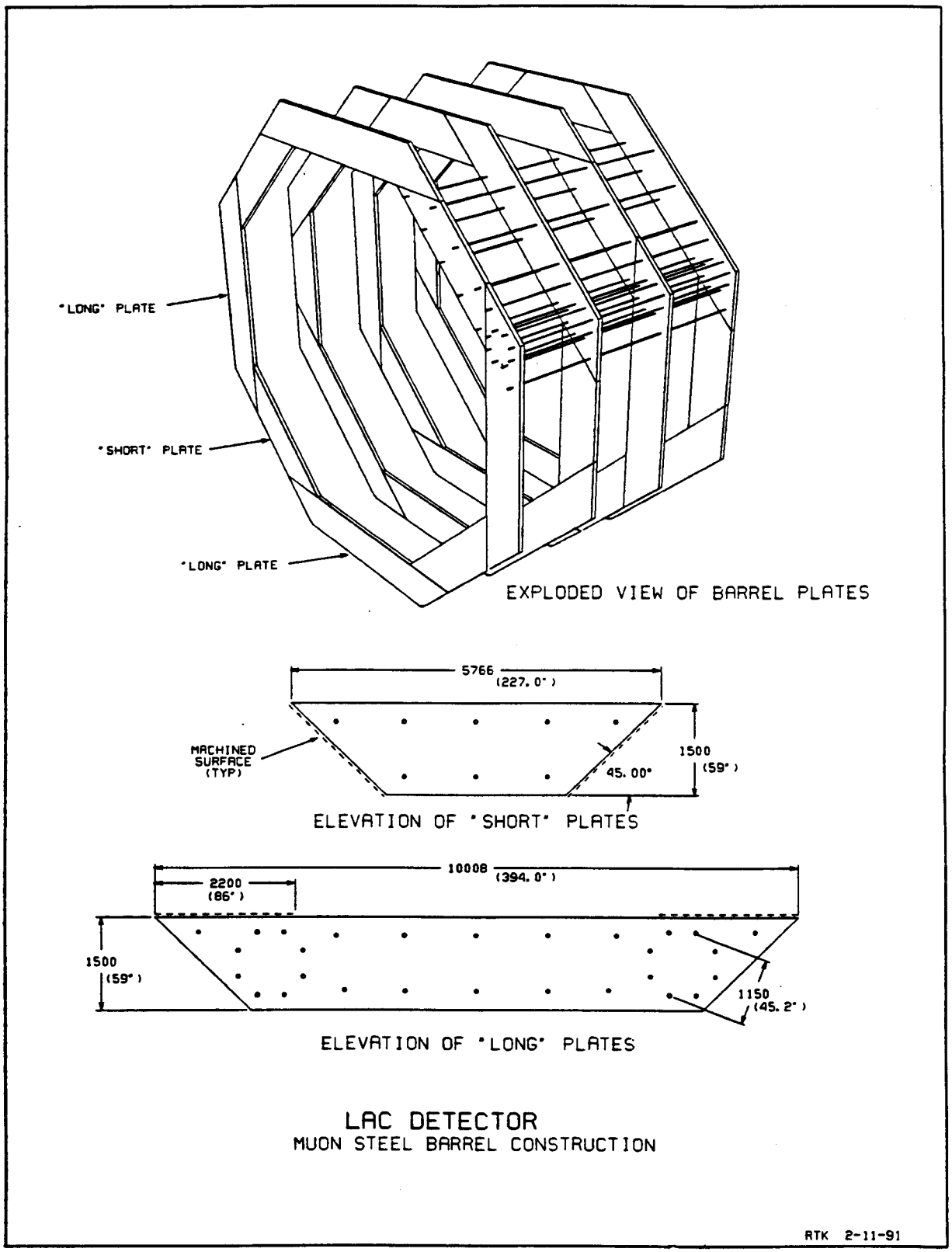

Figure 5.12. LAC Detector—Muon Steel Barrel Construction.

at the interaction point, and a 150-mm (6.0 in.)-thick plate at each end of the barrel. The reason for the three thick plates at the interaction point is to meet the 98% minimum solid material ray penetration criteria. As shown in Figure 5.11, a total of 135 layers make up the 26,140 mm length of the barrel.

Except for the three 380-mm (15 in.)-thick central layers, the plates are ordered from the steel mills in one piece. Because the length of the 380 mm plates exceeds the maximum rolling length available from U.S. mills, these plates must be spliced by partial penetration butt-welding.

The plates may be gas cut from standard rolling widths; however, the sloping edge of the "short" plates, and about 2200 mm (86 in.) long area at each end of the "long" plates are milled for bearing on each other, as shown in Figure 5.12. Except for two grooves for the radial support plates of the barrel, no machining is required.

The strength of the barrel is provided by the overlapping long plates tied together by eight 38-mm (1.5 in.)-diameter high-strength bolts located on a 1150-mm (40 in.)-diameter bolt circle, as shown in the exploded view in Figure 5.12. These bolts provide a slip-critical connection between the long plates, thereby preventing rotation at the corners of the octagonal-shaped barrel. (Slip-critical joints are defined by the codes as joints in which slip would be detrimental to the serviceability of the detector.) Our finite element calculations indicate that the deflection at the top of the barrel is 3 mm (1/8 in.) due to self weight. However, as described below, the gravitational load can be compensated by appropriate adjustment of the erection frame before tightening of the corner bolts. The bolts away from the corners are used to pull the plates together so that the gap between the plates does not exceed 3 mm anywhere in the barrel, and that the criterion of 98% minimum solid material ray penetration is achieved.

We have also investigated the feasibility of using thicker plates, plates in different orientation and arrangement, and plates secured with high-strength bolts tapped into the muon steel. Using thicker plates for the barrel would reduce the number of plates to be installed; however, this is not considered an advantage since the plates may be handled in groups of four or more during shipping and installation. Thicker plates would require larger diameter and/or more bolts in order to pull the plates together and to provide the required strength at the corners of the barrel. Thicker plates cost more, and the machining and general handling costs are also higher.

Plates arranged with mitered ends pointing toward the interaction point would not meet the ray penetration criterion and would require bolts installed in machined pockets and tapped into the muon steel. Longitudinal bolts or plug welds to pull the plates together would also be required. A brief investigation of tapping high-strength bolts (ASTM A490 or Grade 8) into the soft muon steel (Fy=28 ksi) was also made. Theoretically, the length of thread engagement should be about four times the bolt diameter; however, because of shear lag, there will be some yielding of the first few threads of the hole. Normally the strength of the nut (or tapped material) is equal to or higher than

the bolt strength, but in this case the yield strength of the bolt is about four times that of the tapped material. Consultations with experts in this field indicate that this type of connection is very unusual and should be tested for pull-out strength in a laboratory.

As for a plate arrangement where the moment and shear force are transferred through the machined joints by compression on the steel and combined tension and shear of the bolt, we have found that such a joint will have to be machined to a very close angular tolerance. This is because after tightening of bolts, the joint will close tight, and the angular deviation of the machined surfaces from the true will determine the actual shape of the barrel after assembly. Any errors in machining will be hard to correct in the field, so all components of this type of design should be preassembled in the fabrication shop.

The plates of the barrel are drilled with oversized holes to facilitate installation of the longitudinal bolts and to permit adjustments of the barrel shape during assembly. To reduce bolt length, the plates will be pulled together in groups of eight or more The outermost plates (of each group) will have recessed holes on both sides to receive the bolts from the adjacent group of plates. The length of the plates depends on their position in the barrel. The number of each plate type required for the barrel is shown in Table 5.5.

Table 5.5. Plate Count for Muon Barrel Steel Toroid.

Plate Location	Length ¥ Thickness	Number Required	Weight of Each Plate
Central Short Plates	5766 × 380 mm	12	19.09 tonnes
Central Long Plates	10008 × 380 mm	12	38.06 tonnes
Interm. Short Plates	5766 × 190 mm	520	9.54 tonnes
Interm. Long Plates	10008 × 190 mm	520	19.03 tonnes
Short End Plates	5766 × 150 mm	8	7.53 tonnes
Long End Plates	10008 × 150 mm	8	15.03 tonnes

Note: All plates are 1500 mm wide. Length is the overall length of each plate.

To provide maximum chamber coverage the barrel muon steel is supported on two inclined longitudinal plates resting on the concrete floor, as shown in Figure 5.13. The plates are braced together at about 2 m longitudinal intervals to resist buckling and lateral forces on the barrel. As shown in Figure 5.6, the bracings are located between the two outer layers of muon chambers to avoid interference. The base of these supports is designed to facilitate vertical adjustment of the barrel elevation to compensate for the anticipated floor movements described in Section 5.2.3.

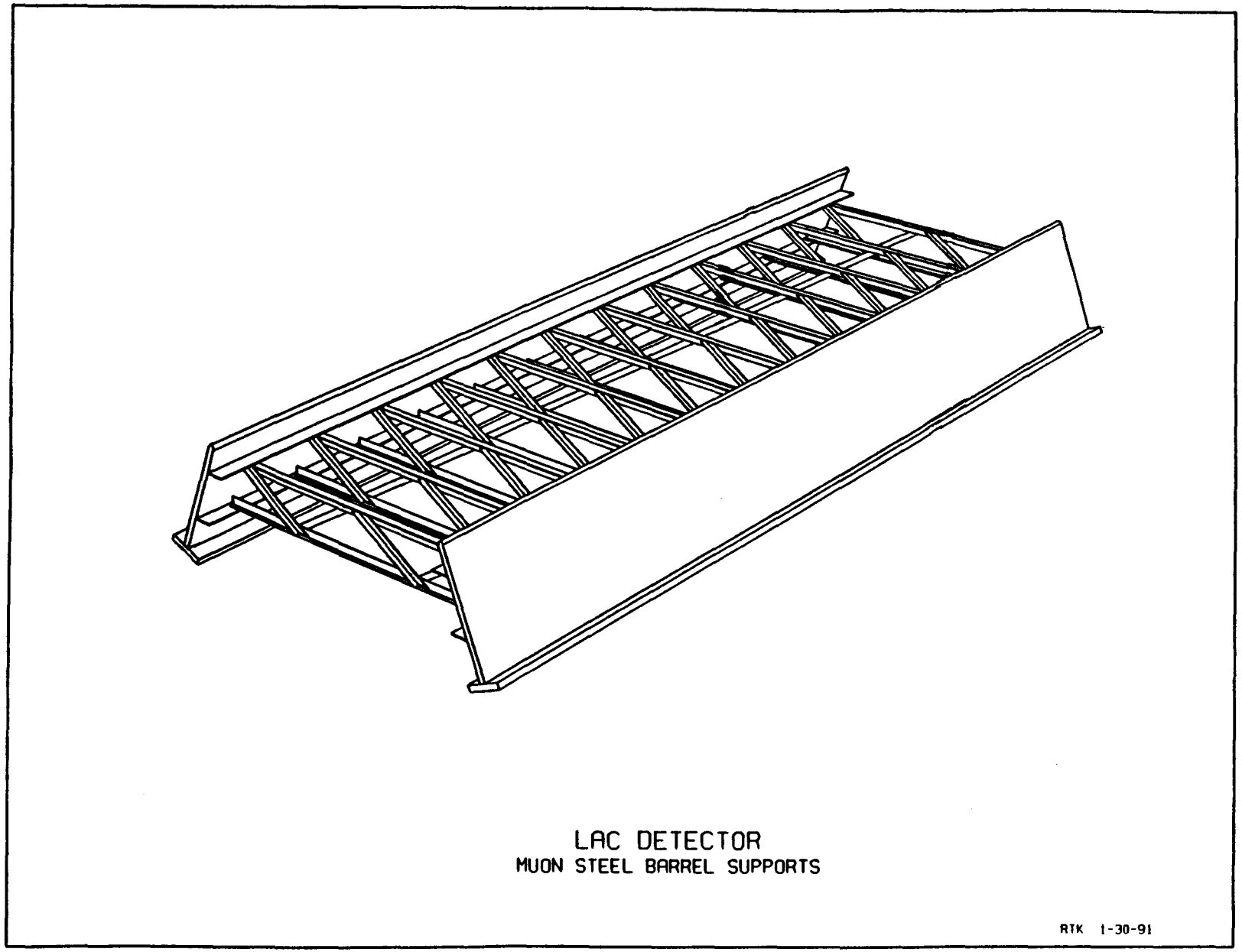

Figure 5.13. LAC Detector—Muon Steel Barrel Supports.

Prior to the muon steel barrel assembly, the two inclined plate supports of the barrel are installed. The muon steel erection rig and the temporary supports of the lower inclined plates of the barrel are also installed at this time. See Figures 5.14 and 5.15.

The barrel steel assembly proceeds as follows. The predrilled and painted steel plates are assembled into jigs on the surface and are lowered into the hall through the construction shaft by the yard crane in groups of four. From the construction shaft laydown area in the hall, the plates are moved to the muon steel staging area by winched carts. After final checkout, the plates are lifted into place by the hall crane in groups of four. One (or two—see Section 5.4.1) erection crews construct the barrel, beginning in the middle of the detector and working out toward opposite ends as follows.

Beginning with the bottom segment of the barrel, four long plates, separated temporarily by 200-mm-wide wood spacers, are placed on the supports. Next, the four inclined long plates are installed on both sides of the barrel, and finally the four short plates are placed between the long plates of the bottom three segments of the barrel. The above procedure is repeated until about 3 m of the bottom segments of the barrel is assembled (Figure 5.16). Note that the number of plates to be lifted by the hall crane at one time does not affect the assembly procedures and may be varied by the assembly contractor.

After the above steps are completed, temporary tracks are installed on the bottom plates, and the assembly frame shown in Figure 5.17 is rolled onto the bottom segment of the barrel. The assembly frame is equipped with adjustable longitudinal beams to support the upper segments of the barrel and to align the plates before tightening of the longitudinal bolts.

In the next step, using the procedures described for the bottom segments, a 3-m length of the vertical and the top three segments of the barrel plates are assembled (Figure 5.18).

After all plates in a 3-m-long portion of the barrel have been installed, the plates are pulled together by hydraulic jacks. The longitudinal bolts are installed next, and after the final alignment check of the barrel is completed, these bolts are tightened to the required tension in a predetermined sequence. The bolt tension is checked with an ultrasonic device prior to assembly of the next group of plates.

The proposed plate arrangement and assembly procedures permit full adjustment of the barrel shape to the required tolerances—including compensations for dead load deflection—without shimming or grinding to correct for fabrication errors.

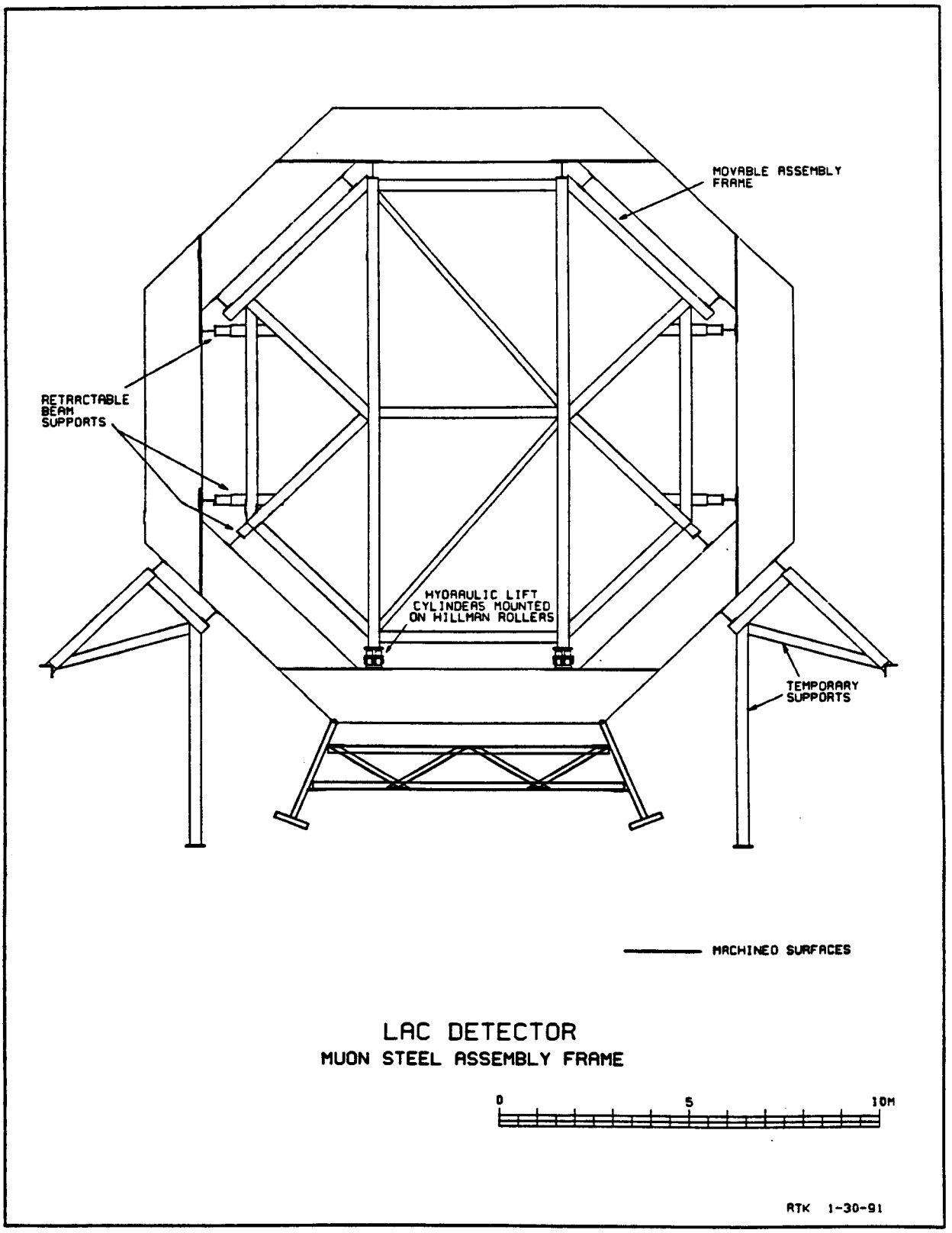

Figure 5.14. LAC Detector—Muon Steel Assembly Frame.

521m9.h11

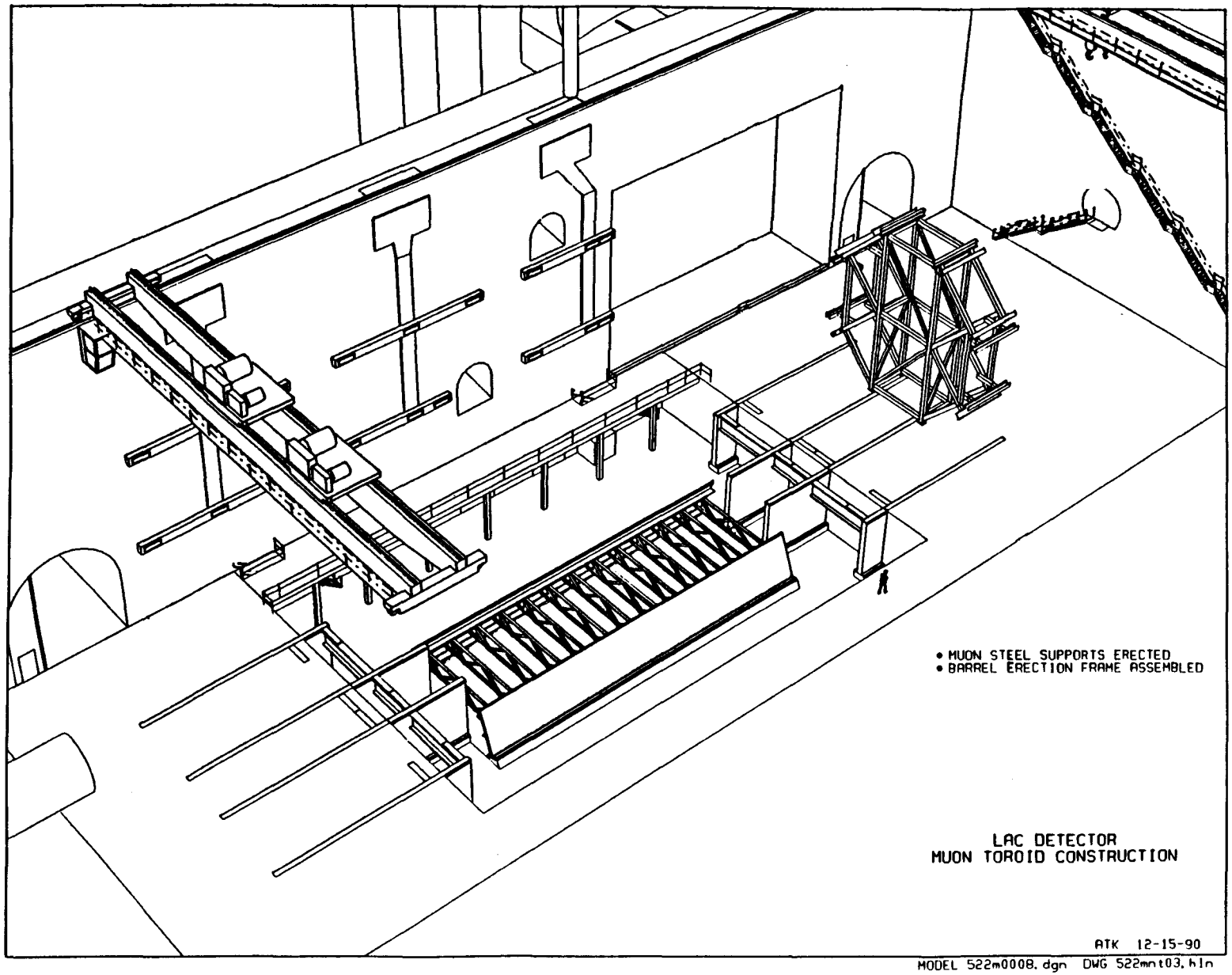

Figure 5.15. LAC Detector—Muon Toroid Construction.

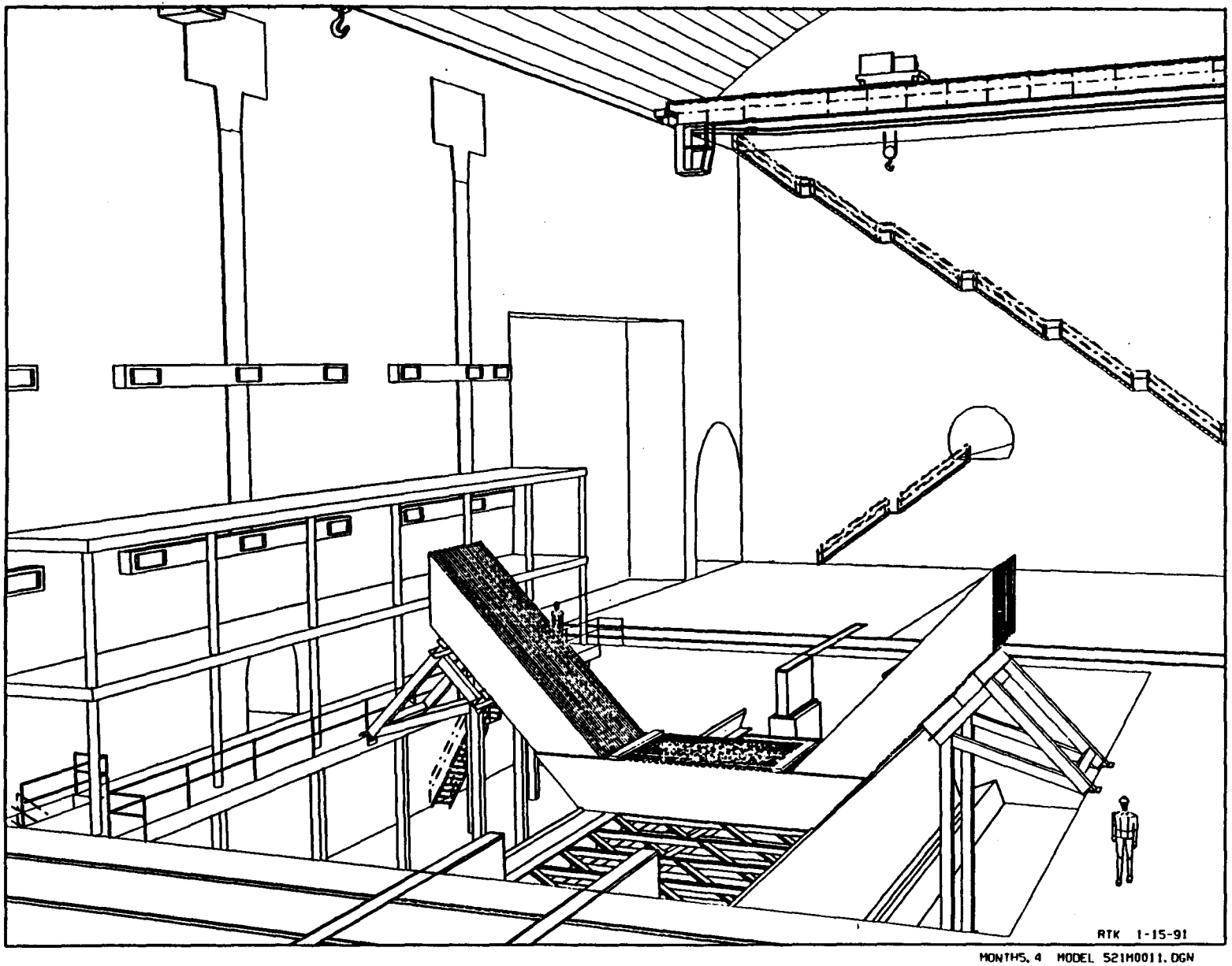

Figure 5.16. LAC Detector—Muon Steel Barrel Assembly (Step 1).

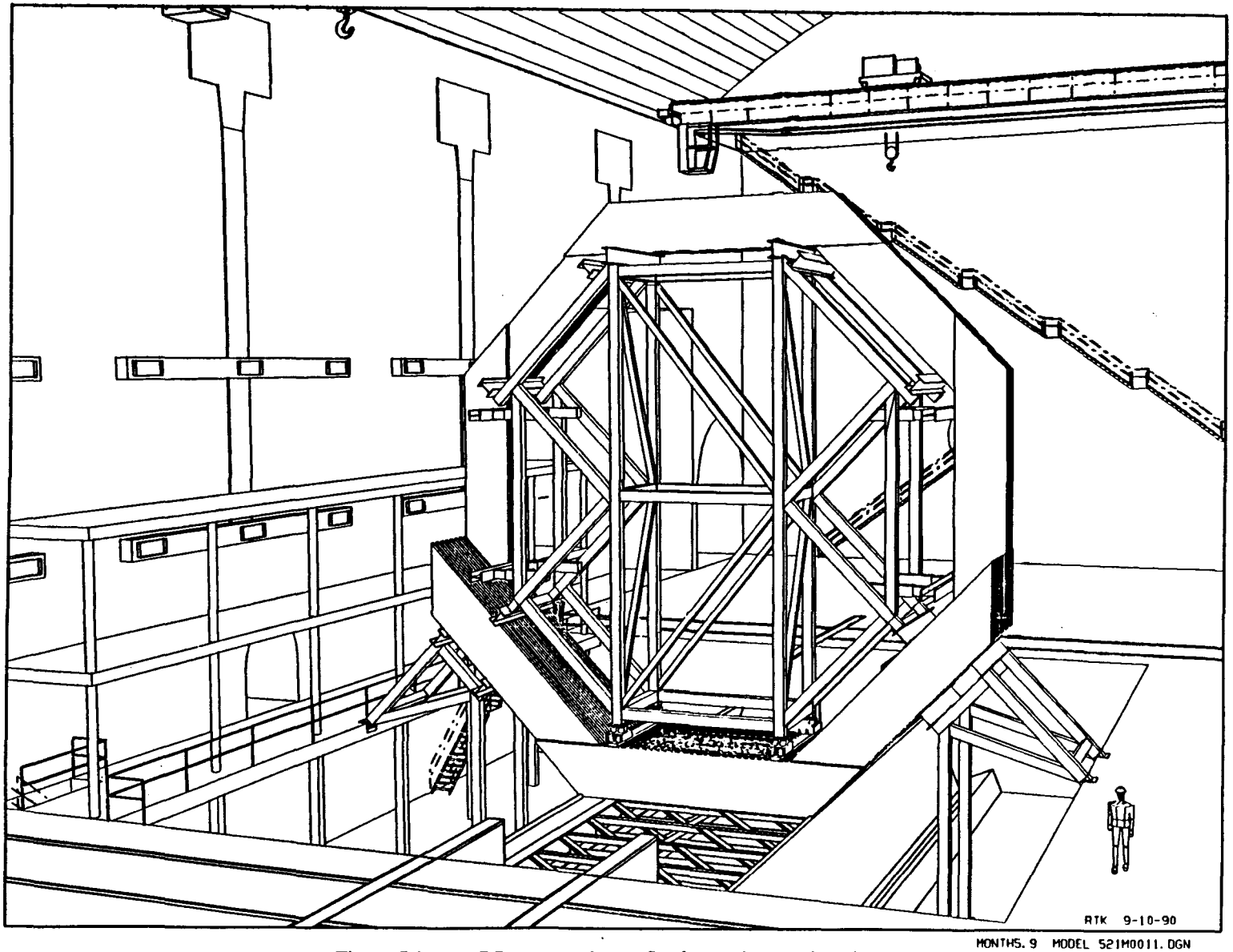

Figure 5.17. LAC Detector—Muon Steel Barrel Assembly (Step 2).

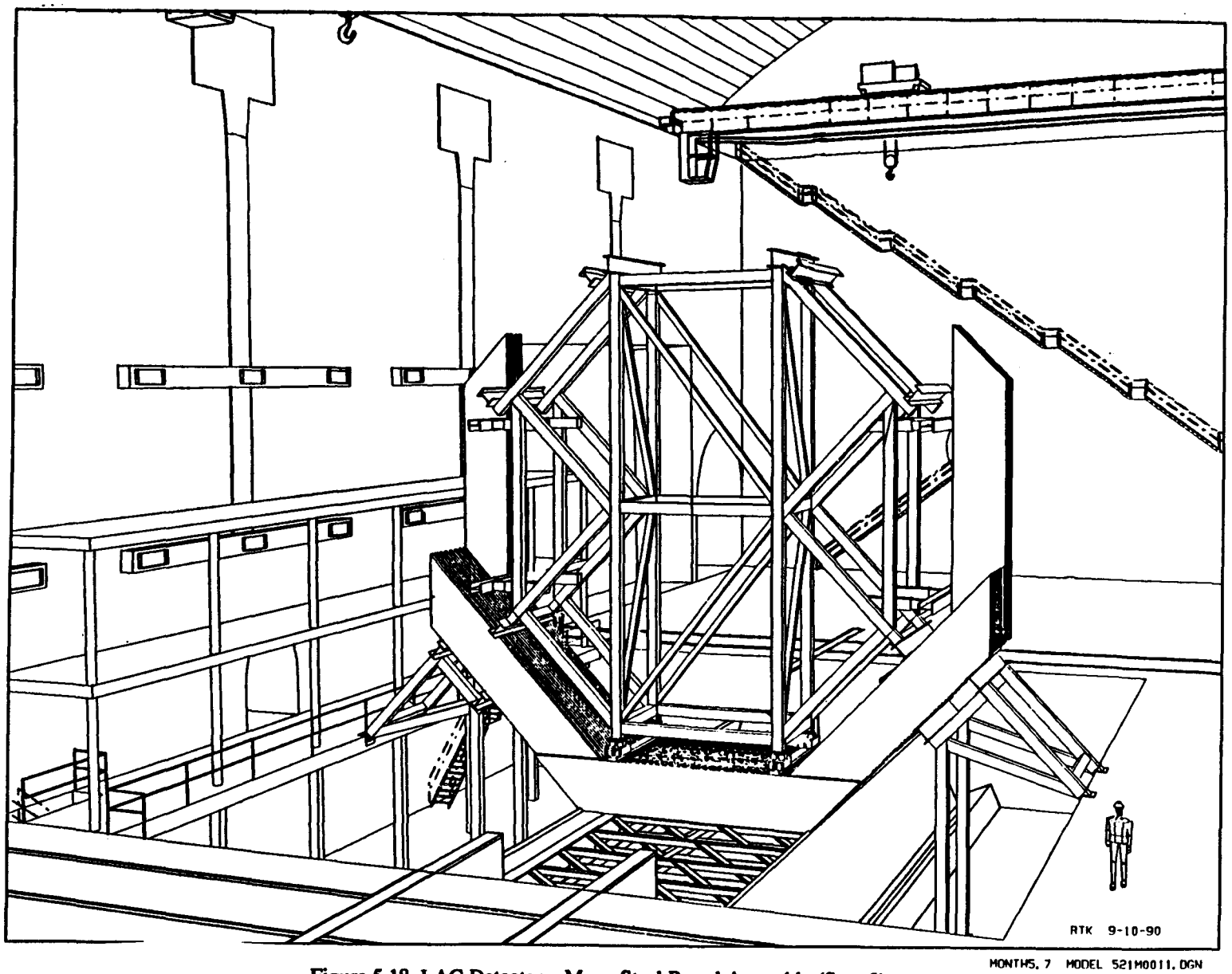

Figure 5.18. LAC Detector—Muon Steel Barrel Assembly (Step 3).

The magnetic field is powered by 16 coils symmetrically located at each corner of the octagonal muon steel. After construction of the barrel steel is complete, 32 "half-coil" packages are lowered into the hall via the construction shaft. These half-coils are pre-assembled modules approximately 26 m long, slightly longer than the full length of the barrel. Each half-coil on the outside of the steel is mechanically and electrically joined at the north and south ends of the barrel toroid to its mate on the inside surface of the steel. Water circuits are completed using flexible tubing.

5.3.2 Muon Endcap Toroid Construction

The muon endcap toroids assembly includes the muon steel toroids, the absorber, and several layers of muon chambers, as shown in Figure 5.19. The entire assembly is supported on a set of Hillman rollers to permit movement when opening the detector for inspection or repair. The assembly consists of two halves bolted together so that they can be separated when the endcap is moved out of the barrel. Before the endcap can be separated, the auxiliary steel framing shown in Figure 5.20 must be bolted to the toroids.

As shown in Figure 5.21, the muon steel toroids are assembled with two alternating shapes of 200-mm (7.9 in.)-thick plates in ten layers. The selected combination of plate size and thickness is available from most domestic mills as a single piece. Larger or thicker plates would require butt welding, which is costly and could be difficult when small flatness tolerances must be maintained. Each layer of the toroid plates is offset by 11.25° to provide an overlap of the wedge-shaped plates. The seven high-strength bolts in this overlap will provide the required strength to resist the gravity and magnetic forces acting on the toroid.

A vertical jig frame, as shown in Figure 5.22, is used to support and align the plates during assembly. The first set of plates is bolted temporarily to the jig while the remaining plates are clamped and/or bolted to the first set and to the core of the jig. During assembly, the bottom plates are supported on temporary steel sleepers that have been shimmed to provide a perfectly horizontal surface at the correct height above the floor. After all ten layers of the muon steel toroid plates are assembled, the permanent high-strength bolts are installed through the oversized holes; they are fully tightened after final alignment of the plates. The second set toroid is assembled using a similar procedure.

Once a toroid is half completed, steel outriggers designed to support the toroid are installed. In the next step the hydraulic jacks and Hillman rollers are installed so that the hydraulic cylinders can lift the whole assembly for moving. The completed half-toroid is shown in Figure 5.23. There is a 850-mm gap between the two toroids to allow for the coils and experimental equipment.

Figure 5.20 shows the conical absorbers assembled from eight cast steel sections on temporary saddles The eight sections are held together by bolting them to heavy plate rings at each end. After assembly the absorbers are rolled into the end toroid and fastened by steel gusset plates to form a rigid unit.

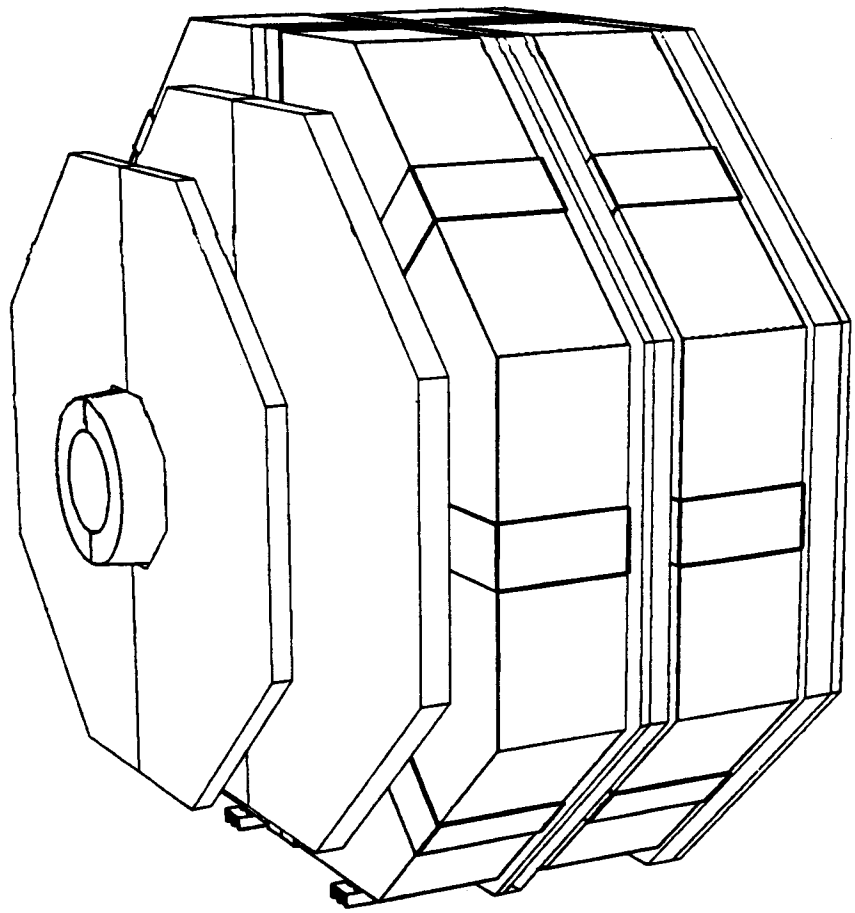

Figure 5.19. LAC Detector—Muon Toroid Assembly.

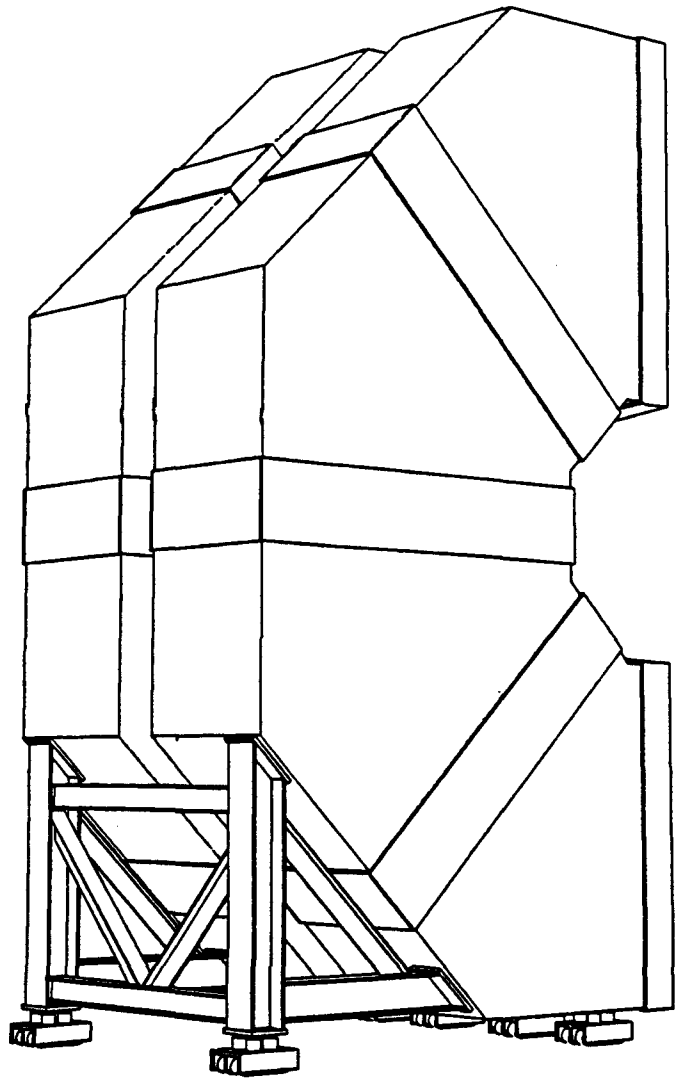

LAC DETECTOR

MUON TOROID
FITTED WITH DISASSEMBLY FRAME

RTK 2-11-91

522m7.h11

Figure 5.20. LAC Detector—Muon Toroid Assembly (Open for Minor Repair).

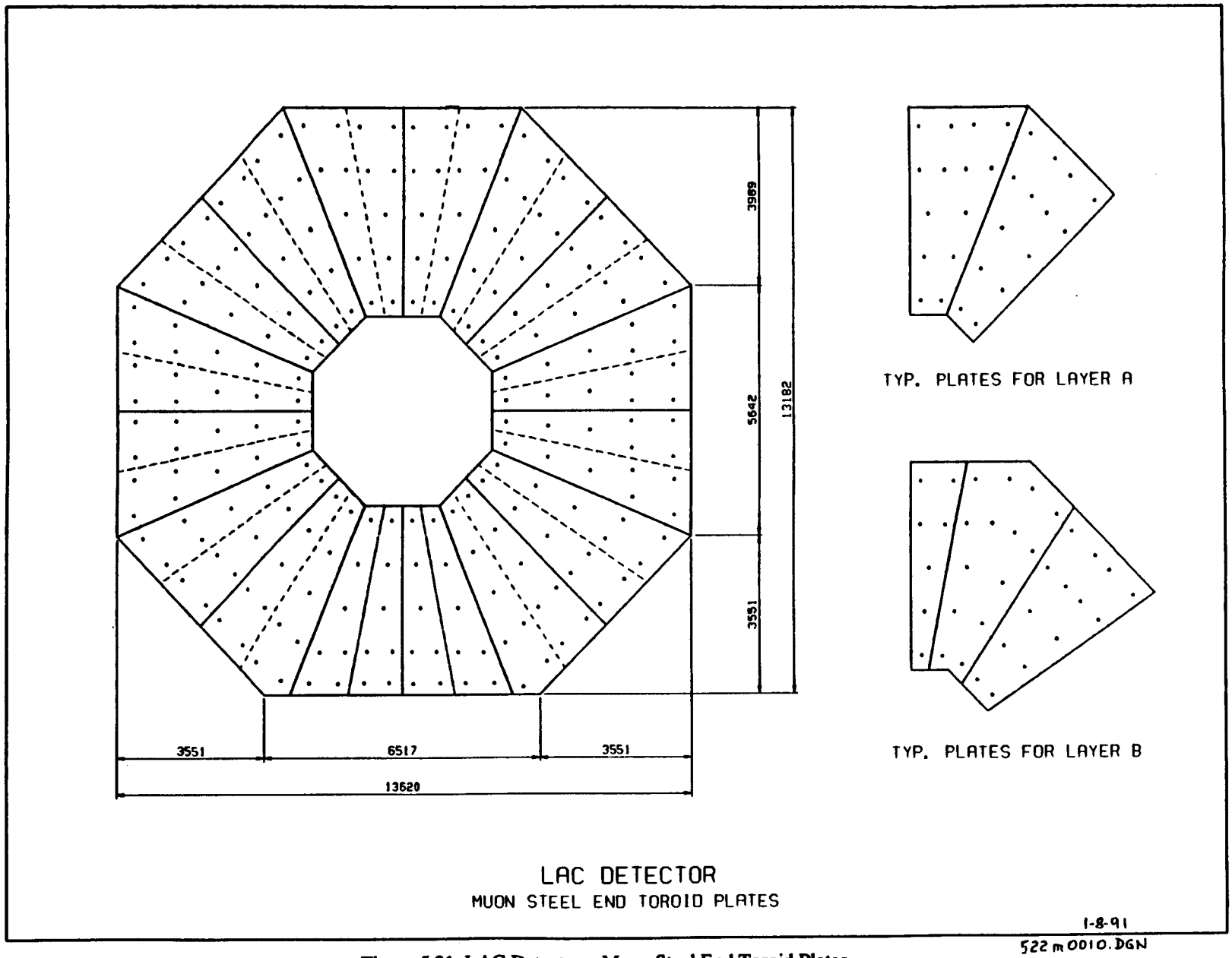

Figure 5.21. LAC Detector—Muon Steel End Toroid Plates.

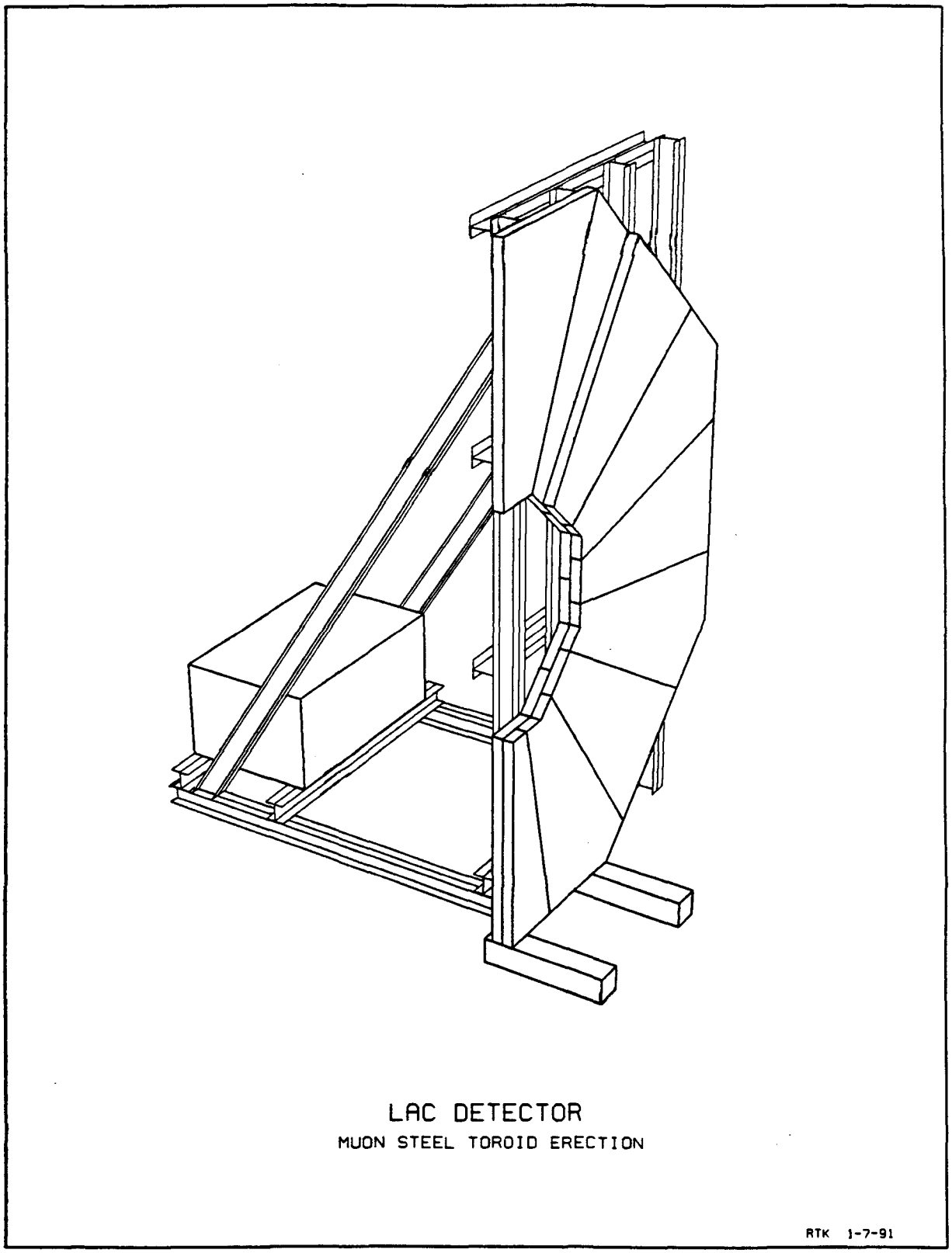

Figure 5.22. LAC Detector—Muon Steel Toroid Erection.

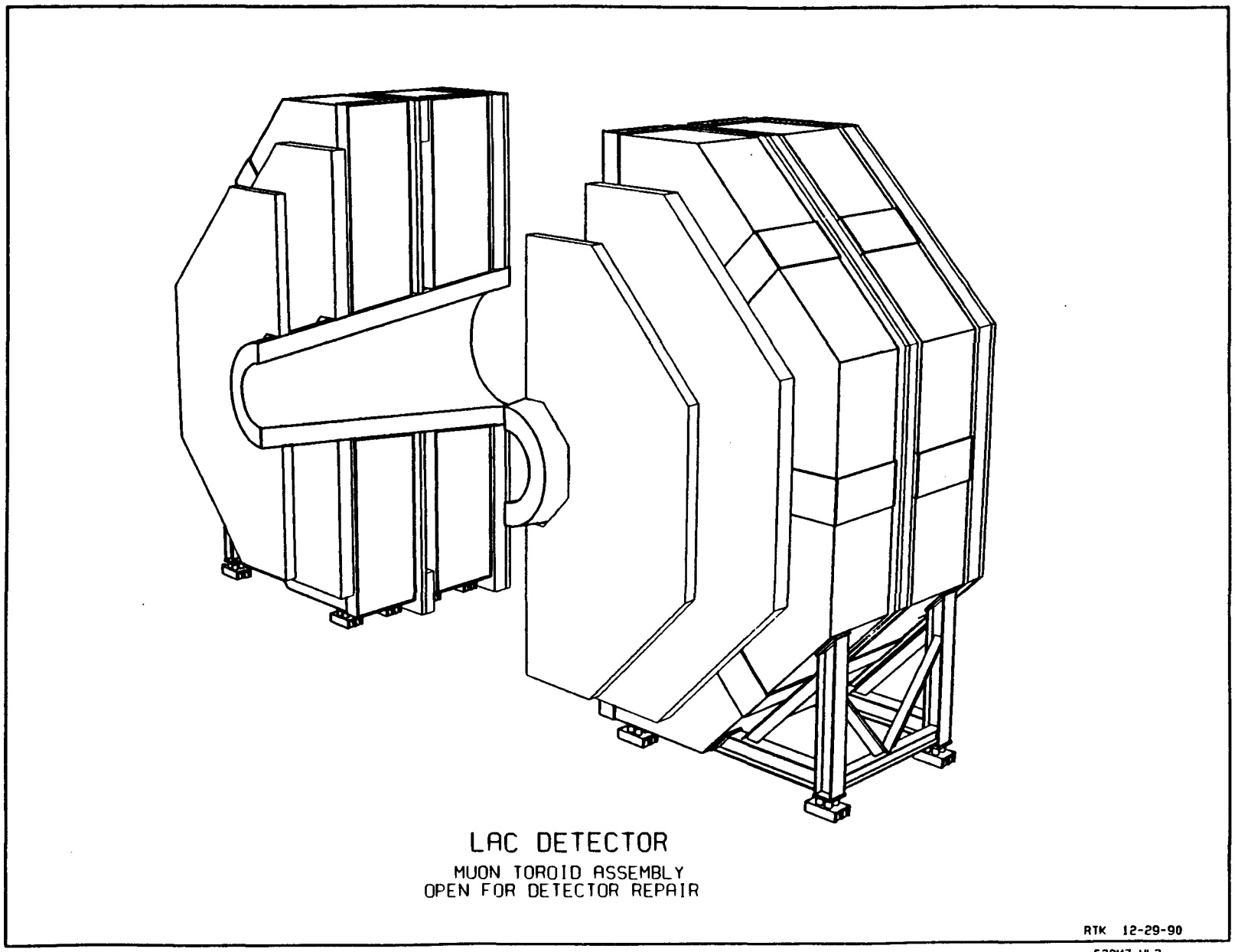

Figure 5.23. LAC Detector—Muon Toroid Half (Fitted with Disassembly Frame and Rollers).

5.3.3 Calorimeter Assembly

The calorimeter for the LAC detector is divided into three components: the barrel calorimeter and two endcaps. For this study, it is assumed that the barrel calorimeter is built in the hall, taking advantage of the hall space and cranes available there. It is also assumed that the endcap calorimeters are built on the surface because of schedule and space availability problems in the hall.

In this section, we briefly describe the assembly method for the barrel calorimeter. Assembly of the endcap calorimeters follows similar steps and is not described.

The barrel calorimeter consists of a liquid argon vessel inside a vacuum insulation vessel. The liquid argon vessel is separated into spaces that contain the active modules of the calorimeter. The liquid argon vessel is supported on four pairs of legs which are located on the same centerline as structural disks for reasons of strength. The vessel is closed on both ends by convex covers. (See the exploded view in Figure 5.24.) The barrel calorimeter is surrounded by flux return iron.

The liquid argon vessel is first lowered to the hall floor and mounted on a special support frame. The support frame is provided with Teflon-coated guides so that the liquid argon vessel can move axially when necessary. On the hall floor the calorimeter modules are inserted into the liquid argon vessel by a specially designed tool (Figure 5.25). Each module is electrically checked after installation and its cables properly routed to cryogenic feed-throughs.

After all the modules have been installed into the liquid argon vessel, it is sealed with the end covers and vacuum leak checked. Superinsulation is then applied to the outside of the liquid argon vessel. The vacuum insulating vessel is now lowered to the hall floor. The vacuum vessel is provided with guides similar to those of the liquid argon vessel support frame so that the liquid argon vessel can slide axially in and out of it. The frames of the two vessels are butted together and the liquid argon vessel is slid into the vacuum vessel by means of horizontal hydraulic jacks fastened to the liquid argon vessel support (Figure 5.26). Numerous electrical connections to the cryogenic feed-throughs are now made. The vacuum vessel is closed and the vacuum leak checked.

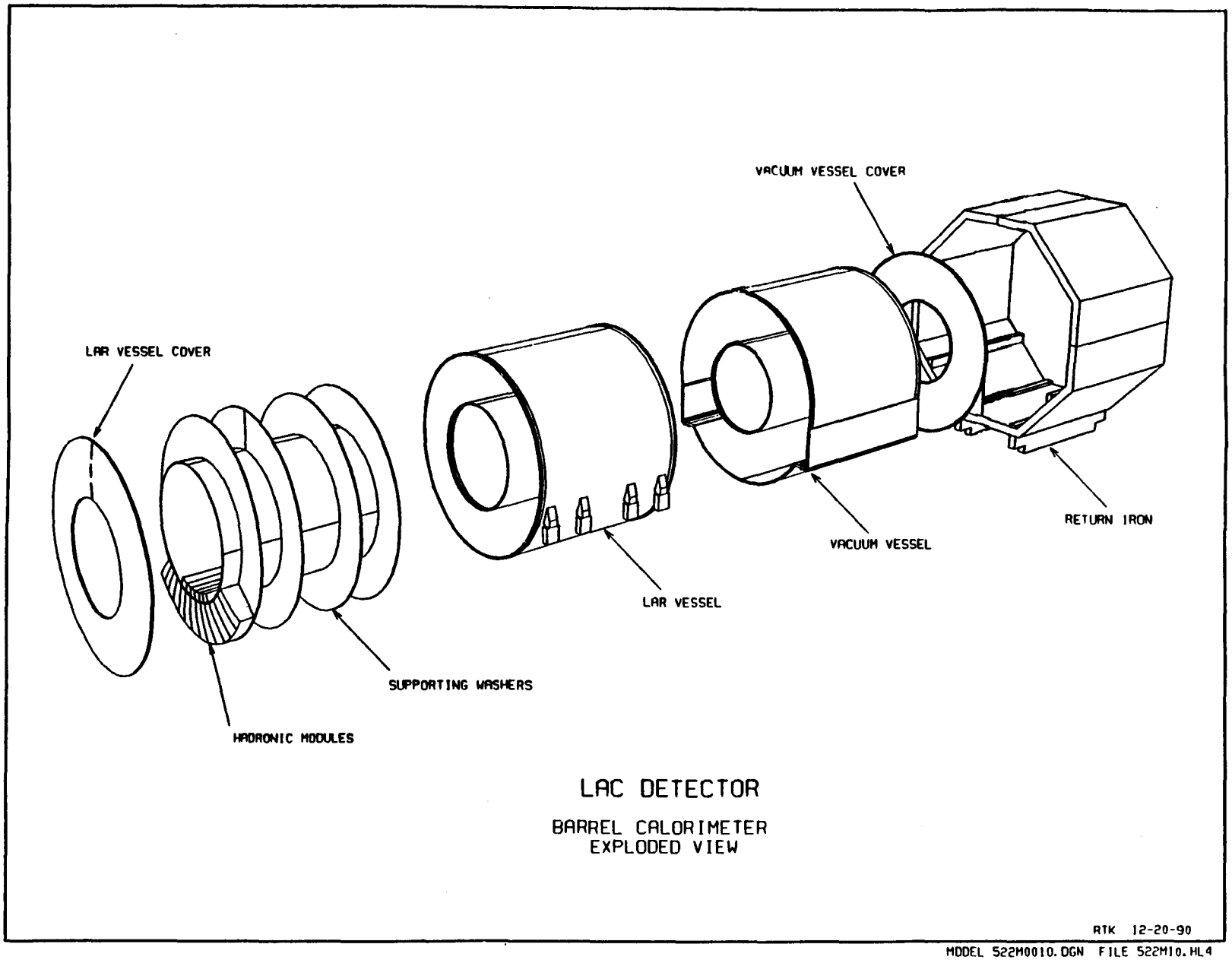

Figure 5.24. LAC Detector—Barrel Calorimeter (Exploded View).

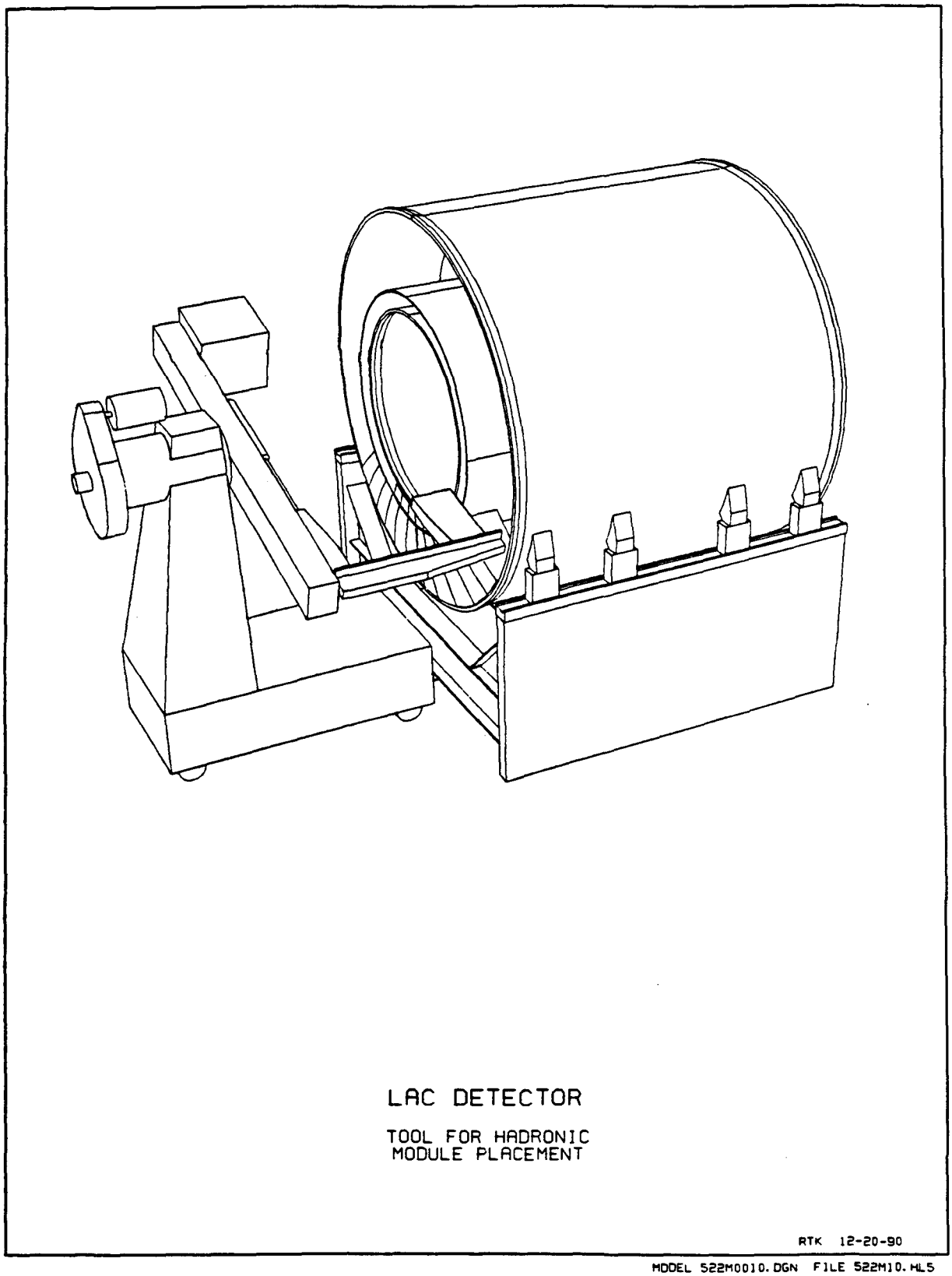

Figure 5.25. LAC Detector—Tool for Hadronic Module Placement.

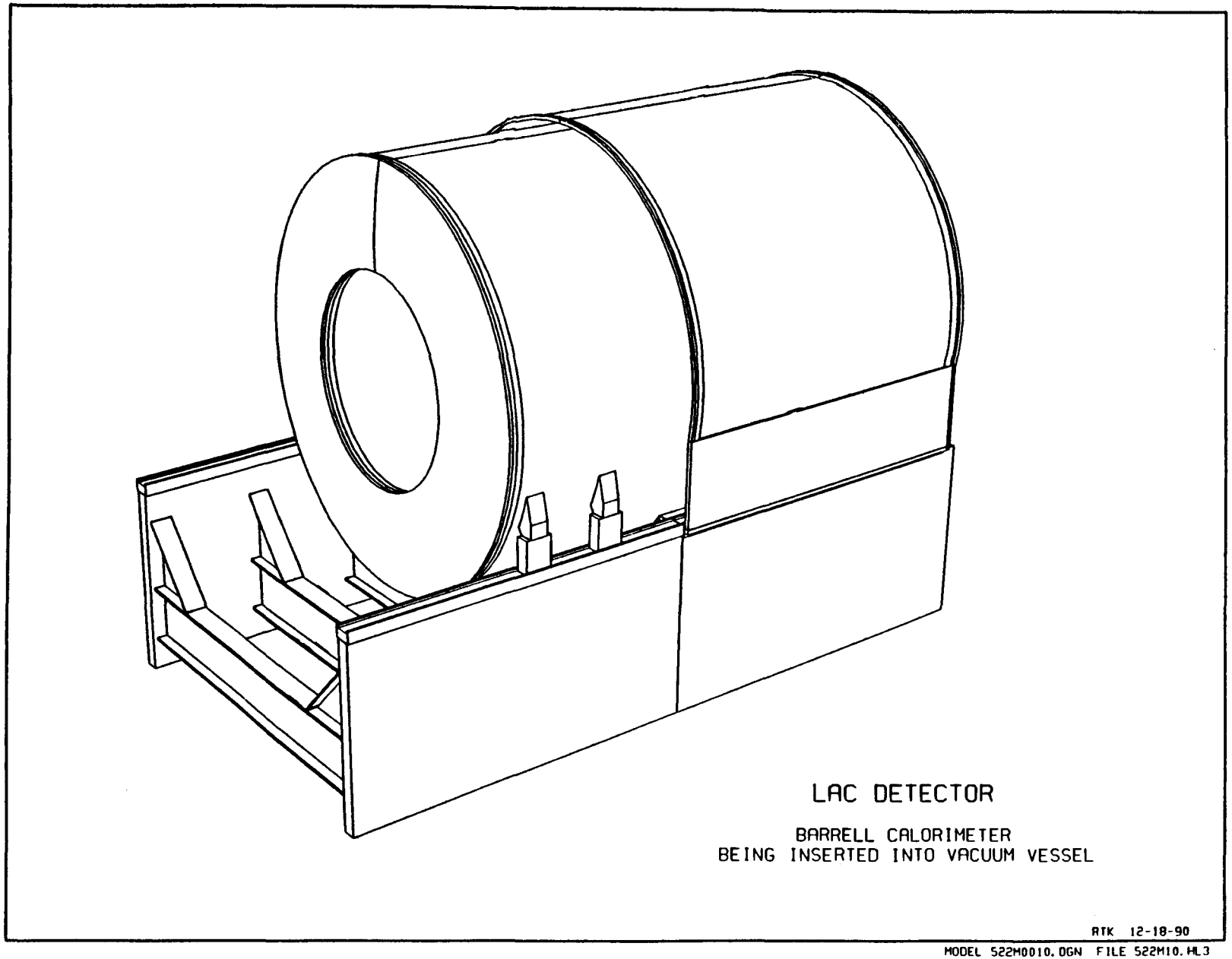

Figure 5.26. LAC Detector—Barrel Calorimeter Being Inserted into Vacuum Vessel.

The flux return steel is fabricated during the calorimeter assembly. The return steel again is provided with Teflon-coated guides for the vacuum vessel to slide on. A method of fabricating this component has not been developed in this report, nor has proper stress been analyzed. Preliminary calculations indicate that with the calorimeter fully loaded on the return iron supports, there will be a significant vertical deflection, measured at the guide surface, which will have to be compensated for in the fabrication. The return steel is transported to its destination in the muon steel barrel by Hillman rollers.

Once the return steel is in place, the calorimeter is transported—supported by Hillman rollers—until the support frame butts against the muon steel. At this point two possibilities exist for transporting the barrel calorimeter from its support frame to the return iron: 1) a special frame and guides is designed to bridge the gap from the support to return iron, and 2) the return iron is moved to the edge of the muon steel to receive the calorimeter and is then rolled back into position by Hillman rollers. These alternatives should be engineered and evaluated.

The procedure for assembly of the endcap calorimeters is similar except that the endcap calorimeter and its return iron are moved as one component.

5.3.4 Muon Chambers

We assume that the muon chambers arrive in the hall as panels several meters on a side and ready to be installed. Support and alignment frames are attached to the muon steel to accept the panels. Transport of the panels is by hall crane. The problems of muon chamber support and alignment have been greatly simplified in this study and need to be addressed further.

5.3.5 Solenoidal Coil

The superconducting solenoidal coil arrives at the detector hall fully assembled and ready to be installed. It is assumed that the coil arrives at the hall mounted on a mandrel which is designed to support the coil during transportation to the site and installation. The coil is lowered into the hall via the construction shaft and is carried to the area previously used for calorimeter assembly by the overhead hall crane. Mounting of the coil on its temporary support trolleys and any other pre-installation work is done in this area. During coil installation, all muon steel work and calorimetry assembly will have been completed, leaving sufficient space available for coil work.

After unpacking and inspection, the coil is installed in the following steps:

1. The coil is first lifted by its mandrel onto the saddles of the temporary supports located at each end of the coil. These temporary supports will hold the coil on the beam line and are designed to roll on calorimeter tracks.

2. After the shipping mandrel is extended by bolting an approximately 12-m-long beam to one end, the coil is rolled into the barrel calorimeter until the end of the cantilever mandrel

extension has emerged from the calorimeter (Figure 5.27). A third movable support stand is bolted to the free end of the mandrel extension, and the middle temporary support stand is removed.

3. The coil is moved into the barrel calorimeter. After installation of the permanent support links to the calorimeter and removal of the shipping ties, the mandrel is rolled out from the coil.

4. Cryogenic and power connections are made.

5. Field mapping takes place after the coil has been cooled and the endcap calorimeters have been temporarily moved into their operating positions.

The superconducting solenoidal coil operates at a cryogenic temperature of 4.5 K by boiling liquid helium in the magnet and by using liquid nitrogen in a shield. The cryogenic valve box is located on top of the north end of the detector. Cryogenic pipes and electric power are connected to the magnet by an approximately 30-cm-diameter chimney. Figure 5.28 shows a schematic layout of the required cryogenic cooling system in the hall and at the surface. The cryogenic and vacuum equipment, such as local dewars and pumps, is located on the gallery at the side of the detector. A walkway from the gallery to the top of the detector is included to facilitate access to the cryogenic valve box.

5.3.6 Central Tracking Device

We assume that the central tracking unit, including the silicon tracking device, arrives at the hall fully assembled on a mandrel and ready to be installed. The central tracking device is lowered into the hall through the larger construction shaft and is carried to the calorimeter assembly area by a hall crane. This area is used for any necessary pre-installation work. After checkout, the tracking unit is installed using the temporary support stands of the coil, in a manner similar to the installation of the coil.

5.3.7 Beam Pipe

The beam pipe arrives at the hall in segments and is assembled on-site. The segments are lowered into the hall through the construction shaft and are either rolled to their installation sites on trolleys or carried by the hall crane. Any preparatory work on the beam pipe can be performed in any area adjacent to the barrel muon steel or in the barrel itself.

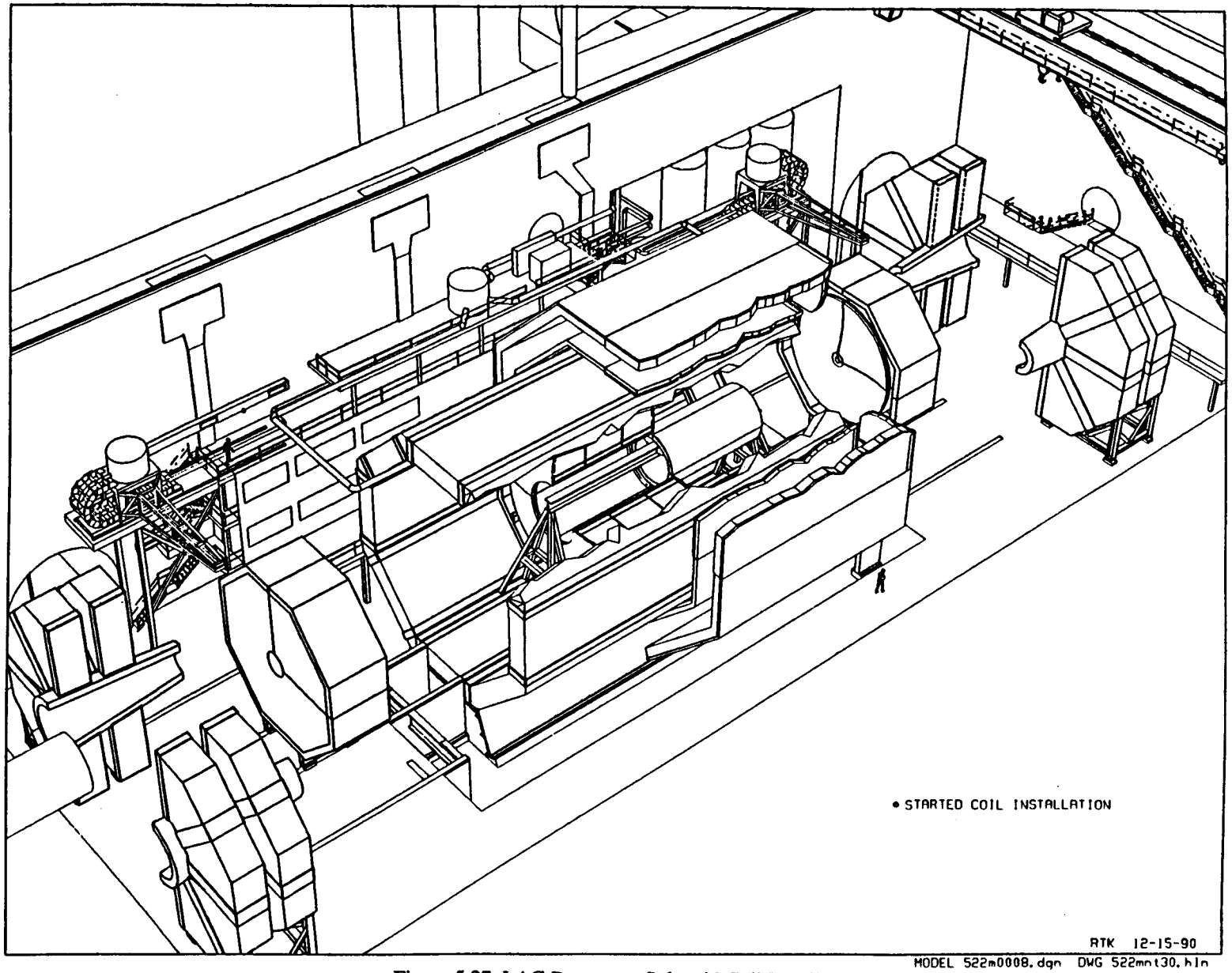

Figure 5.27. LAC Detector—Solenoid Coil Installation.

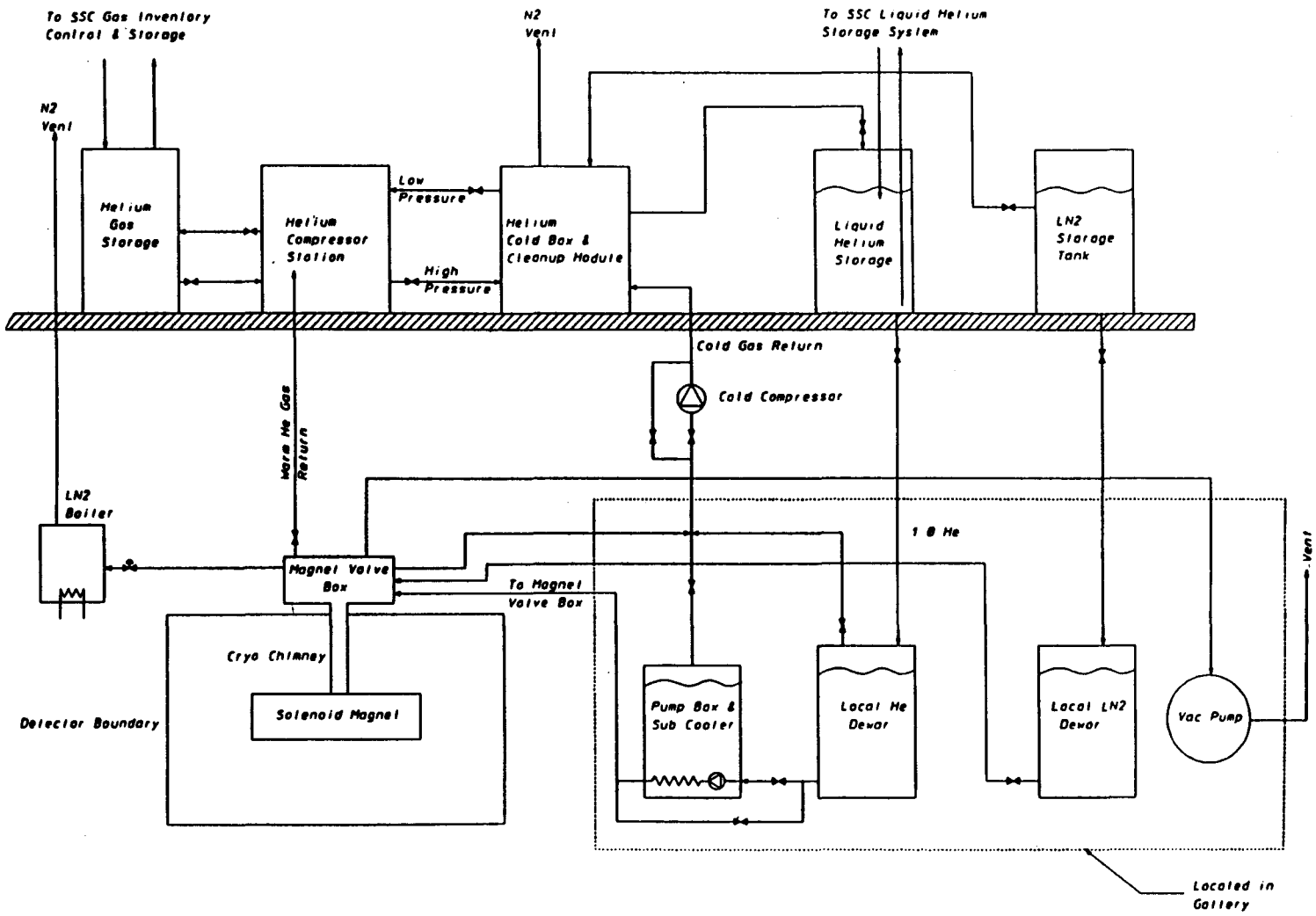

Figure 5.28. Solenoid Cryogenic System Schematic.

5.3.8 Forward Calorimeters

Each forward calorimeter consists of two separate halves, each half consisting of the calorimeter itself, part of the absorber cone, muon chambers, and a support structure. The support is mounted on Hillman rollers, and the muon chambers are bolted to the absorber shell. The Hillman rollers travel on machined steel tracks fastened to the hall floor. The calorimeter halves, together with the absorber and support structure, arrive preassembled at the surface and are lowered to the hall floor through the construction shaft. The muon chambers are added later. These items are shown in Figure 5.29.

The forward calorimeters rest on steel support members from the basement floor. These steel members are removable so that the lower barrel muon chambers can be installed or removed for repair.

5.3.9 Electronics/Triggering

We have not studied the assembly of the readout and triggering electronics necessary for this detector. We have provided space for the electronics and cables. The cables to the surface for the electronics and triggering are carried by the cable shaft.

5.3.10 Accelerator Components

The assembly of accelerator components is carried out in coordination with the SSC Laboratory. We assume that the accelerator components will be brought into the hall through the construction shaft and carried to their installation sites by either of the two cranes in the detector hall. There is space available adjacent to their installation sites for any necessary preassembly work.

5.4 Schedule and Sequential Construction Drawings

5.4.1 Construction Schedule

The construction schedule is shown in Figure 5.30. The total duration from beneficial occupancy to startup is 48 months. The schedule is based on several assumptions:

- Duration of activities are based on the experience of the participants in this report. For the assembly of the calorimeters, durations estimated by Kawasaki Heavy Industries were used. For more accurate durations, activities need to be broken down further and examined in more detail.
- Construction of the endcap calorimeters is performed on the surface while the barrel calorimeter is constructed in the hall.
- One crew (rather than two) is utilized for the building of the muon steel, since the steel is not on the critical path.

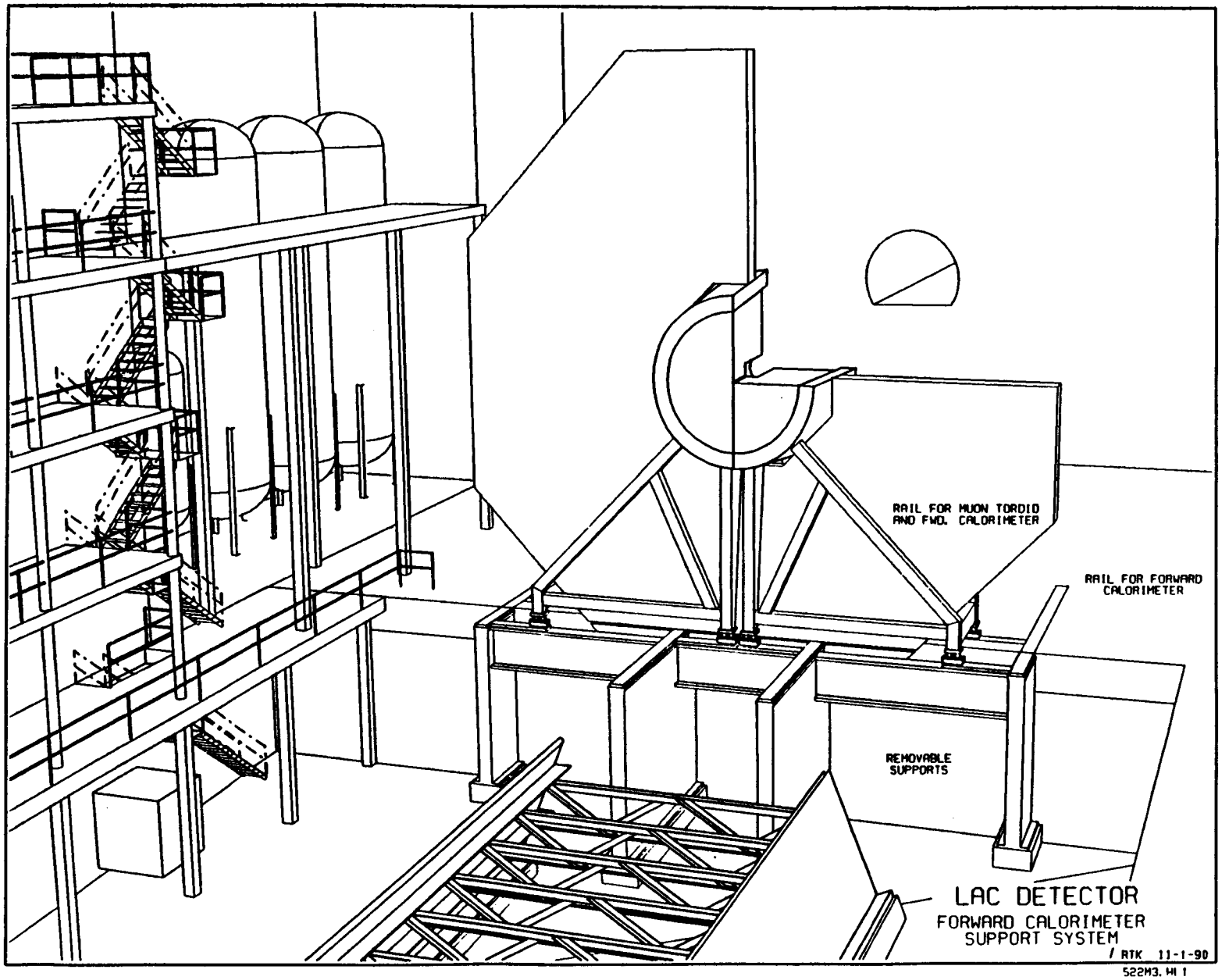

Figure 5.29. LAC Detector—Forward Calorimeter Support System.

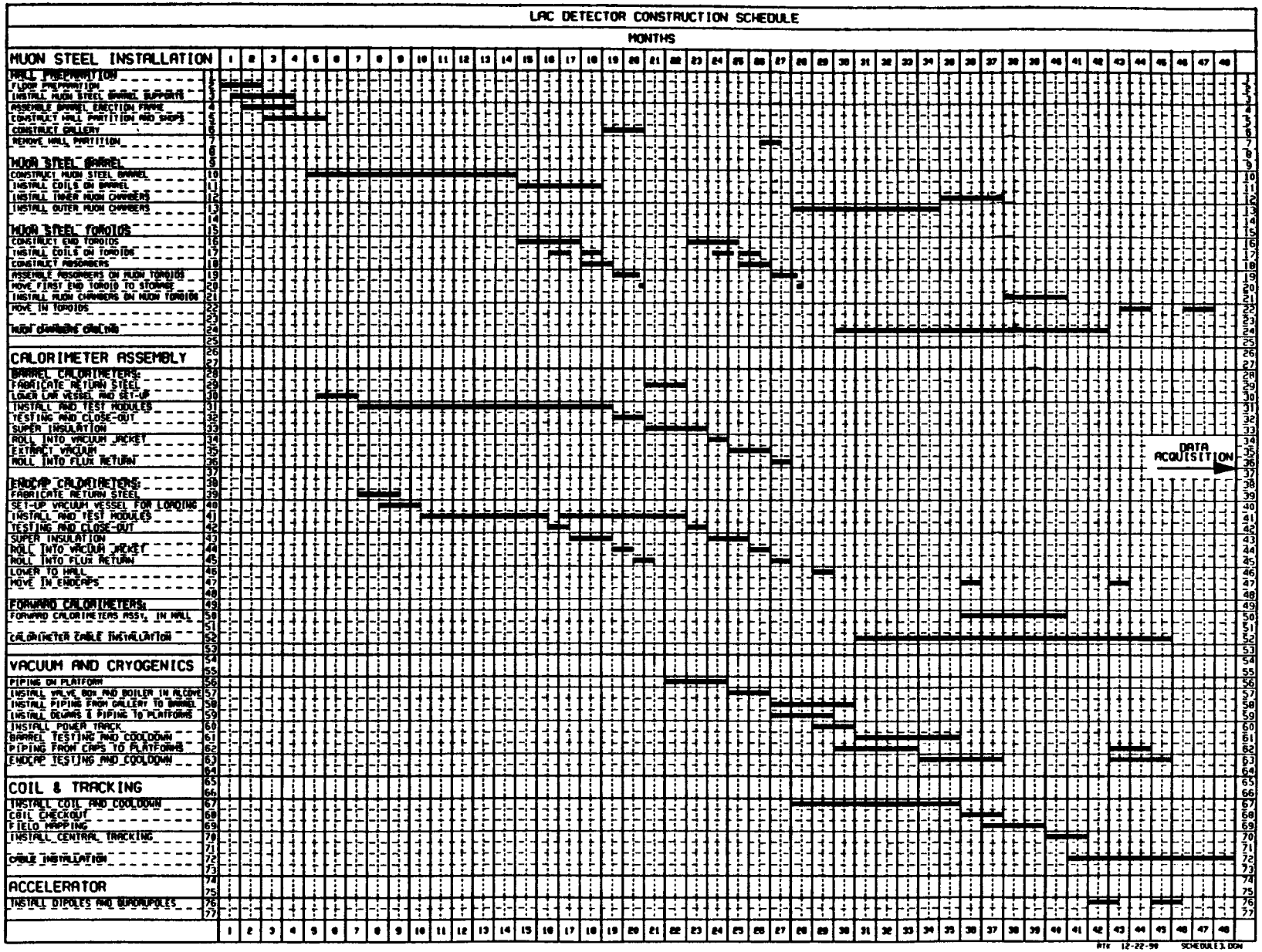

Figure 5.30. LAC Detector Construction Schedule.

The schedule could be accelerated if all calorimeters were assembled on the surface. They could then be built while the hall is under construction; however, this would mean larger surface facilities and a heavier lifting device needed to lower the heavier barrel calorimeter. The muon steel construction in this case would need two crews. The schedule for this option was not studied.

Assembly of the end toroid steel is done by the same crews during the periods when the coils for the barrel toroids are being connected to power and to Low Conductivity Water (LCW) and are being tested for electrical continuity and for integrity of the electrical insulation and cooling system.

Both the barrel and the endcap calorimetry assembly schedules assume that, on average, 1.5 calorimeter modules are installed and tested per day. We foresee the calorimeter installation to utilize two shifts per day, with the day shift installing, and the evening shift testing and calibrating the installed modules. A third shift per day is reserved as contingency.

The bulk of the cryogenic piping construction on the gallery platforms and in the dewar alcove is scheduled for completion just prior to insertio of the calorimeter barrel into the flux return. Dewar installation and connection, along with cryogenic piping to the barrel calorimeter, is completed several months after barrel installation. Vacuum testing and cooldown of the barrel then proceed. Cryogenic piping installation to the first endcap calorimeter takes place at this time, followed by cooldown and testing. The cryogenic connection of the second endcap must wait until the solenoidal field has been measured and the central tracking device has been installed.

The superconducting coil is installed after the barrel calorimeter is located in its final position on the beam line. Prior to installation of the central tracking device, the magnetic field of the solenoidal coil must be measured. This requires that both endcap calorimeters be in position, since they provide part of the return yoke of the magnet. Initial testing of the field-mapping instrumentation can take place simultaneous with the installation and testing of the coil, but the final mapping must wait until all of the magnetic elements are installed and operational.

After the magnetic field has been mapped, the endcap calorimeters are withdrawn, and installation of the central tracking device (including the silicon tracker) can proceed. The unconnected endcap is withdrawn far enough to allow installation of the central tracking device. The central tracking device is assumed to arrive in the hall as a single, pre-tested unit requiring minimal debugging inside the collision hall prior to installation in the detector.

Installation of the muon chambers begins with the successful testing of the barrel iron toroids and their coils. The endcap muon chambers are installed after the end iron toroids and their coils have been assembled and successfully tested.

Estimating the schedule for installation of the electronics is more problematical; we have not considered this schedule in detail. We assume that large-scale testing of the data acquisition system and pathways begins with the installation of the barrel calorimeter. While some of this testing could provisionally be done using the electronics gallery in the hall as a temporary data acquisition

location, prudent planning implies that beneficial occupancy of the operations center should be no later than one year after beneficial occupancy of the collision hall.

5.4.2 LAC Sequential Construction Drawings

In order to better visualize the detector and the construction problems and space requirements, a three-dimensional computer model of the hall and detector has been created comprising several files and a cell library. Different aspects of the construction sequence are placed in different layers that can be turned on or off. Simulation of construction methods and sequences is performed by moving cells or combining the different layers.

The three-dimensional model allows us to accurately establish hall space requirements during construction and repair, and to establish a logical sequence for the construction schedule. The modeling exercise also allows us to take progress pictures of the detector construction and to visualize different situations as assembly progresses. A period of three months between progress pictures is selected as sufficient to highlight construction milestones. These progress pictures can be seen in Figures 5.31 through 5.47.

Figure 5.31 shows the hall at beneficial occupancy or month 0 on the construction schedule. At this time floor preparation begins, which entails preparing all the tools and workstations required for the future construction. Two months is allowed for this activity.

Two weeks after beneficial hall occupancy, installation of the muon steel barrel supports commences. Three months are allowed for this activity, which includes installation of the structural steel and accurate levelling of the edges of the radial plates which serve as the base for the alignment of the detector.

Assembly of the muon steel barrel erection frame begins one month after beneficial occupancy. This frame is a jig around which the muon steel plates are supported before bolting together. Two months is allowed for this activity.

Figure 5.32, month 3, shows the muon steel barrel supports erected and the barrel erection frame assembled. Starting in month 2, the hall partition and shops are assembled. The partition of the hall is necessary to divide the dirty operation of the steel construction from the clean operation of the barrel calorimeter assembly. The partition is provided with sliding doors to allow passage of personnel and tools. Both the shops and the partitions will be built in three months, starting in month 3. The muon steel barrel assembly starts in month 5 with placement of a sufficient number of bottom plates to support the assembly frame. (For more details of the barrel steel construction, see Section 5.3.1.) The liquid argon vessel is lowered to the hall floor in month 5.

Figure 5.33, month 6, shows the hall with the shop platforms built, the partition erected, the barrel calorimeter liquid argon vessel in the assembly position, and the muon steel being erected. Insertion of the barrel calorimeter modules starts in month 7 and continues for 12 months. On the

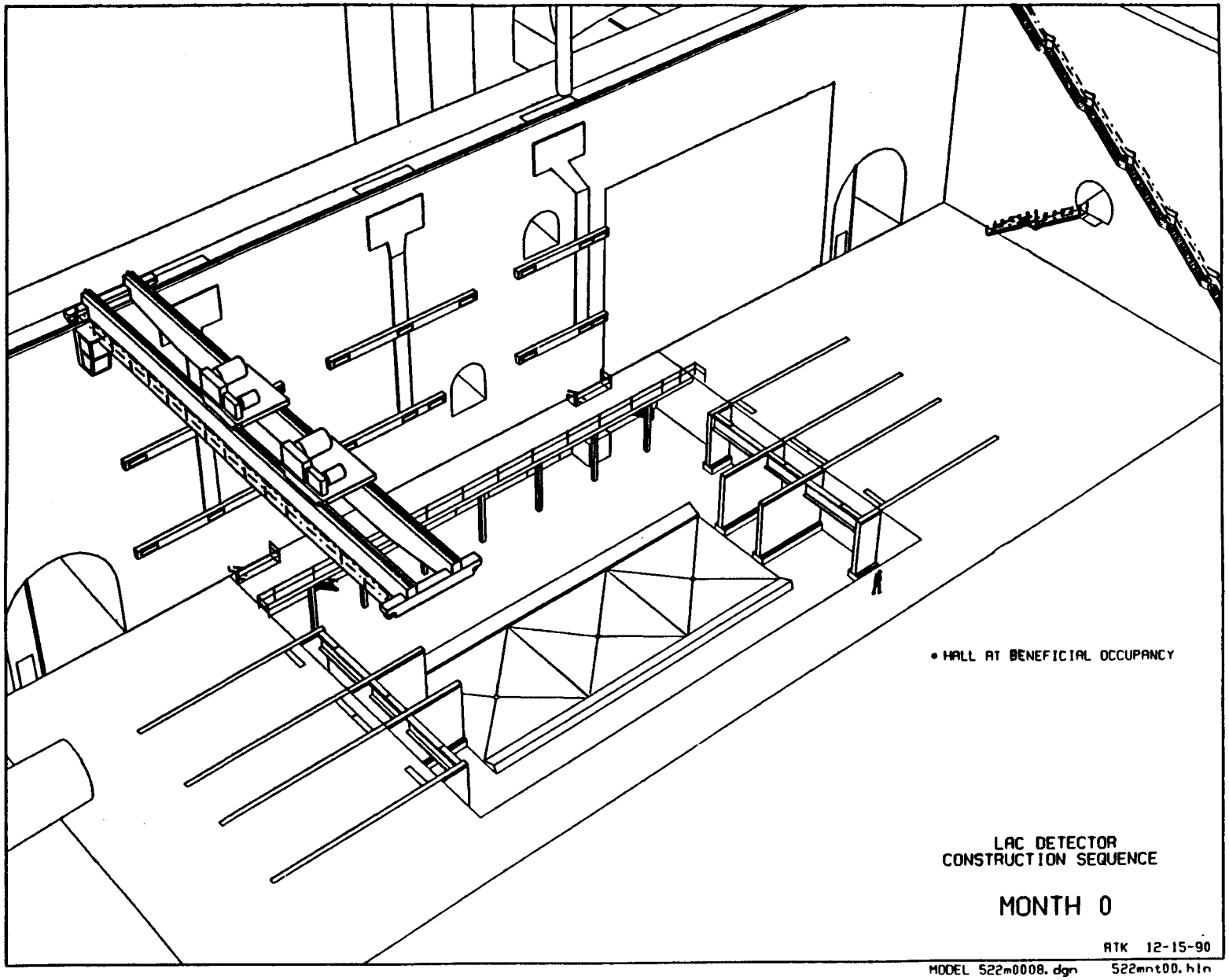

Figure 5.31. LAC Detector Construction Sequence (Month 0).

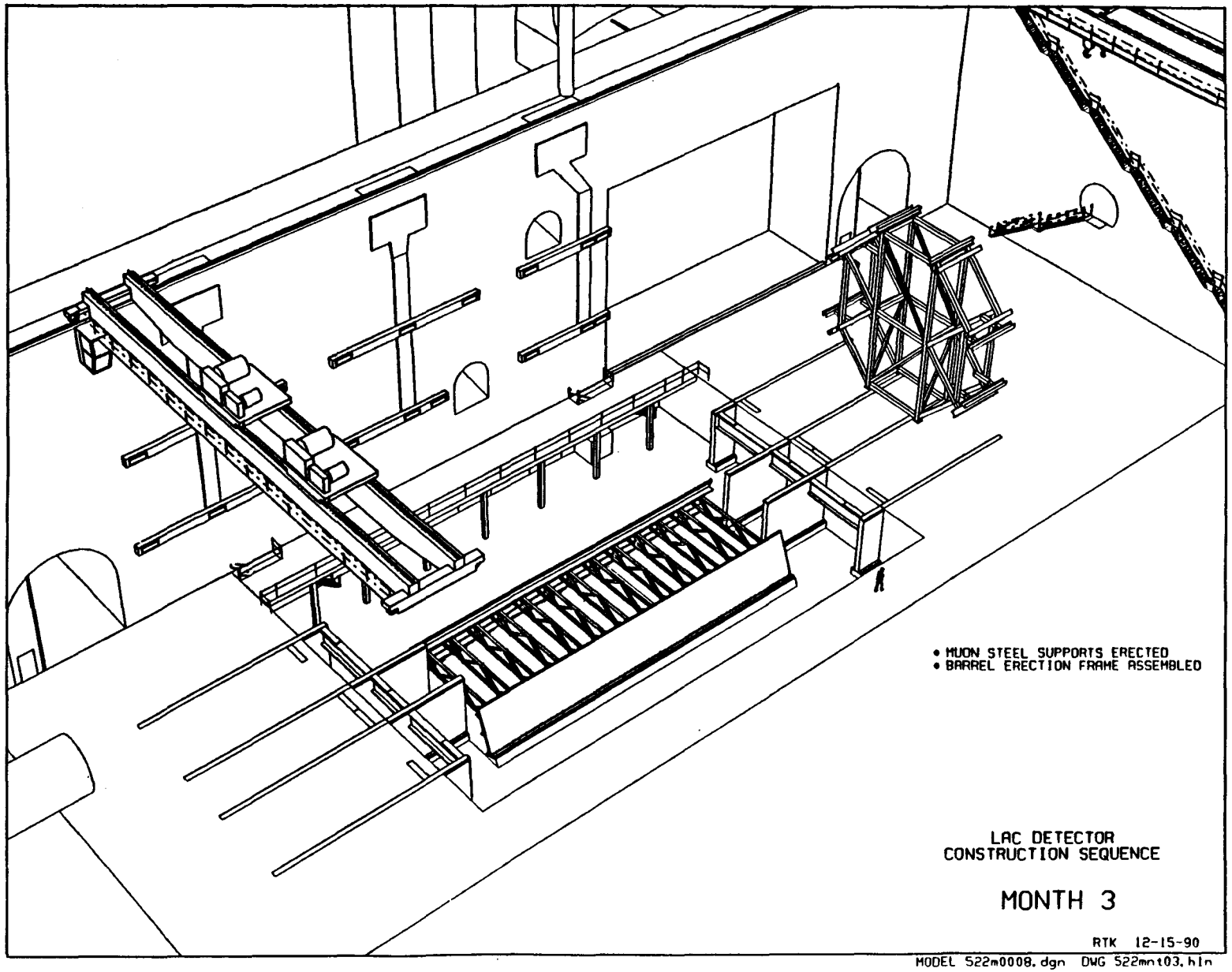

Figure 5.32. LAC Detector Construction Sequence (Month 3).

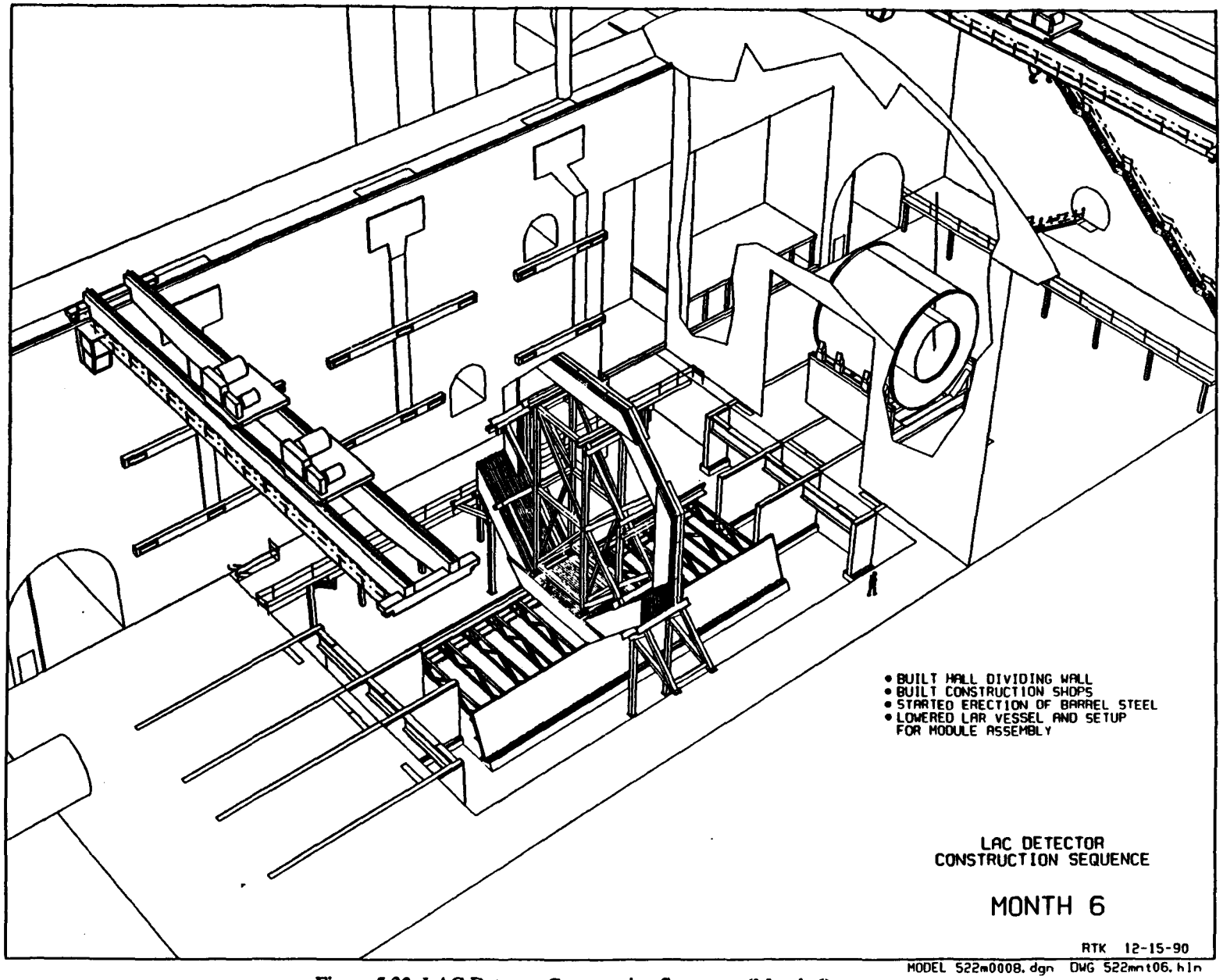

Figure 5.33. LAC Detector Construction Sequence (Month 6).

surface, the fabrication of the flux return steel has begun, as has setup for the the endcap calorimeters assembly.

Figure 5.34 shows the hall at month 9, with the muon steel barrel construction 50% complete and the insertion of modules in the liquid argon vessel continuing. Note the special equipment needed for insertion of modules. The figure shows two insertion machines, but a more detailed study of this operation may reveal that one machine is sufficient to complete the job on time.

Installation of modules into the first endcap calorimeter on the surface starts at month 10 and continues for 6 months.

Figure 5.35, month 12, shows the muon barrel steel 80% complete and the barrel calorimeter module insertion operation 45% complete. Construction of the muon barrel steel is complete at month 14, at which time installation of the muon steel coils begins. Construction of the end steel toroids starts at month 15 following completion of the barrel.

Figure 5.36, month 15, shows the muon steel barrel complete, the barrel steel coil installation undeway, installation of the barrel calorimeter modules 70% complete, and erection of the muon toroids underway.

Coil installation on the first half of the muon end toroids starts in month 16, after erection of a toroid half is complete. In month 17, the second half of the muon toroid is completed and the coil installation is started. In month 16, the first endcap calorimeter module installation is completed on the surface. Module installation of the second endcap calorimeter starts at month 17, as does superinsulation of the first endcap calorimeter.

Figure 5.37 shows the hall at month 18. The first muon steel toroid is complete, the coil installation on the finished toroids is 75% complete, the construction of the absorber is underway, the muon barrel coils are complete, and installation of the barrel calorimeter modules is 95% complete. Construction of the gallery structure starts at month 19 and takes two months to complete, after which installation of the equipment inside the gallery commences.

Construction of the absorbers for the first muon toroid is complete at month 19, and installation of the muon toroid halves is complete at month 20. At this point the two halves of the muon end toroid are joined together and are rolled to the far end of the muon barrel to make room for further construction. Using the same steel erection crew, construction of the barrel calorimeter flux return steel starts at month 21, immediately after construction of the first muon toroid ends.

Installation of the barrel calorimeter module is finished at month 19; closeout and testing last for 1.5 months. The superinsulation of the barrel calorimeter starts in month 21. By the end of month 21, the second endcap calorimeter module insertion is 80% complete, and the first endcap liquid argon vessel has been inserted into its vacuum vessel; the vessel is in turn inserted into the flux return steel casing.

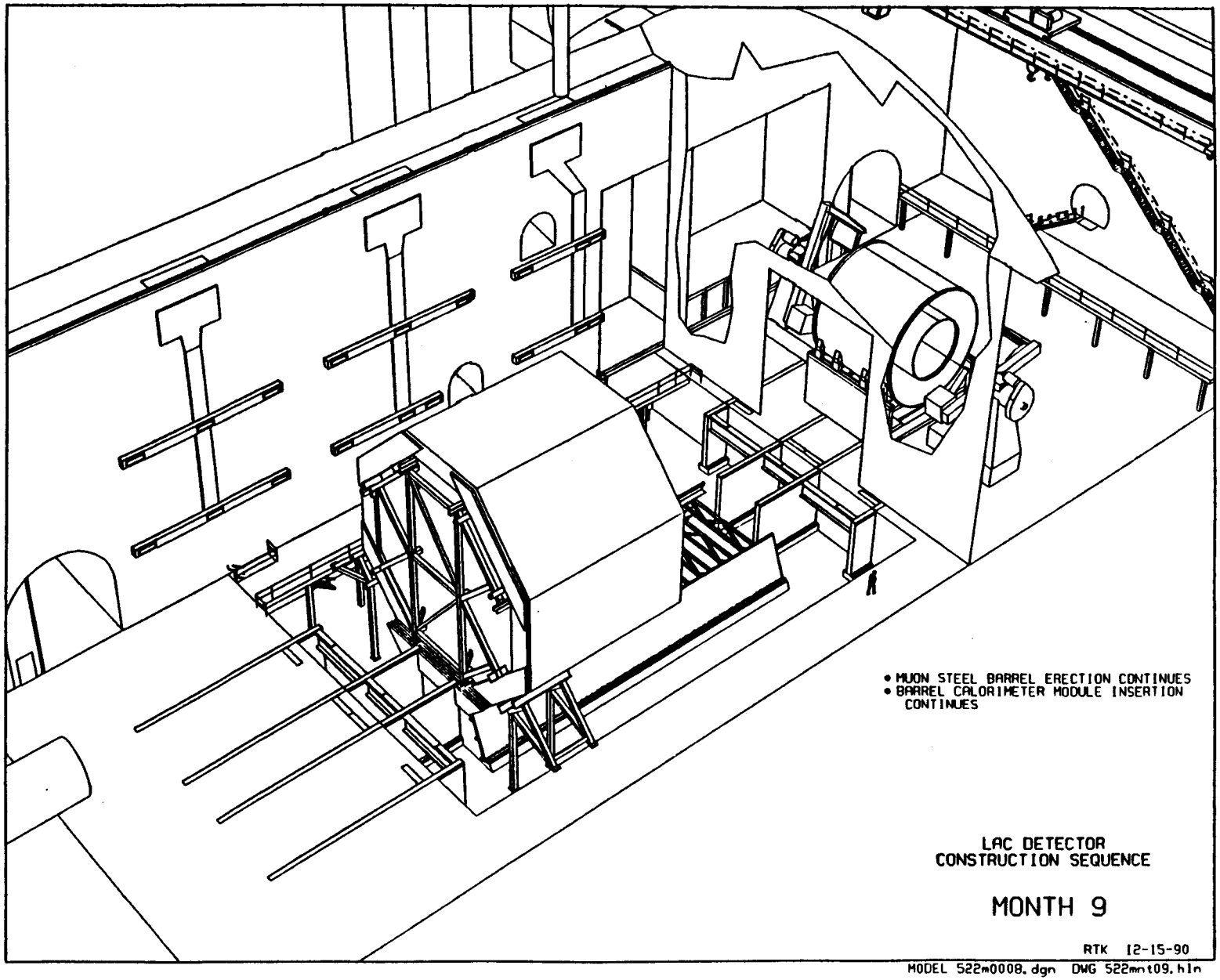

Figure 5.34. LAC Detector Construction Sequence (Month 9).

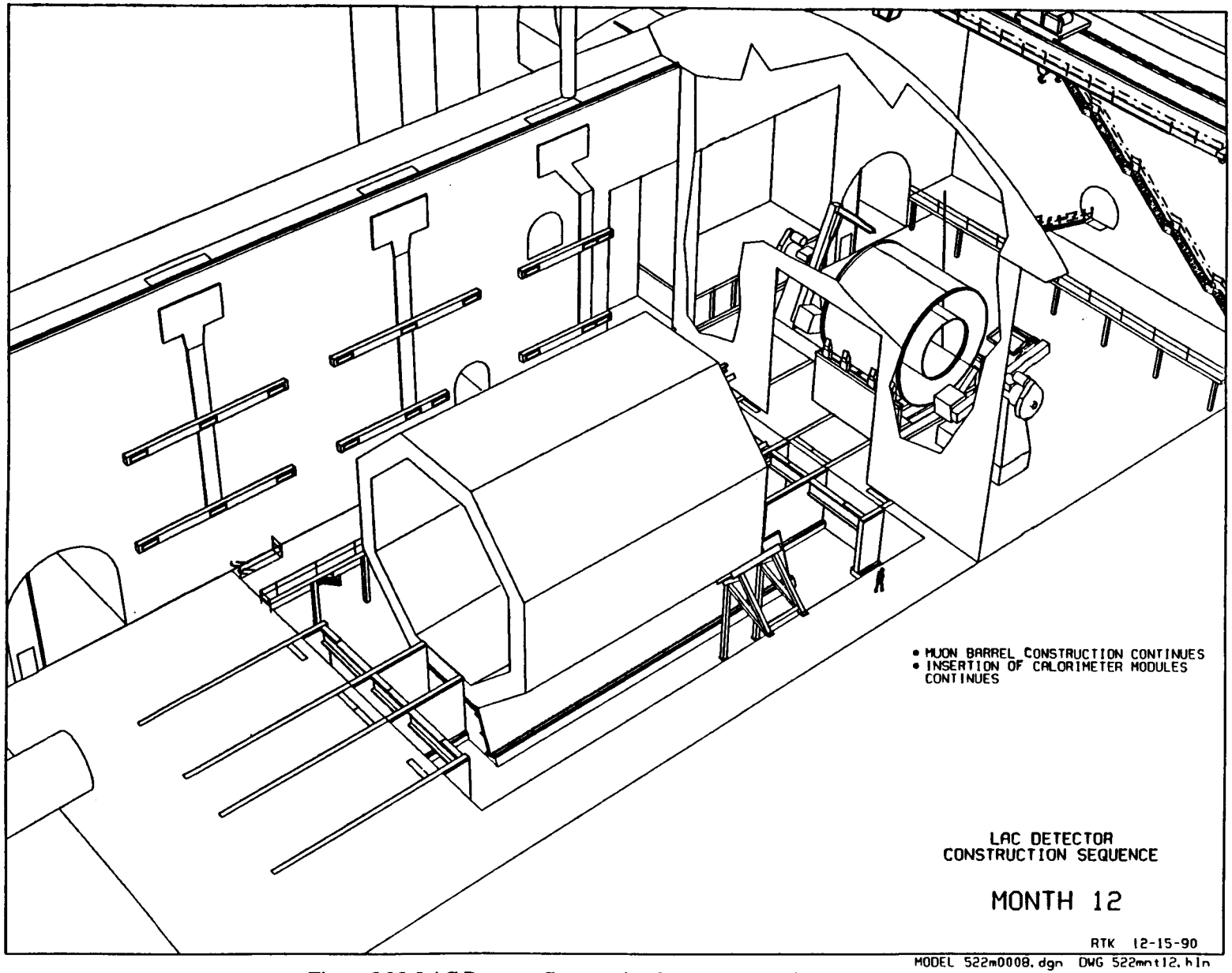

Figure 5.35. LAC Detector Construction Sequence (Month 12).

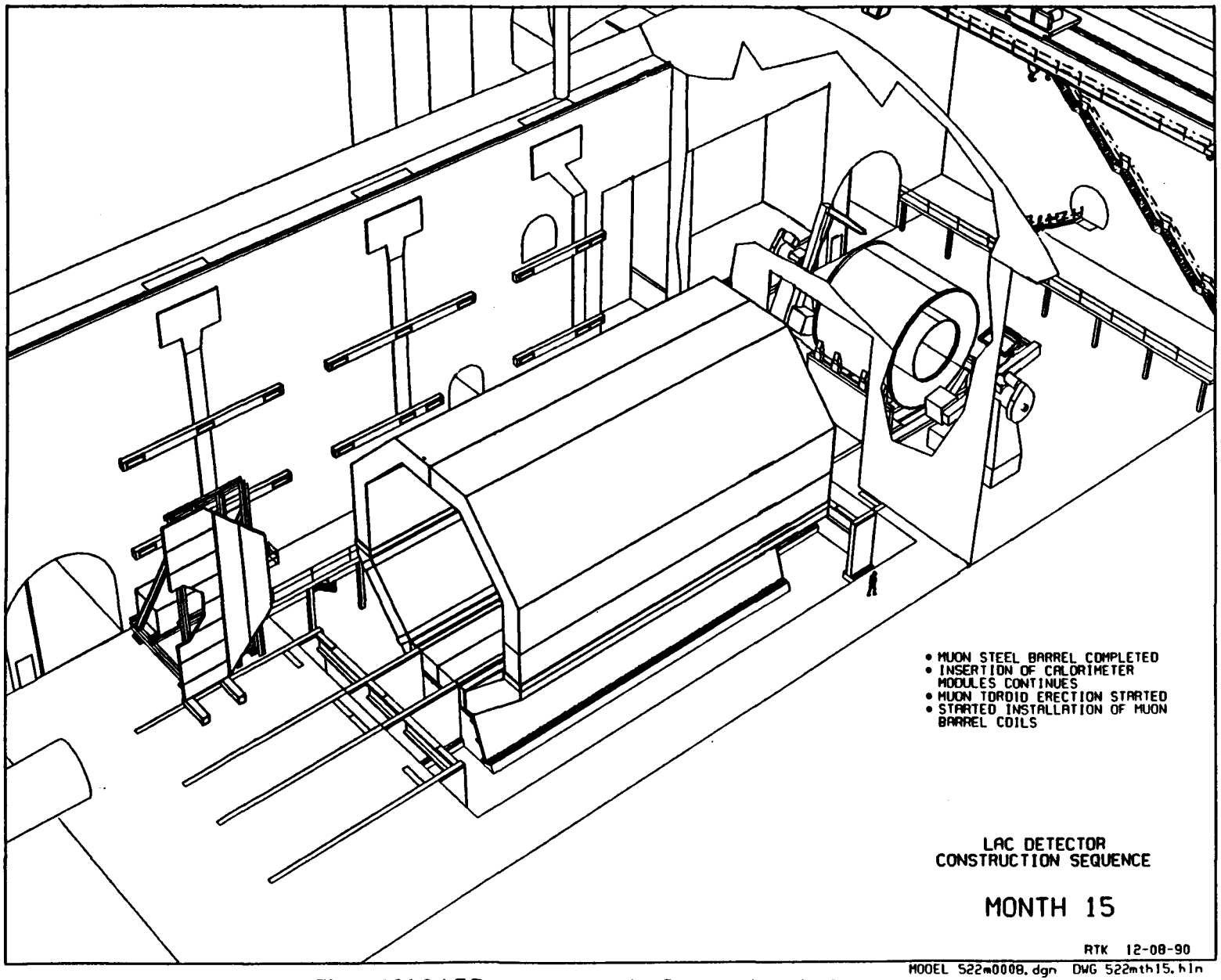

Figure 5.36. LAC Detector Construction Sequence (Month 15).

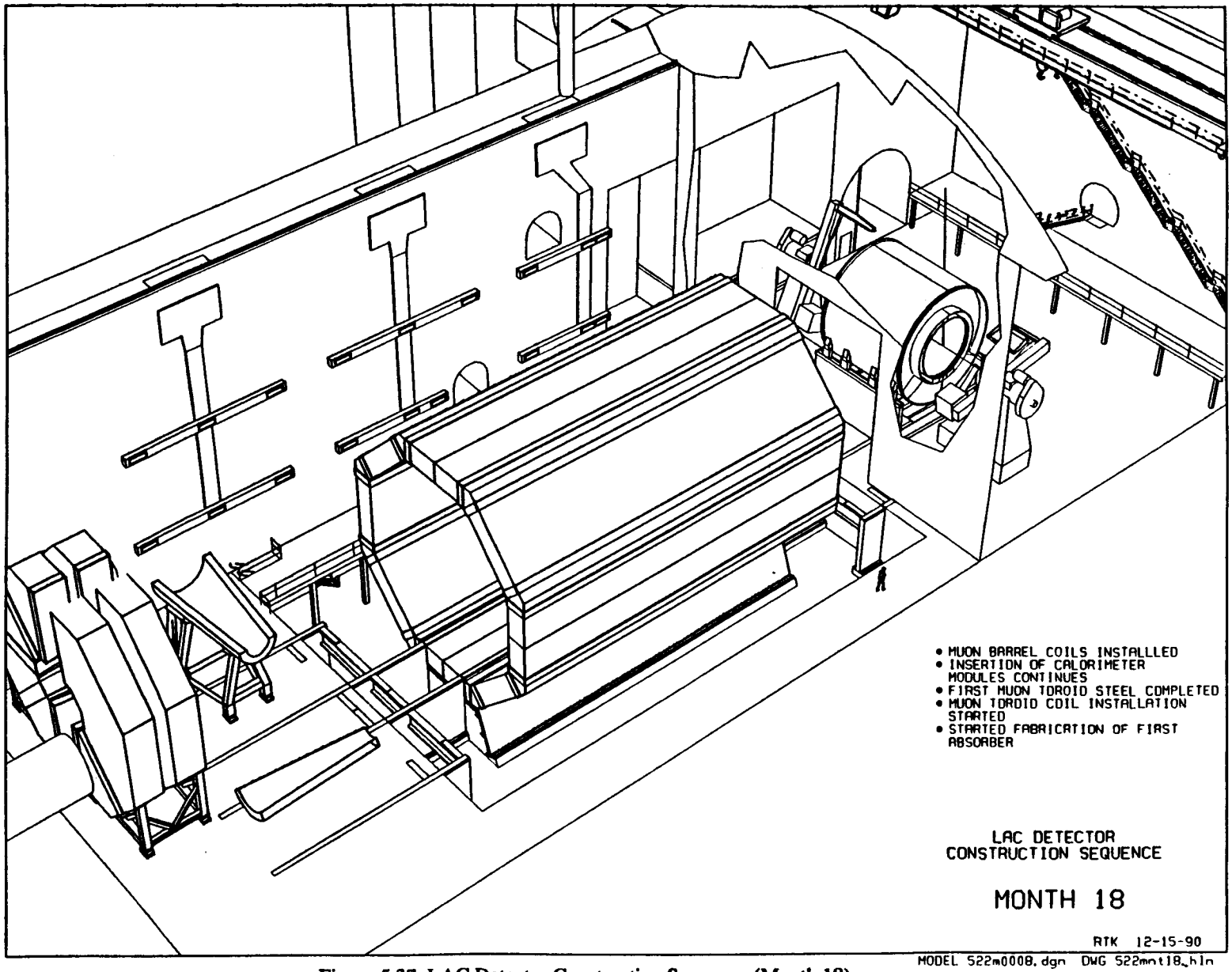

Figure 5.37. LAC Detector Construction Sequence (Month 18).

Figure 5.38 shows the status of construction by the end of month 21. The gallery structure is complete, the first muon steel toroid is finished and stored in the barrel steel, the liquid argon vessel is closed up, and the barrel calorimeter return steel construction is underway. Construction of the return steel for the barrel calorimeter is finished in month 23; it is then installed in the muon barrel steel. The same steel crew begins the second muon steel end toroid in month 23, immediately following completion of the barrel calorimeter return steel.

The barrel calorimeter superinsulation is finished at month 23, and the liquid argon vessel is slipped into the vacuum vessel at month 24. On the surface, installation of the module for the second endcap calorimeter is complete at month 22. The second endcap liquid argon vessel is tested and closed at month 23, and the superinsulation started at month 24.

In month 24 (Figure 5.39), the barrel liquid argon vessel is inserted into its vacuum vessel, construction starts on the second half of the second muon end toroid, and construction and installation of the barrel calorimeter flux return steel is completed. Construction of the second end muon toroid is finished at month 25, and installation of its coils is finished during month 27. The second conical absorber is finished during month 27. This ends all steel fabrication in the hall, thus allowing the hall partition to be removed for component maneuvering on the next detector assembly steps.

Vacuum extraction on the barrel calorimeter is finished by month 26, and the barrel calorimeter is rolled into the return steel during month 27 after the hall partition has been removed. On the surface, the superinsulation for the second endcap is finished in month 25. The liquid argon vessel is slipped into the vacuum vessel, and both are inserted into the flux return steel at month 27. The cryogenic valve box and liquid argon boiler are installed in the alcove at month 26, and cryogenic piping installation from the gallery to the barrel calorimeter begins at month 27.

Figure 5.40, month 27, shows the hall partition removed, the coils for the second muon toroid installed, construction of the conical absorbers finished, the first muon end toroid moved to a storage position, the cryogenic valve box and boiler installed, and the barrel calorimeter in its final position.

Installation of the barrel outer muon chambers starts in month 28 and continues for seven months. Cabling of the muon chambers starts in month 30 and continues for 13 months.

Both endcap calorimeters are lowered into the hall during month 29. Installation of the cryogenic dewars is complete by month 29, and cryogenic piping for the barrel calorimeter and from the dewars to the platforms is finished by month 30. Installation of the power tracks will be accomplished during months 29 and 30.

Installation and testing of the detector superconducting solenoidal coil begins at month 28 and continues for 8 months.

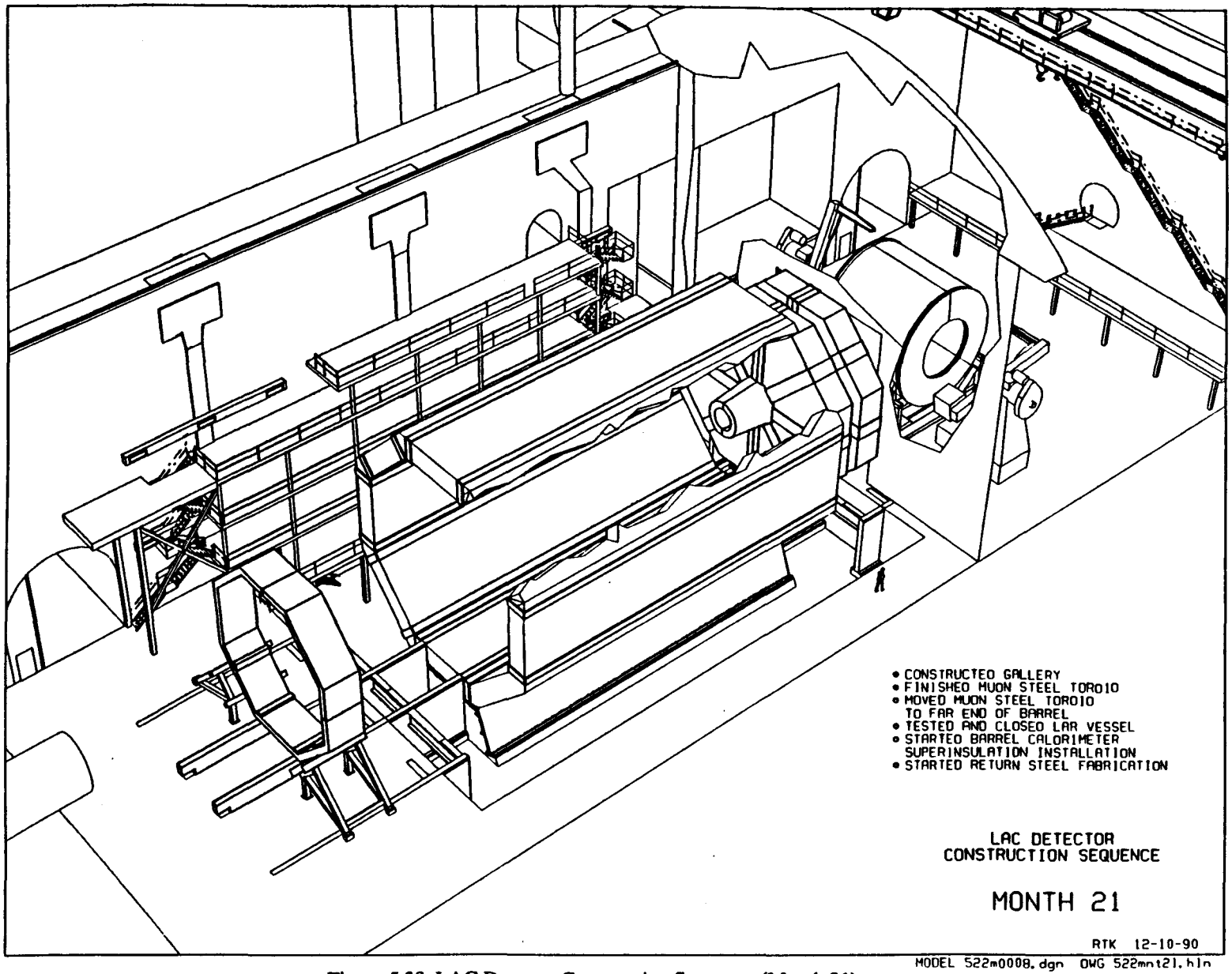

Figure 5.38. LAC Detector Construction Sequence (Month 21).

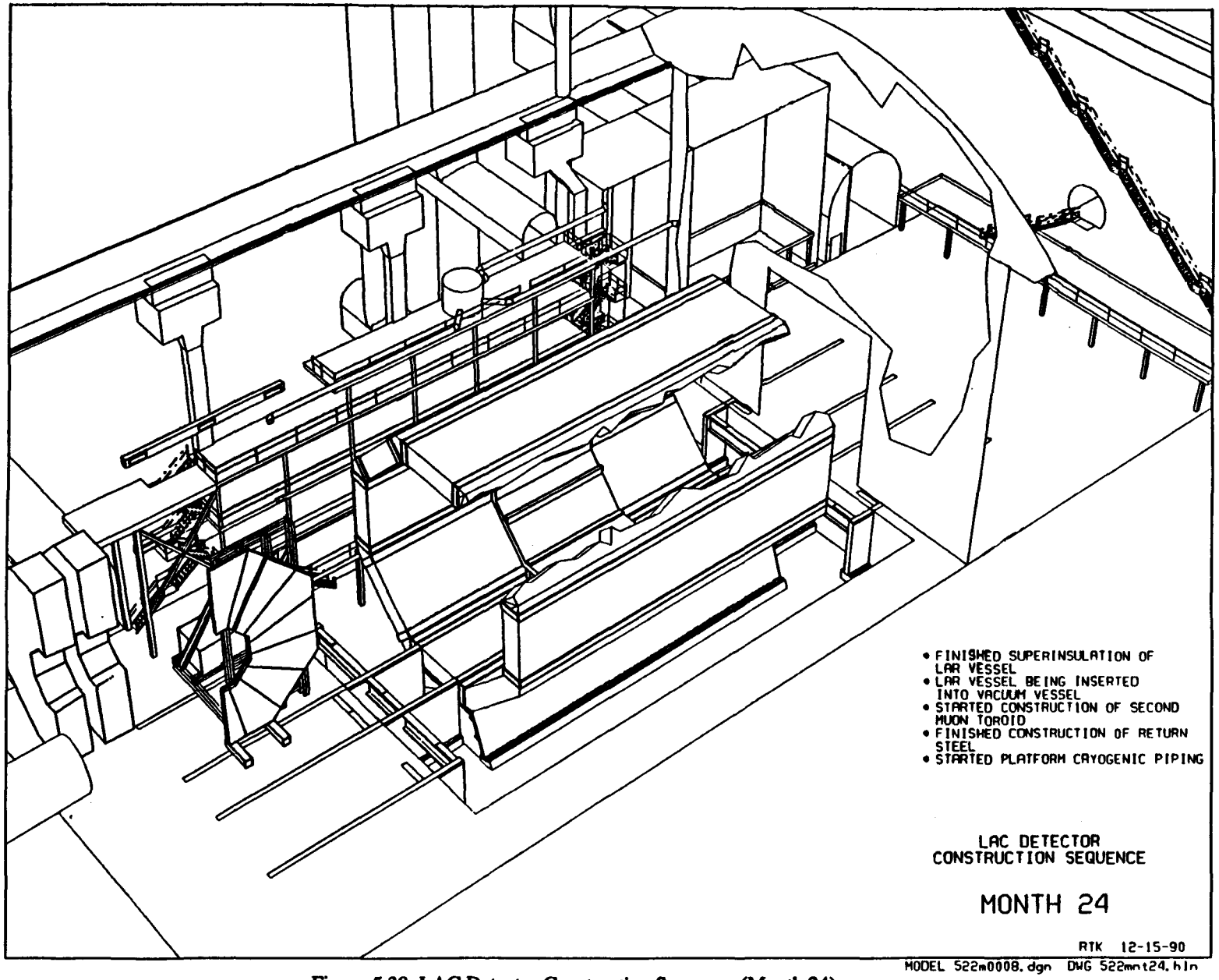

Figure 5.39. LAC Detector Construction Sequence (Month 24).

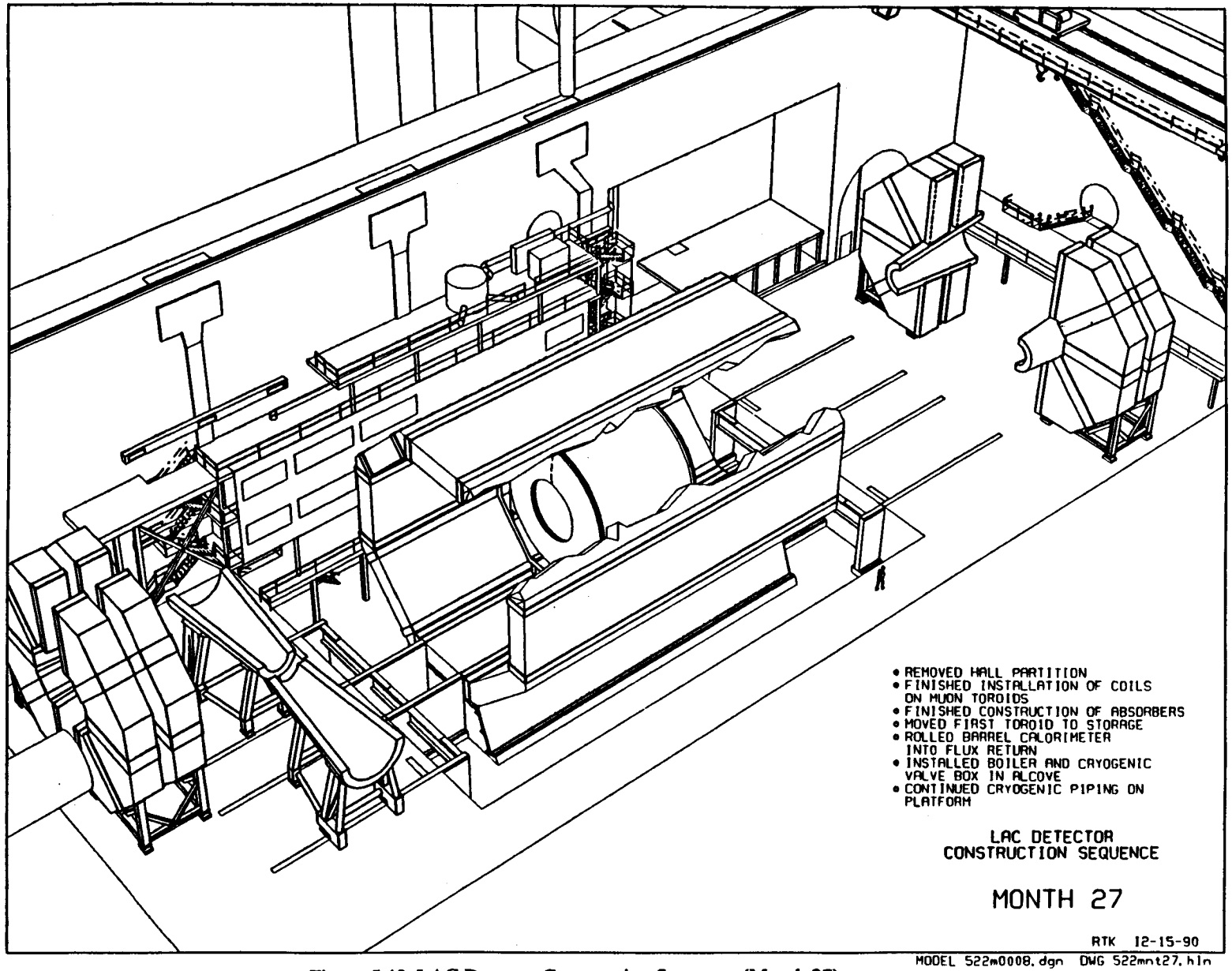

Figure 5.40. LAC Detector Construction Sequence (Month 27).

Figure 5.41, month 30, shows installation of the outer muon chambers underway, installation of the coils completed on the second end toroid, both endcaps lowered to the hall floor, the detector solenoidal coil being prepared for installation, piping from platform to barrel installed, cryogenic dewars installed, and power tracks installed.

Installation of calorimeter cable commences at month 31 and continues for 15 months. Endcap calorimeter cryogenic piping commences at month 31. Cryogenic testing of the barrel calorimeter starts at month 31.

Figure 5.42 shows the hall at month 33. Installation of the barrel exterior muon chamber is 90% complete, solenoidal installation is 80% complete, and endcap cryogenic piping has started.

Installation of barrel exterior muon chambers is finished by month 34, at which time installation of interior muon chambers begins. In actual construction, there is interleaving of exterior and interior muon chamber installation. The object is to keep the installation crew fully occupied during the period.

By month 36 the endcap calorimeters are moved in to allow coil field mapping. Forward calorimeter construction starts by month 36. All cryogenic piping is finished by now except for piping to the east endcap, which needs to move out at a later time to allow for installation of the central tracking devices. Endcap testing of the west endcap starts inmonth 35.

Detector solenoid installation is finished by month 35, and check-out of the coil starts.

Figure 5.43, month 36, shows installation of barrel interior muon chambers underway, the first forward calorimeter constructed, and the endcap calorimeters moved in. Installation of muon chambers on muon toroids begins in month 38, after installation of barrel interior chambers is complete. Testing for the west side endcap will be finished by month 38. Coil check-out and field mapping are accomplished by month 39.

Figure 5.44, month 39, shows installation of muon chambers on muon end toroids to be 70% complete, construction of the forward calorimeters 80% complete, and coil field mapping almost complete. Forward calorimeter construction is finished at month 40. The muon end toroid chambers are complete at month 40, at which time installation of muon chambers on the forward calorimeters is started.

The central tracking device is installed during months 40 and 41. This requires complete removal of the east side endcap and movement of the west endcap to the maximum range of its power track.

Figure 5.45, month 42, shows the central tracking device installed, the west muon toroid halves joined, muon chambers on forward calorimeters installed, and quadrupoles installed on the west side of the hall. The east calorimeter endcap is moved into position for piping, wiring and cooldown during months 43 through 45. During this period, the west side endcap muon toroid and forward calorimeter are moved to their final positions.

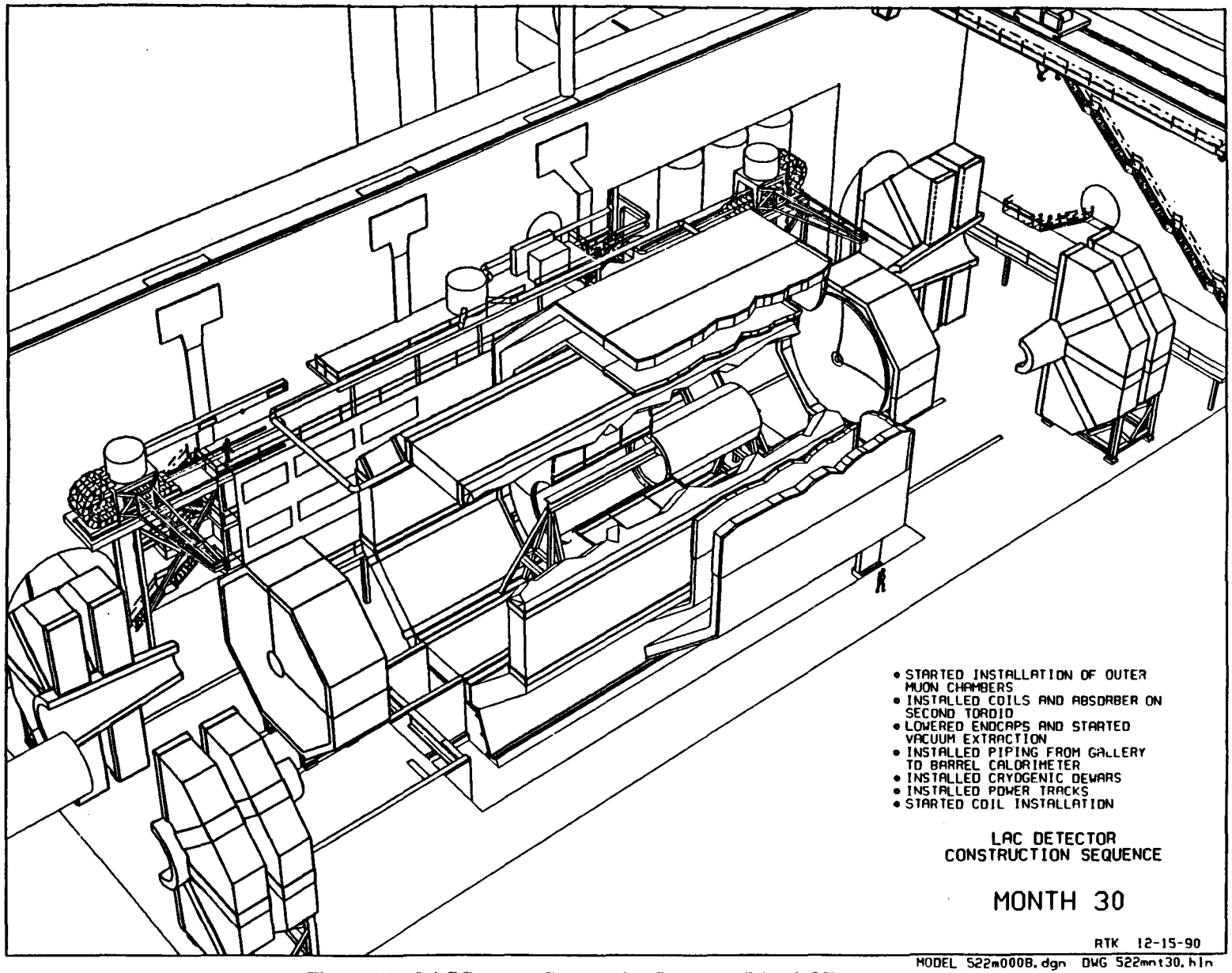

Figure 5.41. LAC Detector Construction Sequence (Month 30).

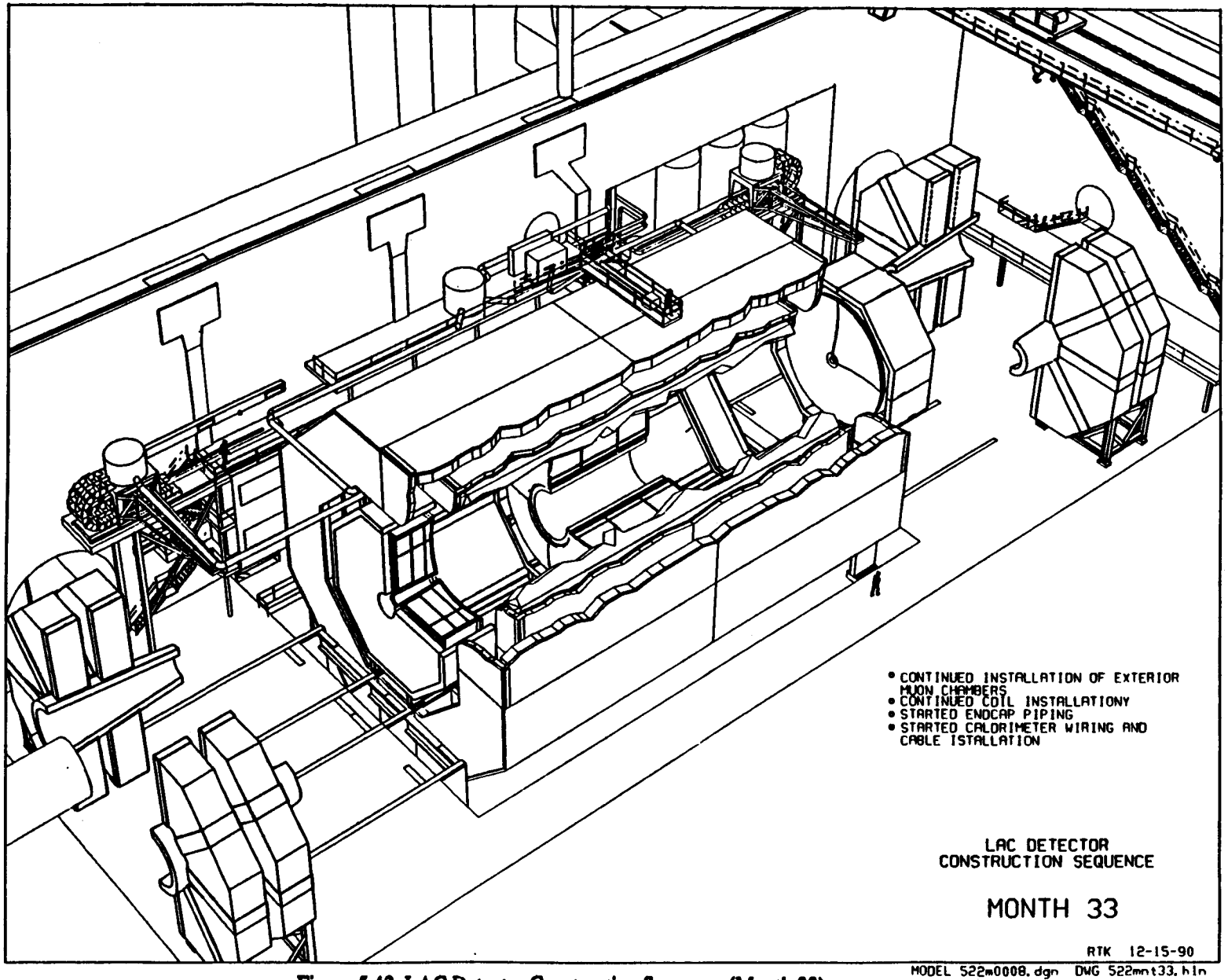

Figure 5.42. LAC Detector Construction Sequence (Month 33).

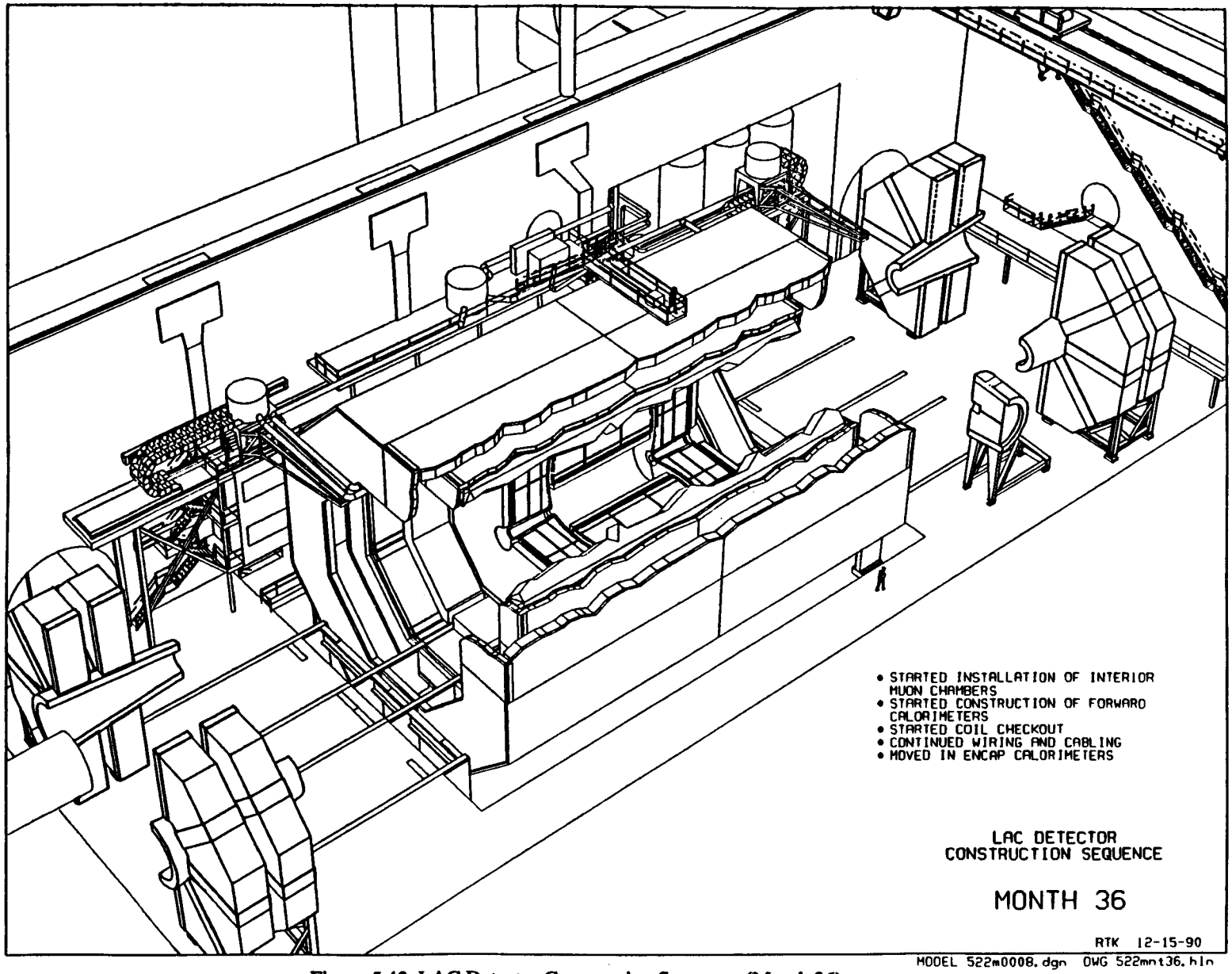

Figure 5.43. LAC Detector Construction Sequence (Month 36).

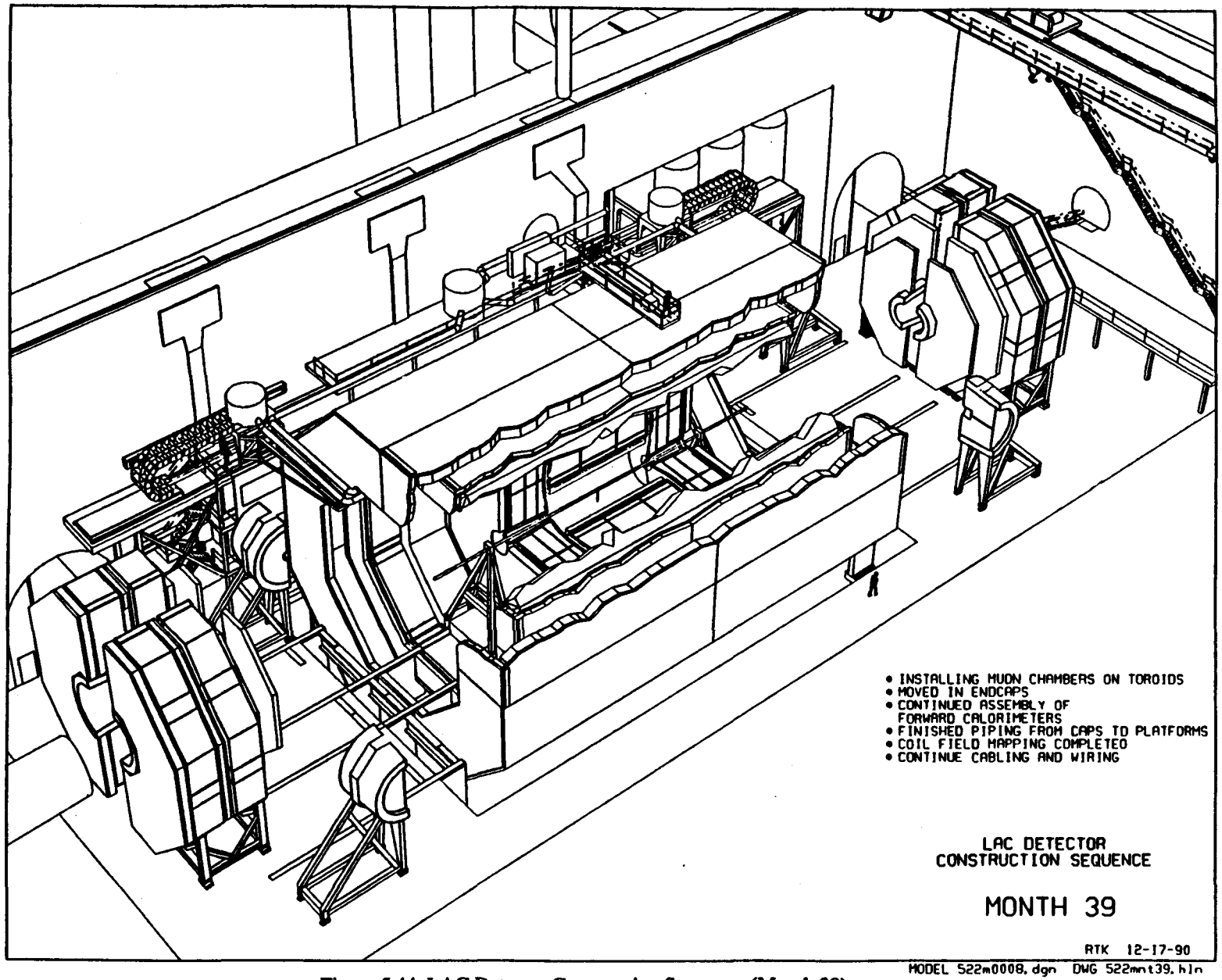

Figure 5.44. LAC Detector Construction Sequence (Month 39).

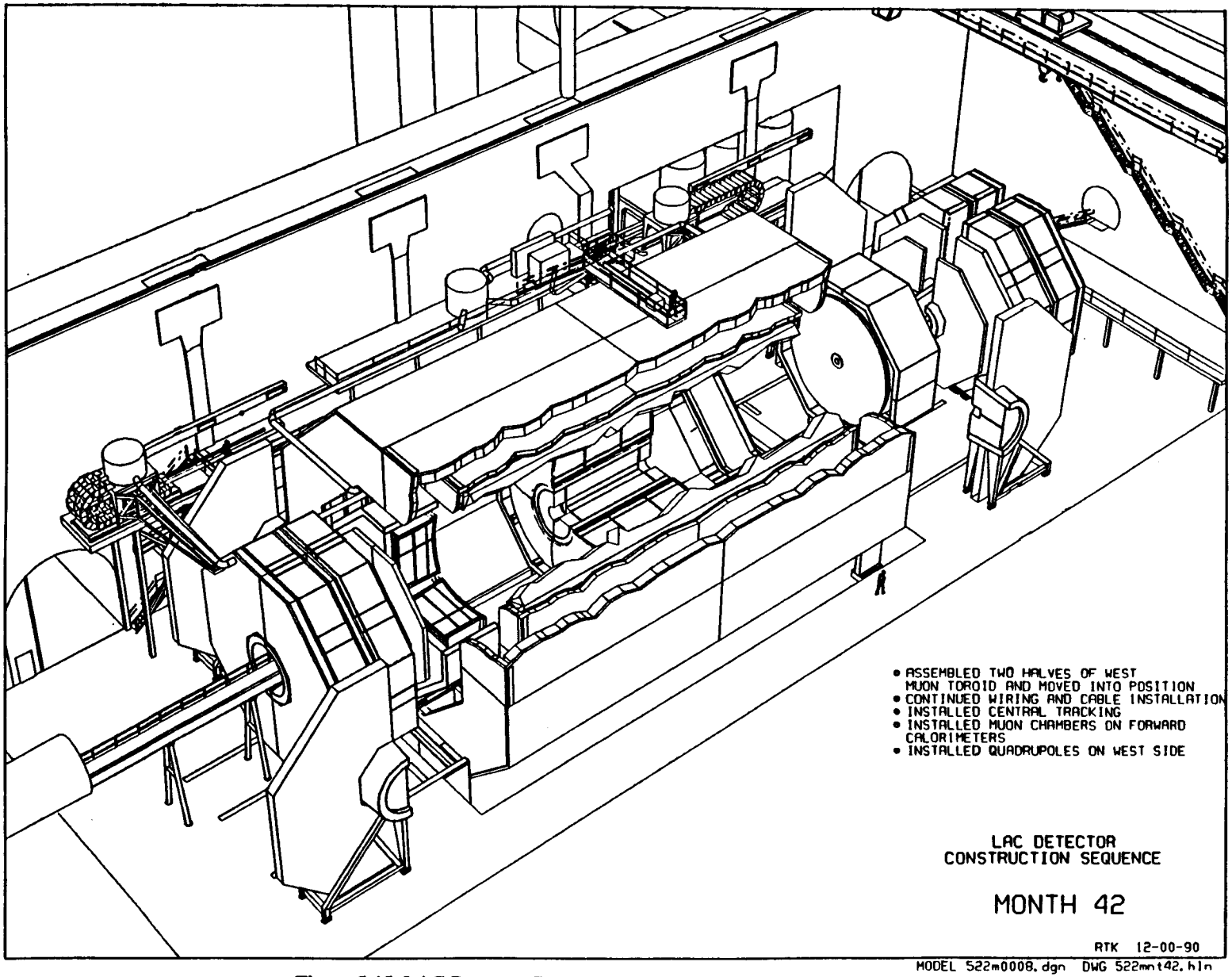

Figure 5.45. LAC Detector Construction Sequence (Month 42).

Figure 5.46, month 45, shows the west end of the detector completed, the east side endcap calorimeter in its final position, the piping and wiring for the endcap calorimeters completed, the east muon end toroid joined, and the east end beamline quadrupoles installed. The east side muon toroid is moved in at month 47, after the final installation of the detector beam tube. The east side forward calorimeter with its muon chamber is moved to its final location in month 48.

Figure 5.47 shows the detector at month 48, completed and in its closed position.

5.5 Disassembly and Repair

Disassembly and repair exercises were performed to ascertain the room required in the hall to repair the detector without raising major components to the surface. (In actual repair, it may be more practical to raise components to the surface.)

Three basic situations are simulated: the detector undergoing service or minor repairs, the detector open for endcap calorimeter repair, and the detector disassembled for barrel calorimeter repair. Situations requiring repair of the coil or components of the central tracking device are not shown; note that these fall under the category of major repairs.

The exercise demonstrates that the floor space developed for constructing the detector is about the same as is required to repair it; therefore, whether the barrel calorimeter is built on the surface or on the hall is not a major influence in determining the hall size if we assume that the endcaps are to be built on the surface.

5.5.1 Minor Repairs

The detector has been designed so that it can be opened for minor repairs without disconnecting the beam tube, removing the beamline quadrupoles, or disconnecting cables and pipes from the endcap calorimeter and muon toroids (Figure 5.48). To accomplish this, the endcap calorimeters and muon toroids are equipped with Hillman rollers running on machined steel tracks. Horizontal hydraulic cylinders push the equipment by fastening one end of the cylinders to the steel tracks.

When opening one end of the detector, the forward calorimeter is the first component that must be moved. It separates from the beam pipe, then each half retracts to a convenient position. Further study is required to learn whether a forward calorimeter can be moved without disconnecting cables. Study also needs to be done on the subject of radiation, which is present when opening the forward calorimeters. A means of automatically introducing shielding may be necessary.

Once the forward calorimeter has been moved out of the way, the muon end toroid is moved axially until it reaches the quadrupole supports. Power tracks are provided at each end to carry the pipes and cables as a calorimeter endcap and toroid move. Maximum total movement is 8.5 m. Because the calorimeter endcap and the power track need to move together, further study should be done on the synchronization of their movements. Another problem that needs further attention is

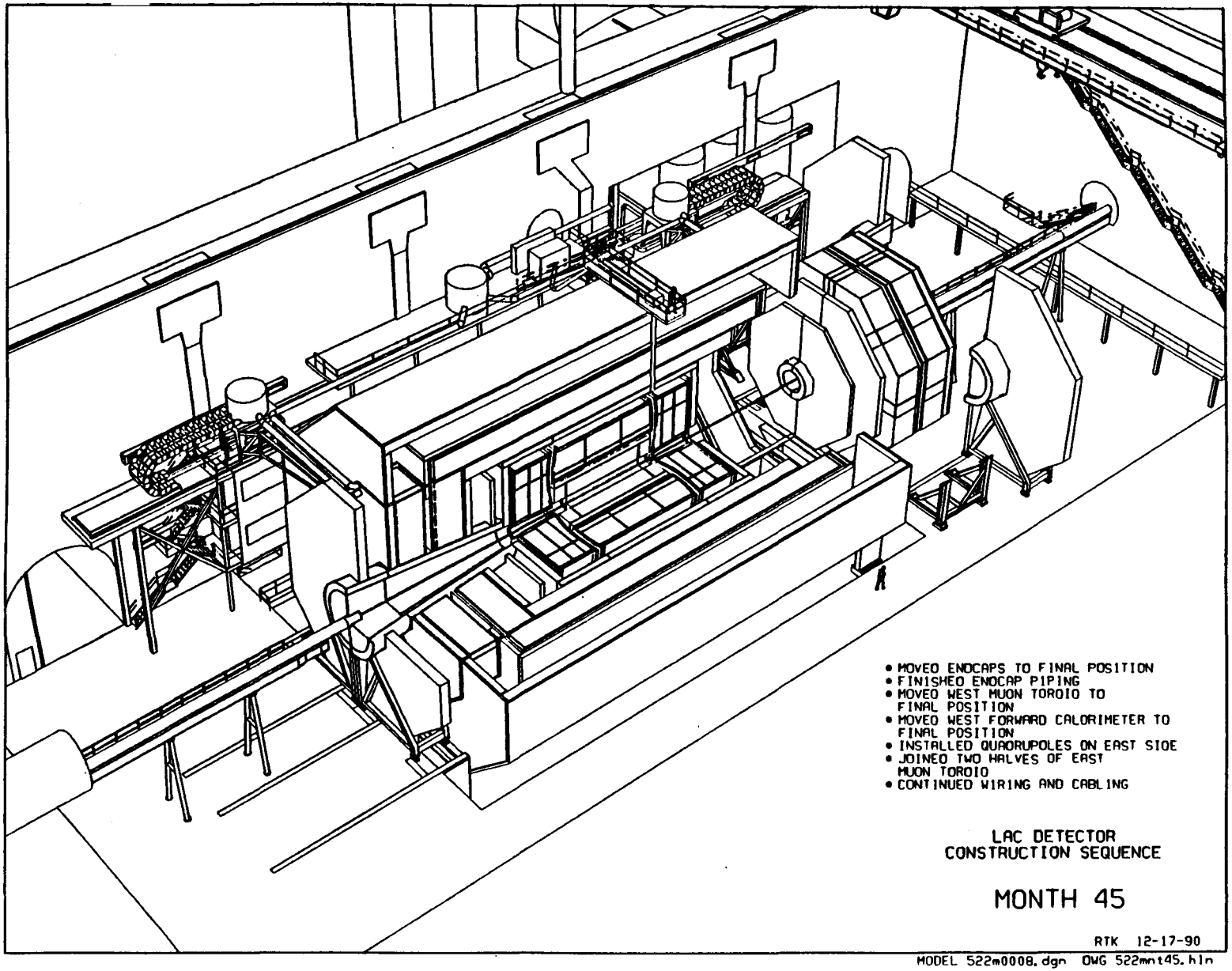

Figure 5.46. LAC Detector Construction Sequence (Month 45).

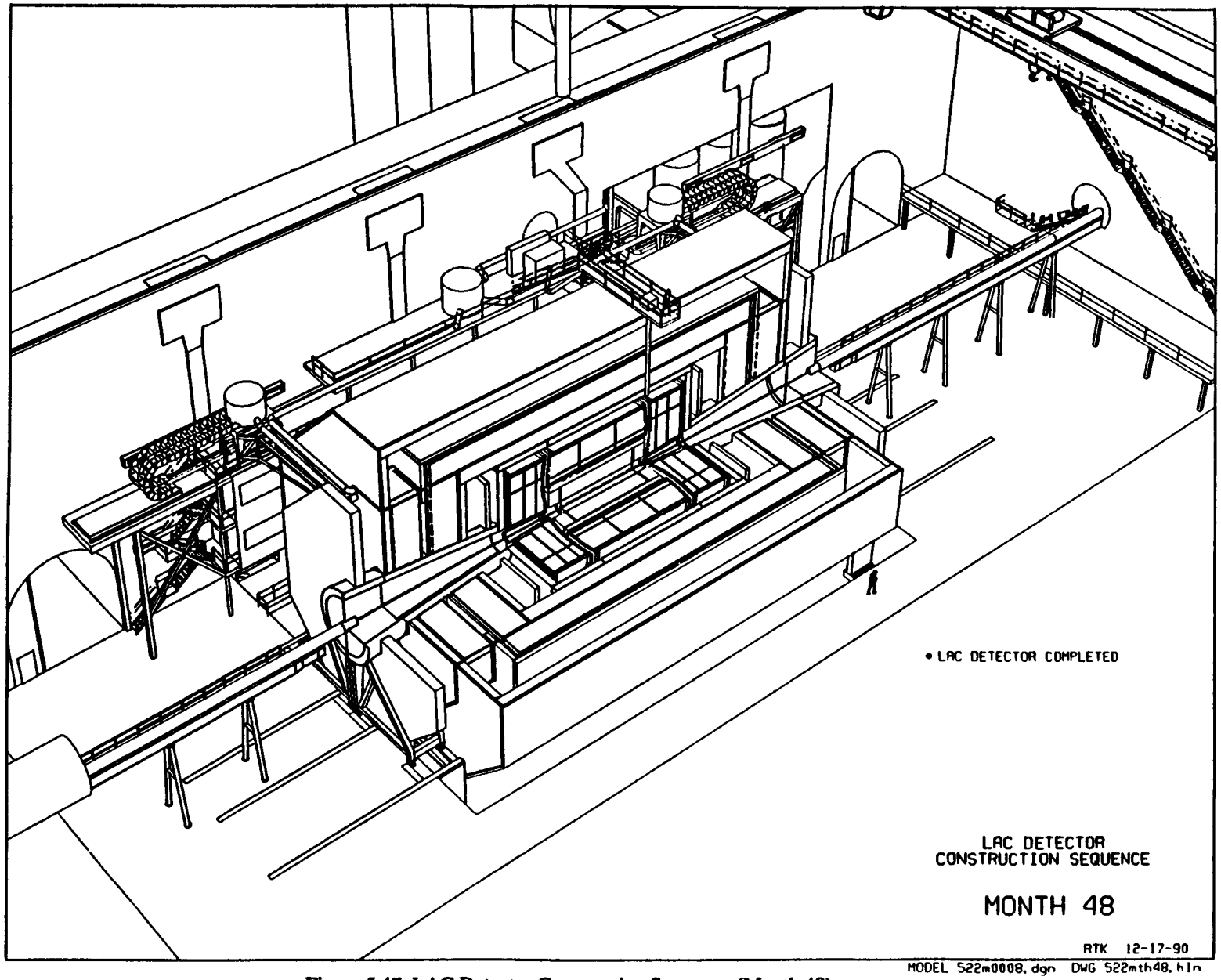

Figure 5.47. LAC Detector Construction Sequence (Month 48).

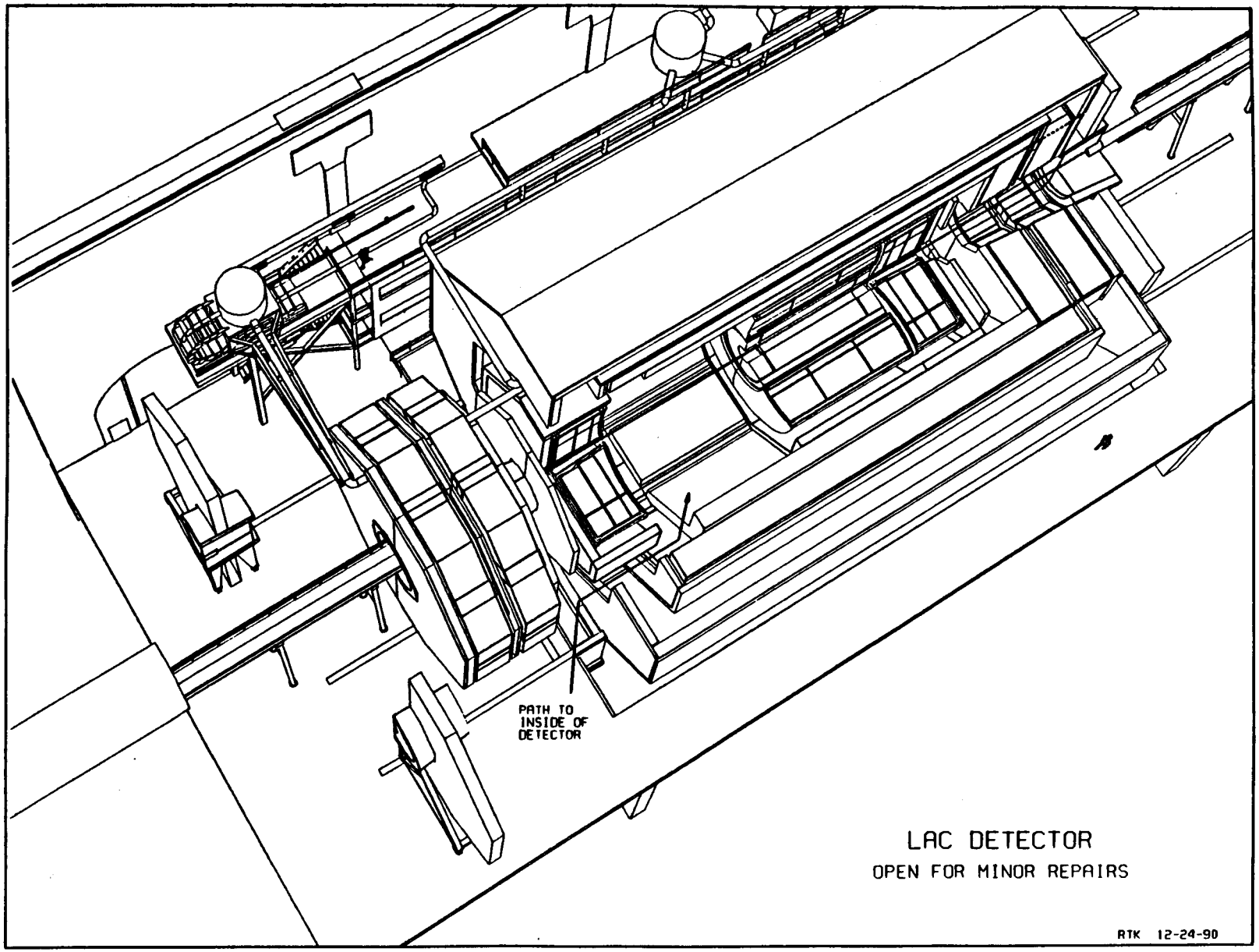

Figure 5.48. LAC Detector Open for Minor Repairs.

the cabling for the muon toroids chambers. If they are connected to the same power track, then the toroid, the calorimeter endcap, and the powertrack need to move together.

Once the movements have been completed, there is a 1.2-m gap between the endcap and the muon barrel which can be used to gain access to the interior of the detector for servicing.

5.5.2 Major Repairs

We define as major any repairs that require breaking the beam tube. Such repairs could entail the replacement of any of the components of the central tracking device, of the coil, or of the calorimeter modules. The duration of these repairs is greater than six months.

Figure 5.49 shows the arrangement when replacing modules on a calorimeter endcap. As can be seen, the floor space is tight, but there is enough room to maneuver all the components. The entire beamline must be disassembled. This repair is shown on the west end of the hall, where there is less space available.

Figure 5.50 shows the arrangement necessary to replace modules on the barrel calorimeter. Here again the floor space is tight but adequate. Once more, the entire beamline must be disassembled. The repair of the solenoidal coil or of any of the components of the central tracking device requires opening the detector in a manner similar to that shown in Figure 5.49. However, because the barrel calorimeter need not be extracted, somewhat less space is required.

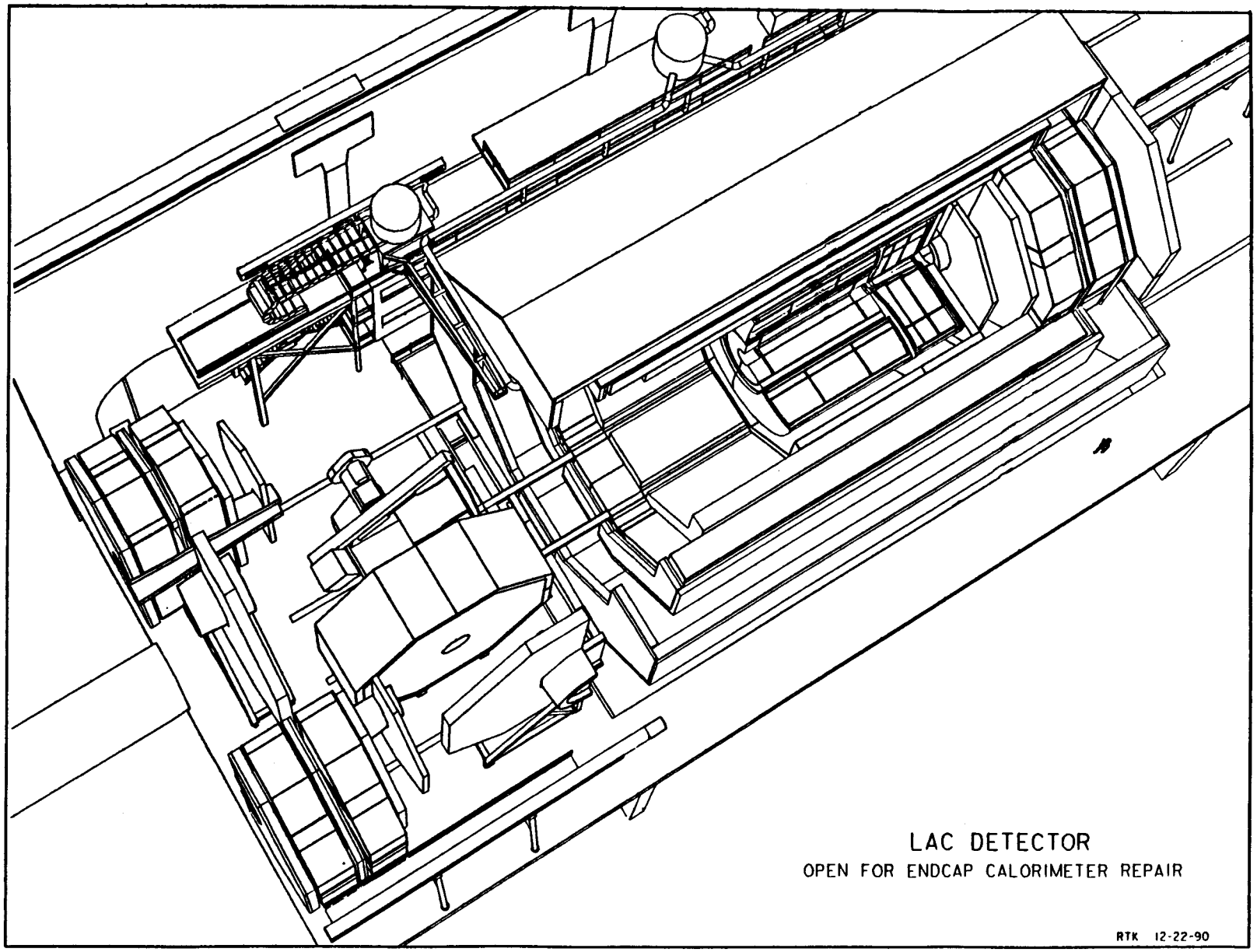

Figure 5.49. LAC Detector Open for Endcap Calorimeter Repair.

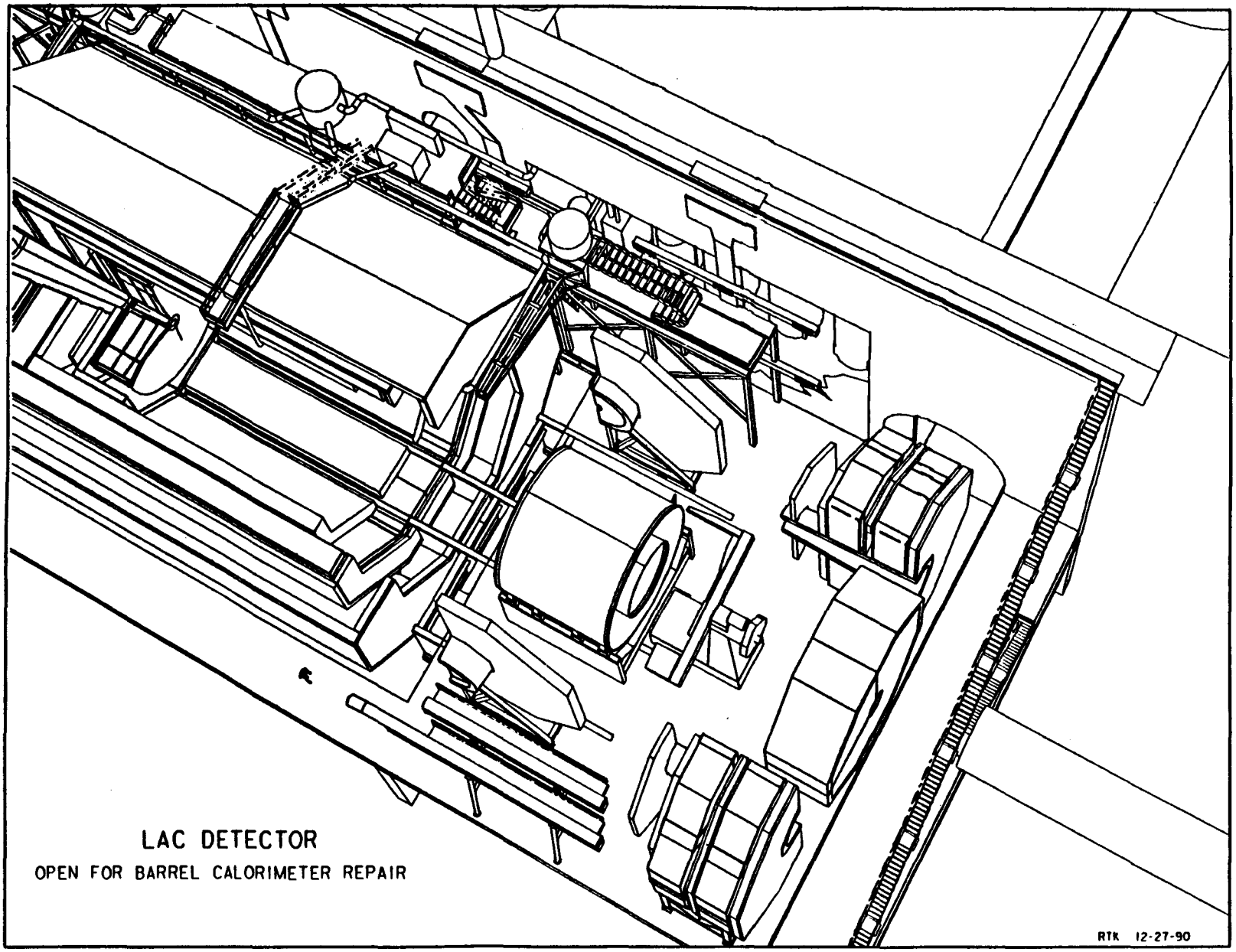

Figure 5.50. LAC Detector Open for Barrel Calorimeter Repair.

REFERENCES

1. Y. Doi et al., "Design Study of a Short Solenoid for the SDC Detector," *Proceedings, International Workshop on Solenoidal Detectors for the SSC*, KEK, April 1990.

2. T. Ballinger et. al., "Engineering Design Study of a Warm Liquid Calorimeter Concept for a Detector at the SSC," EG&G Energy Measurements, Report AVO-395, September 1989.

APPENDIX A

DETECTOR UTILITIES

To determine the electrical and cooling facilities needed for the hall, we have developed a bottoms-up model of power consumption for the detector and hall. Based on this model we estimate the cooling demand for the hall and surface facilities; from the cooling requirements we created a model of the primary and secondary cooling load.

Operating power consumption is determined for three geographic regions: inside the solenoid, between the solenoid and the iron muon toroids, and the remainder of the hall, including shafts and surface buildings. In addition, the type of power used (400 Hz, 60 Hz Detector, 60 Hz other, DC, and line power) is identified, and each load is traced back to the factors. Table A.1 summarizes power information. We also estimate the contingency power capacity (SPARE in Table A.1) for which bussing should be included. Some fraction (DIVERSITY in Table A.1) of the contingency power was also included in the installed transformer capacity. For the baseline detector the total power required is 14,471 KVA.

A model for heat removal was constructed based on load and location. Each thermal load was apportioned between the various cooling systems (ICW, LCW, CHW, butane cooling, and A/C). The net load on the system in each geographical location was tabulated, and results are summarized in Table A.2. The secondary cooling needed to provide the primary cooling is summarized in Table A.3.

Table A-1. Power Consumption.

Location	Numb Chan	Watts Chan	400 Hz Power					60 Hz Detector					60 Hz Other			DC Power			Line Power						
	Chan	Chan	Use	1/Eff.	Load	Spare	Total	Use	1/Eff.	Load	Spare	Total	Load	Spare	Total	Load	Spare	Total	Use	Spare	Div.	1/Eff.	Load	1/PF	Supply
	Kchan		KWatt		Kwatt		KWatt	KWatt		KWatt		KWatt	Kwatt		KWatt	KWatt		KWatt	KWatt	KWatt			KWatt		KVA
Inside Coil:																									
Silicon Vertex			10		10	2	20																		
HV Dissipation								0.66		0.66															
Straw Tracking	240	0.02	4.8		4.8	2	9.6																		
HV Dissipation								0.36		0.36															
Fiber Tracking																									
HV Dissipation																									
Inside Coil Total			14.8		14.8		29.6	1.02		1.02															
Solenoid Magnet:																									
Cryostat																									
Power Leads																									
Ht Leak/Coldwn																									
Solenoid Cryostat																									
Inside Muon Steel:																									
Calorimeter	66	1.5	99	2	198	2	396																		
HV Dissipation								0.99		0.99															
Muon Chamber	35	0.02	0.7	2	1.4	2	2.8																		
HV Dissipation								0.053		0.053															
Muon Trigger	0	1.5	0	2	0	2	0																		
HV Dissipation								0		0															
Inside Tracking PS				2	14.8	2	29.6																		
Total Inside Muon Steel			99.7		214.2		428.4																		
Muon Toroids																									
Barrel																1739	1.25	2174							
Near End Cap																535	1.25	668.8							
Far End Cap																282	1.25	352.5							
Total Muon Toroid																2556		3195							
Outside Muon Steel:																									
Muon Chambers	73	0.02	1.46	2	2.92	2	5.84																		
HV Dissp								0.11		0.11															

* = Not included in totals. PF = Power Factor. Div = Diversity Factor. Eff = 1/(Power Supply Efficiency). Frac = Fraction of Cooling.

Jim Bensinger/Joseph Rasson 1/15/91

Table A-1. Power Consumption (Continued).

Location	Numb Chan	Watts Chan	400 Hz Power					60 Hz Detector					60 Hz Other			DC Power			Line Power						
			Use	1/Eff.	Load	Spare	Total	Use	1/Eff.	Load	Spare	Total	Load	Spare	Total	Load	Spare	Total	Use	Spare	Div.	1/Eff.	Load	1/PF	Supply
	Kchan		KWatt		Kwatt		KWatt	KWatt		KWatt		KWatt	Kwatt		KWatt	KWatt		KWatt	KWatt	KWatt			KWatt		KVA
Muon Trigger	16	1.5	24	2	48	2	96																		
HV Dissp								24		24															
Forward Calorimeter	7	0.4	2.8	2	5.6	2	11.2																		
HV Dissipation								0		0															
Level 1 Trigger			36	2	72	2	144																		
DAQ			14.67	1.5	22.01	2	44.01																		
High Voltage																									
Tracking									2	1.02	2	4.08													
Calorimeter									2	0.99	2	3.96													
Muon Chambers									2	0.162	2	0.324													
Muon Trigger									2	24	2	48													
Monitoring								50		50	2	100													
Liquid Handling													100		100										
Lights													115	1.5	172.5										
Outlet Power													25	1.5	37.5										
* Welding													120	2	240										
* Crane													250	1.5	375										
Air Handling													37	1.5	55.5										
Sump Pumps													25	2	50										
Safety													50	2	100										
Total Outside Muon Steel			78.93		150.5		301.1	74.11		100.3		156.4	352		515.5	0		0							
Utility Shaft																									
Toroid Power Bus																100	2	200							
Solenoid Power Bus																20	2	40							
Total Utility Shaft																120		240							
Surface:																									
DAQ			300	2	600	2	1200																		
Trigger Level 2			56	2	112	2	224																		
Trigger Level 3								90	1.5	135	2	270													

* = Not included in totals. PF = Power Factor. Div = Diversity Factor. Eff = 1/(Power Supply Efficiency). Frac = Fraction of Cooling.

Jim Bensinger/Joseph Resson 1/15/9

Table A-1. Power Consumption (Continued).

Location	Numb Chan	Watts Chan	400 Hz Power					60 Hz Detector					60 Hz Other			DC Power			Line Power						
			Use	1/Eff.	Load	Spare	Total	Use	1/Eff.	Load	Spare	Total	Load	Spare	Total	Load	Spare	Total	Use	Spare	Div.	1/Eff.	Load	1/PF	Supply
	Kchan		KWatt		Kwatt		KWatt	KWatt		KWatt		KWatt	Kwatt		KWatt	KWatt		KWatt	KWatt	KWatt			KWatt		KVA
Control Room								100	2	200	2	400													
Monitoring								100		100	2	200													
Computer System								100		100	2	200													
Cryogenic System																									
Helium Comp.																			800	200	1	1.3	1,300	1.2	1,560
Solenoid Coil PS																			500	125	1	1.3	813	1.2	975
Control/Cold Box													60	2	120										
Compressed Air													20	2	40										
Auxiliary													50		50										
Muon Toroid PS																			2656	739	1	1.3	1,019	1.2	5,296
400 Hz MG Set																			1092	1092	0.3	1.3	426	1.2	2,214
Solenoid Pwr Bus																			20	20	1	1.3	52	1.2	62
Crane																									
HVAC System																									
CHW Prod/Circ													984.9	1.5	1477										
Air Circ Fan													40	1.5	60										
Util Water Pumps													125	1.5	187.5										
Power Transformer																									
60 Hz Detector																			686.3	640.1	0.3	1.3	263	1.2	1,370
60 Hz Other																			1667	841	0.3	1.3	576	1.2	2,994
Vent. Fan													25	1.5	38										
Safety								50		50	2	100													
Noninterruptable Pwr													10	2	20										
Total Surface			356		712		1,424	440		585		1,170	1,315		1,992	0		0	7,421	3,657			4,448		14,471
Total			549		1,092		2,183	515		686		1,326	1,667		2,508	2,676		3,435	7,421	3,657			4,448		14,471

* = Not included in totals. PF = Power Factor. Div = Diversity Factor. Eff = 1/(Power Supply Efficiency). Frac = Fraction of Cooling.

Jim Bensinger/Joseph Rasson 1/15/91

Table A-2. Primary Cooling Requirements

Location	ICW					LCW					CHW					Butane Cooling					A/C				
	Frac	Load	T in	T out	Flow	Frac	Load	T in	T out	Flow	Frac	Load	T in	T out	Flow	Frac	Load	T in	T out	Flow	Frac	Load	T in	T out	Flow
		KWatt	°F	°F	gpm		KWatt	°F	°F	gpm		KWatt	°F	°F	gpm		KWatt	°c	°c	cc/min		KWatt	°F	°F	CFM
Inside Coil:																									
Silicon Vertex HV Dissipation																1	20	10	10	5000					
Straw Tracking HV Dissipation											1	4.8	45	60	2.128										
Fiber Tracking HV Dissipation																									
Inside Coil Total		0			0		0			0		4.8			2.128		20			5000		0			0
Solenoid Magnet:																									
Cryostat Power Leads Ht Leak/Coldwn																									
Solenoid Cryostat		0			0		0			0		0			0		0			0		0			0
Inside Muon Steel:																									
Calorimeter HV Dissipation											1	198	45	60	87.78										
Muon Chamber HV Dissipation																					1	1.4	75	80	903
Muon Trigger HV Dissipation																					1	0	75	80	0
Inside Tracking PS											1	14.8	45	60	6.561										
Total Inside Muon Steel		0			0		0			0		212.8			94.34		0			0		1.4			903
Muon Toroids																									
Barrel						0.98	1704	65	75	1,133											0.02	34.78	75	80	22,426
Near End Cap						0.98	524.3	65	75	349											0.02	10.7	75	80	6,899
Far End Cap						0.98	276.4	65	75	184											0.02	5.64	75	80	3,637
Total Muon Toroid		0			0		2505			1,666		0			0		0			0		51			32,962
Outside Muon Steel:																									
Muon Chambers																					1	2.92	55	75	471

* = Not included in totals. PF = Power Factor. Div = Diversity Factor. Eff = 1/(Power Supply Efficiency). Frac = Fraction of Cooling.

Jim Bensinger/Joseph Resson 1/15/91

Table A-2. Primary Cooling Requirements (Continued).

Location	ICW					LCW					CHW					Butane Cooling					A/C				
	Frac	Load	T in	T out	Flow	Frac	Load	T in	T out	Flow	Frac	Load	T in	T out	Flow	Frac	Load	T in	T out	Flow	Frac	Load	T in	T out	Flow
		KWatt	°F	°F	gpm		KWatt	°F	°F	gpm		KWatt	°F	°F	gpm		KWatt	°c	°c	cc/min		KWatt	°F	°F	CFM
Muon Trigger																					1	48	55	75	7,738
Forward Calorimeter HV Dissipation											1	5.6	50	65	2.483										
Level 1 Trigger											1	72	50	65	31.92										
High Voltage																									
Tracking																									
Calorimeter																									
Muon Chambers																									
Muon Trigger																									
Monitoring																					1	50	55	75	8,060
Liquid Handling																					0.2	20	55	75	3,224
Lights																					1	115	55	75	18,538
Outlet Power																					1	25	55	75	4,030
* Welding																									
* Crane																									
Air Handling																					0.3	11.1	55	75	1,789
Sump Pumps																					0.3	7.5	55	75	1,209
Safety																					0.3	15	55	75	2,418
Total Outside Muon Steel		0			0		0			0		77.6			34.4		0			0		294.5			47476.6
Utility Shaft																									
Toroid Power Bus						1	100	100	130	22															
Solenoid Power Bus						1	20	100	130	4															
Total Utility Shaft		0			0		120			27		0			0		0			0		0			0
Surface:																									
DAQ											1	600	45	60	266										
Trigger Level 2											1	112	45	60	49.65										
Trigger Level 3											1	135	45	60	59.85										

* = Not included in totals. PF = Power Factor. Div = Diversity Factor. Eff = 1/(Power Supply Efficiency). Frac = Fraction of Cooling.

Jim Bensinger/Joseph Resson 1/15/91

Table A-2. Primary Cooling Requirements. (Continued).

Location	ICW					LCW					CHW					Butane Cooling					A/C				
	Frac	Load	T in	T out	Flow	Frac	Load	T in	T out	Flow	Frac	Load	T in	T out	Flow	Frac	Load	T in	T out	Flow	Frac	Load	T in	T out	Flow
		KWatt	°F	°F	gpm		KWatt	°F	°F	gpm		KWatt	°F	°F	gpm		KWatt	°c	°c	cc/min		KWatt	°F	°F	CFM
Control Room											1	200	45	60	88.67										
Monitoring											1	100	45	60	44.33										
Computer System																					1	100	55	75	16,120
Cryogenic System																									
Helium Comp.	1	1300	100	125	348																				
Solenoid Coil PS						1	912.5	100	125	216.1															
Control/Cold Box	1	60	100	125	16																				
Compressed Air																					0.5	10	55	75	1,612
Auxiliary																					0.5	25	55	75	4,030
Muon Toroid PS						1	1019	100	125	270.9															
400 Hz MG Set						1	425.7	100	125	113.2															
Crane																									
HVAC System																					0.3	53	55	75	8,463
CHW Prod/Circ																									
Air Circ Fan																									
Util Water Pumps																									
Power Transformer																									
60 Hz Detector																									
60 Hz Other																									
Safety																					1	50	55	75	8,060
Noninterruptable Pwr																									
Total Surface Cooling		1,360			362		2,257			600		1,147			509		0			0		238			38,285
Total Cooling		1,360			362		4,882			2,290		1,442			639		20			5,000		585			119,627

* = Not included in totals. PF = Power Factor. Div = Diversity Factor. Eff = 1/(Power Supply Efficiency). Frac = Fraction of Cooling.

Jim Bensinger/Joseph Resson 1/15/91

Table A-3. Secondary Cooling Requirements.

Secondary Cooling	Primary Cooling Load BTU/hr	Primary Cooling Flow Rate gpm,cfm	Pump or Blower Δp(psi,in H2o)	Pump or Blower KWatt	Compressor KWatt	Auxilary Pumps/Fans KWatt	Secondary Cooling Pond/Tower Btu/hr
ICW							
100 to 125°F	4,640,320	362	43	11			4,679,085
LCW							
65 to 75 °F	8,546,651	1,667	250	304			
100 to 130 °F	8,109,282	527	53	20			8,178,866
CHW (Primary)							
45 to 60 °F	4,920,786	640	35	16	275		5,913,980
A/C							
55 to 75 °F	1,092,113	51,602	4	37			
75 to 80°F Insd Stl	91,988	17,386	4	12			
Surface Blg	810,350	38,289	4	27			
CHW (Secondary)							
For A/C ΔT = 15 °F	1,994,450	259	35	7	125		2,442,370
For LCW @65°F ΔT=15°F	8,546,651	1,111	35	28	534		10,466,083

Power for CHW Production and Circulation= 985 KW
Hall HVAC Air Handling = 37 KW
Surface Bldg & Hall Ventilation Fans= 40 KW
Line Power= 14,471 KVA Total Ambient Heat Rejec 31,680,383

APPENDIX B

HVAC CONSIDERATIONS

1.0 SYSTEM REQUIREMENTS

Temperature in the hall is controlled to within 0.1°C of a set point of 24°C. The maximum variation due to stratification or localized high-intensity heat sources is 3°C.

General air circulation is approximately two air changes per hour. Based on hall dimensions the rate of air circulation will be approximately 40 m^3/s. Air is drawn from the upper sections of the hall and discharged in the lower sections. This minimizes large temperature variations due to stratification of warm air in the upper level.

Normal ventilation is 25% of the total recirculated air (0.5 air changes per hour). Based on dimensions of the hall, the ventilation rate is 10 m^3/s. This air is delivered at temperatures ranging from 10°C to 30°C, depending on heating and cooling loads.

The ventilation air is exhausted from the hall after it passes through the detector. The air is collected through a gasketed duct adjacent to the gap between the barrel and the end muon toroids. The air enters the detector at approximately 24°C through the gap at the opposite end of the barrel. The 10 m^3/s ventilation rate absorbs 30kW with a temperature rise of 2.5°C.

The opening along the beam line should be minimized to maintain proper air distribution and flow through the detector. During detector assembly the construction shaft is open. The air motion through the shaft will depend on the tightness of the building above the shaft and the relative temperatures in the building and in the underground hall. When the air in the hall is cooler than the air in the building, very little air motion will occur. However, when the reverse is true, air motion may be considerable and is difficult to predict.

The main hall employs a smoke purge system rated at approximately 80 m^3/s. This provides four air changes per hour. This type of ventilation system does not appear to be covered in the codes governing underground structures such as this. Section 1715 of the 1988 Uniform Building Code calls for four air changes per hour for atria. The purpose of atrium ventilation is to remove smoke from a fire in the atrium so that hotel guests can see well enough to find their way out of rooms which open onto balconies around the atrium. In the absence of other guidelines, four air changes per hour has been selected.

Exit stairwells are provided with a pressurization system capable of maintaining 4.1 m/s velocity through an open 0.91 m by 2.1 m door. This is in accordance with ASHRAE Systems Volume, Chapter 58, and is intended to prevent smoke from entering the stairwell from a fire in the

hall. Relief vents are located at the top of the shafts to limit high pressures which would prevent closing the door at the bottom of the shaft.

There may be fluids in the hall which are toxic, flammable, volatile, cryogenic, or otherwise hazardous. The rate of release of these fluids to the air in the hall must be determined. Comparing the release rates with the allowable concentration may indicate a need for additional ventilation.

Humidity will be controlled to a minimum of 30% and a maximum of 50%, so that the dew point of the air in the hall is below the wall surface temperature.

While the calorimeter is being assembled, the calorimeter assembly room at the north end of the hall will be maintained at a slight positive pressure compared to the adjacent area in order to keep construction dirt out of the area.

Table B.1 summarizes the specifications for the HVAC system.

Table B.1. Design Criteria for Temperature, Humidity, and Ventilation.

	Summer	Winter
Outside Dry-bulb	39°C	-8°C
Outside Wet-bulb	24°C	
Inside Dry-bulb	24°C	24°C
Temperature Control	±0.1°C	±0.1°C
Variation Due to Stratification	3.0°C	3.0°C
Inside Dew Point	13°C	10°C
Inside Relative Humidity	50%	40%
Wall Temp. (1)	16°C	16°C
Heat Gains to Air		
Experimental Equipment		
Outside the Detector		400kW
Lighting		115kW
Smoke Purge Rate	4 changes/hour (80 m^3/sec)	
Minimum Air Circulation	2 air changes/hr (40 m^3/sec)	
Minimum Ventilation	0.5 air change/hr (10 m^3/sec)	

2.0 SYSTEM OPTIONS

Two HVAC systems are analyzed. System A uses multiple air-handling units, most of which are located in the hall. System B uses a single large unit located on the surface. The heating and cooling loads are not affected by choice of system. Both systems share several common elements. The detector exhaust system and the stair pressurization systems are identical.

2.1 System A

A schematic of System A is shown in Figure B.1. This system has eight 5 m^3/s air-handling units, four on each side of the hall, spaced according to the cooling load. They are located in equipment rooms outside the walls near the top of the hall. Vertical ducts recessed in the walls carry the supply air to horizontal distribution ducts at various levels. The horizontal ducts project 0.5 m into the hall. These eight units provide two air changes per hour and remove all the heat rejected to the air by the electrical equipment, personnel, and lights.

Outside air for ventilation is delivered by an air-handling unit on the surface through a shaft to the space above the traveling crane. It is distributed by a horizontal duct running the full length of the hall. Each air-handling unit contains a filter, heating coil, cooling coil, and fan, all enclosed in a metal cabinet. Chilled water is distributed to the cooling coils by piping which runs above the base of the roof arch.

Two smoke-purge supply fans located on the surface, each rated at approximately 40 m^3/s, discharge air into the personnel shaft and equipment shaft. The air enters the hall near the floor. A smoke exhaust fan located on the surface and rated at 80 m^3/s is connected by a duct to the top portion of the construction shaft. During a smoke emergency, these three fans provide four air changes per hour for the hall. The normal exhaust fans do not run during a smoke emergency unless the emergency is in the detector.

Estimated electric power requirement are listed in Table B.2.

Table B.2. HVAC Power Requirements (System A).

8 Recirculating Units @ 5 kV	60 kW
1 Ventilation Supply Unit @ 19 kV	19
1 Normal Exhaust Fan @ 6 kW	6
2 Smoke Purge Supply Fans @ 15 kW	30
1 Smoke Purge Exhaust Fan @ 30kW	30
Maximum Simultaneous Load	85 kW

System A has the following advantages:

1) It makes fairly simple the creation of a pressure gradient between the calorimeter assembly area and the remainder of the hall during calorimeter assembly, and it eliminates mixing of air from clean and dirty areas.
2) Temperatures can be controlled separately in eight zones.
3) Failure of an air handling unit will not deprive the whole cooling system.
4) All air-handling units are standard industrial equipment.

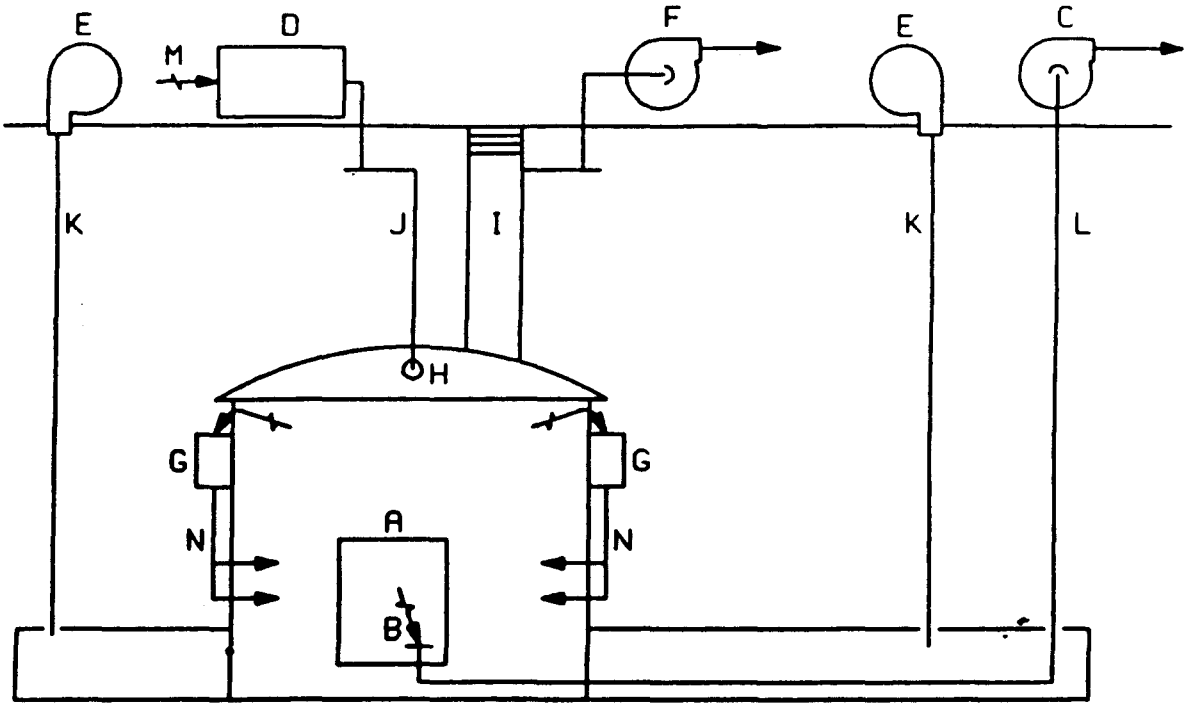

A) Detector

B) Detector Exhaust Slot

C) Detector Exhaust Fan, 21,000 CFM

D) Make-Up Air Unit 21,000 CFM

E) Smoke Control Supply Fan 83,500 CFM (Typical of 2)

F) Smoke Control Exhaust Fan, 167,000 CFM

G) Air Handling Units (Typical of 8) 10,500 CFM

H) Make-Up Air Inlet Duct

I) Construction Shaft

J) Make-Up Air Duct Shaft, 1.2-mø

K) Smoke Control Supply Duct, 1.8 ø, in Personnel Shaft and Equipment Shaft 73,000 CFM each

L) Detector Exhaust Duct,1.2-mø in Personnel Shaft

M) Outside Air Intake, 21,000 CFM

N) Supply Ducts 10,500 CFM 0.75-m x 1.0-m

O) Smoke Exhaust Duct, 2.6-mø

Figure B-1. HVAC System A Schematic $\frac{1}{M}$ A/C Units in Hall.

The disadvantages of System A are:

1) There are eight units to maintain.

2) Additional excavation and form work is required for the spaces to locate the eight air-handling units.

2.2 System B

A schematic of System B is shown in Figure B.2. This system has one approximately 40 m^3/s air-handling unit located on the surface. It discharges air through a separate shaft to a duct running the length of the hall above the crane. Four branch ducts on each side of the main duct deliver air to eight vertical ducts recessed in the walls. The recessed ducts and the distribution system beyond them are similar to those of System A. The air supplied by this system during normal operation is a mixture of 25% outside air and 75% return air. There is no separate outside air unit.

Return air is drawn up the construction shaft by a return air/smoke exhaust fan.

A smoke-purge supply fan rated at approximately 40 m^3/s discharges air through the equipment shaft to the hall. A smoke exhaust fan rated at 40m^3/s exhausts from near the top of the construction shaft. During a smoke emergency the two smoke purge fans, the air-handling unit, and the return/exhaust fan combine to provide four air changes per hour.

Estimated electrical power requirements are listed in Table B.3.

Table B.3. HVAC Power Requirements (System B).

Main Air-Handling Unit	75 kW
Normal Exhaust Fan	6
Return/Exhaust Fan	15
Smoke Purge Supply Fan	15
Smoke Exhaust Fan	15
2 Stair Pressurization Fans @ 0.75	1.5
Maximum Simultaneous Load	96 kW

System B has the following advantages:

1) There is one large air handling unit to maintain vs. nine smaller units.

2) Only one smoke purge supply fan is required because the main air-handling unit replaces one of the supply fans.

The disadvantages of System B are:

1) A failure of the single main air-handling unit would cause a complete system shut-down.

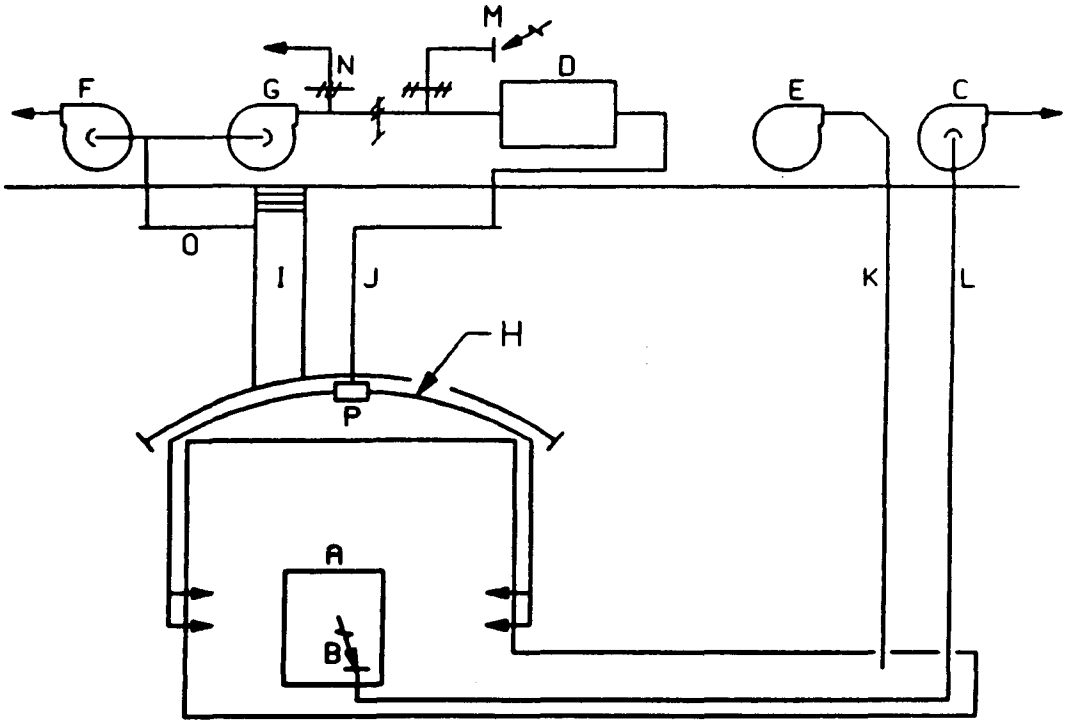

A) Detector

B) Detector Exhaust Slot

C) Detector Exhaust Fan, 21,000 CFM

D) Air Conditioning Unit 83,500 CFM, 25% or

E) Smoke Control Supply Fan 83,500 CFM

F) Smoke Control Exhaust Fan 83,500 CFM

G) Smoke Control Return Fan, 62,500 CFM

H) Supply Ducts, 10,500 CFM, 0.75-m x 1.0-m

I) Construction Shaft

J) Supply Shaft 83,500 CFM, 2.0-mø

K) Smoke Control Supply Duct 83,500 CFM 1.8-mø in Equipment Shaft

L) Detector Exhaust Duct, 1.2-m in Personnel Shaft

M) Outside Air Intake 21,000 CFM

N) Motorized Damper (Typical)

O) Smoke Exhaust Duct, 2.6-mø

P) Supply Duct 83,500 CFM, 1.65-m x 1.65-m

Figure B-2. HVAC System B Schematic $\frac{1}{M}$ A/C Units Above Ground.

2) A long duct must be installed between the personnel shaft and the equipment shaft.

3) Use of the normal ventilation equipment for smoke purge complicates the controls.

4) Half of the smoke purge supply air is introduced into the hall in a uniform distribution instead of near the floor and near one end of the hall. Some of this air may short-circuit directly to the exhaust.

5) The large air-handling unit must be field-assembled instead of factory-assembled, as the smaller units of System A would be.

2.3 System Recommendations

System A, employing multiple underground air-handling units, is recommended. Two advantages of System A are particularly important and outweigh the disadvantages. They are:

1) The ability to provide a pressure gradient and to isolate the calorimeter assembly room during construction.

2) The relatively minor consequences of the failure of one air-handling unit.

The additional complication of System B is the most compelling reason for not choosing it.